Towards the gene-based characterisation of maraena whitefish (*Coregonus maraena*) in local aquaculture

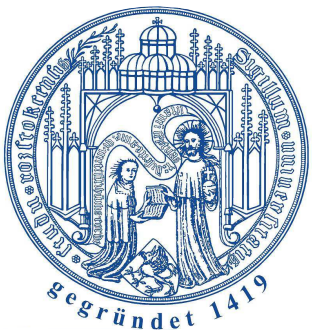

Dissertation
zur
Erlangung des akademischen Grades
doctor rerum naturalium (Dr. rer. nat.)
der Mathematisch-Naturwissenschaftlichen Fakultät
der Universität Rostock

vorgelegt von
Mareen Nipkow, geb. am 12.01.1986 in Schwerin

Rostock, den 18.09.2018

https://doi.org/10.18453/rosdok_id00002528

Date of submission:

18.09.2018

Date of defence:

01.02.2019

Supervisors:

PD Dr. Tom Goldammer
Leibniz Institute for Farm Animal Biology (FBN), Institute for Genome Biology, Fish Genetics Unit, Dummerstorf, Germany

Prof. Dr. Hubert Bahl
Department of Microbiology, Institute of Biological Sciences, University of Rostock, Rostock, Germany

Prof. Dr. Reinhardt Schröder
Department of Genetics, Institute of Biological Sciences, University of Rostock, Rostock, Germany

This work is dedicated to my lovely little daughter Paulina
who came into my life just in time during the writing process
to teach me attentiveness, patience, and serenity,
which contributed a lot to the success of this thesis.

Contents

List of Figures

List of Tables

Nomenclature

A	adenine
aa	amino acid
ACTH	adrenocorticotropic hormone
A.dest.	Aqua destillata (lat.)
ALS	acid labile subunit
ANOVA	analysis of variance
APPs	acute phase proteins
APR	acute phase response
AR	acute temperature rise
A-SAA	acute phase SAA
BLAST	basic local alignment search tool
bp	base pairs
cAMP	cyclic adenosine monophosphate
CCM	cell culture medium
cDNA	complementary DNA
Cq	cycle of quantification
CREB	cAMP response element binding protein
CRH	corticotropin-releasing hormone
C-SAA	constitutive SAA
CXCL8	C-X-C motif chemokine ligand 8 (interleukin 8)
Cy3	cyanine 3 (fluorescent dye)
d	days
DAMPs	danger-associated molecular patterns
DBD	DNA-binding domain
DE	differentially expressed
DEPC-H_2O	diethyl pyrocarbonate treated water
DNA	deoxyribonucleic acid
dNTP	deoxynucleoside triphosphate (A/C/G/T)
dpf	days post fertilisation
dph	days post hatch
dsDNA	double stranded DNA
DTT	1,4-dithiothreitol
E	qPCR efficiency
E.coli	*Escherichia coli*
ED	enhanced stocking density
EDTA	ethylenediaminetetraacetic acid
EEF1A1B	eukaryotic translation elongation factor 1 alpha 1, variant B
e.g.	exempli gratia (lat.)
ELISA	enzyme-linked immunosorbent assay
ENA	European Nucleotide Archive
FC	fold change
FLI	Friedrich-Loeffler-Institute
g	gravitational acceleration (g=9.80665 m/s2)
G+C	guanine+cytosine
GC	glucocorticoids
GCR2	glucocorticoid receptor beta
GCR	glucocorticoid receptor
GHBP	growth hormone binding protein
GH	growth hormone
GHR	growth hormone receptor
GHRH	growth hormone releasing hormone
gp130	glycoprotein 130
GRE	glucocorticoid responsive elements
GR	gradual temperature rise
H_2O_{bidest}	double distilled water
HD	high stocking density
HDL	high-density lipoprotein
HPA axis	hypothalamic-pituitary-adrenal axis
HPI axis	hypothalamic-pituitary-interrenal axis
HR	handling reference (transfer control)
HRP	horseradish peroxidase
HSP70	heat shock protein 70kDa
HSP90	heat shock protein 90kDa
HSPs	heat shock proteins
i.e.	id est (lat.)
IFN	interferon
IGF1	insulin-like growth factor I
IGF1R	IGF-1 receptor
IGF2	insulin-like growth factor II
IGFBPs	insulin like growth factor binding proteins
IGFs	insulin like growth factors

IL12B	interleukin 12 beta
IL1B	interleukin 1 beta
IL6	interleukin 6
i.p.	intraperitoneal
IPTG	isopropyl-1-thio-β-Dgalactopyranoside
kb	kilo base pairs
kDa	kilo-Daltons
LBD	ligand-binding domain
LD	low stocking density
MAPK1	mitogen-activated protein kinase 1
MAPK3	mitogen-activated protein kinase 3
MD	moderate stocking density
min	minutes (unit)
ml	millilitre (unit)
mM	millimolar (unit)
mm	millimetre (unit)
MOPS	3-(N-morpholino) propanesulfonic acid
MR	mineralcorticoid receptor
mRNA	messenger RNA
NCBI	National Center for Biotechnology Information
NK cells	natural killer cells
nm	nanometre (unit)
NR3C1	nuclear receptor subfamily 3 group C member 1
OD	optical density
OmpA	outer membrane protein A
PAMPs	pattern-associated molecular patterns
PCR	polymerase chain reaction
PRR	pattern recognition receptor
PVDF	polyvinylidene fluoride
qPCR	quantitative real time PCR
RACE	rapid amplification of cDNA ends
RIPA	radioimmunoprecipitation assay
RNA	Ribonucleic acid
RPL32	ribosomal protein L32
RPL9	ribosomal protein L9
rpm	rounds per minute (unit)
rRNA	ribosomal RNA
RT	room temperature
SAA	serum amyloid A
SD	standard deviation
SDS-PAGE	sodium dodecyl sulfate polyacrylamide gel electrophoresis
SDS	sodium dodecyl sulfate
SEM	standard error mean
SOB	super optimal broth medium
s	seconds (unit)
T	thymine
TACE	TNF-α-converting enzyme
Taq	*Thermus aquaticus*
TBE	tris/borate/EDTA
TBST	tris-buffered saline and Tween 20
TLRs	toll-like receptors
T_m	melting temperature of an oligonucleotide
TNF	tumor necrosis factor
TP53	tumor protein p53
TR	temperature reference (18°C constant)
TY	tryptone yeast extract
UPR	unfolded protein response
UTR	untranslated region
V	volt (unit)
wph	weeks post hatch
X-gal	5-bromo-4-chloro-3-inodlyl-β-D-galactopyranoside
µl	microlitre (unit)
µM	micromolar (unit)

1. Introduction

The present study on maraena whitefish gives a first overview of morphological and molecular parameters recorded in first breeding trials of this species in a brackish aquaculture facility and in various stress tests. In the long term, these studies aimed at identifying molecular markers for the development of robust and fast-growing whitefish populations, a prerequisite for a sustainable, local, and competitive aquaculture.

1.1. *Coregonus maraena*

1.1.1. Taxonomic classification, morphology, and biology

Coregonus maraena (Bloch, 1779), commonly named maraena whitefish or vendace, in Germany also known as "Maräne" or "Schnäpel", is a salmonid fish (family: Salmonidae) that belongs to the subfamily of "Coregoninae" (see figure 1.1). Taxonomic classification of this species is confusing, as it differs considerably over years and with authors, as Kottelat and Freyhof reported: "systematics of the Coregonidae is traditionally considered as a nightmare". Therefore, at various times, many species within this family were collectively, but falsely referred to as *Coregonus lavaretus*, as happened in the case of *Coregonus maraena* (Kottelat & Freyhof, 2007). Hence, the authors unequivocally clarified that the use of the term *"Coregonus lavaretus"* for any other species than the one of Lake Bourget in France is incorrect (Kottelat & Freyhof, 2007). Since the taxonomic classification of whitefishes published by Kottelat and Freyhof (2007) is the most recent in literature, it is used as a guideline for this thesis.

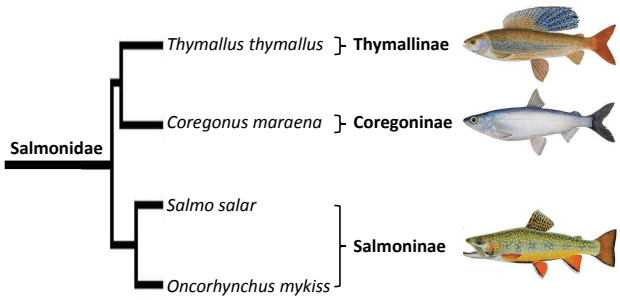

Figure 1.1: ***Coregonus maraena* taxonomy**
Representation of the phylogenetic relation of *Coregonus maraena* within the family of salmonids (figure modified from Macqueen & Johnston, 2014).

Figure 1.2: ***Coregonus maraena* morphology**
Morphology of a nearly one year old *Coregonus maraena*, reared in a flow-through aquaculture facility, having a total length of 25 cm and a total weight of 97.8 g.

Like all salmonids maraena whitefish's morphology (see figure 1.2) is characterised by a spindle shaped, silvery body that is laterally slightly compressed and covered by numerous small scales (Kottelat &

Freyhof, 2007; Hochleithner, 2001). Another characteristic trait of salmonids is the adipose dorsal fin (Kottelat & Freyhof, 2007; Hochleithner, 2001). *Coregonus maraena* can be distinguished from other species in northern Europe by the appearance of 20 - 36 gill rakers, an inferior mouth without teeth, an elongated snout (particularly in males), and a maximum standard length (from snout to the basis of the caudal fin) of 60 cm (Kottelat & Freyhof, 2007). As shown in figure 1.3 the species is naturally distributed throughout the Baltic Sea basin, the south eastern North Sea basin, and the flanking estuaries. Besides from some landlocked populations in lakes, maraena whitefish is an anadromous salmonid, which spawns soonest at three years (Kottelat & Freyhof, 2007; Hochleithner, 2001). Therefore, the fish migrates upstream, and spawning takes place over firm sediments in shallow, freshwater parts of estuaries and lowland rivers (Kottelat & Freyhof, 2007). The spawning period starts depending on water temperature ($< 6\,°C$), and extends from November until December in the southern Baltic Sea area (Kottelat & Freyhof, 2007; Schulz, 2000). The hatching of the eggs takes place from the mid of March until the early April after approximately 250 day degrees, depending on water temperature (at sediment-water border). At a juvenile stage of around one year, the fish actively migrate to feeding grounds in the sea (Kottelat & Freyhof, 2007; Schulz, 2000). Mareana whitefish feeds on mainly insects and crustaceans, but also molluscs, small fishes and fish eggs (Kottelat & Freyhof, 2007; Hochleithner, 2001).

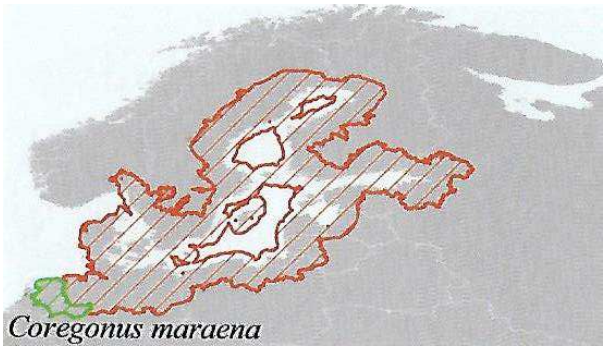

Figure 1.3: **Distribution of *Coregonus maraena*** On the schematic picture of Northern Europe, natural distribution of *Coregonus maraena* is represented by red lines, whereas areas to that *Corenonus maraena* was artificially introduced are marked by green lines. Figure adapted from Kottelat & Freyhof (2007).

1.1.2. Development of a maraena whitefish aquaculture in Mecklenburg-Western Pomerania

Over the last two decades, maraena whitefish has developed to a high-quality food fish in the southern Baltic Sea area. Consequently, this fish is of high commercial value (Bochert *et al.*, 2017; Kottelat & Freyhof, 2007; Jennerich & Schulz, 2011). Since the 1980's, overfishing, the pollution of the natural habitat, and the blocking of spawning grounds by dams and weirs led to a steady decline of the natural population of this highly sensitive fish species that is considered as an indicator species for a clean and healthy habitat (Lorenz, 2012; Arndt, 2001). Thus, the aforementioned conditions resulted in a dramatic drop in catch figures from 32 t in 1980 to 2.7 t in 1995 in Mecklenburg-Western Pomerania (Kottelat & Freyhof, 2007; Schulz, 2000; Arndt & Jansen, 2008). To re-stabilise natural stocks of maraena whitefish in the Southern Baltic Sea, to prevent extinction, and the loss of importance of this species for local fishery, since 1993 annual, aquaculture-based stocking programs were carried out in Mecklenburg-Western Pomerania. To this end, maraena whitefish were artificially brooded and reared in aquaculture facilities until the larvae, and/or juvenile fish (fingerlings) were again released to the Baltic sea (mainly in the Peene river, East Pomeranian bodden chain, and Darß-Zingst bodden chain) (Lorenz, 2012; Schulz, 2000, 2008; Schulz *et al.*, 2012). Despite large-scale stocking programs, the natural population of maraena whitefish was not getting stable again (Arndt & Jansen, 2010; Jansen *et al.*, 2008; Schulz, 2008, 2000; Jennerich & Arndt, 2012a). Indeed, annual catches increased again significantly, but varied considerably from year to year, e.g., between 55 t to 9 t from 2001 until 2010 (Lorenz, 2012; Schulz *et al.*, 2012).

Moreover, catches were not sufficient to meet the raising demand as food fish (Lorenz, 2012; Schulz, 2012; Jennerich & Schulz, 2011). For this reason, based on previous experience from stocking fish production, a whole rearing-period culturing of maraena whitefish in cold-water recirculation and semi-intensive pond systems was initiated in Mecklenburg-Western Pomerania from 2005 to 2008 (Arndt & Jansen, 2008, 2010; Jansen *et al.*, 2008; Jennerich & Arndt, 2012b). Maraena whitefish was then successfully reared in freshwater aquaculture systems, but economically insufficient, since the fish need two summer seasons to reach a marketable body weight (Arndt & Jansen, 2008, 2010; Jansen *et al.*, 2008; Bochert, 2014; Luft *et al.*, 2015). Therefore, from 2012 on, an initiative was launched to culture maraena whitefish in intensive recirculation aquaculture systems (usually termed RAS; tempered and supplied by brackish water) and thus productivity was increased to an economic level, since a year-round production, as well as a off-season reproduction of maraena whitefish has been realised (Luft *et al.*, 2015; Bochert, 2014).

1.2. Immune target genes

For this study, the focus was clearly directed on the innate immune system[1], as it plays the fundamental role in mediating defence mechanisms in fish, while the adaptive immune system is limited in its functions compared to mammals (Rebl & Goldammer, 2018; Uribe *et al.*, 2011; Bayne & Gerwick, 2001; Zwollo, 2018; Magnadóttir, 2006). The knowledge accumulated by the Fish Genetics Unit (FBN Dummerstorf) on innate immune regulation in rainbow trout, was the starting point to investigate the early immune response of maraena whitefish. Hence, the cytokines tumor necrosis factor "TNF" (Rebl *et al.*, 2012, Brietzke *et al.*, 2015), interleukin 1 beta "IL1B" (Brietzke *et al.*, 2015), interleukin 6 "IL6" (Rebl *et al.*, 2012, Zante *et al.*, 2015), C-X-C motif chemokine ligand 8 "CXCL8" (Rebl *et al.*, 2014; Brietzke *et al.*, 2015) and the acute phase protein serum amyloid A "SAA" (Rebl *et al.*, 2009, 2011), have been chosen as "immune target genes" for the subsequent analysis of the innate immune response in maraena whitefish, since all these factors proved to be critical in early immune response of rainbow trout upon experimental infection. Subsequently, based on a functional analysis (see 2.7.3) using IPA software, another cytokine, namely interleukin 12 beta "IL12B", and the two mitogen-activated protein kinases 1 and 3 termed "MAPK1" and "MAPK3" have been identified as suitable candidates complementing the set of "immune target genes", since they are intensively networking with the previously selected cytokines as to be seen in figure 1.4.

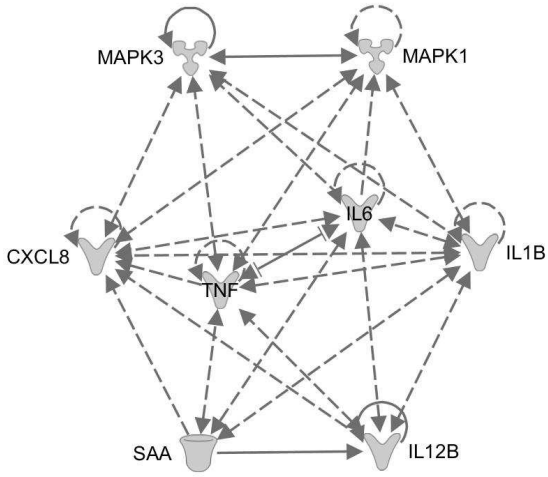

Figure 1.4: **IPA network of immune target genes** Based on IPA functional analysis, additional candidate genes were identified and the connectivity of the whole set of immune target genes was examined and subsequently displayed as a functional network. All symbols given in the network are in greyscale because the network is based solely on theoretical information from the IPA database and not on self-generated gene expression data. Full and broken lines indicate a direct or indirect interaction between two factors and the arrows represent the direction of interaction and activation.

[1]The description of the immune factors and mechanisms of innate immunity in section 1.2 are based on information adopted from IPA database, from the scientific textbook Janeway *et al.* (2001), and literature as cited.

1.2.1. The role of innate immunity in fish and major functions of the selected immune genes

The fish's immune system, in principle, is very similar to the mammalian one, since fish possess lymphoid tissues, humoral and cellular immune functions, and the immune cells are divided in a myeloid and lymphoid lineage (Tort *et al.*, 2003; Riera Romo *et al.*, 2016). Nevertheless, there are some decisive differences. For example, the bone marrow is completely missing, as well as lymphoid nodes, whilst the thymus is present in fish, and seems to be the site of T cell maturation, (Tort *et al.*, 2003; Uribe *et al.*, 2011; Riera Romo *et al.*, 2016). However, germinal centres — known as site of B cell maturation of higher vertebrates — are suggested to be partly represented by macrophage aggregates called melanomacrophage centres (MMCs) in teleost fish (Steinel & Bolnick, 2017). These MMCs are mainly found in the kidney, but also in the spleen and liver (Steinel & Bolnick, 2017; Uribe *et al.*, 2011). Moreover, like mammals, teleosts posses a multi-lineage myeloid system, hence macrophages as well as the three types of granulocytes, namely neutrophils, eosinophils and basophils, were identified in teleost fish (Ellis, 1977; Crippen *et al.*, 2001; Arnold, 2009). However, the abundance of the different granulocyte types is highly species-specific (Ellis, 1977). In salmonids, neutrophils are the predominant granulocytes, whilst basophils are absent, as in most teleost species (Secombes, 1996).

In contrast to higher vertebrates, the spleen has only limited immune functions in salmonids and is mainly responsible for blood filtration and storage, as well as for the destruction of aged blood cells, e.g., erythrocytes (Fänge & Nilsson, 1985; Uribe *et al.*, 2011; Press & Evensen, 1999). However, the major immune organ in teleosts, and particularly in salmonids, is the head kidney, the anterior part of the kidney (Fänge & Nilsson, 1985; Uribe *et al.*, 2011; Press & Evensen, 1999; Tort *et al.*, 2003). The head kidney assumes functions similar to the mammalian bone marrow and is therefore the main site of haematopoiesis (Press & Evensen, 1999; Tort *et al.*, 2003; Uribe *et al.*, 2011). But this organ is also responsible for phagocytic activities and antigen processing, whilst the multitude of its MMCs might be the site of IgM and immune memory formation, which indeed is still controversial (Tort *et al.*, 2003; Steinel & Bolnick, 2017; Kum & Sekkin, 2011; Parra *et al.*, 2015). Besides its lymphopoietic functions, the head kidney is also the main organ for the development and differentiation of myeloid cells, such as macrophages and granulocytes (Crowhurst *et al.*, 2002; Romano *et al.*, 2002). Additionally, the head kidney has functions homologous to the mammalian adrenal gland and mediates important endocrine functions, adopting the role of a key regulator of immune-endocrine and neuroimmune-endocrine interactions, which makes the head kidney unique in its functions for teleost fish (Tort *et al.*, 2003; Rebl & Goldammer, 2018; Geven & Klaren, 2017).

Altogether the different organisation of immune-related organs and particularly the low complexity of teleostean lymphoid tissues results in limited mechanisms of acquired immunity (Tort *et al.*, 2003; Uribe *et al.*, 2011; Riera Romo *et al.*, 2016). Though, the teleostean adaptive immunity is characterised by a slow antibody response and low number and affinity of immunoglobulins, relying mainly on natural poly-reactive IgM, compared to the fast and highly specific reactions in homoiothermic vertebrates (Tort *et al.*, 2003; Uribe *et al.*, 2011; Riera Romo *et al.*, 2016). However, the fish's innate immunity is much more complex compared to higher vertebrates, since it is based on a more extensive repertory in TLRs and a much higher diversity for specific complement factors, cytokines, and natural killer cells (Rebl & Goldammer, 2018; Magnadóttir, 2006; Zou & Secombes, 2016; Secombes *et al.*, 2011; Riera Romo *et al.*, 2016). In general, the evolutionary older innate immune system is characterised by unspecific mechanisms that respond fast to external stimuli and their functions are less temperature-sensitive, which is advantageous for the poikilothermic nature of fish (Tort *et al.*, 2003; Abram *et al.*, 2017; Magnadóttir,

2006). Thus, the average ambient temperature of the fish's habitats, as well as the structural composition of the immune organs could be causative for the predominance of the innate immune system in fish (Tort *et al.*, 2003; Uribe *et al.*, 2011; Riera Romo *et al.*, 2016).

The innate immune system mediates fast defence mechanisms as a first response to infection and tissue injury and it also triggers the subsequent activation of the adaptive immunity. The early immune response is mainly initiated by the extracellular binding of specific particles to germline-encoded receptors, called pattern recognition receptors (PRR), which are particularly expressed on phagocytic cells, but also on other immune and non-immune cells, e.g., epithelial and endothelial cells (Vallés *et al.*, 2014; Akira *et al.*, 2006; Magnadóttir, 2006). PRRs recognize both, pathogenic substances, collectively referred to as pathogen associated molecular patterns (PAMPs) but also substances released by the body's own damaged or stressed cells, commonly referred to as danger-associated molecular patterns (DAMPs) (Vallés *et al.*, 2014; Akira *et al.*, 2006). Among the different types of PRRs, the best studied is the family of toll-like receptors (TLRs) that can bind both PAMPs and DAMPs, which in turn activates immune cells, like macrophages, and thus triggers the inflammatory cascade (Vallés *et al.*, 2014; Akira *et al.*, 2006). The figure 1.5 gives an overview of the main functions of the selected immune target genes as mediators of the innate immune response based on the network given in figure 1.4.

As described above, in case of infection, trauma, or tissue injury of an organism, mainly macrophages are activated locally at the site of disorder and secrete pro-inflammatory cytokines, of which the main ones are included in the immune target gene set, namely IL1B, IL6, CXCL8, IL12B, and TNF. These cytokines immediately cause a local inflammation reaction, besides other pleiotropic regulatory functions in innate and also in acquired immunity. CXCL8 is one of the first factors secreted by macrophages in case of infection, and due to its chemotactic effect on neutrophils, CXCL8 leads to a fast and massive invasion of these polymorphonuclear cells into the affected tissue. Like macrophages, the neutrophils eliminate pathogens by phagocytosis. In a process called respiratory burst, the phagocytic cells release reactive oxygen species (H_2O_2, O_2^-, NO) from their granula into the phagolysosome, which are directly toxic to bacteria. Further, the cytokines IL1B, TNF, and IL6 mobilise neutrophils, induce the expression of complement factors, and above all are critical for the initiation of the acute phase response (APR), a systemic reaction of the innate immune system, which leads to the synthesis of acute phase proteins (APPs). Even in fish, APPs are predominantly synthesised in the liver, and then released to circulation (Bayne & Gerwick, 2001). Through extracellular binding to their respective membrane-bound receptors, namely TNF receptor (TNFR) for TNF, IL1 receptor-1 (IL1R1) for IL1B, IL6 receptor (IL6R) and glycoprotein 130 (gp130) for IL6, these cytokines trigger a change in hepatocyte metabolism, which in turn initiates the APP synthesis (Grover *et al.*, 2016; Gruys *et al.*, 2005). During APR, plasma concentrations of particular proteins are reversed and though the APPs are classified into positive and negative factors, depending on whether their concentration significantly increases (positive APP) or decreases (negative APP) (Grover *et al.*, 2016; Gruys *et al.*, 2005; Urieli-Shoval *et al.*, 2000; Steel & Whitehead, 1994). Whereas signaling cascades activated by TNF mainly cause the down-regulation of normal plasma proteins, IL1B, but mainly IL6 causes the synthesis of a wide variety of APPs. IL1B has rather a potentiating effect in APR, since it induces further synthesis of IL6, which in turn stimulates the synthesis of APPs. IL6 signaling is mediated by three signal transduction cascades, namely the phosphorylated signal transducer and activator of transcription 3 (STAT3P) pathway, the nuclear factor kappa-light-chain-enhancer of activated B cells (NFκB) pathway, and the mitogen-activated protein kinase (MAPK) pathway[2] that includes the two

[2]The MAPK pathway is also termed Ras-Raf-MEK-ERK pathway (rat sarcoma-rapidly accelerated fibrosarcoma-MAPK/ERK kinase-ERK pathway) according to the main signal transduction proteins included (Roskoski, 2012).

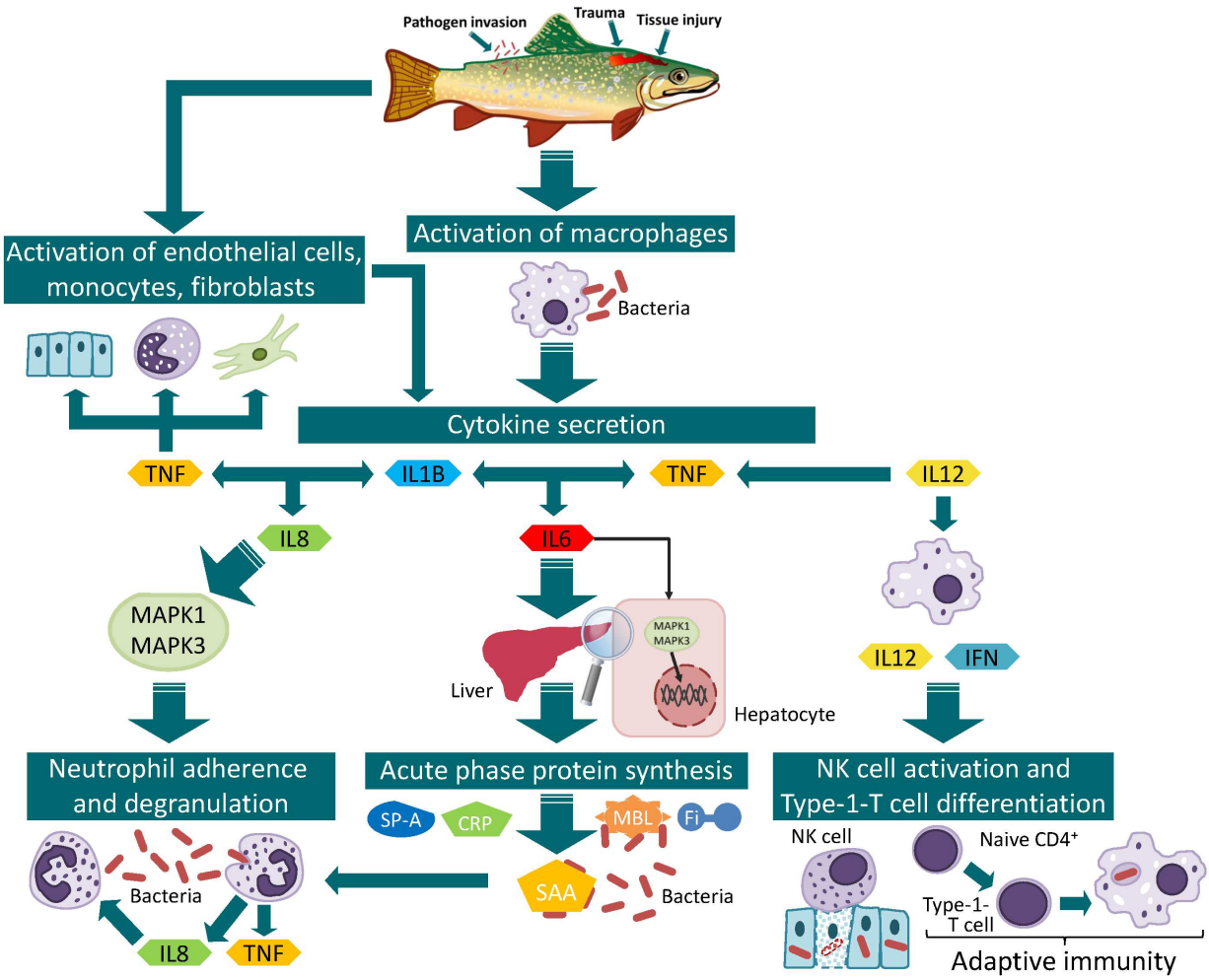

Figure 1.5: **The immune target genes and their major functions in innate immunity**
Schematic overview of the involvement of the selected immune genes in establishing an inflammatory response, a main function of the innate immune system.

immune target genes MAPK1 and 3. The activation, i.e., the phosphorylation of MAPK1 and 3, leads to their translocation from the cytoplasm to the nucleus, where the kinases, in turn, activate transcription factors (e.g., NF-IL6 (nuclear factor IL6) and Elk1(Ets-like transcription factor 1)) by phosphorylation (Roskoski, 2012). Eventually, all three pathways promote the synthesis of different APPs, like C-reactive protein (CRP), fibrinogen (Fi), mannan-binding lectin (MBL), surfactant protein A (SP-A), and serum amyloid A (SAA). The APPs fulfil a wide variety of functions in host defence, such as opsonisation of pathogens, which enhances the activity of phagocytic cells, repairing tissue damage, and restoring of homoeostasis (Bayne & Gerwick, 2001). SAA, which is also included in the set of immune target genes is a major APP, since its serum levels are up-regulated 100- to 1000-fold in response to inflammatory stimuli, at least in humans as reviewed by Gruys *et al.* (2005) and Grover *et al.* (2016). However in fish no, or a medium to strong up-regulation has been reported (Kania *et al.*, 2014; Villarroel *et al.*, 2008; Starliper, 2011). SAA, is a multifunctional protein, and although its operations during APR are not fully elucidated so far, it is known to be involved in the detoxification of endotoxins, in the inhibition of lymphocyte and endothelial cell proliferation, in the cholesterol metabolism and transport (redirects HDL from hepatocytes to macrophages), and it directly modulates the inflammatory response (Grover *et al.*, 2016; Gruys *et al.*, 2005; Urieli-Shoval *et al.*, 2000). Within the early immune response, at such high concentrations given during APR, SAA dissociates from HDL and acts as a chemoattractant of

polymorphonuclear cells and monocytes, enhancing extravasation of these cells to the inflammatory site (Badolato *et al.*, 2000, 1994). Moreover, even at low concentrations and in presence of HDL, Hari-Dass *et al.* (2005) and Shah *et al.* (2006) found SAA to be an opsonin of the innate immune system, binding to the outer membrane protein A (OmpA) of Gram-negative bacteria, which results in an increased phagocytic activity of neutrophils and macrophages and further stimulates the respiratory burst in neutrophils and the cytokine secretion (TNF and IL10) of macrophages (Shah *et al.*, 2006). Further, in their study He *et al.* (2003) showed that SAA also has cytokine-like functions, since it stimulates neutrophils to release pro-inflammatory cytokines, like CXCL8, TNF and IL1B, which in turn leads to the attraction of more neutrophils to the site of infection or injury. Moreover, He *et al.* (2006) reported that SAA exerts its cytokine-like effect on monocytes and macrophages and therefore promotes IL12B expression.

The cytokine IL12 is also released by macrophages during the early immune response. IL12 stimulates the secretion of TNF and another cytokine, namely interferon (IFN), by macrophages and moreover, by its autocrine effect, IL12 promotes its own synthesis. The main function of IL12, together with IFN, is the activation of natural killer cells (NK cells), which are large granular lymphocytes that can detect infected or damaged cells and trigger apoptosis to eliminate intracellular pathogens or to support tissue healing. Further in mammals, IL12 mediates the differentiation of naive $CD4^+$ T cells into T helper 1 (T_H1) cells, an immunomodulatory function of this cytokine that connects innate and adaptive immunity. In fish, there is mounting evidence for the existence of Type-1-T cells and similar functions of IL12 for the induction of T cell differentiation are suggested (Wang *et al.*, 2014b; Matsumoto *et al.*, 2016).

Within this study, the immune target genes were exclusively applied to examine the modulation of the early immune response after challenging of maraena whitefish with inactivated bacteria, namely *Aeromonas salmonicida* subsp. *salmonicida* (*A. salmonicida*). *A. salmonicida* is a pathogenic, Gram-negative, non-motile and rod-shaped bacterium, which is facultatively anaerobic (Hochleithner, 2001; Schachte, 2002; Austin & Austin, 2012). It is the oldest known fish pathogen and causes acute and chronic furunculosis, a disease characterised by blistered haemorrhages on fins, gills, skin and internal organs, as well as skin ulcerations (Austin & Austin, 2012; Hochleithner, 2001; Schachte, 2002). Outbreaks of furunculosis were observed in wild and cultured salmonids at any stage of life and mostly dependent from water quality and temperature, since above 15°C water temperature, severe losses can occur that cause great economic damage to aquaculture (Austin & Austin, 2012; Tam *et al.*, 2011). Regarding this crucial role for infections, especially for farmed salmonids, *A. salmonicida* has been chosen as an appropriate pathogen for this study. Further, via *in vitro* experiments, the immune-gene expression was analysed, following stimulation of head kidney primary cells, to study the merged immune and endocrine functions of this organ (see 1.3.1).The immune-gene set was additionally used to assess the impact of stocking density and temperature on mareana whitefish's innate immune response.

1.2.2. Major features of the selected immune genes

1.2.2.1. IL1B IL1B is a member of the interleukin 1 superfamily, consisting of cytokines that all bind to similar receptors, and thus share similar signal transduction pathways (Krumm *et al.*, 2014). The cytokines of the IL1 superfamily are important regulators of the innate and the adaptive immune response (Zou & Secombes, 2016). In fish, IL1B is the best-studied member of the IL1 superfamily and its functions have been proven to be conserved in vertebrates, as reviewed by Zou & Secombes (2016). Although they share very low sequence similarities, the three-dimensional structure of the proteins is highly conserved (Krumm *et al.*, 2014; Zou *et al.*, 1999; Secombes *et al.*, 1999; Zou & Secombes, 2016).

The expression of IL1B is induced by inflammatory stimuli and it acts as an agonist of the constitutively expressed IL1A (Krumm *et al.*, 2014). In contrast to IL1A, the cytosolic precursor form of IL1B is biologically inactive and must be cleaved at a specific aspartic acid residue. However in fish, this specific cleavage site is lacking and it is not yet fully understood if and how IL1B is processed in fish to become an active protein (Secombes *et al.*, 1999; Zou & Secombes, 2016). Further, IL1B has regulatory functions on other cytokines like IL6 and CXCL8, and it is induced by TNF and bacterial LPS.

1.2.2.2. IL6 IL6 belongs to the family of interleukin-6-type cytokines that commonly share the membrane-bound glycoprotein 130 (gp130) as receptor and signal transducer subunit (Scheller *et al.*, 2011; Rose-John, 2018; Iliev *et al.*, 2007). Although the sequence of the *IL6* gene is phylogenetically poorly conserved from mammals to fish, the conserved synteny of the IL6 locus allowed the identification of this gene, as reported for different fish species by Varela *et al.* (2012) and Iliev *et al.* (2007). IL6 initially binds to the IL6 receptor (IL6R) and then the complex associates with gp130, which in turn triggers signal transduction Scheller *et al.* (2011). Whereas gp130 is constitutively expressed, IL6R expression is mainly restricted to hepatocytes and several leukocyte subtypes but a second soluble form of IL6R, which was recently discovered in fish as well, allows a wide variety of cells to interact with IL6, which is decisive for its pro-inflammatory functions (Scheller *et al.*, 2011; Zou & Secombes, 2016). IL6 is primarily produced at sites of acute and chronic inflammation by macrophages and endothelial cells, but also by T cells and its synthesis is mainly induced by pathogenic stimuli like LPS and Poly I:C RNA, and additionally by cytokines such as TNF and IL1B (Tanaka *et al.*, 2014; Secombes *et al.*, 2011). Besides the various pro-inflammatory functions, e.g., the induction of fever, the synthesis of acute phase proteins and the differentiation of T and B cells, IL6 also acts as an anti-inflammatory reactant as reviewed by Scheller *et al.* (2011) and Tanaka *et al.* (2014).

1.2.2.3. CXCL8 The cytokine CXCL8, also referred to as interleukin 8, belongs to the subfamily of CXC chemokines. All molecules accounted to the chemokine family have key functions for the activation and mobilisation of specific leukocytes to the site of inflammation. In most fish species the CXCL8 orthologs lack the typical ELR motif, which, e.g., in trout, is replaced by an aspartic acid-leucine-arginine (DLR) sequence (Laing *et al.*, 2002; Rebl *et al.*, 2014). Despite the presence of the DLR instead of the ELR motif, which is decisive for the chemoattractive effects of CXCL8 on neutrophils in mammals, piscine CXCL8 exerts the same functions and is suggested to be an evolutionary older form of the mammalian CXC cytokines (Harun *et al.*, 2008; Cai *et al.*, 2009). While in humans only one CXCL8 gene is known that produces several isoforms, in fish there is emerging evidence for the presence of two lineages of CXCL8 chemokines. The first lineage is specific for teleosts and the second corresponds more to the mammalian CXCL8 gene, albeit both lineages represent functional homologues of their mammalian counterpart (van der Aa *et al.*, 2010; Abdelkhalek *et al.*, 2009). A common feature of all CXCL8 chemokines is the signal transduction through binding to their specific receptors, namely interleukin-8 receptor A (IL8RA) and interleukin-8 receptor B (IL8RB). At least as reported for humans, CXCL8 needs to form a dimer for successful receptor binding (Skelton *et al.*, 1999; Liu *et al.*, 2016a). Further, CXCL8 expression is mainly stimulated by the cytokines IL1B and TNF, as well as by the pathogenic reagents LPS and Poly I:C, as was found in mammals and fish (Bird & Tafalla, 2015). In response to inflammatory stimuli, the chemokine is produced by macrophages, monocytes, fibroblasts and endothelial cells.

1.2.2.4. IL12B IL12 is a heterodimeric cytokine encoded by the genes *IL12A* and *IL12B* that are structurally related to the IL6 family (Trinchieri, 2003; Zou & Secombes, 2016). In fish, IL12 is the only member of its family, which has been subjected to functional studies so far (Zou & Secombes, 2016). Further, in salmonids three IL12A and IL12B paralogues have been identified, which are differentially expressed and modulated due to pathogenic stimuli (Zou & Secombes, 2016; Wang & Husain, 2014; Wang *et al.*, 2014b). Whereas in mammals, expression of IL12A is constitutive and of IL12B induced (e.g., in activated macrophages), the situation in fish is much more complex, since the different IL12A and IL12B isoforms associate according to the given pathogenic stimuli to trigger a suitable immune response (Wang & Husain, 2014; Wang *et al.*, 2014b). IL12 exerts its pro-inflammatory and pro-stimulatory effects through binding to the heterodimeric IL12 receptor (IL12R), whose expression is rapidly up-regulated after activation of NK cells and T cells (Trinchieri, 2003; Wang & Husain, 2014). Further, IL12 acts as an regulator of TNF and is itself regulated by LPS and Poly I:C RNA (Wang & Husain, 2014).

1.2.2.5. TNF TNF is a multifunctional cytokine that belongs to the tumor necrosis factor (TNF) superfamily, which is characterised by distinctive cytoplasmic death domains (Vinay & Kwon, 2011). The binding of TNF, either to the membrane bound TNF receptor 1 (TNFR1) or TNF receptor 2 (TNFR2), triggers many biological functions of this molecule. TNF associates with its receptors in form of a homotrimeric protein and it leads to local inflammation and endothelial activation. Functional homologues of TNF have been identified in various fish species and even in invertebrates (Zou & Secombes, 2016). Evidence is mounting concerning the presence of multiple TNF homologues in teleosts, suggesting the existence of three phylogenetic TNF groups, namely type I TNFα, TNFN and type II TNFα that additionally produce multiple isoforms, e.g., in salmonid and cyprinid species, as reviewed by Zou & Secombes (2016). Whereas type I TNFα and TNFN reveal a conserved synteny to their human counterparts, type II TNFα seems to be teleost-specific (Savan *et al.*, 2005; Hong *et al.*, 2013). TNF is mainly produced by macrophages, but also NK-cells and T-cells and it regulates CXCL8 and IL6, while itself is regulated by pathogenic LPS and Poly I:C RNA.

1.2.2.6. SAA SAA belongs to a family of small 12 kDa apolipoproteins that associate with high-density lipoprotein (HDL) in the circulation (Gruys *et al.*, 2005; Steel & Whitehead, 1994; Grover *et al.*, 2016; Kania *et al.*, 2014). As reviewed by Uhlar & Whitehead (1999), SAA proved to be highly conserved among species and has been identified in various vertebrates, including mammals (Steel & Whitehead, 1994; Cray *et al.*, 2009), birds (Ericsson *et al.*, 1987), fish (Bayne & Gerwick, 2001; Heinecke *et al.*, 2014; Jørgensen *et al.*, 2000; Kania *et al.*, 2014; Rebl *et al.*, 2009; Uhlar & Whitehead, 1999; Wei *et al.*, 2013), as well as invertebrates (Santiago *et al.*, 2000; Qu *et al.*, 2014). Two different forms of SAA have been identified so far: (i) the acute phase SAA (A-SAA), which is a major acute phase protein, and (ii) the constitutively expressed SAA (C-SAA) that was found in humans and mice only (Uhlar & Whitehead, 1999; Gruys *et al.*, 2005; Grover *et al.*, 2016). In fish, only one SAA gene, encoding an A-SAA, has been identified to date, however, in mammals a multi-gene family evolved, e.g., in mice five and in humans four SAA isoforms are known (Uhlar & Whitehead, 1999; Rebl *et al.*, 2009; Fujiki *et al.*, 2000; Wei *et al.*, 2013; Kania *et al.*, 2014; De Buck *et al.*, 2016). Two of the human and three of the murine SAA genes encode A-SAA variants, whereas two additional genes code for a C-SAA and a pseudo-gene, respectively (Uhlar & Whitehead, 1999). Hence, the inducible A-SAA form, which is the only present in lower vertebrates, seems to be evolutionary more conserved than the C-SAA form (Rebl *et al.*, 2009).

1.2.2.7. MAPK1 and MAPK3 MAPK1 (also called ERK2) and MAPK3 (also called ERK1) are related protein-serine/threonine kinases, that are ubiquitously expressed and highly conserved in sequence and function between vertebrates (Buscà *et al.*, 2015). Moreover, in their study on the evolution of MAPK1 and 3, Buscà *et al.* (2015) identified only one ancient precursor of the *MAPK1* gene in cartilaginous fish, whereas due to a single gene duplication, teleost fish and tetrapodes possess a *MAPK1* and a *MAPK3* gene. Both kinases are proline-directed, i.e., both preferentially catalyse the phosphorylation of substrates containing a Pro-Xxx-Ser/Thr-Pro sequence (Roskoski, 2012). Prior to their enzymatic activity, the kinases themselves have to be activated by the phosphorylation of tyrosine and threonine residues mediated by MAPK/Erk kinase 1/2 (MEK1/2). Thus, MAPK1/3 participate in signal transduction cascades from the cell surface to the interior by phosphorylating a wide variety of regulatory molecules or transcription factors, in the cytoplasm or following translocation, even in the nucleus (Roskoski, 2012). For regulatory purposes, MAPK1/3 can be de-phosphorylated again, mediated by different phosphatases. The nuclear transcription factors that are activated by MAPK1/3 participate in the immediate early gene response (Roskoski, 2012).

1.3. Stress target genes

Particularly farmed fish have to cope with various stressors that, according to Barton (2002), Moreira & Volpato (2004), and Nardocci *et al.* (2014), can mainly be classified into three groups: (i) physical stressors (e.g., temperature, handling, confinement, noise, vibration, pain), (ii) social stressors (e.g., space availability, dominance-subordinance behaviour), and (iii) chemical stressors (e.g., concerning water quality in terms of contaminants, pollutants, oxygen deficit, acidification). Stress itself is not necessarily harmful but becomes a negative stressor if it compromises the fish's homoeostasis and consequently induces a stress response, as defined in literature (Moreira & Volpato, 2004; Barton, 2002).

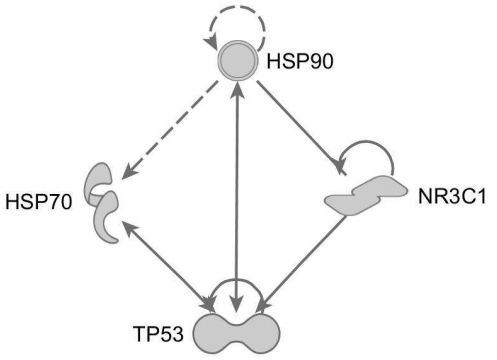

Figure 1.6: **IPA network of stress target genes**
Based on IPA functional analysis, suitable stress-related candidate genes were identified and their connectivity was displayed as a functional network. All symbols given in the network are in grey-scale because the network is based solely on theoretical information from the IPA database and not on self-generated gene expression data. Full and broken lines indicate a direct or indirect interaction between two factors and the arrows represent the direction of interaction and activation.

As previously described for the immune-gene set, also stress-relevant candidate genes were determined in previous studies on rainbow trout within the Fish Genetics Unit (FBN Dummerstorf). Thus, in rainbow trout, several members of the HSP90 and the HSP70 family were found to be up-regulated due to elevated temperature and moreover TP53 and glucocorticoid receptor pathways were predicted to be affected within the heat-stress response (Verleih *et al.*, 2015; Rebl *et al.*, 2013). Subsequently, based on literature research and an IPA functional analysis, the suitability and connectivity of several potent candidate genes has been confirmed. Consequently, the genes *HSP70*, *HSP90*, *TP53* and *NR3C1* have been selected as "stress target genes" for the initial investigation of the stress response in maraena whitefish, since those four genes are reported to be involved in the response to various stressors, not only temperature (Roberts *et al.*, 2010). The interaction of the selected stress genes is represented by the

IPA based network given in figure 1.6.

1.3.1. The stress response in fish and major functions of the selected stress genes

In general, as reviewed by Barton (2002) and Nardocci *et al.* (2014), the fish's response to environmental stressors can be subdivided into three categories, depending on the magnitude and duration of a stressor and the respective mechanisms that were activated to regain homoeostasis of the organism. The primary stress response is characterised by the initial activation of neuroendocrine signaling, leading to the release of catecholamines and glucocorticoids (Barton, 2002; Nardocci *et al.*, 2014). In case of a prolonged stressor (still short-term, or acute), the secondary response is initiated and due to an increased energy demand, cortisol-driven changes occur in metabolism that affect ion and metabolite levels, and moreover catecholamines trigger the immune response, which leads to enhanced innate immunity (Barton, 2002; Nardocci *et al.*, 2014). Moreover, the secondary response includes the activation of heat-shock proteins (Barton, 2002). If the fish is exposed to a chronic stress stimuli, the stress response culminates in the tertiary response that affects the whole body and has various suppressive effects on growth (leading to a lower protein content), immunocompetence (hampered resistance to diseases), reproductive capacity, as well as alterations in behaviour and feed intake (Pottinger *et al.*, 1994; Barton, 2002; Nardocci *et al.*, 2014; Rebl & Goldammer, 2018). In fish, similarly to mammals, the hypothalamus is the central mediator that coordinates two different signaling cascades in response to stress, as shown in figure 1.7. The first, the hypothalamic-sympathetic-chromaffin axis, provides a very fast, transient (within seconds) response to an acute stress stimuli, since the signal is directly transduced from the central nervous system (CNS) via sympathetic nerve fibres to the chromaffin cells (homologous to the mammalian adrenal medulla) in the head kidney, which then release catecholamines (Barton, 2002; Nardocci *et al.*, 2014). However, the second, the hypothalamic-pituitary-interrenal axis (HPI axis), a homologue to the mammalian hypothalamic-pituitary-adrenal axis (HPA axis), is activated not before several minutes, hours, or even days, but leads, in comparison to the first, to a prolonged response to acute and chronic stress (Barton, 2002; Nardocci *et al.*, 2014). The volatility of the sympathetic-based stress response, in contrast to the comparably well accessibility to effector molecules of the HPI-based stress response, made the latter of tremendous importance for stress studies in fish

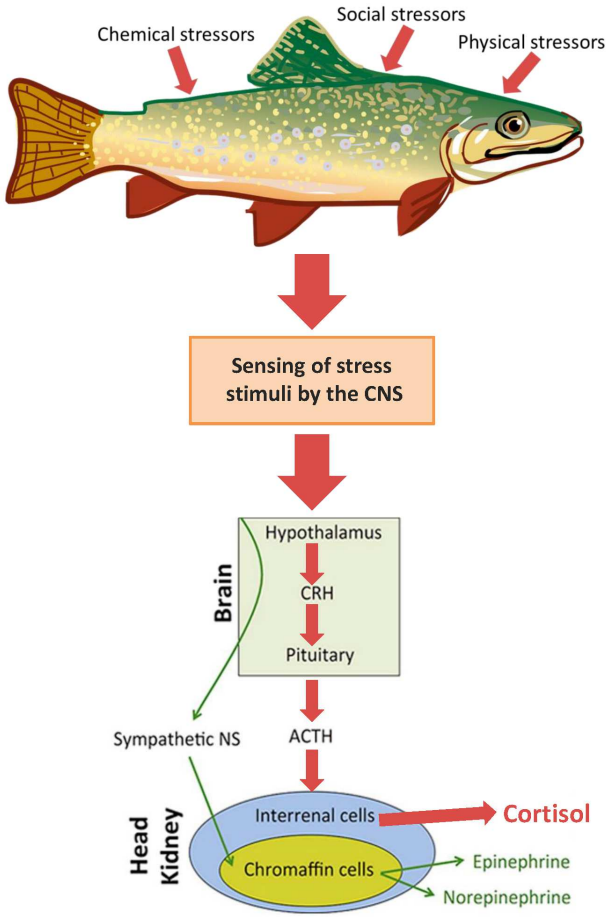

Figure 1.7: **The neuroendocrine stress response in fish**
Schematic representation of the two signaling cascades, namely the hypothalamic-sympathetic-chromaffin axis and the hypothalamic-pituitary-interrenal axis, that were activated in fish in response to stressors. Figure modified from Nardocci *et al.* (2014).

and thus components of the HPI-axis were focused within this work, as well. During HPI-axis signaling, the hypothalamus secretes corticotropin-releasing hormone (CRH) to stimulate the anterior pituitary to release adrenocorticotropic hormone (ACTH). This in turn, stimulates the interrenal cells of the head kidney, which are homologous to the adrenal gland in mammals, to release cortisol, the principle glucocorticoid in fish (Weyts *et al.*, 1999; Barton, 2002; Stolte *et al.*, 2006; Nardocci *et al.*, 2014; Rebl & Goldammer, 2018). Cortisol is then released into circulation and due to its lipophilicity and small size, it passively diffuses, or is passively transported via plasma proteins through cell membranes within target tissues (Mommsen *et al.*, 1999; Inaba & Pui, 2010). Subsequently, cortisol elicits its diverse effects via binding the inactive glucocorticoid receptor (GCR) hetero-complex, residing in the cytosol, as represented in figure 1.8. As known mainly from studies in mammals, the GCR hetero-complex consists of various chaperones, like HSP70 and HSP90, and cochaperones, of which, at least HSP70 and HSP90 are very likely to be involved in piscine GCR-complex formation, respectively (Kirschke *et al.*, 2014; Stolte *et al.*, 2006; Mommsen *et al.*, 1999). HSP70, is thought to be responsible for the early steps of GCR folding, for the initial delivery of the GCR to HSP90, for keeping the GCR biologically inert by unfolding its ligand binding domain, and for ligand removal (Kirschke *et al.*, 2014). In addition to HSP70, a HSP90 homo-dimer is bound to the C-terminal ligand binding domain of the GCR, which is indispensable for folding, stability, and ligand binding, since HSP90 reverses the HSP70-mediated GCR inactivation, and

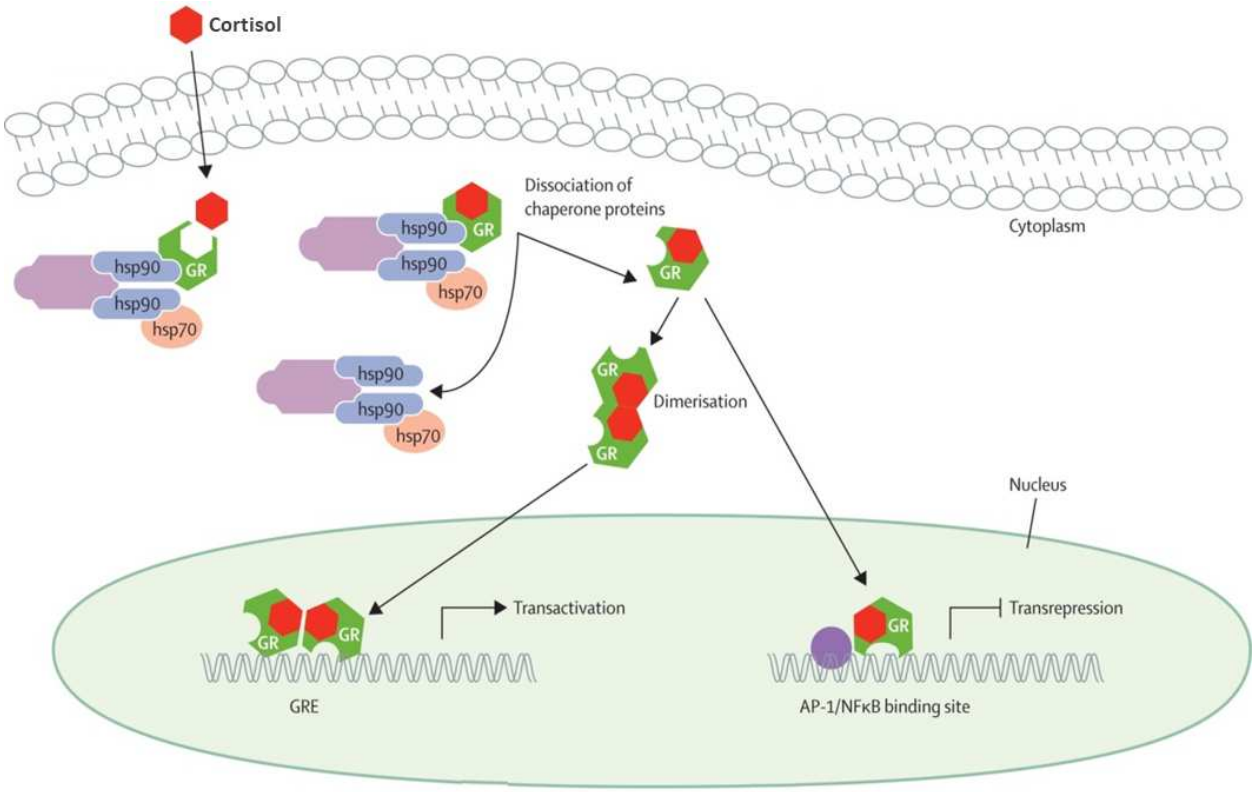

Figure 1.8: **The glucocorticoid receptor signaling cascade**
Representation of the cortisol dependent signaling of the glucocorticoid receptor (for reasons of space abbreviated as GR, instead of GCR as found within the text). Figure modified from Inaba & Pui (2010).

therefore is essential for receptor activation (Mommsen *et al.*, 1999; Inaba & Pui, 2010; Kirschke *et al.*, 2014). Though, in presence of its ligand, cortisol, the GCR hetero-complex is activated and undergoes a significant conformational transformation, which leads to the dissociation of the previously bound proteins. Subsequently, the GCR-cortisol complex translocates into the nucleus in form of homo-dimers

or monomers. Within the nucleus, the DNA-binding domain of the homo-dimeric GCR-cortisol complex serves to interact with glucocorticoid-responsive elements (GRE) and to induce transcription of target genes, whilst the monomer interacts with transcription factors such as activating protein-1 (AP-1) or NFκB to inhibit their stimulatory effects on gene transcription, particularly of immune related genes (Mommsen *et al.*, 1999; Inaba & Pui, 2010; Kirschke *et al.*, 2014; Petta *et al.*, 2016; Rebl & Goldammer, 2018). The trans-activating capacity of the GCR-cortisol complex mainly influences metabolic functions, e.g., it causes an enhanced gluconeogenesis in fish hepatocytes, similarly to mammals, and additionally it promotes proteolytic (white muscle) and lipolytic (adipose tissue, red muscle) actions to meet the augmented energy demand during stressful situations (Mommsen *et al.*, 1999; Wiseman *et al.*, 2007; Rebl & Goldammer, 2018). As noted in section 1.2.1, in teleost fish, immune and endocrine functions are combined within the head kidney and this local proximity allows and supports a close interaction of both systems (Weyts *et al.*, 1999; Nardocci *et al.*, 2014; Rebl & Goldammer, 2018). Therefore, the cortisol-dependent stress response in fish has many immune regulatory functions, which are, in an overwhelming majority, immunosuppressive (Stolte *et al.*, 2006; Castro *et al.*, 2011; Nardocci *et al.*, 2014; Rebl & Goldammer, 2018). These effects are, e.g., a decrease in phagocytic activity of macrophages and head kidney cells, a strong inhibition of respiratory burst activity and chemotaxis, an induction of apoptosis in macrophages, a decrease in expression of pro-inflammatory cytokines, HSPs, acute phase proteins, and GCR, and a reduction in circulating lymphocytes (Nardocci *et al.*, 2014; Rebl & Goldammer, 2018). Within these various regulatory actions of the GCR, the transcription factor TP53 is thought to play an important role. At least in mammals, it is suggested that TP53 is important for the trans-repressive functions of the GCR, since it supports its interaction with NFκB and thus prevents the latter from DNA binding (Petta *et al.*, 2016). Moreover, there is also evidence for a TP53-dependent targeting of the GCR to the promoter regions of its target genes within trans-activation, as reviewed by Petta *et al.* (2016). Moreover, though only in mammals, it was shown that HSP90 and HSP70 act as chaperones for TP53 upon heat shock, but HSP90 is also important for stability and DNA binding ability of TP53 at physiological temperatures (Wang & Chen, 2003; Müller *et al.*, 2004; Walerych *et al.*, 2009). Further, a role for HSP70 for the nucleic dissociation of the TP53 tetramer during recovery from heat stress is suggested (Zylicz *et al.*, 2001).

In the present study, a major focus has been placed on the head kidney, due to its central importance in the combined processing of stress and immune-related stimuli, as described in detail in this paragraph and in 1.2.1. Therefore, the influence of neuroendocrine and immune-related stimuli on maraena whitefish's head kidney has been assessed by an *in vitro* stimulation experiment of head kidney primary cells, using the sets of immune and stress genes. Further, similarly to the set of immune genes, the modulation of the stress gene set has been examined due to stocking-density and thermal stress.

1.3.2. Major features of the selected stress genes

1.3.2.1. HSP70 and HSP90 The two genes *HSP70* and *HSP90* encode heat shock proteins, which are commonly referred to as "chaperones". According to their molecular mass of approximately 70 kDa and 90 kDa, HSP70 and HSP90 are classified into two major subgroups within the family of heat shock proteins (HSPs). The HSPs are unique regarding their extraordinary high conservation in amino acid sequence and function, as was found for a multitude of organisms for all three kingdoms of life (Iwama *et al.*, 1998; Roberts *et al.*, 2010; Lindquist & Craig, 1988; Basu *et al.*, 2002). Since these proteins were first identified in response to temperature shock, they were referred to as "heat shock proteins", but

nowadays it is well known that HSPs are also induced by a wide variety of abiotic and biotic stressors, such as cold, anoxia, hypoxia, toxins, protein degradation, acidosis, nutritional deficiency, and microbial invasion (Iwama *et al.*, 1998; Bukau & Horwich, 1998; Roberts *et al.*, 2010; Basu *et al.*, 2002; Lindquist & Craig, 1988). Therefore, HSPs are considered to be fundamental components of the cellular stress response. In response to stressors, HSP90 and HSP70 recognize and non-covalently bind non-native states of various proteins and therefore protect them from irreversible aggregation and assist in the refolding, to restore or maintain their functional conformation (Iwama *et al.*, 1998; Bukau & Horwich, 1998; Roberts *et al.*, 2010; Basu *et al.*, 2002). Moreover, even at normal, unstressed conditions, HSPs are constitutively expressed, mainly in the cytosol of nearly all cells, since they have key functions in cellular protein and lipid metabolism and are also involved in signal transduction (Iwama *et al.*, 1998; Bukau & Horwich, 1998; Roberts *et al.*, 2010; Basu *et al.*, 2002; Horváth *et al.*, 2008).

In fish, HSPs have mainly been studied on protein level, but data about the *HSP70* and *HSP90* genes are still few, thus little is known about the gene distribution within the piscine HSP70 and HSP90 subfamilies, as well as about the existence of gene variants and isoforms, compared to vast amounts of data provided for mammals, bacteria and yeast. For comparison, the human HSP70 family is extraordinarily diverse, containing overall six typical, cytosolic *HSP70* genes, each encoding several transcript variants and isoforms (Brocchieri *et al.*, 2008). Thus, over the last two decades, data about the existence of several piscine *HSP70* genes were piling up and it seems that at least two distinct lineages of heat inducible *HSP70* genes have evolved in fish (Yamashita *et al.*, 2010; Ojima *et al.*, 2005a; Eid *et al.*, 2016). The first piscine HSP70 lineage is very likely to contain homologues of human *HSP70-1* and *HSP70B'* genes, while the second has rather emerged by gene duplication of the first lineage and is therefore fish-specific (Yamashita *et al.*, 2010).

At least one homologue, for each of the two closely related, cytosolic genes *HSP90A* and *HSP90B*, known from mammals, could be identified in various teleost species (Basu *et al.*, 2002; Garcia de la serrana & Johnston, 2013; Ojima *et al.*, 2005b). Further, phylogenetic analyses performed by Garcia de la serrana & Johnston (2013) unveiled the presence of four paralogues for the inducible *HSP90A* and two paralogues for the constitutive *HSP90B* gene in Atlantic salmon and rainbow trout.

1.3.2.2. NR3C1 The gene *NR3C1* codes for a nuclear transcription factor, termed glucocorticoid receptor (GCR), according to the ligands it depends on, namely the glucocorticoids (GC). The GCR system is highly conserved among all vertebrates studied so far, regarding function and sequence identity, the latter particularly within the DNA-binding and ligand-binding region (Stolte *et al.*, 2006). The GCR is mainly expressed in the cytosol and, activated by ligand binding, it translocates into the nucleus, where it binds to glucocorticoid responsive elements to specifically regulate gene transcription (Nardocci *et al.*, 2014; Rebl & Goldammer, 2018). The GCR ligands, the GCs, form a major subclass within the group of the steroid hormones and are all, similarly in mammals and fish, synthesised from their precursor cholesterol (Tokarz *et al.*, 2015; Mommsen *et al.*, 1999). In fish, according to current knowledge, cortisol is the only ligand of the GCR, which therefore mediates the cortisol-dependent regulation of carbohydrate, lipid, and protein metabolism, osmoregulation, stress and immune responses, as well as growth and reproduction (Tokarz *et al.*, 2015; Ducouret *et al.*, 1995; Mommsen *et al.*, 1999; Cruz *et al.*, 2013). In contrast to other vertebrates, teleost fish provide duplicated GCR genes, as reported for rainbow trout, Nile tilapia and common carp (Bury *et al.*, 2003; Stolte *et al.*, 2006; Tokarz *et al.*, 2015). Further, one of the duplicated GCRs is alternatively spliced, which results in a nine-amino-acid insert in the DNA binding region and seems to be specific for teleost fish (Stolte *et al.*, 2006). The different teleost GCR

isotypes studied so far, are biologically functional and tend to have a species specific expression pattern and cortisol sensibility (Stolte *et al.*, 2006).

1.3.2.3. TP53 The gene, tumor protein p53, codes for a transcription factor, which is, besides TP63 and TP73, one of three members of the p53 family that is characterised by a tetrameric organisation (Joerger *et al.*, 2014). In evolutionary terms, bony fish are the first vertebrates, containing all three genes of the p53 family, whereas cartilaginous fish possess two and invertebrates only one related ancestor gene *(Belyi* et al.*, 2010)*. The TP53 gene, compared to its two sister genes, TP63 and TP73, is small and reveals the highest variation in its DNA binding site among different vertebrates species *(Belyi* et al.*, 2010)*. Nonetheless, TP53 is structurally and functionally highly conserved from fish to human *(Belyi* et al.*, 2010; Storer & Zon, 2010)*. The evolutionary oldest function of the TP53 gene, is the surveillance of DNA integrity in somatic stem cells, regarding the protection from environmental damage and stress *(Belyi* et al.*, 2010)*. In fish, as in mammals, TP53 is a master regulator and modulates, in response to stressors, the expression of genes involved in apoptosis and cell cycle regulation, and though additionally acts as a tumor suppressor protein *(Belyi* et al.*, 2010; Storer & Zon, 2010; Mandriani* et al.*, 2016)*. Hence, TP53 is induced by a plethora of physiological stresses that are mainly involved in DNA damaging events *(Belyi* et al.*, 2010; Storer & Zon, 2010)*. Upon activation, TP53 is post-translationally modified, translocates to the nucleus and forms the functional active tetramer, capable of binding p53 responsive elements in the promoter region of target genes (Zylicz *et al.*, 2001). Taken together, compared to an overwhelming number of literature concerning cancer research for the mammalian TP53, there is little information about sequences and functions of piscine TP53, mostly relying on studies in zebrafish (Storer & Zon, 2010; Liu *et al.*, 2011).

1.4. Growth factors

Based on literature research, the insulin-like growth factors IGF-1 and IGF-2 were found to be interesting candidates in the search for biomarkers, since both play important roles in growth, development and metabolism in vertebrates (Daughaday & Rotwein, 1989; de Pablo *et al.*, 1990; Duan, 1998; Forbes, 2016). Hence, IGFs in general, and particularly IGF-1, are broadly discussed in literature for its potential as biomarker for growth in fish (Brown *et al.*, 2012; Picha *et al.*, 2008; Gonzaga *et al.*, 2010), whilst IGF-1 is already used as biomarker in human diagnostics (Bielohuby *et al.*, 2014; Nedić *et al.*, 2007; Lodhia *et al.*, 2015; Peters *et al.*, 2003; Clemmons, 2007). Both insulin-like growth factors are single-chain polypeptide hormones with structural homology to pro-insulin, and are highly conserved between species (Rinderknecht & Humbel, 1978b,a; Shimatsu & Rotwein, 1987). As shown in figure 1.9, the IGFs are integrated into the growth hormone-insulin like growth factor axis (GH-IGF axis) and mediate their mitogenic effects on cells of target tissues via this pathway. Joining exogenous (photoperiod, temperature) and endogenous (nutritional status, humoral factors) stimuli, the GH-IGF axis is initially regulated by two somatotrophic hormones of the hypothalamus (Picha *et al.*, 2008; Moriyama *et al.*, 2000; McCormick *et al.*, 2000). Whilst somatostatin acts as an inhibitor of GH, the growth hormone releasing hormone (GHRH) stimulates the release of growth hormone (GH) from somatotrophs in the anterior pituitary. GH directly acts on different target tissues through binding to the membrane-bound growth hormone receptor (GHR), or circulates bound to growth hormone binding protein (GHBP) in the plasma, but mainly it binds to GHR in the liver and thus stimulates the hepatic synthesis of insulin like growth factors (IGFs), insulin like binding proteins (IGFBPs), and acid labile subunit (ALS) (Argente

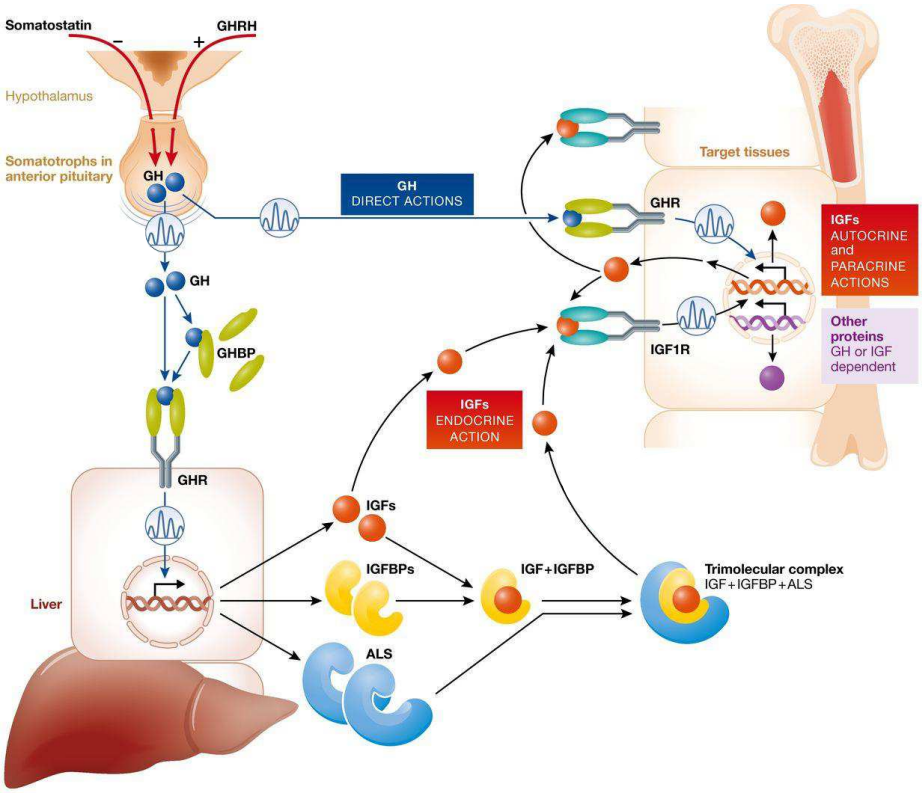

Figure 1.9: **The growth hormone-insulin like growth factor axis**
The abbreviations are the following: GHRH (growth hormone releasing hormone); GH (growth hormone); GHBP (growth hormone binding protein); GHR (growth hormone receptor); IGFs (insulin like growth factors); IGFBPs (IGF binding proteins); ALS (acid labile subunit); IGF1R (IGF-1 receptor). The figure was modified from Argente *et al.* (2017).

et al., 2017; Puche & Castilla-Cortázar, 2012). The synthesised IGFs are transported from the liver via the bloodstream to the target tissues, where they bind to membrane-bound IGF-1 receptor (IGF1R) to mediate their growth promoting actions. The activated IGF1R, in turn, can cause the synthesis of IGFs, which then mediate their actions in an autocrine and paracrine manner on cells of target tissues. Mainly, circulating IGFs are bound to acid labile subunit (ALS) and to high-affinity IGF binding proteins (IGFBPs), which in this way regulate the concentration of freely available IGFs, to ensure normal growth and development (Duan, 1997; Argente *et al.*, 2017). From a total of six IGF binding proteins known in mammals, the four proteins IGFBP-1, IGFBP-2, IGFBP-3 and IGFBP-5 are identified in fish so far (Reinecke *et al.*, 2005; Duan, 1997; Hwa *et al.*, 1999; Kelley *et al.*, 1996; Reinecke & Collet, 1998).

As mediators of growth hormone, IGFs influence reproduction, osmoregulation, and the immune system (Duan, 1997; Roith *et al.*, 2001; Wenger *et al.*, 2014; Reinecke, 2010; Mancera & McCormick, 1998; Franz *et al.*, 2016), but primarily IGFs are relevant for pre- and postnatal growth, as shown for human, mice and several fish species (Reinecke *et al.*, 2005; Baker *et al.*, 1993; Duan, 1998). Because of this key function in growth and development, IGFs have been selected as "growth target genes" within this study, since they might be useful candidate genes, which could possibly display or even more importantly predict fish growth rates (Picha *et al.*, 2008; Vera Cruz *et al.*, 2006). As to that, IGFs could be helpful parameters to evaluate optimal rearing conditions including the continuous observance of aquaculture related stressors affecting fish growth, as already discussed in literature (Picha *et al.*, 2008; Vera Cruz *et al.*, 2006; Brown *et al.*, 2012; Dyer *et al.*, 2004). Therefore, in the course of this study, IGF-1 and IGF-2 were analysed during pre- and post-hatching development and in marketable juvenile maraena whitefish.

Moreover, the effect of different incubation temperatures on *IGF1* and *IGF2* transcript levels, during embryonic development and early life stages post-hatching of maraena whitefish larvae were analysed, since not only a fast fish growth is crucial for a highly productive aquaculture, but also initial steps of egg incubation, hatching, and the onset of feeding are elementary.

1.5. Aim of the study

The present work was contributed the pilot project "Ostseeschnäpel" (VI-560/730-32614) that was kindly funded by the European Fisheries Fund (EFF) and the Ministry of Agriculture, Environment, and Consumer Protection Mecklenburg-Western Pomerania. The overarching objective of the project was to assess the fish's suitability for local aquaculture, founded on the following central hypothesis:

- Maraena whitefish, as a native species, provides a good capability of adaptation to local brackish water conditions, although due to the lack of breeding selection, under aquaculture conditions, a high stress susceptibility of this sensitive fish species is to be expected

In the context of these investigations, the present study aimed at the collection and evaluation of selected morphological and molecular biological data to initially characterise maraena whitefish within this anthropogenic environment and to identify or confirm candidate genes, as well as to derive guidelines for suitable cultivation conditions of this species. As to that, within this study, the following three main priorities have been focused concerning maraena whitefish:

1. Innate immune response
2. Stress response
3. Growth and development

Based on these three main topics the candidate genes were selected and the aims of the present study were defined as follows:

- Recording and evaluation of parameters characterising the growth performance in different aquaculture facilities
- Isolation and structural and functional characterisation of the selected candidate genes, comprising an immune-gene, stress-gene and growth-factor-gene set
- Targeted analysis of alterations in physiological parameters and in the tissue-specific expression of immune- and stress-related candidate genes in response to the following typical aquaculture-related stressors:
  - Stocking density
  - Rearing temperature
  - Exposure to pathogenic agents
- Development of a head kidney primary cell culture for detailed analyses of the joined neuroendocrine- and immune-driven expression of the stress- and immune-gene sets
- Analysis of growth-factor gene expression during early ontogenetic development and depending on incubation temperature

Within the artificial environment, this already sensitive fish species, is exposed to a plethora of potential stressors, which might compromise growth performance, health status, and the general body constitution. Therefore, the analysis of gene-based responses of maraena whitefish to different stressors are of high importance, as these are first indicators supporting the identification of molecular markers. Hence, the long-term objective of this work is the establishment of molecular markers supporting the development of a highly productive and robust whitefish population for local aquaculture, which is well adapted to local farming conditions and characterised by a low stress susceptibility and an efficient pathogen defence. Moreover, in the interests of a sustainable aquaculture, the development of a local and robust breeding strain offers an important alternative to the otherwise necessary use of drugs, antibiotics, and vaccines.

2. Materials and Methods

2.1. Animals, experiments, and sampling procedures

2.1.1. Maraena whitefish — experimental animals

All animals and sample material used in the course of this study originated from maraena whitefish, that were provided by the Institute for Fisheries of the State Research Centre for Agriculture and Fishery Mecklenburg-Vorpommern. Annually from 2013 to 2015, eggs and milt stripped from wild-caught maraena whitefish (caught in the Stettiner Haff; baltic sea) were artificially fertilised and transferred to the aquaculture testing station of the Institute for Fisheries in Born (Germany). There, eggs were kept in zuger jars provided with fresh water at 4°C until hatching. Then, alevins were transferred to tanks supplied by a fresh water recirculation system at 18°C. *Ad libitum* feeding of larvae with *Artemia salina* set in after complete yolk sac resorption. At a body mass of about 10 g and after complete fin development, fry were transferred either to a recirculation system provided with purified (bio filter and drum filter), disinfected (UV light) brackish water, tempered to 20°C, or to a flow-through system supplied with untreated brackish water without temperature control. In both systems water parameters like NH_4^+, NO_2^-, NO_3^-, NH_3 concentrations, pH value, temperature and oxygen saturation were constantly gathered. However, only for the recirculation system water parameters were stabilised constantly. Maraena whitefish were reared in tanks of the respective aquaculture system at a 12 h day and night light period until slaughter age. The fish were fed commercial dry pellets (Biomar, Inicio Plus, 4.5 mm) at a daily rate of 0.8 - 4.0% depending on their biomass. Throughout this study, maraena whitefish were applied to several experiments, that are detailed in the following from 2.1.2 to 2.1.8. Prior to blood sampling and dissection, fish were always killed by an overdose of 2-Phenoxyethanol (0.5 ml/l; Sigma-Aldrich).

2.1.2. Phenotype characterisation

Phenotype characterisation of maraena whitefish comprised the monitoring of total length, total weight, and the body constitution regarding injuries and infections. Therefore, at fry stage maraena whitefish aged 12 wph and weighing ≈10 g per individual, were separated into two cohorts and subsequently reared simultaneously, one in a recirculation system and the other in a flow-through system, as indicated in 2.1.1. Coincident sampling of 7 fish per cohort was carried out every 3 to 5 weeks, starting 17 weeks post hatch (wph) until slaughter age at 48 wph as indicated in figure 2.1. Subsequently, Fulton's condition factor (Ricker, 1975; Richter *et al.*, 2000) was used to analyse the fish's weight to length relation, according to formula (1). The variables were defined as follows: M = body mass, K = condition factor and L = body length. K was specifically calculated for the collected phenotype data by non-linear regression using formula (2) as a model in GraphPadPrism® software (version 5.01).

$$K = \frac{M}{L^3} * 100 \tag{1}$$

$$M = \frac{K}{100 * L^3} \tag{2}$$

Further, length and weight gain over time were analysed by Bertalanffy growth equations (Ricker, 1975; Sparre & Venema, 1998). Therefore formula (3) served as a model to quantify the length-based growth over time and formula (4) to calculate the weight-based growth over time, respectively. The variables of

both formula were defined as follows: L_t = length at age t, L_∞ = theoretical maximum length, K = growth coefficient, t_0 = theoretical age at $L = 0$, W_t = weight at age t, W_∞ = theoretical maximum weight.

$$L_t = L_\infty(1 - e^{(-K(t-t_0))}) \tag{3}$$

$$W_t = W_\infty(1 - e^{(-K(t-t_0))})^3 \tag{4}$$

To estimate initial values for the parameters L_∞, W_∞ and K Ford-Walford plots (Ricker 1975; Sparre & Venema 1998) were constructed plotting length and weight data. Then, to determine intercept and slope from the graphs and to subsequently calculate initial L_∞, W_∞ and K values from therespective Ford-Walford plots (see graphs in appendix B.1) linear regression was carried out in GraphPadPrism® software (version 5.01). Best fitting values for L_∞, W_∞, K and t_0 for the respective data set were then calculated by non-linear regression using the Bertalanffy equations (3, 4) as models together with the previously determined initial values for L_∞, W_∞ and K in GraphPadPrism® software (version 5.01).

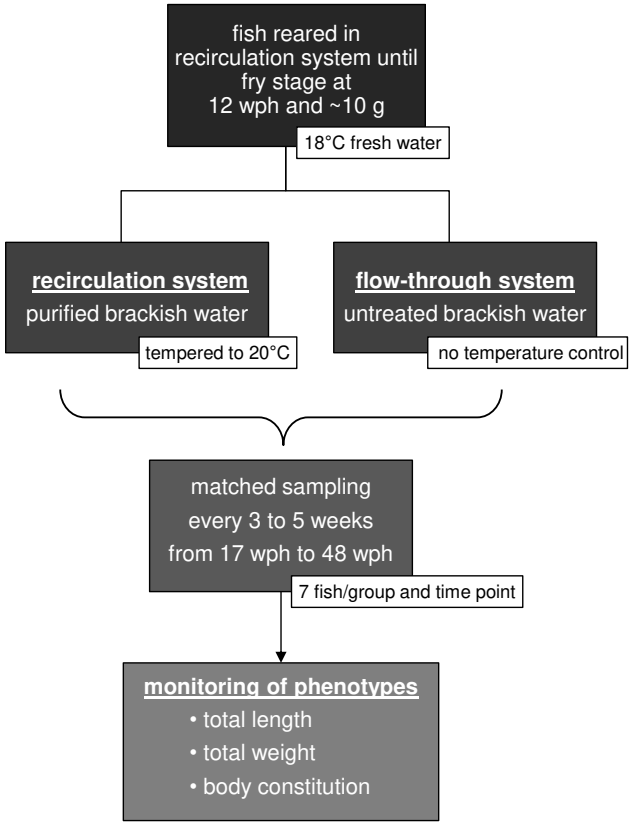

Figure 2.1: **Phenotype characterisation overview**

2.1.3. Tissue profiling

In order to examine the tissue-specific mRNA levels of target genes, various tissues (skin, kidney, muscle, spleen, liver, gills, gonads, eye, brain, heart) were dissected from four juvenile fish that were reared in a recirculation system until the age of 344 dph (48 wph), a total weight of $\bar{x} = 300.9 \pm 88.4$ g, and a total length of $\bar{x} = 30.6 \pm 2.4$ cm .(see figure 2.2). The sampled tissues were applied to RNA isolation (2.2.1) and cDNA synthesis (2.2.3). Finally, qPCR assays (2.2.4.8) were carried out to determine tissue-specific mRNA quantities of target genes using the LightCycler®96 System (2.2.4.8.1), as well as semi-quantitative PCR in case of the IGFs.

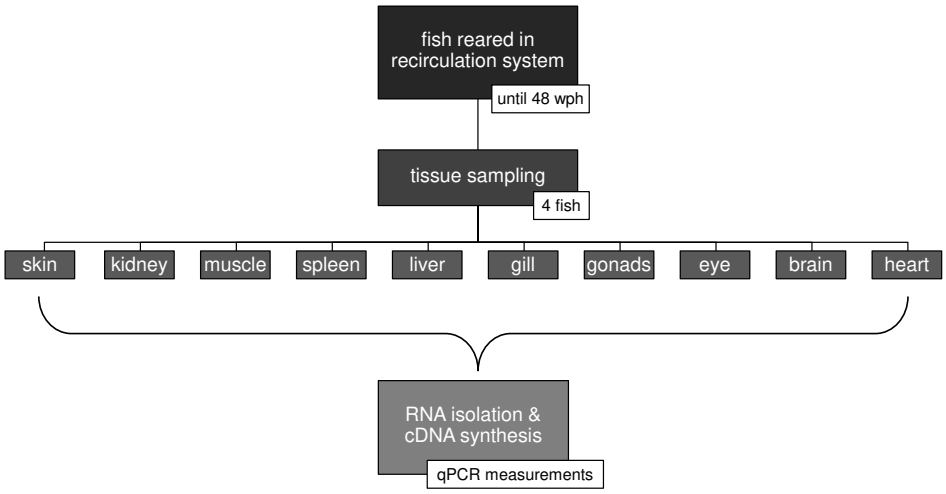

Figure 2.2: **Tissue profiling overview**

2.1.4. Density stress

The density stress experiment was performed to analyse the influence of different stocking densities on maraena whitefish. Prior to the experiment, fish were reared until the age of 29 wph, a total weight of $\bar{x}$= 87.7 ± 22.2 g, and a total length of $\bar{x}$= 21.4 ± 1.4 cm in the recirculation system of the aquaculture testing station of the Institute for Fisheries in Born (Germany) according to 2.1.1. For the density stress experiment, the fish were kept in 300 l glass aquaria, that are connected to the recirculation system, and thus provide the same conditions regarding water quality (pH $\bar{x} = 7.3 \pm 0.1$;$\bar{x} = 9.8 \pm 1.7$ O_2mg/l) and temperature ($\bar{x} = 19.6 \pm 0.7$ °C) as the latter. Throughout the experiment all water-quality parameters were constantly controlled and kept at safe levels. The experiment comprised a short-term density stress and an acute density stress approach as specified in figure 2.3. Therefore, the fish were weighed and transferred to the glass aquaria according to the different tested stocking densities, indicated in table 2.1.

Table 2.1: **Stocking density scheme**

Treatment category	Stocking density (SD)	SD per aquarium (300 l)	Extrapolated SD per 1 m³	Number of fish (per iteration 1/2)
Short-term density stress	low	3 kg	10 kg	34/33
	moderate	10 kg	33 kg	101/103
	enhanced	18 kg	60 kg	185/181
	high	30 kg	100 kg	309/305
Acute density stress	moderate	10 kg	33 kg	104/99
	high	30 kg	100 kg	308/309

For the short-term density stress approach, the fish were kept at four different stocking densities for 8 days (d), whereas for the acute stress approach, the fish remained at two different stocking densities for 24 h. The whole experiment has been performed in duplicate. Thus, two times four fish per stocking density of each approach were sampled after 24 h or 8 d, respectively. Prior to fish dissection, blood was collected from the caudal vein using 0.8 x 40 mm cannula (Sterican®, Braun) on 5 ml syringes (Injekt®, Braun) equipped with 100 µl 0.5 x EDTA/1 ml blood as anticoagulant. Blood samples were stored 60 min

on ice, and then centrifuged for 30 min at 2500 x g and 4°C. The blood plasma (supernatant) was pipetted into new 1.5 ml reaction tubes (Sarstedt) and stored until use in glucose (4.1) and cortisol assays (2.3) at -20°C. Sampled fish were applied to dissect liver, spleen, kidney, and gill tissue. The obtained tissues were sliced, immediately flash frozen in liquid nitrogen and stored at -80°C until RNA isolation (2.2.1). Subsequently, RNA was used for qPCR (2.2.4.8), as well as microarray analyses (2.2.10).

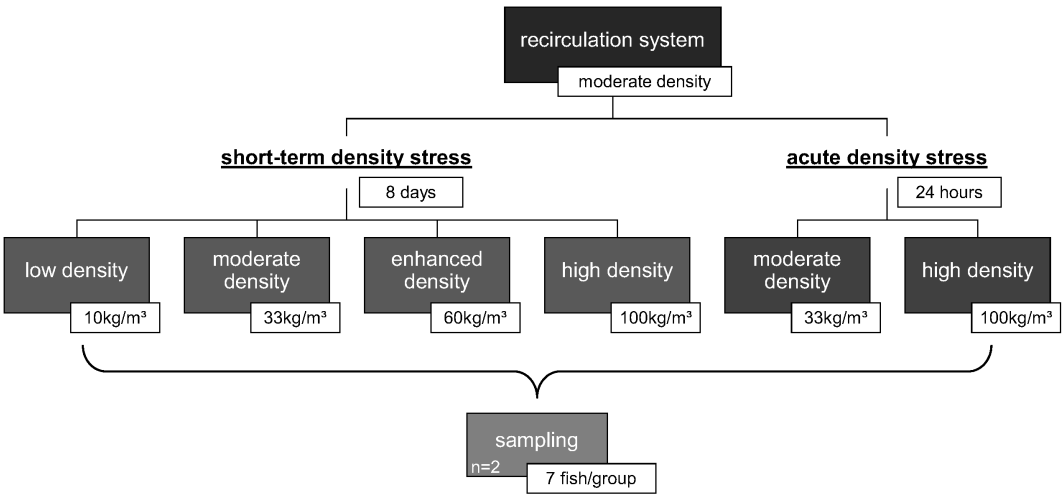

Figure 2.3: **Density stress experiment overview**

2.1.5. Temperature stress

For the purpose of studying the impact of temperature on maraena whitefish a temperature stress experiment was carried out. Therefore, maraena whitefish (aged 49 wph) having a total weight of $\bar{x} = 300.6 \pm 68.4$ g and a total length of $\bar{x} = 30.3 \pm 1.7$ cm, reared in the recirculation system (2.1.1) were transferred to 300 l glass aquaria. Water quality was identical to the recirculation system, but temperature was adjusted to 18°C, thus an acclimation period of 10 d was conducted. Throughout the experiment water-quality parameters were maintained at safe levels. The temperature stress experiment comprised two different approaches, i.e., a gradual and an acute temperature rise as indicated in figure 2.4. For the gradual temperature rise, water temperature of the respective aquaria was increased by 1°C/2 d from 18°C to 24°C within 12 d.

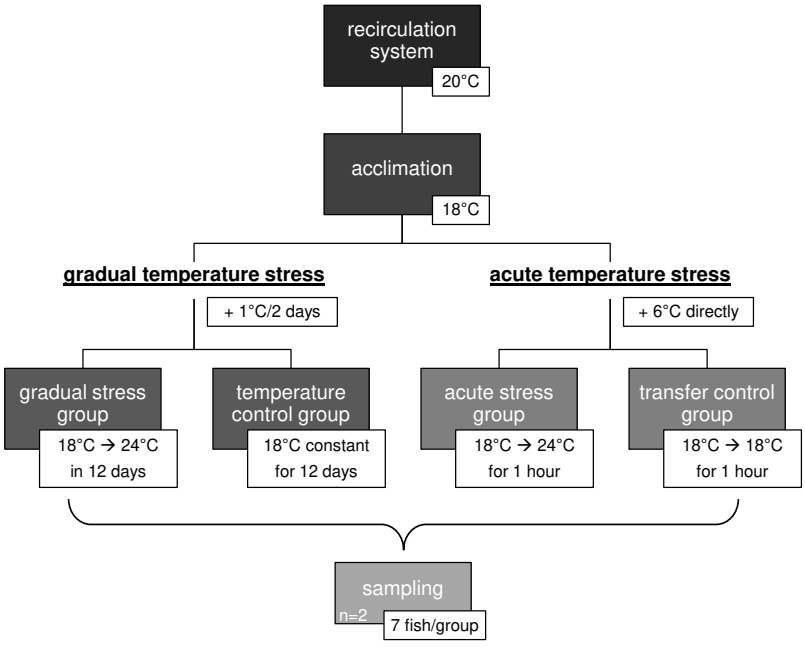

Figure 2.4: **Temperature stress experiment overview**

Subsequently, fish were kept for another 24 h at 24°C and then applied to sampling. For the acute temperature rise fish were reared 7 d at 18°C, directly transferred to 24°C aquaria and sampled after 1 h. Simultaneously to the acute temperature stress procedure, a transfer-control was carried out, whereby fish were transferred from one 18°C aquaria to another and sampled after 1 h, to measure the handling stress. In addition, a control group of fish were reared throughout the experiment at 18°C and sampled concurrently. All in all, seven fish per group (gradual and acute temperature rise; transfer and 18°C control) were sampled, blood was collected and liver, spleen, kidney and gill tissue were dissected. The procedure of blood and tissue sampling, as well as the subsequent application of samples was carried out as described in section 2.1.4. The temperature stress experiment has been performed in duplicate.

2.1.6. Stimulation of maraena whitefish with *Aeromonas salmonicida*

The stimulation experiment was performed, headed by Tomáš Korytář, at the Institute of Immunology of the Friedrich-Loeffler-Institut (FLI), the Federal Institute for Animal Health in Riems/Greifswald (Germany). Juvenile maraena whitefish were obtained from the aquaculture testing station of the Institute for Fisheries in Born (Germany). There, fish were reared in a recirculation system until the age of 205 dph as indicated in 2.1.1. For the stimulation experiment the fish were transferred to the experimental facility of the FLI and acclimated in 300 l glass aquaria at 18°C and freshwater for two weeks. The bacterium *A. salmonicida* ssp. *salmonicida* (wild type strain JF 2267) was used for the stimulation of maraena whitefish. The cultivation and inactivation of *A. salmonicida*, as well as the subsequent preparation and storage of the bacterial suspension (5×10^7 cells/ml) was carried out according to a standard protocol as described in detail by Korytár *et al.* (2013). In total, 18 maraena whitefish (i.e., $n = 6$ per time point) were injected i.p. a 100 µl bacterial suspension containing 5×10^6 inactivated bacteria. As negative control, simultaneously, 15 maraena whitefish (i.e., $n = 5$ per time point) were administered 100 µl sterile PBS solution. 24 h, 48 h and 72 h post treatment stimulated and control fish were sampled and dissected. Thus, liver, spleen, head kidney, gills and peritoneal cells were obtained, immediately flash frozen in liquid nitrogen and stored at -80°C. The tissue samples were applied to RNA extraction (2.2.1) and subsequent qPCR measurements with the Fluidigm® BioMark™ HD-System (2.2.4.8.2). Figure 2.5 gives an overview of the experimental design.

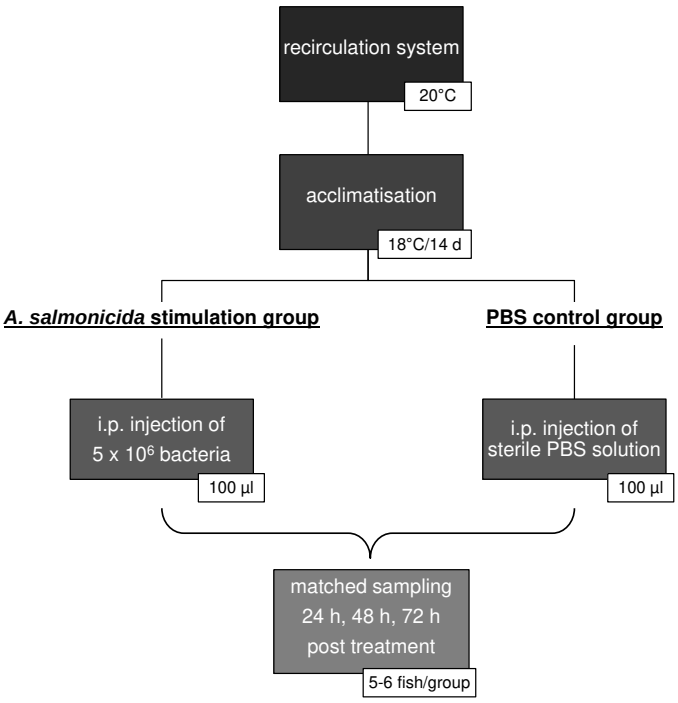

Figure 2.5: ***A. salmonicida* stimulation experiment overview**

2.1.7. Primary cell stimulation

The primary cell experiment was conducted to analyse target gene mRNA numbers of maraena whitefish immune cells after a stimulation with PAMP reagents and/or the steroid hormone cortisol. To this end, head kidney primary cells were isolated according to the protocol in section 2.5. After 15 h of incubation at 20°C and 5% CO_2 atmosphere, the cells were applied to cell stimulation experiments as specified in figure 2.6. Therefore, hydrocortisone (600 ng/ml; Sigma-Aldrich) and/or a mixture of the PAMP reagents listed in table 2.2 were added directly onto the cells growing on 6-well plates. The cells were incubated again at 20°C and 5% CO_2 atmosphere, until each time 3 wells per treatment were harvested after 1 h, 3 h, 6 h, 12 h, 24 h and 48 h. Further, at least 3 - 5 wells were kept untreated as negative controls. The primary cell stimulation experiment was repeated three times independently. The harvested cells were applied to RNA isolation according to 2.2.1, and the RNA was used for IFC chip based real time PCR measurements on the Fluidigm® BioMark™ HD-System (2.2.4.8.2).

Table 2.2: **PAMP reagents used for primary cell stimulation**

Reagent	Specification	Applied concentration
LPS-EB	lipopolysaccharide from *E.coli*	10 µg/ml
FSL-1	synthetic bacterial lipoprotein	100 ng/ml
Pam2CSK4	synthetic diacylated lipoprotein	100 ng/ml
Pam3CSK4	synthetic triacylated lipoprotein	300 ng/ml
FLA-ST	purified flagellin from *S. typhimurium*	10 ng/ml
Poly(I:C)-LMV	synthetic analogue of dsRNA	10 µg/ml

Reagents were all purchased from InvivoGen SAS, Toulouse, France

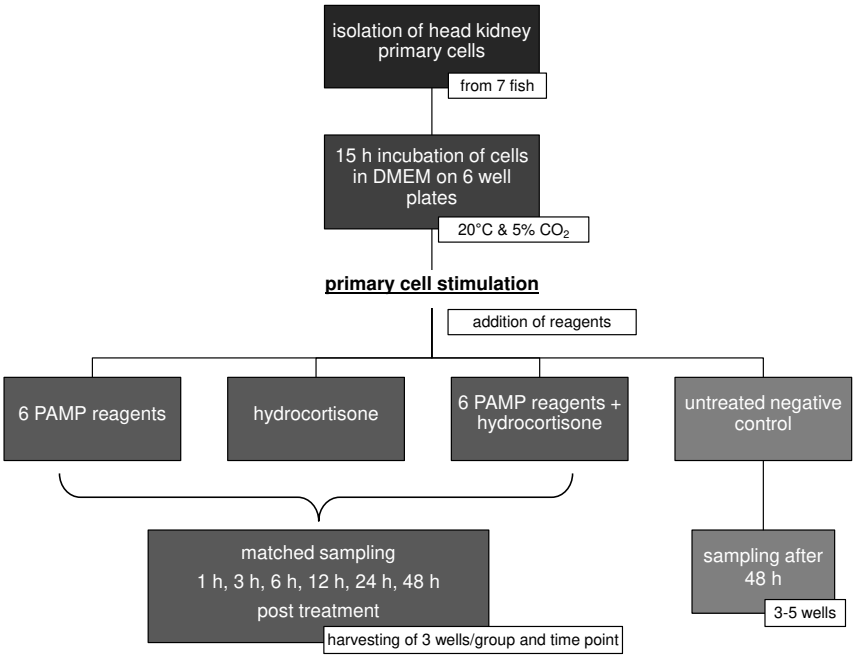

Figure 2.6: **Primary cell stimulation schedule**

2.1.8. Ontogenetic development

2.1.8.1. Ontogenetic development from egg to fingerling This experiment was performed to survey maraena whitefish ontogenetic development from unfertilised egg until early fingerling stage. For this purpose, eggs obtained from wild-caught maraena whitefish (Stettiner Haff; Baltic sea) were sampled and stored in RNAlater™ (Qiagen), prior to the artificial fertilisation with milt. Then, eggs were transferred

to zuger jars (4°C) at the aquaculture testing station of the Institute for Fisheries in Born (Germany). Incubation of fertilised eggs, and subsequent rearing of larvae in fresh water recirculation tanks (18°C), and of fry in flow-through tanks was performed as described in section 2.1.1. Transfer of fry to the flow-through system, that is directly supplied with unfiltered, non tempered brackish water, was conducted at age of 59 days post hatch (dph). Throughout the experiment, sampling was carried out at least once a week and samples were immediately stored at -80°C until further use. Four eggs were always merged to one pool, whereas larvae and fry were collected individually. Hence, each time four pools of eggs and four larvae, fry, or fingerlings were applied to RNA isolation (2.2.1) per sampling time point. The extracted RNA was then used to examine the expression of target genes by qPCR measurements (2.2.4.8).

2.1.8.2. Temperature dependent ontogenetic development The aim of this experiment was to examine the influence of different incubation temperatures on developing eggs and on maraena whitefish's development post hatch. Initially, fertilised eggs were incubated in zuger jars until 27 days post fertilisation (dpf) as indicated in 2.1.1.

Then, eggs were split into three groups and simultaneously incubated in zuger jars at 4°C, 6°C and 9°C, respectively. Sampling of eggs started approximately two weeks before, and was carried out weekly until four weeks post hatch for each group, respectively. Immediately after hatch, alevins were transferred to fresh water recirculation tanks (18°C) and sampling was proceeded once a week. The sampling procedure, as well as the subsequent preparation and usage of samples was the same as in the previous experiment (2.1.8.1). Figure 2.7 gives an overview of the experimental procedure.

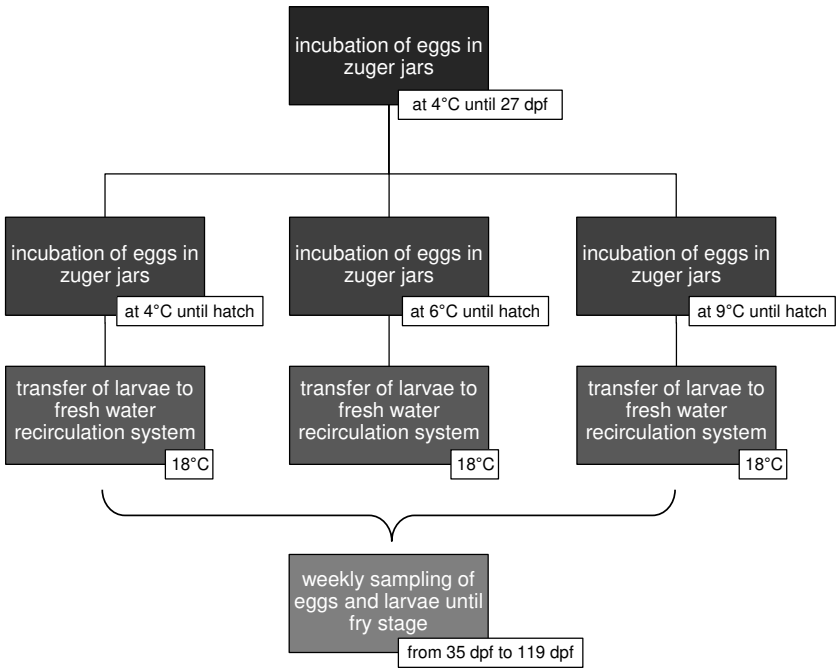

Figure 2.7: **Temperature dependent ontogenetic development overview**

2.2. Molecular biological techniques

2.2.1. Isolation of total RNA from maraena whitefish tissue and cells

Total RNA was extracted by an improved single-step method of RNA isolation using TRIzol® Reagent (Life Technologies) based on an acid guanidinium thiocyanate-phenol-chloroform extraction, originally developed by Chomczynski & Sacchi (1987). Small pieces of ca. 0.1 g frozen tissue were put into 2 ml screw-cap tubes (Sarstedt) together with five sterile ceramic beads of 2.8 mm diameter (Precellys® ,

Peqlab Biotechnologie) and 1 ml TRIzol® Reagent (Invitrogen). Then tissue samples were homogenised for 30 s at 6000 rpm with the Precellys®24 Homogeniser and directly incubated on ice for at least 5 min. Subsequently, 200 µl chloroform were added, the tubes were thoroughly mixed for 15 s by inversion and then incubated at RT for 3 min. Next, the mixture was centrifuged for 15 min at 14000 rpm and 4°C to separate the aqueous phase containing the RNA, from the lower phenol-chloroform phase and the interphase. Solely the aqueous supernatant was pipetted into a new 1.5 ml tube (Sarstedt). In order to precipitate RNA 500 µl of isopropanol were added, followed by 10 min of incubation at RT. Sedimentation of the RNA was acquired by a centrifugation step for 10 min at 14000 rpm at 4°C. Then the RNA pellet was washed in 1 ml ice-cold 80% ethanol, sedimented again (5 min, 14000 rpm, RT) and resuspended in 100 µl RNase-free water. For further purification and removal of residual amounts of DNA the RNA was treated with the RNeasy Mini Kit (Qiagen) according to the manufacturer's protocol. Subsequently, the RNA quality was assessed by horizontal electrophoresis on 1% agarose gels through checking the integrity of the 28S- and 18S-rRNA bands.
RNA isolation of maraena whitefish cells was performed without previous TRIzol®(Invitrogen) treatment using only the RNeasy Mini Kit (Qiagen) according to the manufacturer's instructions. Finally, the RNA concentration was determined using the NanoDrop 1000 Spectrophotometer (Peqlab Biotechnologie) (see section 2.2.2). RNA was then stored at -80°C until further use.

2.2.2. Quantification and quality control of nucleic acids

Prior to further use the concentration and purity of RNA and DNA samples was assessed by measuring the absorbance at 230 nm (peak absorbance of organic compounds like phenol), 260 nm (peak absorbance of nucleic acids) and 280 nm (peak absorbance of proteins) using the NanoDrop 1000 Spectrophotometer (Peqlab Biotechnologie). Therefore, 1 µl of RNA or DNA sample were applied to determine the amount of nucleic acid in the sample, as well as the presence of contaminants. The 260/280 nm ratio should be around 2.1 for RNA and 1.8 for DNA, whereby lower values indicate a protein contamination of the sample. The 260/230 nm ratio should be around 2.0 for RNA and DNA respectively, whereas ratios < 1.8 indicate an organic contamination of the sample.

2.2.3. cDNA synthesis

The SuperScript™ II Reverse Transcriptase Kit (Invitrogen, Life Technologies) was used for the synthesis of first-strand cDNA (complementary DNA) from purified total RNA. For this purpose 1.5 µg RNA were filled up to a volume of 10 µl with DEPC-H_2O. Then, according to manufacturer's protocol 1 µl Oligo(dT) primer (100 µM) and 1 µl dNTP Mix (10 mM each) were added and the mixture was heated to 65°C for 5 min. Next, while keeping the solution on ice, 4 µl of 5 x First Strand Buffer, 2 µl DTT and 1 µl of the SuperScript™ II Reverse Transcriptase enzyme were added followed by a 50 min incubation at 42°C. Finally, the enzyme reaction was inactivated by heating the solution up to 70°C for 15 min. The resulting cDNA was purified using the High Pure PCR Product Purification-Kit (Roche) as described in section 2.2.6. Then, the cDNA was usually diluted in 100 µl *A. dest.* and stored at -80°C until further use for PCR and qPCR analyses.

Table 2.3: **Preparation of diethyl pyrocarbonate treated water**

DEPC-H_2O	
diethyl pyrocarbonate	10 ml
H_2O	1000 ml

The solution was mixed under stirring over night and subsequently autoclaved.

2.2.4. Polymerase chain reaction-based methods

The polymerase chain reaction (PCR) is a method to generate large amounts of specific DNA sequences using sequence-specific oligonucleotides and a template DNA according to Saiki *et al.* (1988). In the course of this study, a range of PCR methods were carried out, e.g., to isolate unknown DNA sequences and to amplify DNA fragments prior to a DNA cloning experiment (standard PCR, touch down PCR), to elucidate unknown UTRs of cDNAs (3'/5'-RACE PCR), or to quantify cDNA copies of a specific sample (semi-quantitative PCR, qPCR). By using different cycling or temperature profiles, polymerases and oligonucleotides, the PCR was adjusted to meet the specific requirements of a certain experiment, as indicated in the following. PCR reactions were usually carried out in 0.2 ml tubes (Sarstedt) using the Thermocycler T1 (Biometra). The obtained PCR products were always assessed by agarose gel electrophoresis (2.2.5).

2.2.4.1. Primer design All primers used in this study were custom-made by Sigma-Aldrich and diluted to a final concentration of 20 µM, unless specified otherwise. All primers used and/or generated in the course of this study can be found in the appendix (A.2).

2.2.4.1.1. Standard PCR primers Primer design for already known sequences was performed with the online interface of the Primer3Plus software (Untergasser *et al.*, 2007). Generally, the program settings were adjusted to generate primers with a size of 18 to 27 bp, a G+C content of 40 to 60%, and a T_m (melting temperature) ranging between 63 to 66°C.

2.2.4.1.2. Consensus and degenerate primers If no sequence information for the target gene was available, consensus and/or degenerate primers were designed using the online interface of the software packages ClustalOmega (Sievers *et al.*, 2011) provided by the EMBL-EBI (European Molecular Biology Laboratory - European Bioinformatics Institute) and PrimaClade (Gadberry *et al.*, 2005). Initially, a multiple sequence alignment was carried out using ClustalOmega with at least three or more orthologous sequences from closely related species, that were available on the online NCBI (National Center for Biotechnology Information) Nucleotide Database. Next, the multiple sequence alignment was supplied to PrimaClade to design "consensus primers" that were specific for highly conserved sequence regions, identified among the selected species. In some cases, the derived primer sequences contained nucleotide exchanges among the species, so that "degenerate primers" were designed. Primers with a maximum of 2 degenerate base positions, were synthesized as a mixture of similar oligonucleotides, differing only in the two or more required bases at the respective position. Degenerate nucleotides of the primers were indicated by the respective characters of the *IUPAC* (International Union of Pure and Applied Chemistry) *Ambiguity Code* (Cornish-Bowden, 1985). The general primer settings, regarding primer size, G+C content and T_m were adjusted as indicated for standard PCR primers (2.2.4.1.1). Usually, consensus and degenerate primers were used in a touch down PCR program (2.2.4.3) to increase the PCR specificity.

2.2.4.1.3. Real time PCR primers Primers for qPCR assays were designed using the PSQ Assay Design Software 1.0 (Biotage AB, Uppsala, Sweden). Primer settings were always adjusted to the following parameters: primer size between 18 to 24 bp, optimal amplicon length ranging from 150 to 180 bp, but not larger than 220 bp, and a T_m between 64.0 - 66.0°C. Only primer sets were chosen that

reached a PSQ primer set score > 90% to avoid internal secondary structures and primer dimerisation through (self-) complementarity.

2.2.4.2. Standard PCR procedure The standard PCR procedure was performed to specifically amplify DNA fragments with a maximum length of 2.0 kb. Therefore, the HotStar Taq® *Plus* DNA Polymerase (Qiagen) together with the supplied PCR Buffer (Qiagen) or CoralLoad PCR Buffer (Qiagen) was used. As needed, 10 µl, 15 µl or 25 µl PCR reactions (see table 2.4) were prepared as a master mix that was adjusted to the total number of required PCR assays. The final volume of the master mix always included an excess of 10% and one negative control (without template DNA/cDNA) for each pair of applied primers. The standard PCR program was run as indicated in table 2.5. The annealing temperature was set between 55 to 60°C according to the $T_m$of the applied primers. Further, the elongation time was adapted to the expected size, and the cycle number to the assumed abundance of the requested DNA fragment.

Table 2.4: **Standard PCR reaction**

onefold PCR master mix for a final volume of:	10 µl	15 µl	25 µl
Reagent	**Volume**	**Volume**	**Volume**
10 x PCR buffer	1.0 µl	1.5 µl	2.5 µl
dNTP mix (10 mM each dNTP)	0.4 µl	0.6 µl	1.0 µl
Hot Star Taq® *Plus* DNA Polymerase (5 U/ µl)	0.04 µl	0.06 µl	0.1 µl
forward primer (20 µM)	0.4 µl	0.6 µl	1.0 µl
reverse primer (20 µM)	0.4 µl	0.6 µl	1.0 µl
H_2O_{bidest}	7.36 µl	11.04 µl	18.4 µl
template DNA/cDNA	0.4 µl	0.6 µl	1.0 µl

Table 2.5: **Standard PCR cycling program**

Step	Temperature	Time	Cycle number
Initial denaturation	95°C	5 min	
Denaturation	94°C	30 s	
Annealing	55 - 60°C	30 s	30 - 40
Elongation	72°C	30 - 150 s	
Final elongation	72°C	6 min	
Rest	8°C	∞	

2.2.4.3. Touch Down PCR In order to decrease the number of unspecific DNA fragments, especially when running a PCR with consensus or degenerate primers (2.2.4.1.2) or a 3'/5'-RACE PCR (2.2.4.6, 2.2.4.7) a touch down PCR program was performed. Since the binding of a primer to its template is most specific just below the primer T_m, the initial annealing temperature was set comparatively high, and was then gradually reduced until it was several degrees below the specific T_m of the primer. Thus, the touch down protocol increased the specificity of the PCR due to a gradual decrease of the annealing temperature by 1°C at each cycle. The target sequences, already bound to its specific primers, were then amplified in the following standard PCR procedure. The touch down PCR reactions were prepared analogous to the standard PCR (see table 2.4) and the cycling program was performed as indicated in table 2.6. Equally to the standard PCR procedure (2.2.4.2), the elongation time and the cycle number was adjusted to the specific requirements of every touch down PCR assay.

Table 2.6: **Touch down PCR cycling program**

Step	Temperature	Time	Cycle number
Initial denaturation	95°C	5 min	
Denaturation	94°C	30 s	
Annealing	68°C*	30 s	10 - 15
Elongation	72°C	30 - 150 s	
Denaturation	94°C	30 s	
Annealing	55 - 60°C	30 s	30 - 40
Elongation	72°C	30 - 150 s	
Final elongation	72°C	6 min	
Rest	8°C	∞	

*(-1°C per cycle)

2.2.4.4. High Fidelity PCR High Fidelity PCR was carried out using the Q5®High-Fidelity DNA Polymerase Kit (New England BioLabs/NEB) according to the manufacturer's protocol. The Q5®High-Fidelity DNA Polymerase was used to amplify long and "difficult" DNA fragments, since it has a 3'-5' exonuclease activity (proof reading) and a very low error rate (according to NEB: > 100-fold lower than that of *Taq* DNA Polymerase). As recommended by the manufacturer the NEB T_mCalculator was used to determine the specific melting temperature of the applied primers and to subsequently adapt the annealing temperature of the PCR cycling program.

2.2.4.5. Semi-quantitative PCR Semi-quantitative PCR was carried out to rapidly analyse transcript levels of specific target mRNAs in several samples, particularly from different tissues. For proper quantification of target gene mRNA levels by semi-quantitative PCR the resulting bands on the agarose gel must be clearly visible, but not saturated. Thus, an appropriate cycle number for every specifically analysed mRNA of the respective sample set was determined by PCR pretests. Semi-quantitative PCR was always performed using real time PCR primers (2.2.4.1.1) for the respective target mRNA, since these generate amplicons with a maximum size of 220 bp. The PCR reaction was prepared in one master mix (15 µl each reaction) for all tested samples according to table 2.4, and the PCR cycling program was set as indicated in table 2.7. Further, all PCR assays were run in the same thermocycler device and subsequently exactly the same amount of each sample (5.0 µl) was applied on the same agarose gel, to minimize variations for each tested sample. Based on band intensities, gene-specific mRNA of the assayed samples, was quantified by densitometric analysis with Image Lab™ Software Version 4.1 (Bio-Rad).

Table 2.7: **Semi-quantitative PCR cycling program**

Step	Temperature	Time	Cycle number
Initial denaturation	94°C	5 min	
Denaturation	94°C	30 s	
Annealing	60°C	30 s	31
Elongation	72°C	20 s	
Final elongation	72°C	10 min	
Rest	8°C	∞	

2.2.4.6. 3'-Rapid Amplification of cDNA Ends (3'-RACE) In order to analyse unknown 3'-regions of a mRNA transcript the 3'-RACE (rapid amplification of cDNA ends) method was carried out. Therefore, RNA was reverse transcribed into a cDNA copy applying a Oligo-(dT)-Primer with a known anchor

sequence in the 5'-region according to 2.2.3. Following, a PCR was performed using an anchor-specific primer and a gene-specific primer derived from the already known sequence region. The resulting PCR product was then applied as a template in a second so called nested-PCR to reduce the probability of amplifying a wrong locus. Therefore, a second set of nested-primers with specific binding sites within the first PCR product are used to increase the specificity of the amplified fragment. The obtained DNA fragments were separated on 1.5% agarose gels (2.2.5) and then applied to DNA cloning (2.2.7) and subsequent sequencing (2.2.9).

2.2.4.7. 5'-Rapid Amplification of cDNA Ends (5'-RACE) The 5'-RACE (rapid amplification of cDNA ends) method serves to obtain unknown 5'-regions of a partly known mRNA transcript. Analogous to the 3'-RACE (2.2.4.6), mRNA was initially reverse transcribed into first-strand cDNA (2.2.3) modifying the given protocol in terms of employing a gene-specific primer instead of the usual Oligo(dT) primer. Further steps of the 5'-RACE were carried out using the 2nd Generation 5'/3' RACE Kit (Roche), that bases on the enzyme activity of a recombinant terminal transferase. This enzyme is a template independent polymerase, that adds deoxynucleotides to the 3' hydroxyl terminus of cDNA molecules and thus allows to amplify unknown 5'-regions of a mRNA transcript. According to the manufacturer's protocol two runs of nested-PCRs with two antisense gene-specific nested-primers were performed. The obtained PCR products were tested on 1.5% agarose gels (2.2.5) and then applied to DNA cloning (2.2.7) and subsequent sequencing (2.2.9).

2.2.4.8. Quantitative real time PCR methods In order to quantify the abundance of a target cDNA, previously reverse transcribed from mRNA (2.2.3), in a specific sample, quantitative real time PCR (qPCR) was carried out. The qPCR method bases on fluorescence dyes, that intercalate the newly synthesised DNA within qPCR and emit fluorescence signals only when bound to double stranded DNA. Thus, when the proceeding qPCR reaction leads to increasing amounts of target cDNA, it consequently causes an increase in fluorescence emission, as well. The qPCR assays were performed either in the LightCycler®96 System (Roche) or the BioMark™ HD-System (Fluidigm). Both qPCR instruments detect and monitor the fluorescence emission of fluorescence dyes (at 530 nm) during the exponential phase of the PCR. Further, both qPCR devices plot the respective amplification curves displaying the fluorescence intensity against the number of amplification cycles. Based on the amplification curve the qPCR instruments automatically calculate a Cq value, that reveals the first amplification cycle at which the fluorescence signal of a sample exceeds the threshold level (background signal). The Cq value correlates to the amount of target cDNA copies of the tested sample and thus is needed to calculate absolute or relative transcript quantities. Generally, low Cq values indicate high, whereas high Cq values point to a low abundance of target cDNA at the beginning of the qPCR. In general, if Cq values were ≥ 35, the respective target gene was considered as "not expressed".

The qPCR assays were always performed with real time PCR primers (2.2.4.1.3), that were assessed by melting curve analysis regarding their specificity to the target sequence after every run and for every examined sample. Additionally, since the used fluorescence dyes were not sequence specific, a standard PCR protocol (2.2.4.2) was run once for each applied primer pair. The resulting PCR products were, purified (2.2.6), quantified (2.2.2) and subsequently verified by sequencing (2.2.9).

Further, the PCR product of every primer set was used as external standard to generate a standard curve. Therefore, via the concentration and the size of the DNA fragment the specific number of molecules in 1 µl of the sample was calculated using the Molbiol online tool (`http://www.molbiol.ru/`

ger/scripts/01_07.html). Then, serial dilutions (10^3 - 10^6) of the PCR product were prepared and measured by qPCR to generate a standard curve of known concentrations. For absolute quantification of target molecules, the sample-specific Cq value and the standard curve served to interpolate copy numbers using formula (5).

$$copy\,number = 10^{\frac{Cq - intercept}{slope}} \tag{5}$$

Furthermore, the standard curve was used to determine the efficiency (E) of the qPCR reaction for every primer set according to formula (6). At optimal experimental conditions the efficiency of the reaction equals E = 2, i.e., the amount of qPCR products doubles within every cycle.

$$E = 10^{\frac{-1}{slope}} \tag{6}$$

Subsequently, the three reference genes *EEF1A1B*, *RPL9* and *RPL32* (Altmann *et al.*, 2014) were used to calculate a normalisation factor. Therfore, the copy number of each target gene sample is divided by the average copy number of the reference gene for the same condition. From the three different reference genes, the three resulting factors were used to calculate the geometric mean to obtain the normalisation factor. Then, the copy numbers of each target gene (interpolated from the standard curve) were multiplied by the normalisation factor. Data obtained from qPCR experiments were always normalised this way, unless otherwise stated.

2.2.4.8.1. Real time PCR with LightCycler®96 System Small-scale qPCR assays were carried out with the LightCycler®96 System (Roche) using the SYBR® Green fluorescence dye of the SensiFAST™ SYBR®No-ROX Kit (Bioline) on a clear LightCycler®480 Multiwell Plate 96 (Roche) closed with a LightCycler®480 Sealing Foil (Roche). Usually, 1.5 µg RNA of the required sample were reverse transcribed into cDNA (2.2.3) prior to the qPCR run. The qPCR reactions were always prepared according to the protocol in table 2.8, as a mastermix with 10% excess and one negative control for every applied primer pair. Further, the qPCR cycling program was performed as indicated in table 2.9. Following qPCR, the obtained DNA fragments were run on a 2% agarose gel (2.2.5) to assess the integrity and specificity of the applied primer sets for the examined samples.

Table 2.8: **qPCR reaction**

Reagent	Volume
SYBR®Green I Mastermix (2x)	6.0 µl
forward primer (20 µM)	0.5 µl
reverse primer (20 µM)	0.5 µl
template cDNA	5.0 µl

Table 2.9: **qPCR cycling program**

Step	Temperature	Time	Cycle number
Initial denaturation	95°C	5 min	
Denaturation	95°C	20 s	
Annealing	60°C	15 s	40
Elongation	72°C	15 s	
Fluorescence measurement	72°C	10 s	
Capture of melting curve: denaturation	95°C	5 s	
Melting	70 - 95°C	60 s	

2.2.4.8.2. IFC chip based real time PCR with BioMark™ HD-System Large-scale qPCR assays were carried out on 192.24 Dynamic Array™ IFC chips (Fluidigm®) with EvaGreen® fluorescence dyes

(Bio-Rad) using the BioMark™ HD-System (Fluidigm®). The integrated fluidic circuit (IFC) technology of the Fluidigm®microfluidic chips permits qPCR measurements in nano-litre volumes, thus very high sample numbers, as well as small quantities of RNA could be analysed. The applied 192.24 Dynamic Array™ IFC chip (Fluidigm®) enables the simultaneous measurement of 192 samples in combination with 24 primer sets. The complete IFC chip qPCR run comprises 7 steps as described in the following.

1. Preparation of RNA samples

RNA samples were isolated as described in section 2.2.1 and the RNA concentration was determined according to 2.2.2. Subsequently, the RNA samples were pipetted onto 96-well plates (Thermo Fisher Scientific) and diluted to final concentrations ranging between 5 ng/µl to 150 ng/µl in respective volumes of RNase free water.

2. cDNA synthesis

On new 96-well plates (Thermo Fisher Scientific), each time 1 µl of the prepared RNA samples were reverse transcribed into cDNA using the Reverse Transcription Master Mix (Fluidigm®) according to the manufacturer's protocol. The cycling protocol for cDNA synthesis was adjusted as specified by the manufacturer and performed in a Thermocycler T1 (Biometra).

The resulting cDNA was used to generate one or more standards from cDNA sample mixtures. Therefore, each time 0.4 µl of at least 5 different cDNAs were pipetted into a 1.5 ml reaction tube (Sarstedt) to generate one "standard mix". The standard mixes were then applied in the cDNA pre-amplification step.

3. Pre-amplification of cDNA

In order to increase the amount of initial cDNA a pre-amplification step was carried out prior to the qPCR run. Pre-amplification was carried out using the PreAmp Master Mix (Fluidigm) and a "primer master mix" with a final concentration of 500 nM per primer pair.

The applied real time primers (2.2.4.1.3) for IFC chip based qPCR assays were always delivered in 200 µM dilutions (customized by Sigma Aldrich). To generate a "primer master mix", 100 µM mixes of all applied primer sets were prepared. To this, 50 µl of the forward and the reverse primer of each primer pair were mixed in a 0.5 ml reaction tube (Sarstedt). Next, the "primer master mix" with a final concentration of 500 nM per primer pair was prepared. Hence, 1.0 µl of each previously prepared primer mix were pipetted in a 1.5 ml reaction tube (Sarstedt) and filled up to a final volume of 200 µl with DNA Suspension Buffer (Affymetrix).

Then, on new 96-well plates (Thermo Fisher Scientific) the cDNA pre-amplification was performed, employing the PreAmp Master Mix (Fluidigm®), the "primer master mix" and the cDNA samples according to the manufacturer's instructions. To generate the external standard a respective amount of wells were prepared and filled with 1.25 µl of "standard mix" instead of cDNA sample. The cycling protocol for pre-amplification reaction was adjusted as specified by the manufacturer and performed in a Thermocycler T1 (Biometra). Based on the initial concentration of the RNA samples (5 ng/µl to 150 ng/µl) the number of amplification cycles was adapted in a range between 11 (high initial concentration) to 21 (low initial concentration).

4. Exonuclease I treatment

To remove unincorporated primers following the cDNA pre-amplification, a treatment with Exonuclease I (ExoI; New England BioLabs) was performed according to the manufacturer's protocol in a Thermocycler T1 (Biometra). Following the Exo I treatment, the cDNA samples were diluted by adding 43 µl of TE buffer (Qiagen), whereas only 10.5 µl were added to wells containing the "standard mix".

Further, to generate a serial dilution for a standard curve, 5 µl of the previously diluted "standard mix" were mixed with 20 µl TE buffer (Qiagen) in a new 0.5 ml reaction tube (Sarstedt). Then, serial dilutions were prepared by pipetting 6 times 1 µl of the previous dilution into 40 µl TE buffer (Qiagen) in new 0.5 ml reaction tubes (Sarstedt).

5. Loading the IFC chip

Prior to the qPCR run the primers and samples, as well as the 192.24 Dynamic Array™ IFC chip (Fluidigm®) were prepared according to the Fluidigm® 192.24 Fast/Standard Gene Expression Workflow. Therefore, 0.2 µl of the previously prepared 100 µl dilutions of every primer set (see step 3) were added to a master mix of DNA Suspension Buffer (Affymetrix) and 2 x Assay Loading Reagent (Fluidigm®) on a new 96-well plate (Thermo Fisher Scientific). In parallel, on new 96-well plates (Thermo Fisher Scientific) 1.8 µl of the standard mix dilutions and of the cDNA samples were added to a master mix containing of SsoFast™ EvaGreen® Supermix with Low ROX (Bio-Rad) and 192.24 DELTAgene™ Sample Reagent (Fluidigm®). The primer and sample (including standard) master mixes were transferred from the 96-well plates (Thermo Fisher Scientific) to the assay and sample inlets on the IFC chip. The loading of primers and samples on to the IFC chip was carried out automatically, using the IFC Controller RX (Fluidigm®) and the LoadMix (169x) script of the respective IFC Controller RX software (Fluidigm®) according to the manufacturer's instructions.

6. Chip run

After automatic loading of primers and samples, the IFC chip was transferred to the BioMark™ HD-System (Fluidigm®) to perform the qPCR assay using the BioMark HD Data Collection Software v.3.1.2 (Fluidigm®) and the GE 192 x 24 Fast PCR+Melt v2.pcl cycling program with parameter settings according to the manufacturer's Fluidigm® 192.24 Fast/Standard Gene Expression Workflow protocol.

7. Analysis of qPCR data

The obtained qPCR data were analysed using the Fluidigm®RealTime PCR Analysis Software v. 3.0.2. The qPCR measurements for the standard dilutions were used to generate a relative standard curve for each applied primer set. Based on this standard curve, relative copy numbers were interpolated for all tested samples applying formula (1). If not otherwise specified, the relative copy numbers were normalised as described in 2.2.4.8.

2.2.5. Agarose gel electrophoresis

Following DNA amplification by PCR or qPCR the resulting DNA fragments were separated and visually checked with the help of horizontal gel electrophoresis. Agarose concentration of the gel varied from 0.5% to 2.5%, since it was adjusted to the expected size of the DNA fragments. The corresponding amount of agarose was solved in 0.5 x TBE electrophoresis buffer (see A.1.1) by shortly boiling up the mixture in a microwave oven. Under soft stirring the solution cooled down and ethidium bromide was added to a final concentration of 0.05 ‰. Then the gel was poured into a casting tray with a sample comb. After complete gelation, samples mixed with 0.2 volumes of loading buffer (see A.1.1) were load to the gel. Additionally, alongside the tested samples a DNA ladder of known fragment sizes was run on the gel. On this, according to the expected size of the assessed samples 5 µl FastRuler Low Range DNA Ladder (50 - 1500 bp) (Thermo Scientific), or 5 µl GeneRuler 1 kb DNA Ladder (250 - 10000 bp) (Thermo Scientific) were deployed. Electrophoresis was carried out at 100 V in 0.5 x TBE electrophoresis buffer until complete and sharp separation of the DNA fragments. Due to the ethidium bromide staining

of the nucleic acids during electrophoresis the DNA fragments could be visualised using the ultraviolet transilluminator function of the ChemiDoc MP (Bio-Rad).

2.2.6. Purification of PCR products and cDNA

For efficient subsequent use PCR products and cDNA were purified from primers, salts, unincorporated nucleotides and thermostable DNA polymerases with the help of the *High Pure PCR Product Purification Kit* (Roche). Therefore 100 µl of binding buffer were added to 25 µl sample, mixed and applied to a *High Pure Filter Tube*. Through centrifugation for 30 s at 10000 rpm (RT) DNA > 100 bp was bound to the filter. Next, the DNA was purified twice by adding wash buffer (500 µl; 200 µl) and subsequent spinning for 60 s at 10000 rpm (RT). The DNA was eluted by adding 10-100 µl *A. dest.* to the tube and was then, after 20 min of incubation, spun down for 2 min at 14000 rpm (RT). Finally, the supernatant was transferred to a new 1.5 ml or 0.5 ml tube (Sarstedt) and stored at -20°C (DNA) or -80°C (cDNA).

2.2.7. DNA cloning

2.2.7.1. Preparation of competent *E.coli* XL1 Blue-Cells The preparation of *E. coli* $CaCl_2$ competent cells was performed according to a modified protocol originally developed by Hanahan (1983). Initially, from a frozen stock of *E.coli* XL1-Blue cells (Stratagene), one inoculation loop was streaked onto a TY agar plate (supplemented with tetracycline; see appendix A.1.2) and incubated over night at 37°C. Then, three colonies were picked off the TY agar plate, inoculated into 5 ml SOB medium (A.1.2) and incubated over night at 37°C and 180 rpm on a rotary shaker. 5 ml of the liquid culture were then transferred into 50 ml of PSI broth (A.1.2) and grown in an Erlenmeyer flask up to a OD_{600} of 0.45 to 0.55. Subsequently, 50 ml of the culture were decanted into 50 ml centrifuge tubes (Roth), incubated on ice for 15 min and pelleted (15 min at 3000 x g). The cell pellet was resuspended in 16 ml ice-cold RF1-solution (A.1.2), again incubated on ice (10 min) and pelleted (15 min at 3000 x g). The cell pellet was resuspended in 4 ml ice-cold RF2-solution (A.1.2) and incubated on ice (15 min). Finally, 40 µl aliquots of competent cells were pipetted into 1.5 µl reaction tubes (Sarstedt) and immediately flash frozen in liquid nitrogen. The competent *E.coli* XL1-Blue cells (Stratagene) were stored at -80°C until further use.

2.2.7.2. Ligation of PCR fragments into the pGEM®-T Easy Vector For efficient sequencing of the whole fragment, PCR products were inserted into a vector with single 3'-terminal thymidine overhang via the TA cloning method (Zhou *et al.* 1995). Since thermostable polymerases like the *Taq* (polymerase from *Thermus aquaticus*) often add a single 3'-terminal adenosine to dsDNA the efficiency of the PCR product ligation is highly enhanced by T-overhangs at the insertion site of the vector (Zhou & Gomez-Sanchez, 2000). Additionally, the T-overhangs prevent a recirculation of the linearised vector. Ligation was carried out using the pGEM®-T Easy Vector System (Promega) as follows: 7.6 µl of purified PCR product (2.2.6) were mixed in a 1.5 µl tube (Sarstedt) with 1.0 µl 10 x Ligation Buffer, 1.0 µl T4 DNA Ligase and 0.4 µl pGEM®-T Easy Vector. The mixture was briefly centrifuged for 20 s at 10000 rpm and then incubated at RT for at least two hours or preferentially at 4°C over night. Ligation reaction was stored at -20°C or immediately applied to subsequent transformation (2.2.7.3).

2.2.7.3. Transformation of pGEM®-T Easy Vector into competent *E.coli* cells The ligation reaction (2.2.7.2), i.e., the pGEM®-T Easy Vector containing the ligated target PCR product, was applied

to transformation into $CaCl_2$competent *E.coli* XL1-Blue cells (Stratagene) (2.2.7.1). Therefore, the ligation reaction was heated at 60°C for 5 min, cooled down on ice and pipetted into a tube containing a 40 µl aliquot of competent *E.coli* XL1-Blue cells (Stratagene). Then, the transformation reaction was incubated on ice for 20 min and subsequently heat shocked at 42°C for 90 s in a heating block. The tube was immediately put on ice for 2 min while adding 160 µl of SOC medium (A.1.3) and then incubated for at least 1 h at 37°C on a heating shaker (180 rpm). The transformation reaction was entirely plated on TY agar plates supplemented with X-gal, IPTG and ampicillin (for blue-white colour screening; see A.1.3) and following incubated over night (12-16 h) at 37°C. Next, a colony PCR was carried out to screen for positive clones that contain plasmids with the desired DNA insert. To this, 10 white colonies were picked off the TY agar plates with sterile pipette tips and dipped each in a tube containing a PCR reaction with vector- and/ or insert-specific primers. Then, a standard PCR procedure with a final volume of 10 µl was performed according to 2.2.4.2, but the amount of template DNA was substituted by *A. dest*. The PCR products were tested for proper DNA insert size by agarose gel electrophoresis (2.2.5). Positive clones containing the desired DNA insert were inoculated into 1.5 ml TY liquid growth medium (supplemented with ampicillin; see A.1.3) and grown over night on a rotary shaker (180 rpm) at 37°C. Finally, the bacterial cultures were applied to plasmid mini-preparation as described in section 2.2.8.

2.2.8. Plasmid mini-preparation

Plasmid mini-preparation was performed to isolate plasmid DNA from a small-scale bacterial culture (0.5 - 5 ml) by the method of alkaline lysis, originally developed by Bimboim *et al.* (1979). An overnight culture of successfully transformed *E.coli* XL1-Blue cells (2.2.7.3) was pelleted (1 min, 12000 x g, RT) and applied to plasmid isolation and subsequent purification using the ZR Plasmid Miniprep™-*Classic* kit (Zymo Research) according to the manufacturer's instructions. In case of large DNA inserts > 1500 bp a restriction reaction was performed instead of the colony PCR, to verify the exact integration of the expected DNA insert into the plasmid. Therefore, plasmid DNA, previously purified by mini-preparation, was digested according to the protocol given in section A.1.4 using appropriate restriction enzymes. After restriction digestion, the correct size of the resulting DNA fragments were assessed by agarose gel electrophoresis (2.2.5). Purified plasmid DNA containing the required DNA insert was then supplied to sequencing (2.2.9).

2.2.9. Sequencing

The sequencing of purified plasmid DNA or PCR products was performed either in the service laboratory for DNA sequencing of the Leibniz Institute for Farm Animal Biology (FBN-Dummerstorf) with the ABI Prism 377 DNA Sequencer (Applied Biosystems), applying the chain termination method developed by Sanger *et al.* (1977), or by the Qiagen sequencing service (Hilden,Germany). Primers used for sequencing were specific for the T7 and SP6 RNA polymerase promoters flanking the multiple cloning region of the pGEM®-T Easy Vector, or specific for the target gene. Prior to publication of DNA sequences in the European Nucleotide Archive (ENA), every single nucleotide position was confirmed as consensus from at least three independent sequencing reactions.

2.2.10. Microarray analysis

2.2.10.1. Sample preparation and measurement Tissue samples obtained in the course of the density stress (2.1.4) and the temperature stress (2.1.5) experiment were additionally employed to perform microarray analyses. Therefore, total RNA was extracted from liver, spleen and kidney samples of 7 maraena whitefish obtained from the different examined experimental conditions, respectively. Then, 600 ng/µl pools for the density stress and 500 ng/µl pools for the temperature stress experiment were prepared for each tissue and condition. The pooled RNA samples were supplied to Miltenyi Biotec GmbH. Subsequently, RNA quality control, Cy3-labeling of the RNA, and the hybridisation of the cRNA samples to 8 x 60 K Salmon Oligo Microarray chips (Agilent-049158; GEO platform: GPL21057) were performed by the Miltenyi Biotec microarray service according to the Agilent 60-mer oligo microarray processing protocol. For both experiments (density stress and temperature stress) each time one chip per tissue was applied, containing double pools for all tested conditions, since both experiments were carried out in duplicates.

2.2.10.2. Microarray-data analysis The resulting microarray raw data, delivered by Miltenyi Biotec, were subsequently computed using the limma package (version 3.34.9;Ritchie *et al.*, 2015) of the Bioconductor project in the open source user interface RStudio (version 1.1.419) of the programming language R (version 3.4.3). Initially, raw data files were imported to R, then limma was used to correct the data regarding background signals and additionally the arrays were normalised to exclude technical effects (Smyth & Speed, 2003). Finally, based on linear models and the statistical technique of Empirical Bayes the limma software identified genes that were differentially expressed (DE) between different experimental conditions (Phipson *et al.*, 2016; Smyth, 2004). Genes were considered differentially expressed if the adjusted p-value was $p < 0.05$ and the absolute fold change was at least $FC > 2$. The identified DE genes were re-annotated using BLAST algorithm, and for subsequent analyses only those genes were taken into account that met the following criteria: coverage and sequence identity of $> 80\%$ and an E-value $< 1 \times 10^{-4}$.

2.2.10.3. Construction of Venn diagrams To get an overview of the DE genes for the different experimental conditions and tissues tested, the DE-gene sets from the microarray-data analysis were used to create area-proportional Venn diagrams. Therefore, lists of DE genes, based on Agilent gene names, were constructed and load to BioVenn software (Hulsen *et al.*, 2008). The BioVenn software automatically identifies redundant genes and joins them to only one entry.

2.2.11. Transcriptome sequencing

Previously isolated and sequenced DNA fragments were verified and complemented by alignments with transcriptome data of *C. maraena* using the bioinformatics software Unipro UGene (Okonechnikov *et al.*, 2012). *C. maraena* transcriptome analysis was carried out to gain a first insight into transcriptome composition of maraena whitefish. Therefore, various tissues (liver, spleen, gills, muscle, gonads, brain) from several juvenile maraena whitefish were used to isolate total RNA (2.2.1). RNA concentration was then adjusted to tissue-specific pools of 200 ng/µl and supplied to LGC Genomics GmbH (Berlin, Germany). The cDNA preparation and library construction was carried out by the LGC Genomics sequencing service, as well as the sequencing in a 454 Genome Sequencer FLX system (Roche) and the subsequent contig

assembly. Final assessment of the obtained *C. maraena* transcriptome data was proceeded as described by Brietzke *et al.* (2016).

2.3. Cortisol enzyme immunoassay

Cortisol concentrations of plasma samples, obtained from the density stress (2.1.4) and the temperature stress (2.1.5) experiment, were determined using the DRG Cortisol Enzyme Immunoassay Kit (DRG Instruments GmbH). Prior to the test procedure blood samples were centrifuged (4°C and 1700 rcf) and the supernatant was kept on ice until the measurement.The ELISA test procedure of the kit bases on competitive binding of cortisol (cortisol of samples versus cortisol of enzyme conjugate of the kit) to a cortisol-specific monoclonal antibody. The cortisol assay procedure was performed according to the manufacturer's protocol and the entire set of samples was analysed at the Beckman Coulter DTX 800/880 Series Multimode Detector (Beckman Coulter). Each sample was measured two times independently, mean values were calculated and the resulting data were analysed by a 4 parameter logistic curve fit using the GraphPadPrism® software (version 7.03).

2.4. Western blot

Specific detection of proteins in various tissue samples was carried out by an antibody-based staining in a Western blot procedure. Previously, protein extracts were isolated from liver, gills and muscle samples of 3 maraena whitefish, respectively. To this, 0.1-0.3 g of frozen tissue were put into 2 ml screw-cap tubes (Sarstedt) containing four sterile ceramic beads (2.8 mm Ø; Precellys®, Peqlab Biotechnologie) and 1.5 ml RIPA buffer (see A.1.5) supplemented with complete Mini (Roche) as protease inhibitor. The tissue samples were homogenised 2 x 30 s at 6000 rpm using the Precellys®24 Homogeniser (Peqlab Biotechnologie) and then immediately incubated on ice for 20 min. The tissue samples were centrifuged for 10 min at 14000 rpm and 4°C, the supernatant was decanted in to a new 1.5 ml reaction tube (Sarstedt) and the whole cell lysate protein content was determined using the NanoDrop 1000 Spectrophotometer (Peqlab Biotechnologie). Subsequently, a concentration of 80 µg protein per sample were load on a 12% TGX Stain-Free™ FastCast™ SDS-Gel (Biorad) and separated under non reducing conditions by SDS-PAGE. Samples were then transferred onto 0.2 µm PVDF membranes (Merck Millipore) for 1 h at RT, followed by a stain-free based transfer control as recommended in the manufacturer's protocol (Biorad). Prior to incubation with the primary polyclonal antibodies, the membranes were blocked for 1 h in 5% bovine serum albumin dissolved in TBST (Tris-buffered saline and 0.05% Tween 20; pH 7.4) at RT. Then, the antibodies rabbit anti-barramundi IGF-1 (1:500; GroPep) or rabbit anti-salmon/trout IGF-2 (1:50; GroPep) dissolved in TBST were added onto the membrane and incubated over night at 4°C. Next day, after washing membranes in TBST, the secondary antibody (HRP-conjugated anti-rabbit IgG; 1:2500; Santa Cruz Biotechnology) was added to the membranes and incubated for 1 h at RT. Detection of the protein signal was carried out by enhanced chemiluminescence with the ChemiDoc MP System (Biorad) using the reagent Luminata Forte (Merck Millipore). Throughout the Western blot assay, salmon IGF-1, as well as salmon/ trout IGF-2 recombinant proteins (rsIGF-1; rsIGF-2; GroPep) were used as positive controls for the IGF-1 and IGF-2 target proteins. For more details see also Nipkow *et al.* (2018).

2.5. Cell culture techniques

2.5.1. Isolation of head kidney primary cells

In order to perform *in vitro* cell stimulation experiments, head kidney cells were isolated from eight juvenile maraena whitefish, aged 65 to 69 wph, having a total weight of $\bar{x} = 131.9 \pm 42.0$ g, and a total length of $\bar{x} = 25.1 \pm 2.1$ cm, that were previously reared in a flow-through system as described in 2.1.1. The given protocol was developed referring to methods published by Mackenzie *et al.* (2003) and MacKenzie *et al.* (2006). Throughout the whole experiment cell culture medium (CCM) was prepared as follows: Dulbecco's Modified Eagle Medium (DMEM; Gibco) was supplemented with 10% heat-inactivated fetal bovine serum (FBS; PAN-Biotech) and an antibiotic antimycotic solution (Sigma-Aldrich) containing final concentrations of 100 units/ml penicillin, 0.1 mg/ml streptomycin and 0.25 µg/ml amphotericin B.

For isolation of head kidney cells, the fish were killed by an overdose of 2-Phenoxyethanol (Sigma-Aldrich) and subsequently bled to decrease red blood cells in head kidney tissue, and general bleeding within the procedure (Goetz *et al.*, 2012). The fish's surface was sterilised with 70% ethanol and the head kidney was dissected under sterile conditions in a laminar flow hood (HERAsafe® KS, Heraeus®). Each head kidney was transferred into a sterile petri dish (Sarstedt) containing 2.0 ml of CCM and incubated for 5 min at RT. Then, the tissue was squeezed through a steel sieve (0.1 mm, Roth) with the help of a spatula to isolate cells. The CCM containing the separated cells was strained through two additional sieves (200 µm, PluriSelect; 100 µm, BD Falcon) attached to 50 ml centrifuge tubes (Roth). To improve the cell straining, up to 3 ml CCM were added to wash out residual cells from the sieves. The cells were pelleted for 5 min at 1500 rpm (RT) and subsequently resuspended in 1.0 ml 1 x PBS solution (Biochrom AG). Next, the isolated cells were counted in a Neubauer chamber (neoLab) and the cell size and viability was assessed using a Cellometer® Auto 2000 (Nexcelom Bioscience) then pelleted again (5 min, 1500 rpm, RT). The cell pellets were resuspended in appropriate volumes of CCM. Subsequently 2.0 ml medium containing 0.5×10^6/ml cells were plated on 6-well Poly-D-Lysin plates (Cellcoat®, Greiner Bio-One) and incubated over night at 20°C and 5% CO_2 atmosphere. Next day, the isolated head kidney cells were used for cell stimulation experiments as indicated in 2.1.7.

2.5.2. Characterisation of primary head kidney cells by flow cytometric analysis

After isolation from head kidney, primary cells have been resuspended in 1 x PBS solution and then subjected to a flow cytometric cell sorting using a MoFlo XDP high-speed cell sorter (Beckman Coulter, USA) equipped with an air cooled coherent sapphire laser (488 nm; 100 mW). Optimal settings to sort the cells were provided by a 70 µm nozzle at 60 psi in purify mode. The trigger signal used for all measurements was the forward scatter. The cells were sorted according to lower side scattering (corresponding to cell granularity) and higher side scattering intensities. The purified fractions were collected in PBS and re-analysed. The sorting efficiency was $94 \pm 3\%$. Fractions were centrifuged (500 x g, 5 min) and the supernatant was removed to get a dry pellet. Pellets were flash frozen in liquid nitrogen and then stored at -70°C for subsequent RNA isolation (2.2.1).

2.6. Bacterial strains and plasmids

Escherichia coli strain XL1-Blue MRF	Stratagene, La Jolla, USA
Aeromonas salmonicida subsp. *salmonicida*- wild type strain JF 2267	Microbank™, Pro-Lab Diagnostics, Cheshire, UK
pGEM®-T easy Vector system	Promega, Mannheim, Germany

2.7. *In silico* analyses

2.7.1. Sequence analysis

Analysis and assessment of data resulting from sequencing experiments (2.2.9) was always performed with the bioinformatics software Unipro UGene (Okonechnikov *et al.*, 2012). Additionally, Unipro UGene was used to perform alignments, to calculate sequence identities and to deduce protein sequences from isolated cDNA sequences. Additionally, ExPASy webpage (SIB; Swiss Institute of Bioinformatics) was used to identify ORFs. The secondary structure of putative protein sequences were predicted with the help of the NCBI conserved domain database (Marchler-Bauer *et al.*, 2017), the Scan Prosite tool (de Castro *et al.*, 2006) and the Swiss Model tool (Bienert *et al.*, 2017; Waterhouse *et al.*, 2018; Guex *et al.*, 2009) from the ExPASy webpage (Swiss Institute of Bioinformatics), as well as with the SignalP 4.1 Server (Nielsen, 2017; Petersen *et al.*, 2011) provided by the Technical University of Denmark. Graphical representations of sequence alignments were created and edited using CLUSTALW on PRABI webpage (Combet *et al.*, 2000)from the Institute of Biology and Protein Chemistry, Lyon (France).

2.7.2. Phylogenetic analysis

Based on evolutionary analyses phylogenetic trees were generated using the software MEGA 7 (version 7.0.26;Tamura *et al.*, 2013). Prior to this, the deduced protein sequences were applied to a multiple sequence alignment as described in 2.7.1. Subsequently, phylogenetic distances were calculated in MEGA 7 using the Neighbour-Joining method (Saitou & Nei, 1987) to construct a bootstrap tree (Felsenstein, 1985) inferring from 10,000 replicates and evolutionary distances were computed using the Poisson correction method. The trees are drawn to scale, with branch lengths in the same units as those of the evolutionary distances used to infer the respective phylogenetic tree. All positions containing gaps and missing data were eliminated. All evolutionary analyses are based on nucleotide or protein sequences of the same species, as available from the NCBI GenBank, unless otherwise stated. These were: *Onchorynchus mykiss* (rainbow trout), *Salmo salar* (Atlantic salmon) and *Danio rerio* (zebrafish) for the bony fish, *Callorhinchus milli* (Australian ghostshark) or *Squalus acanthias* (spiny dogfish) for the cartilaginous fish, *Gallus gallus* (chicken or red junglefowl) as the representative of the birds, and *Mus musculus* (mouse) and *Homo sapiens* (human) for the mammals.

2.7.3. Gene-network generation

Gene networks shown in this study were generated using the software Ingenuity® Pathway Analysis (IPA, Qiagen). Lists of DE genes, resulting from the limma-based microarray calculations (see section 2.2.10) were assigned to functional pathways within the IPA analysis. Therefore, data sets containing gene identifiers and corresponding expression values were uploaded into the application. Within this study expression values were always uploaded as average fold changes of the different tested tissues for a specific

gene of interest. Then, each identifier was mapped to its corresponding object in Ingenuity's Knowledge Base and networks were algorithmically generated (Krämer *et al.*, 2014) based on their connectivity. The following functional analysis, identified the biological functions that were most significant to the molecules in a certain network. Additionally, the upstream regulator analysis predicted factors that were very likely to have caused the differential expression of the tested gene-set for a certain experiment. Since the Ingenuity Knowledge Base is constructed from investigations in mammalian (human, mouse, and rat) in vivo and in vitro systems, the resulting pathways were carefully reviewed with regard to their presence and function in teleosteans. Right-tailed Fisher's exact test was used to calculate a p-value determining the probability that each biological function assigned to that network is explained by chance alone. Moreover, standard scores (z-scores) were calculated to assess whether certain pathways were activated ($z > 1$), inhibited ($z < 1$), or not affected (z-scores around 0). If no prediction could be made for a pathway, this is indicated by "n.a." (not available) at the respective position.

2.7.4. Computing and plotting

Raw data obtained in this study, e.g., Cq values from qPCR experiments, were analysed and computed using Microsoft Excel 2010 and GraphPadPrism® software (version 5.01 and 7.03). The subsequent plotting of the data, unless otherwise specified, was always performed with GraphPadPrism® software (version 5.01 or 7.03).

Unless otherwise specified, the box-plots given in this study are arranged as described in the following: The left to right border of the boxes indicate the 25 to 75 percentiles and the vertical line within the box mark the median. The whiskers represent the 10 to 90 percentiles (from left to right) and values below or above the whiskers are drawn as individual points.

Heat maps were computed with the help of the open source user interface RStudio (version 1.1.419) of the programming language R (version 3.4.3) and the heatmap.2 function of the gplots package (version 3.0.1). The mRNA copy numbers were previously calculated as fold changes (FC) of a given reference (e.g., a control group). If the resulting FC was less than one, the reciprocal (-1/FC) was calculated and listed in the heat map (e.g., $FC = 0.5$ was transformed into -2, i.e., target gene expression was 2-fold down-regulated at a certain treatment compared to the control group).

2.7.4.1. Statistical analysis Statistical analyses were performed with GraphPad Prism® Software (GraphPad Prism 7.03), using one-way or two-way ANOVA followed by Tukey or Bonferroni post-tests, respectively. P-values < 0.05 were considered significant. In figures significance levels were indicated by asterisks as specified in table 2.10.

Table 2.10: **Significance levels**

Icon	P-value	Significance level
*	$p < 0.05$	significant
**	$p < 0.01$	highly significant
***	$p < 0.001$	extremely significant

3. Results

In the course of this study, several experiments were performed to examine the potential of maraena whitefish as a new native species for local, sustainable and economically competitive aquaculture. Therefore, maraena whitefish was analysed on phenotypic and molecular biological level to compose a first picture of the fish's general constitution during the farming procedure and to further characterise its molecular response to specific conditions of the new and artificial environment. Subsequently, the experiments served to estimate the fish's susceptibility regarding aquaculture relevant parameters like, water quality and temperature, stocking density and pathogens.

3.1. Phenotypic analysis of maraena whitefish in different aquaculture systems

To get a first insight into the fish's capability of coping with aquaculture conditions, maraena whitefish were reared simultaneously in two different aquaculture systems, and phenotypes were compared regarding weight and length gain. At the age of 12 wph and an average weight of 10 g maraena whitefish were separated into two cohorts and transferred from fresh water recirculation system into two different aquaculture systems, i.e., a recirculation and a flow-through system (2.1.1, both supplied by brackish water). From the age of 17 wph until 48 wph, matched sampling of seven fish per system was carried out to determine fish length and weight. Then, data was used for comparative analysis of body condition (weight to length relation) and time-dependent growth of fish in both systems, as described in detail in section 3.1.1, as well as 3.1.2.

3.1.1. Analysis of the fish's weight to length relation by Fulton's condition factor

In fisheries science the relation of weight to length is used as indicator for the fish's health. Therefore, figure 3.1 displays fish weight plotted as function of fish length for fish grown in a recirculation system (3.1a), as well as in a flow-through system (3.1b). Further linear regression was carried out using Fulton's equation as a model (2.1.2) to determine the specific condition factor K for fish reared in the respective system. The high values for the coefficient of determination $R^2 = 0.98$ and $R^2 = 0.97$ for recirculation and flow-through data, indicate that the fitted curves are very close to the given data points for both data sets. Further, the data clearly revealed a much higher growth of fish reared in the tempered and purified brackish water of the recirculation system, compared to fish kept in the non-tempered, untreated brackish water of the flow-through system. That is reflected by a much higher condition factor of $K = 1.09$ for fish of the recirculation system compared to $K = 0.86$ for fish of the flow-through system. By comparison, this means that at the same length, fish reared in the recirculation system showed higher weights than respective fish of the flow through system. Apart from that, length and weight values for fish grown in the recirculation system were generally higher.

3.1.2. Analysis of time-dependent length and weight gain

Time-dependent growth of fish in both aquaculture systems was analysed in terms of length and weight gain, as shown in figure 3.2. The plotted curves were fitted by non-linear regression using the Bertalanffy growth equations as model (2.1.2). Analysis of maraena whitefish length gain over time (see figure 3.2a) revealed at all time points examined, that the total length of fish kept in the recirculation system was plainly higher than that of fish kept in the flow-through system. Additionally, there was no overlap of the

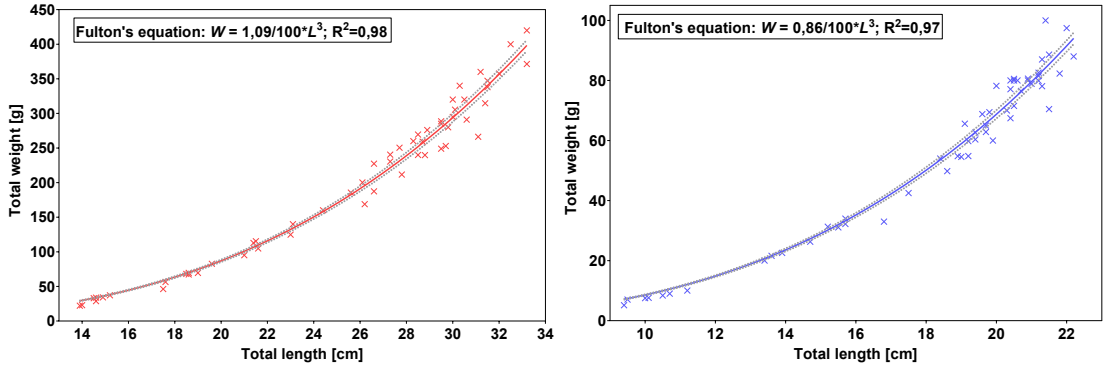

(a) Recirculation system (b) Flow-through system

Figure 3.1: **Analysis of weight-to-length-relation of maraena whitefish reared in a recirculation or a flow-through system**
In each case, the total length and total weight of all in all 56 fish of the recirculation (3.1a) and the flow-through system (3.1b) were determined and plotted. Data points were analysed by non-linear regression using Fulton's equation as a model. The resulting best fit curve is figured as a red line for the recirculation data (3.1a), as well as a blue line for the flow-through data (3.1b). The respective 95% confidence intervals of the curves are depicted as grey dashed lines.

calculated 95% confidence intervals of both best fit curves. Fish kept in untreated brackish water (flow-through) reached only about 70% of the body length fish gained in tempered, purified brackish water (recirculation). Thus, the final body length, determined after 48 wph, was on average 20.61 cm for fish of the flow-through system compared to 31.43 cm for fish of the recirculation system. Figure 3.2b displays the comparative time-dependent weight gain of maraena whitefish in the two tested aquaculture systems. Overall the weight gain of maraena whitefish was clearly higher in the recirculation system, although at the beginning of the assessment at 17 wph the 95% confidence intervals of the two calculated curves showed an overlap. Nonetheless, at all examined time points the body weight of maraena whitefish in the flow-through system, was averaged merely 30% of the fish's body weight in the recirculation system. There was a sharp increase in total weight for fish reared in the recirculation system, since the predicted

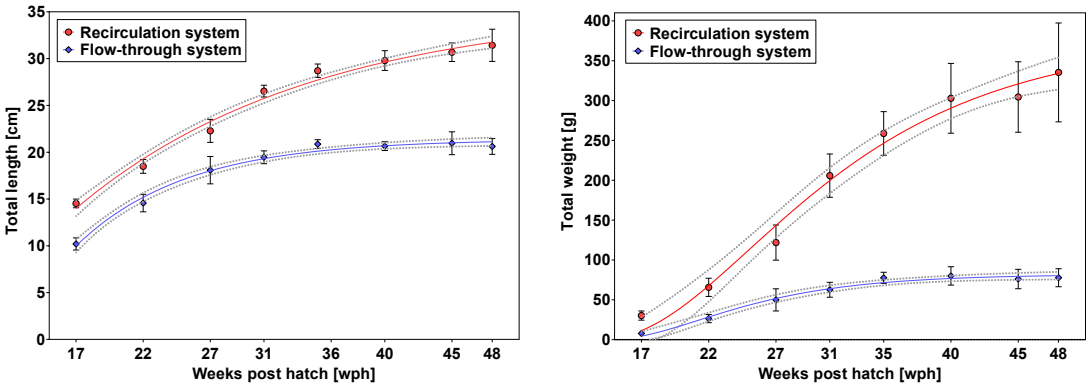

(a) Time-dependent length gain (b) Time-dependent weight gain

Figure 3.2: **Time-dependent length and weight gain of maraena whitefish reared in a recirculation or a flow-through system**
Over a time period of 31 weeks the data for total length and total weight of seven fish per time point of the recirculation or the flow-through system were gathered. Figure 3.2a displays fish length as mean ± SD, whereas figure 3.2b displays the mean ± SD of fish weight. All data sets were analysed by non-linear regression using Bertalanffy's growth equations as models. The resulting best fit curves are figured as red lines for the recirculation data, or as blue lines for the flow-through data. The 95% confidence intervals of the respective curves are depicted as grey dashed lines.

growth curve clearly drifts apart from the one displaying the weight gain of fish in the flow-through system. Accordingly, fish of the recirculation system gained slaughter age at 48 wph with an average weight of 335.34 g, whereas the body weight was averaging not more than 77.68 g at the same time point for fish of the flow-through system. Moreover, length and especially weight gain for fish kept in the recirculation system were still increasing as indicated by the upward sloping curves. Whereas the flattening curves for both, length and weight gain for fish grown in the flow-through system remained nearly static from 40 wph onwards.

3.2. Isolation and characterisation of target genes

In the course of this study, three different target-gene sets were analysed, which were selected based on previous experiments performed in rainbow trout, through network analysis using IPA software, or by literature research, as explained in sections 1.2, 1.3, and 1.4. Since maraena whitefish, is a relative new salmonid species in aquaculture compared to well domesticated trout, gene expression data regarding its ability to cope with aquaculture relevant conditions and stressors are rare or still completely missing. Hence, to get a first overview of the influence of farming procedures and the exposure to aquaculture related stressors on maraena whitefish's gene expression, the selected target-gene sets cover three main areas of interest: (i) immune response, (ii) stress response , and (iii) growth and development.

In order to analyse the target-gene sets, initially sequences of the open reading frames (ORFs) were isolated -completely or partially- from maraena whitefish. Since no sequence information was available for the selected genes at that time, consensus primers were derived from orthologous genes of other closely related salmonid species, or if not available, from other teleost species, as explained in section 2.2.4.1.2. Table B.2 in the appendix summarises all species used to derive consensus primers, as well as the primers itself and the respective fragment lengths in maraena whitefish. Moreover, the table in section C gives an overview of all maraena whitefish isolates obtained and published in the course of this study. These were characterised regarding their structure and evolutionary conservation as described below.

3.2.1. Characterisation of immune genes

For the immune target genes, partial cDNAs of all genes were successfully amplified within this study.

The isolated maraena whitefish *IL1B* cDNA was 886 bp in length, comprising 65 bp of the 5' UTR, a 780 bp ORF region, and 41 bp of the 3' UTR. The ORF codes for a putative 260 aa protein with a predicted molecular weight of 29 kDa, which is well conserved within the family of salmonids ($>90\%$) but has a notable low sequence identity compared to other vertebrates, irrespective of whether fish, birds, or mammals (26-31%). For the maraena whitefish IL1B protein sequence, a comparably well conserved IL1-family signature could be identified (LESARFRNWFISTAMQQDNTKTV) and a salmonid specific N-glycosylation site as shown in figure B.2a. Further, the start of the mature peptide (marked by the first of twelve typical ß-sheet motifs) was predicted to be located in the region of aa residue 103-105 on the maraena whitefish IL1B sequence, which is four aa residues downstream from the mammalian IL1B cleavage site, marked by an aspartic acid residue (D), that is missing in maraena whitefish. For the evolutionary analysis, using additional sequences for salmonid IL1B2 (type II) and IL1B3 (type I), the hypothetical maraena whitefish IL1B could be assigned to type II IL1B proteins, since it was clearly clustered together with IL1B2 from rainbow trout, whilst the IL1B3 sequences built their own cluster within the resulting phylogenetic tree (see figure B.2b). Notably, all putative teleostean IL1B proteins

were grouped together in one major branch, whereas IL1B proteins from all other analysed species, comprising cartilaginous fish, birds and mammals, were clustered in a second one.

For the IL6 gene, a partial 731 bp maraena whitefish *IL6* cDNA was isolated that included 20 bp of the 5' UTR and 45 bp of the 3' UTR, flanking a 666 bp ORF region that codes for a putative 222 aa protein of approximately 24.8 kDA, which revealed a comparably high sequence homology (< 89%) within the family of salmonidae, compared to the very low conservation to all other analysed vertebrate species (< 27%). However, the putative maraena whitefish IL6 protein was structurally well conserved, containing a N-terminal signal peptide, the four indicative α-helices, the IL-6 signature (C-x(9)-C-x(6)-G-L-x(2)-[FY]-x(3)-L) with the two highly conserved cystein residues (C, marked by black asterisks) that are decisive to form a disulfide bond, all of which are shown in figure B.3a. Evolutionary analysis proved the much higher similarity of maraena whitefish IL6 to its homologues in other salmonids, compared to the ones of other vertebrates. Accordingly, in the phylogenetic tree, given in figure B.3b, the putative maraena whitefish IL6 was clustered together with rainbow trout and Atlantic salmon, whilst the zebrafish built an own group within the one main teleostean branch, which was juxtaposed with the second main branch that grouped together cartilaginous fish, birds, and mammals.

The partial maraena whitefish *CXCL8* cDNA, obtained within this study was 784 bp in length, of which 4 bp belonged to the 5' UTR, 291 bp to the coding region, and the remaining 489 bp account for the full 3' UTR. The ORF encodes a comparable small putative protein of only 97 aa, having an estimated molecular weight of 10.8 kDa. With the help of structural analysis, characteristics of CXCL8 peptides were identified on the predicted maraena whitefish CXCL8 protein (see figure B.4a), such as the N-terminal signal peptide, the salmonid-specific DLR motif (similar to the mammalian ELR motif), and the four highly conserved cystein residues on positions 34, 36, 60 and 77, of which the first two form the C-x-C pattern that is decisive for these chemokines. Like previously shown for IL1B and IL6, the predicted maraena whitefish CXCL8 aa sequence revealed a high sequence identity within the family of salmonids (> 94%), an average conservation to other teleosts (> 60%), but it is poorly conserved compared to cartilaginous fish, birds, and mammals (< 38%). Based on evolutionary analyses the putative maraena whitefish CXCL8 chemokine was assigned to the CXCL8 lineage 1, since it was clearly clustered together with the fish-specific lineage 1 homologues (99% bootstrap support) of rainbow trout, common carp, and zebrafish, whilst the common carp lineage 2 CXCL8 was grouped together with its counterparts in birds and mammals as it is slightly closer related to these (≈ 30% coverage versus < 25% identity to all analysed piscine CXCL8 homologues), as to be seen in the phylogenetic tree in figure B.4b.

The gene *IL12B*, codes for one of the two subunits of IL12 and is also termed *IL12p40* in response to the molecular weight of the gene product. The partial maraena whitefish *IL12B* cDNA obtained in this study is 1130 bp in length, comprises 5 bp of the 5' UTR, besides a full ORF region of 1002 bp and a 3' UTR of 122 bp. The deduced maraena whitefish IL12p40 protein encoded by the isolated cDNA is 334 aa long and has a predicted molecular weight of ≈ 38 kDa. Further, the aa sequence shows high identity with several homologues of other salmonids (> 89%), whilst it is poorly conserved to the designated IL12p40b forms of salmonids (≈ 23%), as well as to other putative vertebrate IL12B proteins (≤ 34%), as to be seen in the multiple sequence alignment in figure B.5. These results were confirmed by evolutionary analysis, however the resulting phylogenetic tree (B.5) indicated that the predicted maraena whitefish IL12p40 protein is a member of the IL12p40c lineage, since it was clearly separated from the cluster of IL12p40a and IL12p40b, as well as from the cluster of higher vertebrate IL12p40, but grouped together with IL12p40c of common carp, supported by a high bootstrap value of 99%. According to is poor conservation to higher vertebrate IL12p40 proteins, the predicted maraena whitefish IL12p40 aa

sequence lacks several, characteristic features like the cystein residue (aa position: 211), which is regarded decisive for the formation of a disulphide bridge between the two subunits (IL12p35 and IL12p40) of the IL12 hetero-dimer. Further, not a single N-glycosylation motif (NxT/S) was identified for the three potential salmonid IL12p40c members. Nonetheless, for the putative maraena whitefish IL12p40c, three (aa positions:95,139, 152) out of the eight (aa positions: 54, 95, 139, 152, 181, 205, 324, 351) conserved cystein residues known from mammals were identified, and three additional conserved cystein residues (aa positions: 41, 146, 170) were located near to the conserved mammalian ones. Moreover, the three aa residues (E,Y, D; aa positions: 215, 284, 336) that are crucial and two out of four aa residues (Y, P; aa positions: 144, 212) that are important for the formation of the IL12p70 hetero-dimer are conserved for the potential maraena whitefish IL12p40c. Additionally, the C-terminus of the potential salmonid IL12p40c sequences exhibit a WSxWT motif, which is highly similar to the conserved WSxWS motif (WSxWAS in humans), present in all vertebrate sequences analysed, except from rainbow trout and common carp IL12p40b and mouse IL12p40 sequences.

The isolated maraena whitefish *TNF* cDNA of 801 bp, comprises 35bp of the 5' UTR and 766 bp of the OPR region, which codes for a partial protein of 255 aa residues. The putative maraena whitefish TNF protein shares high sequence identity to salmonid TNF-α1 and TNF-α2 isoforms ($>89\%$), but the similarity to rainbow trout TNF-α3 is significantly lower ($\approx 49\%$), as well as to other piscine TNF isoforms ($\approx 40\%$) and the ones of reptiles and mammals ($<27\%$). Structural analyses showed, that the maraena whitefish TNF aa sequence contains a transmembrane domain (aa position: 48-68), a TNF-α-converting enzyme (TACE) cut site between T (Threonine) and L (Leucine) residues at aa position 102 and 103, a conserved TNF-family signature motif ([LV]-x-[LIVM]- x_3-G-[LIVMF]-Y-[LIVMFY]$_2$-x_2-[QEKHL]) (except from an "I" (Isoleucine) instead of a "L" (Leucine) or "V" (Valine) in the first position), as well as two highly conserved cystein residues that most likely form a disulphide bridge (aa position: 173, 218), all of which are indicative for TNF members (see figure B.7a). Further, the phylogenetic tree shown in figure B.7b, summarises the relationship of the putative maraena whitefish TNF to several other vertebrate TNF proteins. The tree was divided into two main branches, one for all piscine TNF's and another for those of reptiles and mammals. The maraena whitefish TNF protein was clustered together with the salmonid TNF-α1 and TNF-α2 isoforms (100% bootstrap support), whereas the TNF-α3 isoform of rainbow trout built an out-group within the salmonid clade. However, all other teleostean TNF's were grouped together in a second independent clade within the main branch of piscine TNF molecules.

Within this study, for the *SAA* gene, a partial maraena whitefish *SAA* cDNA of 419 bp was isolated comprising a 363 bp ORF region, flanked by 37 bp of the 5' UTR and 16 bp of the 3' UTR. The ORF codes for a putative protein of 121 aa, containing a N-terminal signal peptide, followed by the typical hydrophobic region. In the middle domain of the predicted maraena whitefish SAA protein the highly conserved SAA signature pattern (A-R-G-N-Y-[ED]-A-x-[QKR]-R-G-x-G-G-x-W-A) was identified and the molecular weight of the mature protein was estimated to be 11.6 kDA. Multiple sequence alignment showed the relatively high conservation of the putative SAA aa sequence compared to other vertebrates, which was by far highest within the family of salmonids ($>90\%$), followed by average values ($>63\%$) for other teleosts and mammalian A-SAA (see figure B.8a). However, the lowest sequence identity of the maraena whitefish SAA was determined in comparison to its homologue in chicken ($<60\%$) and to the mammalian C-SAA forms ($<49\%$). Consequently, these results were reflected within evolutionary analysis, since all vertebrate SAA proteins were clustered together, except from the mammalian C-SAA proteins, which built an own major branch, as to be seen in the phylogenetic tree in figure B.8b.

Nonetheless, the second major branch, which contained the piscine SAA and the mammalian A-SAA proteins, was again subdivided into several clades, in which the mammalian and avian SAA molecules were distinctly separated (bootstrap support of 99%) from their homologues in teleosts. Moreover, within the teleostean sub-tree, the salmonid SAA proteins were grouped together with a high bootstrap value of 99%.

For the two genes *MAPK1* and *MAPK3*, encoding two closely related protein-serine/threonine kinases, cDNAs of 215 bp and 784 bp length were obtained within this work. The partial maraena whitefish *MAPK1* cDNA is located completely within the ORF region, coding for 71 aa residues, whilst the partial maraena whitefish *MAPK3* cDNA comprises 756 bp of the ORF and 28 bp of the 3' flanking region and codes for a sequence of 251 aa residues. The deduced aa sequences of maraena whitefish MAPK1 and MAPK3 were analysed using multiple sequence alignment, which clearly unveiled the high degree of conservation of these kinases. Since the sequence for maraena whitefish MAPK1 was relatively short, it revealed a considerably high similarity of $>94\%$ among all included vertebrate species (see figure B.9a), nonetheless for the much longer sequence of maraena whitefish MAPK3 $>90\%$ aa identity were calculated, compared to teleosts and mammals (see figure B.9b). Further, for the maraena whitefish MAPK1 and MAPK3 aa sequences highly conserved structures were identified, such as a catalytic loop, an activation segment, and for MAPK3, additionally a kinase insert domain. Evolutionary analysis of the deduced maraena whitefish MAPK1 aa sequence resulted in unreliable bootstrap values $<10\%$ and therefore nucleotide sequences were used to create a phylogenetic tree, including both *MAPK1* and *MAPK3* cDNAs for different vertebrate species. The phylogenetic tree, given in figure B.10, was clearly separated into one major branch for all *MAPK1* sequences and another for all *MAPK3* cDNAs, supported by a high bootstrap value of 98%. Moreover, within the two subtrees of *MAPK1* and *MAPK3* cDNAs, the ones of mammals and teleosts were clustered in distinct clades, respectively. Within the teleostean MAPK3 cluster the salmonid- and the cyprinid-specific sequences were grouped separately and far apart from each other, however for the *MAPK1* gene no suitable sequence data was available, neither for zebrafish, nor for common carp.

3.2.2. Characterisation of stress genes

Regarding the stress-gene set, a partial 1002 bp maraena whitefish *HSP70* cDNA was isolated, which is located completely within the ORF region of this gene. The isolated maraena whitefish *HSP70* cDNA is highly conserved between species (sequence identity: $>97\%$ in salmonids, 85% for teleost fish, $>76\%$ for mammalian and avian species). The deduced protein sequence of 331 aa contains two HSP70 family signature sequences, namely "IDLGTTYS" in the N-terminal domain and "IFDLGGGTFDVSIL" in the middle domain (see figure B.11a). Additionally, between position 133 and 140 an ATP/GTP-binding site (AEAYLGQK) was identified. The multiple sequence alignment of the partial protein, revealed that it is highly conserved between teleost fish species, showing $>90\%$ identity (within salmonids even $>96\%$) and compared to mammalian and avian homologues, conservation is still very high ($>85\%$).These results were confirmed by phylogenetic analysis, as one major branch was constructed for all teleostean species, including also branches for members of avian and mammalian species, whilst a second major branch was calculated for the supplemented cartilaginous spiny dogfish (see figure B.11b in the appendix).

The isolated partial cDNA for maraena whitefish *HSP90* was 920 bp, including 8 bp of the 5' UTR and 912 bp of the ORF region, coding for a putative partial 304 aa protein. All in all, three conserved HSP90 family signature sequences and a typical ATP-binding motif (GxxGxG) were identified within

the N-terminal or the middle domain of the the derived aa sequence. A multiple sequence alignment of the deduced partial maraena whitefish HSP90 protein with HSP90A and HSP90B protein sequences from seven different species, comprising teleost and cartilaginous fish, birds, and mammals, showed a very high conservation for all tested amino acid sequences, ranging between 80-84%, equally for HSP90A or HSP90B (see figure B.12a in the appendix). Further, the multiple sequence alignment data were subjected to evolutionary analysis. Within the resulting phylogenetic tree, all tested HSP90A and HSP90B sequences were clustered together in their own major branch, even though with low likelihood (20%), whilst the putative maraena whitefish HSP90 protein built an out-group.

For the glucocorticoid receptor gene *NR3C1*, a partial cDNA was isolated, comprising 42 bp of the 5' UTR, the complete ORF region (2298 bp) and 65 bp of the 3' UTR. The maraena whitefish *NR3C1* cDNA codes for at putative 765 aa protein, with a molecular weight of approximately 84 kDa, having the typical structure of the nuclear receptor superfamily: a variable N-terminal region, a centrally located DNA-binding domain (DBD), a species-specific hinge region and a C-terminal ligand-binding domain (LBD), as indicated in figure B.13a in the appendix. Further, the DBD contains two C4-type zinc finger motifs, which are characteristic for the glucocorticoid receptor. A multiple sequence alignment of the putative protein revealed a high degree of conservation within salmonids ($> 92\%$), whilst for non-salmonid fish species, as well as for avian and mammalian species, the sequence identity was significantly lower (52-67%). However, the inter-species homology was very high within the functionally important DBD and LBD for all tested sequences (see figure B.13a) For evolutionary analysis of the putative GCR, protein sequences for the glucocorticoid receptor beta (GCR2) and the mineralcorticoid receptor (MR) were included. Within the resulting phylogenetic tree the putative maraena whitefish GCR was clustered together only with GCR sequences of other salmonids, whereas the salmonid GCR2 was separated in an own branch, likewise the GCR and/or GCR2 sequences for all other tested species. However, all analysed MR sequences were clearly separated in one major branch for all tested species.

Since there was already a GenBank entry for the *Coregonus lavaretus TP53* cDNA (EU978857), only a short segment of the maraena whitefish *TP53* cDNA was isolated within this study, comprising 408 bp of the ORF region and 32 bp of the 3' UTR, which was then aligned with the first one, resulting in 100% nucleotide identity (see figure B.14a). The partial ORF was translated into a putative aa sequence of 114 bp, which was highly conserved within salmonid species ($> 93\%$) and the identified conserved TP53-family DBD and the characteristic tetramerisation motif, revealed a high homology for all vertebrate species included in the analysis, as shown in figure B.14b. Based on the multiple sequence alignment, a phylogentic tree was created, that consisted of two major branches, one for all teleostean TP53 proteins and a second for those of higher vertebrates. However, for the fish-specific clade, all salmonids were clustered together in one branch, whilst the zebrafish and the Australian ghostshark were each grouped into separate branches (see figure B.14c).

3.2.3. Characterisation of growth-factor genes

The two partial maraena whitefish cDNAs *IGF1* and *IGF2* have been identified within this study, both starting within the 5' region, spanning the whole ORF and reaching within the 3' region. The resulting ORF regions comprise 567 bp for maraena whitefish *IGF1* and 645 bp for *IGF*2, coding for putative proteins of 189 amino acid and 215 amino acids, respectively. In order to analyse the evolutionary conservation of the typical IGF domains, both deduced protein sequences were aligned with selected homologous sequences (see figures B.15a and B.15b). These analyses clearly unveiled a very high degree

of conservation for the A-, B-, C-, and D-domains of the mature protein—that is, 70 amino acid residues for IGF-1 and 69 amino acid residues for IGF-2. However, the pre-peptide region and the E-domain belonging to the pre-propeptide are diverse.The highest sequence identity between the examined species emerged in the A-domain of IGF-1 and IGF-2 protein sequences with 95%. We found a relatively high grade of conservation for the IGF-1 B-domain (90%), followed by the D-domain (83%) and the B-domain (78%) of IGF-2. The C- and D-domains of IGF-1, as well as the C-domain of IGF-2, revealed a lower degree of conservation (less than 58%). Additionally, the evolutionary relationship of vertebrate IGF-1 and IGF-2 amino acid sequences was visualised by a phylogenetic tree (figure B.16), which showed plainly (with 100% bootstrap support) that maraena whitefish IGF-1 and IGF-2 share highest identity with their orthologues in other salmonids. Nonetheless, the zebrafish, another teleost species, is grouped together with salmonids, whilst sequences from chicken and mammalian orthologues were grouped together in an own branch. Overall, the phylogenetic analysis clearly unveils the high conservation of IGFs within salmonids and also for teleosts. Additionally, it shows that teleostean IGFs are more closely related to their avian and mammalian orthologues than to those in cartilaginous fish.

3.3. Tissue profiling of maraena whitefish

The tissue profiling experiments served to get a general overview of the tissue-specific expression of the stress, immune, and growth target genes in slaughter-aged, healthy maraena whitefish. Therefore, gene-specific qPCR measurements were performed in the following 10 tissues: brain, eye, gills, gonads, heart, kidney, liver, muscle, skin and spleen. For the growth factor genes *IGF1* and *IGF2*, semi-quantitative PCR was performed prior to qPCR assays. Additionally, the tissue-specific expression of the IGF-1 protein was examined by Western blot analysis. Statistical evaluation (one-way ANOVA and Tukey-Kramer post-test) of the qPCR measurements, revealed significant differences in transcript numbers of the different tested tissues for each of the three reference genes (*RPL9, RPL32, EEF1A1B*). Consequently, for the tissue profiling, all transcript levels were calculated as direct copy numbers related to 1 µg RNA, and not normalised by reference genes. Statistical evaluation of the target gene qPCR data was equally performed by one-way ANOVA in combination with Tukey-Kramer multiple comparison tests. In section B.3 of the appendix additional diagrams are given, displaying the qPCR data of the stress and immune target genes as mean values ± SEM.

3.3.1. Analysis of tissue-specific mRNA transcripts of maraena whitefish immune genes

The expression of the maraena whitefish immune target genes *IL1B*, *IL6*, *CXCL8*, *IL12*B, *TNF, SAA, MAPK1,* and *MAPK3* was determined by qPCR in 10 different tissues. Transcripts were detected in every examined tissue and for each target gene as diagrammed in the heat map given in figure 3.3a. The overall highest expression levels of all immune target genes revealed *SAA* ranging between ≈3.5 million copies/µg RNA in the muscle, and ≈73.5 million copies/µg RNA in the spleen. The *MAPK1* mRNA levels were also comparably high in nearly all tested tissues (minimum value of ≈130,000 copies/µg RNA in the liver), but maximum values were measured in brain and gonads (≈1.3 mio to ≈ 2.5 mio copies/µg RNA). Similarly, high numbers of *MAPK3* transcripts were found in all tissues examined (minimum of ≈180,000 copies/µg RNA in the muscle), whereby mRNA levels were particularly high in gills, spleen, and brain (≈2.2 mio to ≈2.6 mio copies/µg RNA), and the topmost copy numbers were found in gonads (≈9.2 mio copies/µg RNA). However, the overall lowest expression levels were measured for *TNF* showing a minimum value of 4,000 copies/µg RNA in muscle, and a maximum value of ≈240,000

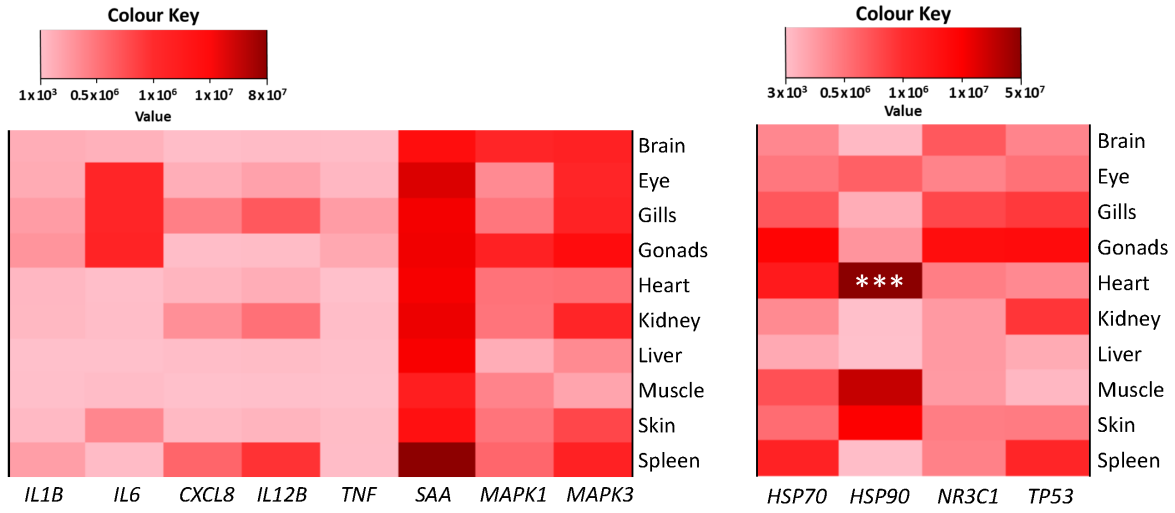

(a) Immune genes (b) Stress genes

Figure 3.3: **Tissue-specific mRNA levels of immune and stress genes in maraena whitefish measured by qPCR**
The heat-maps above represent mRNA levels of the immune target genes (3.3a) and the stress target genes(3.3b) in 10 different tissues of maraena whitefish. The mean values ($n = 4$) of direct transcript numbers related to 1 µg RNA are represented as colours in the given heat map. The colour key (on top) indicates the range of values on which the colouring of the heat map is based. The target genes are represented in columns and the tissues in rows. Significant differences in expression levels between tissues of each gene, were computed by one-way ANOVA and Tukey-Kramer multiple comparisons tests. Significant differences in expression levels between tissues of the respective gene are marked with white asterisks (***, $p \leq 0.001$).

copies/µg RNA in gills. *IL1B* transcript numbers were in the same range as those of *TNF*, but beside gills, *IL1B* transcripts were also highly abundant in spleen and gonads ($\approx$220,000 to $\approx$290,000 copies/µg RNA). *IL6* was mainly expressed in gills, eye, and gonads ($\approx$1.0 mio to $\approx$1.8 mio copies/µg RNA) and to a little lesser extend in skin tissue ($\approx$375,000 copies/µg RNA). However, the main site of expression for *CXCL8* and *IL12B* was gill, kidney, and splenic tissue, ranging between $\approx$320,000 to $\approx$590,000 copies/µg RNA for *CXCL8*, and $\approx$520,000 to $\approx$930,000 copies/µg RNA for *IL12B*. Statistical evaluation verified no significant differences in the tissue-specific transcript numbers for any target gene, since the transcript levels varied considerably over all tested tissues.

3.3.2. Analysis of tissue-specific mRNA transcripts of maraena whitefish stress genes

The mRNA levels of maraena whitefish stress-related genes *HSP70, HSP90*, *NR3C1*, and *TP53* were examined in 10 different tissues as shown in the heat map in figure 3.3b. Taken as a whole, the qPCR analysis revealed gene expression of all tested genes in all tissues. The overall highest variation in tissue-specific copy numbers was detected for *HSP90,* revealing a maximum of $\approx$48.5 mio copies/µg RNA in the heart ($p < 0.001$) and a minimum of $\approx$4000 copies/µg RNA in the liver, which is a $>$12,000-fold difference. Additionally, *HSP90* was highly expressed in the muscle and in the skin ($\approx$26.5 mio copies/µg RNA and $\approx$8.5 mio copies/µg RNA). Similarly to the latter, *HSP70* was least expressed in the liver ($\approx$150,000 copies/µg RNA), whereas considerably high transcript numbers were found in splenic ($\approx$1.6 mio copies/µg RNA), and heart tissue ($\approx$3.2 mio copies/µg RNA), and the topmost value of $\approx$7.4 mio copies/µg RNA was measured in the gonads. Except from a peak value of $\approx$5.8 mio copies/µg RNA in the gonads, *NR3C1* was most regularly expressed within the other tested tissues, since

transcript numbers varied only by a factor of < 3.0 ($\approx$250,000 copies/µg RNA in the muscle to $\approx$680,000 copies/µg RNA in the brain). The main site of *TP53* transcript expression were by far the gonads ($\approx$6.1 mio copies/µg RNA), followed by mRNA levels of $\approx$1.1 mio copies/µg RNA to $\approx$890,000 copies/µg RNA in the spleen, kidney, and gills. However in muscle tissue, *TP53* was least expressed ($\approx$62,000 copies/µg RNA). Compared to all other tested tissues, statistical evaluation verified a significantly higher transcript number of the gene *HSP90* in the heart, indicated by a value of $p < 0.001$.

3.3.3. Multi-level analysis of maraena whitefish growth factors in various tissues

3.3.3.1. Analysis of maraena whitefish growth factors on mRNA level by semi-quantitative PCR In order to get a first insight into the tissue-specific expression of the growth factor genes *IGF1* and *IGF2*, semi-quantitative PCR was performed as a pretest in only 4 different tissues (gills, kidney, liver, muscle). The tissue-specific expression of genes was determined as relative quantities by densitometric analysis as described in section 2.2.4.5. Therefore, *EEF1AB1* was used as an internal reference and the band intensities representing the gene expression in the respective tissues were set 100%. Consequently, the tissue-specific band intensities of *IGF1* and *IGF2* were determined in relation to the reference gene.

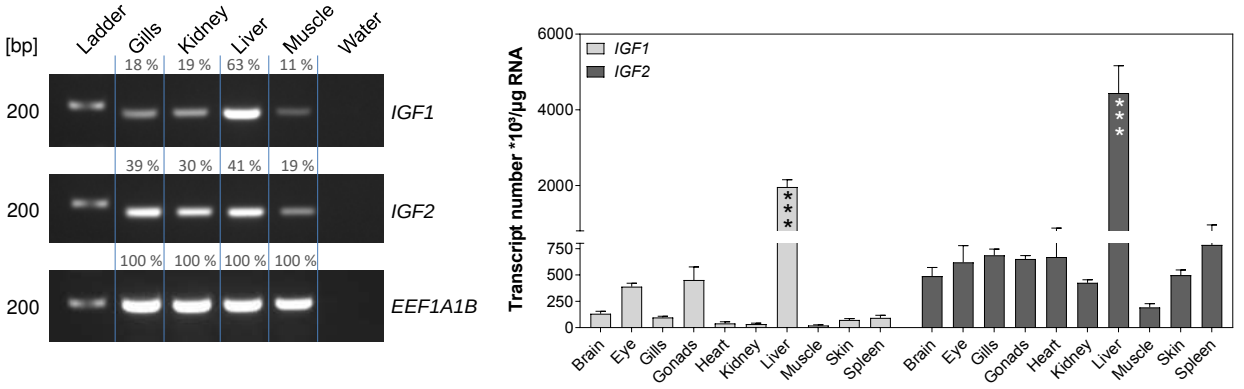

(a) semi-quantitative PCR (b) qPCR

Figure 3.4: **Tissue-specific mRNA levels of IGFs measured by semi-quantitative PCR and qPCR** Figure 3.4a shows representative agarose gels of the tissue distribution of maraena whitefish *IGF1* (164 bp) and *IGF2* (158 bp) target genes, as well as the *EEF1A1B* (189 bp) reference gene, determined by semi-quantitative PCR. The expression levels were examined using cDNA mixtures of four juvenile maraena whitefish for each of the four analysed tissues, respectively. *EEF1A1B* was used as internal reference in every tissue and the respective band intensities were set to 100%. Band intensities of *IGF1* and *IGF2* were calculated relative to the reference values of *EEF1A1B* for each tissue. Relative quantities of the band intensities are given in percentage terms (grey-coloured) above the agarose gels. For all three agarose gels, the last lane displays the negative control, containing water instead of a cDNA sample. In figure 3.4b the distribution of *IGF1* and *IGF2* mRNA in 10 different tissues of maraena whitefish is depicted. The bar graph displays the means ($n = 4$) of direct transcript numbers related to 1 µg RNA. *IGF1* is represented in light grey, and *IGF2* in dark grey bars. The respective tissues are given on the x-axis. Significant differences in expression levels between tissues of each gene, were computed by one-way ANOVA and Tukey-Kramer multiple comparisons tests. Values were considered significant if gene expression in a specific tissue was determined as significant compared to all other tissues for the same gene and are marked with black or white asterisks (***, $p \leq 0.001$) for *IGF1* or *IGF2*, respectively. Figures modified from Nipkow *et al.* (2018).

Overall, band intensities for *IGF1*, as well as for *IGF2* were relatively variable between the tissues and always lower than the reference gene *EEF1AB1*. Further, the highest expression was measured in liver tissue for both *IGF1* and *IGF2* with values of 63% and 41%, respectively. Both genes revealed moderate band intensities in gill and kidney tissue, accounting for 18% and 19% for *IGF1*, as well as 39% and 30%

for *IGF2*. However, the least intense bands were determined in muscle tissue for *IGF1* (11%) and *IGF2* (19%), respectively. In general, in all tissues higher band intensities were calculated for *IGF2* than for *IGF1*, except for the liver.

3.3.3.2. Analysis of maraena whitefish growth factors on mRNA level by qPCR The expression levels of *IGF1* and *IGF2* transcripts were examined in 10 different tissues by qPCR and plotted as a bar graph as seen in figure 3.4b. Both genes were expressed in all tissues examined, and the mRNA transcripts ranged between ≈19,500/µg RNA (muscle tissue) and ≈2,100,000/µg RNA (liver tissue) for *IGF1* and between ≈190,000/µg RNA (muscle tissue) and ≈4,300,000/µg RNA for *IGF2*, respectively. Thus, *IGF1* and *IGF2* gene expression was lowest in muscle, and highest in liver tissue. Additionally, in the liver, both *IGF1* and *IGF2* expression was significantly higher than in all other tissues examined ($p < 0.001$). In contrast to the result from the semi-quantitative PCR, the liver-specific *IGF2* expression determined by qPCR was higher (> 2-fold) than that of *IGF1*. However, the qPCR analysis confirmed the higher levels of *IGF2* mRNA compared to *IGF1*, that were previously detected by semi-quantitative PCR. Thus, expression levels computed for *IGF2* were overall 1.5 (eye tissue) to 18.2-fold (heart tissue) higher than for *IGF1*.

3.3.3.3. Analysis of maraena whitefish IGF-1 on protein level by Western blot In collaboration with the Signal Transduction Unit of the FBN, it was possible to study the tissue-specific expression of IGFs on protein level, as the group has expertise in the analysis of IGF proteins. Thus, IGF-1 protein levels were determined in gills, liver and muscle tissue of three animals by Western blotting as seen in figure 3.5. The same procedure was performed for the detection of IGF-2, but the protein was not traceable,

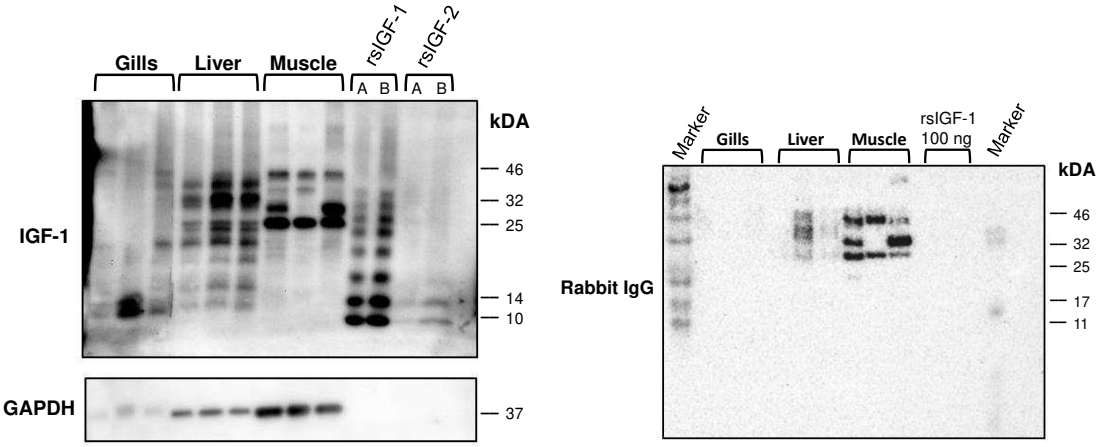

(a) Specific IGF-1 antibody (b) Secondary control antibody

Figure 3.5: **Expression analysis of maraena whitefish IGF-1 protein in different tissues by Western blot technique**
Figure 3.5a shows expression of the IGF-1 protein in gills, liver, and muscle of juvenile maraena whitefish determined by Western blot analysis. Tissue extracts of three animals (80 µg total protein), were added to each lane. The recombinant salmon (rs) proteins rsIGF-1 and rsIGF-2 were used as controls for antibody binding in two different dilutions (A: 150 ng/lane; B: 250 ng/lane). Additionally, GAPDH was used as loading control. Figure3.5b displays a second PVDF membrane that was solely incubated with the secondary antibody (anti-rabbit IgG) to detect unspecific bands. Figure modified from Nipkow *et al.* (2018).

since the anti-salmon/trout IGF-2 antiserum (raised in rabbits) failed to specifically bind to IGF-2 (data not shown). As shown in figure 3.5a, several bands were detected for IGF-1 in all three examined

tissues, as well as for the positive controls rsIGF-1 and rsIGF-2. Due to the presence of various signals, the secondary antibody (rabbit-IgG) was tested concerning non-specific binding. As shown in figure 3.5b , the rabbit-IgG antibody bound proteins unspecifically at molecular weights >25 kDA in liver and muscle tissue. Consequently, four variants of IGF-1 protein <25 kDa were specifically detected in similar concentrations in the liver of all three tested animals (see figure 3.5a). In gills, two variants of IGF-1 were traceable at molecular weights of ≈ 10 kDa and ≈ 14 kDa that revealed different expression patterns between the tested animals. However, in muscle tissue no IGF-1 variant could be verified. Additionally, several bands with molecular weights of approximately 10 to 43 kDa, were detected for the positive control rsIGF-1 with strongest signals at ≈ 10 kDa and ≈ 14 kDa. Moreover, figure 3.5a displays, that at molecular weights of ≈ 10 kDa and ≈ 14 kDa the anti-IGF-1 antibody exhibited a cross reactivity of approximately 15% of the IGF-1 signal with rsIGF-2.

3.4. Influence of density stress on maraena whitefish mRNA levels and physiology

In order to examine the influence of different stocking densities on maraena whitefish, an acute stress experiment, as well as a short-term density stress experiment were performed. For the acute density stress experiment, fish were kept for 24 h at moderate (33 kg/m³) or high density (100 kg/m³) until sampling. However, for the short-term density stress experiment fish were kept at low (10 kg/m³), moderate (33 kg/m³), enhanced (60 kg/m³) or high density (100 kg/m³) for eight days until sampling (for more details see 2.1.4). The tissue and blood samples obtained during the experiment, were subsequently analysed by qPCR, microarray, and glucose and cortisol assays as described in the following.

3.4.1. Modulation of immune gene transcript levels due to different stocking densities

The mRNA concentrations of the respective target genes were measured two times independently (4 individuals in each case ($n=8$)) in liver, spleen, kidney, and gills (the latter only for acute density stress) by qPCR using the LightCycler®96 System. The resulting mRNA levels were calculated as described in 2.2.4.8, but the copy numbers were solely normalised by the reference gene *RPL9*, since it proved as the only stable gene within this experiment. Since moderate density (MD) conditions were set as control, the mRNA copy numbers were calculated as fold changes of low density (LD), enhanced density (ED), and high density (HD) relative to MD. Subsequently, the data were plotted as heat maps using the RStudio software as described in section 2.7.4. Additionally, individual copy numbers ($n=8$) of each gene and treatment were visualised as box-whisker plots (2.7.4) showing the median, the 25 and 75 percentiles (box), and the 10 to 90 percentiles (whiskers).

3.4.1.1. Acute-density stress The acute high-density experiment (100 kg/m³ for 24 h) was affecting five out of eight immune target genes (i.e., $FC>2$ or $FC<-2$) as illustrated in the heat map in figure 3.6.A. Compared to the copy numbers measured at MD, the overall highest up-regulation of $FC=7.7$ was calculated for *IL1B* in kidney, followed by *IL6* ($FC=3.7$) and *SAA* ($FC=2.5$). In spleen, gene expression was approximately three fold increased for *SAA* ($FC=2.8$), more than two fold for *IL1B* ($FC=2.2$), and exactly two fold for *TNF*. In the liver, an up-regulation higher than two fold, relative to MD, was determined for *IL6* ($FC=2.1$) and *SAA* ($FC=2.5$). On the contrary, *CXCL8* revealed the overall topmost down-regulation of 2.5 fold in the liver. The only gene reaching a $FC>2$ in gill tissue was *SAA* ($FC=2.7$), compared to the MD control group. The expression of the genes *IL12B*, *MAPK1,* and *MAPK3* were hardly affected by the acute high-density conditions, since the respective ratios ranged from $FC=-1.9$

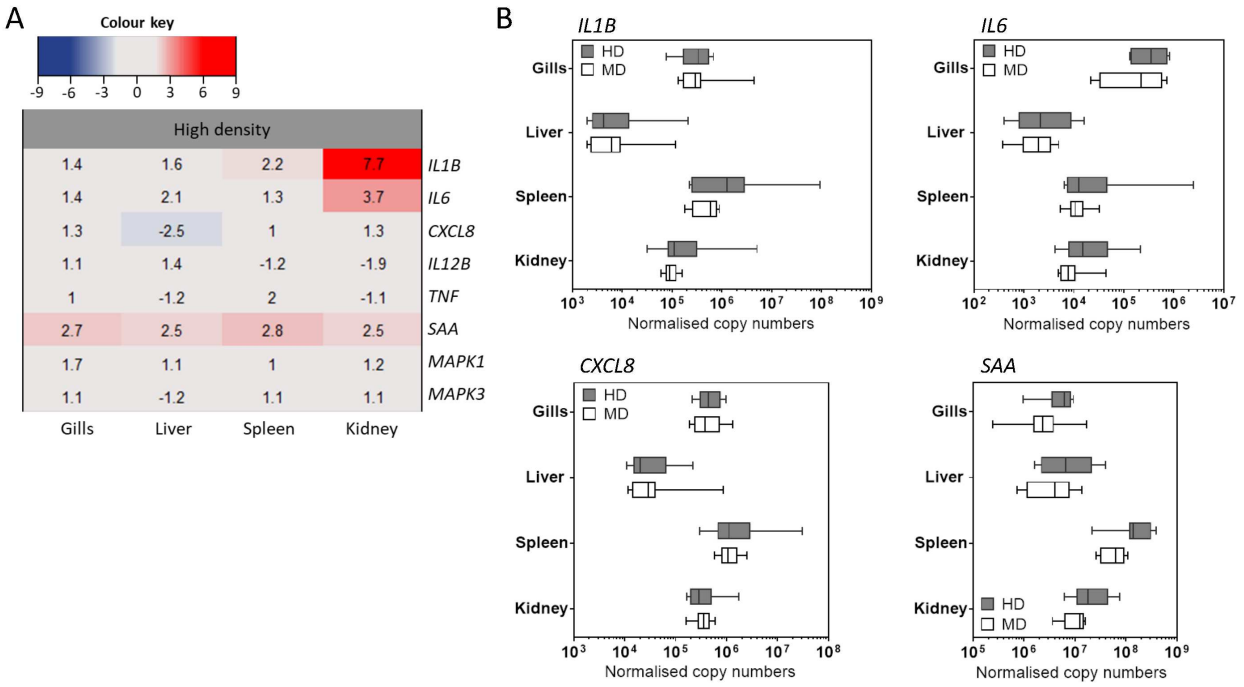

Figure 3.6: **Influence of high-density conditions on maraena whitefish immune genes**
The heat map (**A**) illustrates average expression ratios as fold changes of high density relative to moderate density for the immune target genes *IL1B*, *IL6*, *CXCL8*, *IL12B*, *TNF*, *SAA*, *MAPK1* and *MAPK3* (listed in rows) measured by qPCR (n = 8). The different tested tissues are given in columns. The bar above the heat map indicates the analysed density category. A colour key is indicated on top. The box-whisker plots (**B**) depict the individual copy numbers (abscissa) of the target genes (indicated above the plot) in the different tissues (ordinate), normalised by the reference gene *RPL9*. The different treatment categories given in the plot are high density (HD) in dark grey, and moderate density (MD) in light grey.

up to FC = 1.4, relative to MD, in every tested tissue. Figure 3.6.B additionally shows individual copy numbers of the top four regulated genes (*IL1B*, *IL6*, *CXCL8*, and *SAA*,) as box-whisker plots (see B.4.1.1 for plots of the non-affected genes). Although, for some genes and tissues the copy numbers reveal high variances, a clear shift of the high-density bars to the right, compared to the moderate-density bars, can be seen in specific tissues for the top regulated genes, indicating the up-regulation discussed above. As already shown in the heat map, for *SAA*, the copy numbers at HD were clearly higher than for MD in all tested tissues. This is to be seen particularly in spleen, where > 90% of the HD values were higher than the MD values. Moreover, the box-plot clearly shows that the spleen was the main site of *SAA* expression within this experiment, as well as for *IL1B* and *CXCL8*. However, *IL6* was mainly expressed in the gills, but likewise for HD and MD. Notably, *CXCL8* was accounted as down-regulated (FC > -2) in the liver, and fittingly the copy numbers in this tissue were considerably low.

3.4.1.2. Short-term density stress Fold change values of HD, ED, and LD for the eight analysed immune genes (*IL1B*, *IL6*, *CXCL8*, *IL12B*, *TNF*, *SAA*, *MAPK1*, *and MAPK3*), relative to the MD control were depicted as a heat map in figure 3.7.A. HD conditions had the highest effect on gene expression, since here, three out of the eight target genes showed a FC > 2. The all in all highest up-regulation in all three tissues was determined for *SAA*, reaching a higher than eight fold up-regulation in kidney (FC = 8.6) and spleen (FC = 8.3), and a topmost fold change of 12.2 in the liver, compared to MD. At HD, also *IL1B* (FC = 3.6) and *CXCL8* (FC = 3.9) expression were up-regulated in the liver, as well as in the kidney (*IL1B,* FC = 4.5; *CXCL8,* FC = 2.2), but much lesser than *SAA*. However in the spleen,

besides the top-regulated *SAA* gene, an up-regulation of nearly four-fold could be determined for *IL1B* (FC = 3.7). At ED (60 kg/m³ for 8 d) the analysed genes reached only low fold changes relative to MD, ranging between -1.5 and 1.7 in all three tissues, except from *SAA*. Red shades in the heat map clearly indicate that *SAA* expression was affected by ED as well, particularly in the liver (FC = 4.0) but also in spleen (FC = 3.7) and kidney (FC = 3.1). For LD (10 kg/m³ for 8 d) copy numbers of all tested immune

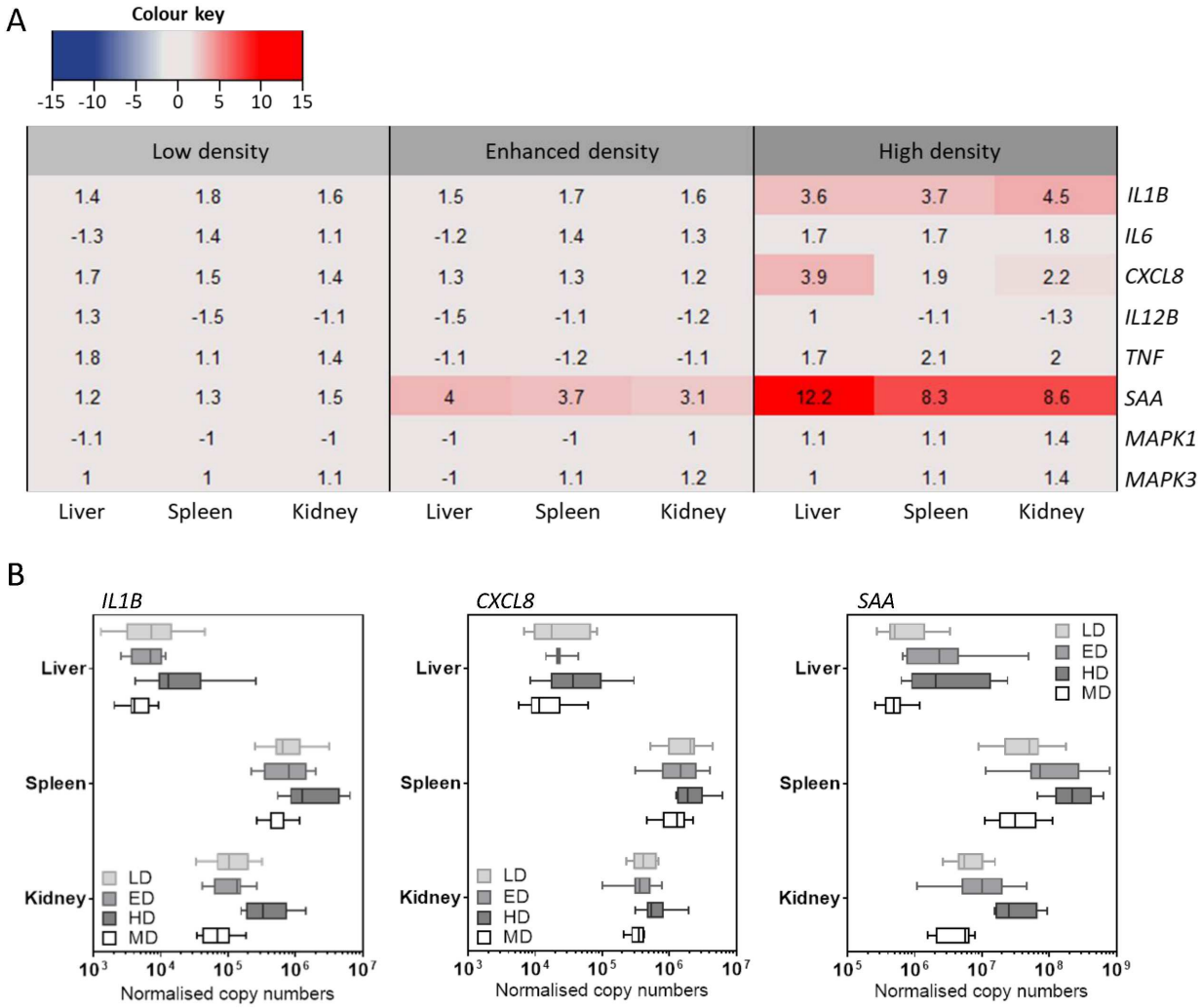

Figure 3.7: **Influence of a short-term exposure of maraena whitefish to different stocking densities on immune genes**
The heat map (**A**) illustrates average expression ratios as fold changes of low density, enhanced density and high density relative to moderate density for the immune target genes *IL1B, IL6, CXCL8, IL12B, TNF, SAA, MAPK1*, and *MAPK3* (listed in rows) measured by qPCR (n = 8). The different tested tissues are given in columns. The bar above the heat map indicates the analysed density categories and a colour key is given on top. The box-whisker plots (**B**) depict the individual copy numbers (abscissa) of the target genes (indicated above the plot) in the different tissues (ordinate), normalised by the reference gene *RPL9*. The treatment categories given in different shades of grey in the plots are: low density (LD), enhanced density (ED), high density (HD), and moderate density (MD).

genes were nearly on the same level as at MD (values varied between -1.5 and 1.8). *IL12B, MAPK1*, and *MAPK3* expression ratios were barely affected by the short-term density stress experiment. In figure 3.7.B copy numbers of the three top-regulated genes *IL1B*, *CXCL8*, and *SAA* were plotted for each of the four treatments (see B.4.1.2 for plots of the non-affected genes). For each of the three genes, highest copy numbers were measured in splenic tissue and the lowest in the liver. Moreover, for *IL1B* the HD-box

plots clearly shifted to the right, compared to MD, indicating the increase of the copy numbers in all three tissues examined. However for *SAA*, the same is to be seen for HD, and to a little lesser extend for ED-box plots.

3.4.2. Modulation of stress gene transcript levels due to different stocking densities

Data for the mRNA concentrations of the stress target genes were measured, calculated, and plotted exactly in the same way as previously described for the immune target genes in section 3.4.1.

3.4.2.1. Acute density stress The expression ratios of the stress target genes *HSP70*, *HSP90*, *NR3C1*, and *TP53* were poorly affected by the acute density stress experiment (see figures in B.4.2.1). Related to MD, the ratios of all tested genes ranged between 1.4 and -2 in the analysed tissues. The highest regulation, indicated by a fold change of -2 was determined for *HSP90* in the spleen.

3.4.2.2. Short-term density stress Within the short-term density stress experiment (8 d) the three different density categories scarcely influenced the expression of most stress genes as shown by the dominance of grey shades in the heat map in figure 3.8.A. At LD and HD conditions, none of the tested

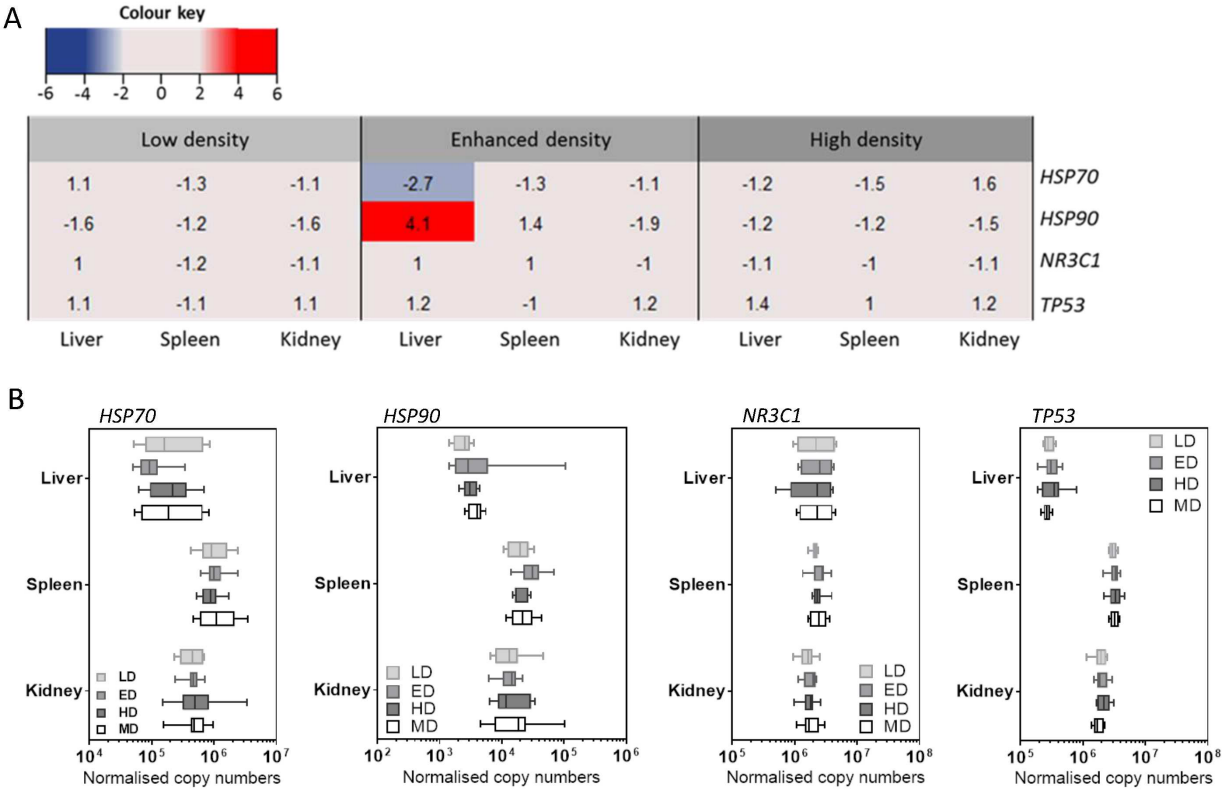

Figure 3.8: **Influence of a short-term exposure of maraena whitefish to different stocking densities on stress genes**
The heat map (**A**) illustrates average expression ratios as fold changes of low density, enhanced density and high density relative to moderate density measured by qPCR (n = 8). The examined stress target genes *HSP70*, *HSP90*, *NR3C1*, and *TP53* are given on the right side and the different tested tissues are listed below the heat map. The bar above the heat map indicates the three different density categories analysed. A colour key is given above the scheme. The box-whisker plots (**B**) depict the individual copy numbers (abscissa) of the target genes (given above the plot) in the different tissues (ordinate), normalised by the reference gene *RPL9*. The different treatment categories given in the plot are high density (HD) in dark grey, and moderate density (MD) in light grey.

genes showed a down- or up-regulation higher than -2 or 2 in liver, spleen, or kidney, relative to the expression at MD. At ED conditions, *HSP70* was down-regulated nearly three fold (FC = 2.7) in the liver. Moreover, *HSP90* reached a ratio of FC = 4.1 at ED in the liver, which was the overall highest regulation within this treatment. *NR3C1* and *TP53* were poorly affected, since the FC values ranged between -1.2 and 1.4 at all three stocking densities. The box-whisker plots in 3.8.B, additionally display the low degree of regulation, since the boxes, representing individual copy numbers of each stress gene and treatment, are arranged relatively centrally on top of each other.

3.4.3. Holistic analysis of gene expression at different stocking densities

In addition to qPCR analyses, microarray technique was used to investigate the influence of stocking density on gene expression and to record differentially expressed (DE) genes at a holistic level. This served for two purposes, firstly to confirm results from the qPCR measurements of the pre-selected target-gene sets and secondly, to identify further candidate genes that might interact with the target genes in a functional pathway. Therefore, DE genes were computed using the limma package of the programming language R (for further details see section 2.2.10) by performing comparisons of the LD, ED, and HD data sets to the MD data set, for liver and kidney tissue, respectively. Based on the lists of DE genes, area-proportional Venn diagrams (see section 2.2.10.3) were calculated with the BioVenn software (Hulsen *et al.*, 2008) and functional pathway and upstream regulator analyses were conducted using the Ingenuity® Pathway Analysis software (IPA, Qiagen).

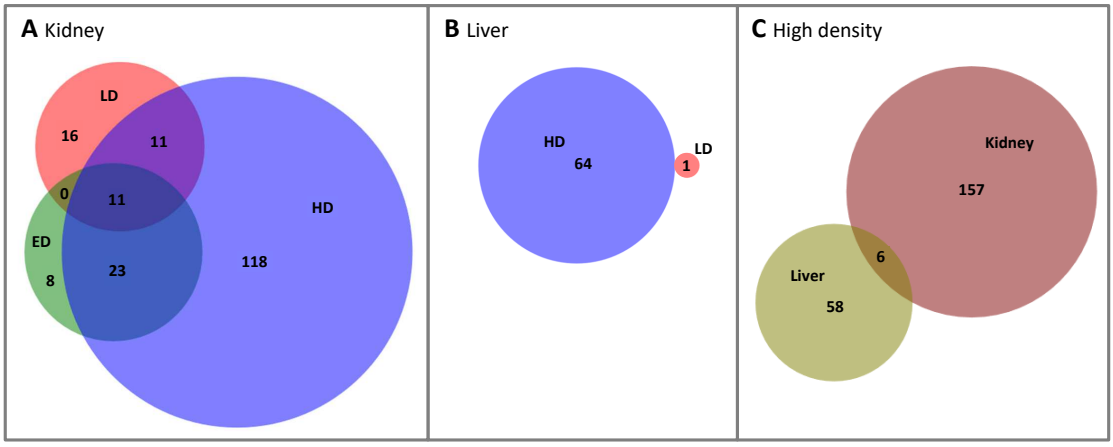

Figure 3.9: **Venn diagrams show DE genes after short-term exposure of maraena whitefish to different SD's**
The Venn Diagrams show the overlap of DE genes at different stocking densities in (**A**) kidney and (**B**) liver, each time compared to MD conditions. In the liver, for the comparison of ED to MD no DE genes could be identified. In (**C**) the sets of DE genes for HD vs. MD were compared in kidney and liver. Whereas numbers in the pure-colour areas indicate the respective DE genes for one specific feature (as labeled individually), the numbers in the mixed-colour intersections indicate DE genes, that were shared by more than one of the tested features (see labels). This analysis is based on Agilent-ID's and only annotated DE genes with an absolute FC > 2, and a corrected p-value < 0.05 were considered.

Microarray analysis revealed a total number of 187 genes affected in the kidney of maraena whitefish kept at LD, ED, and HD (compared to MD), as shown in the Venn diagram in figure 3.9.A. The by far the highest proportion of 63.1% (118) of all DE genes in the kidney were determined for the comparison of HD to MD conditions, while for LD and ED conditions compared to MD, only 16 and 8 DE genes

were found. Moreover, as indicated by the intersections, a comparably high number of 23 genes were differentially expressed at HD and ED treatment (relative to MD). However, HD and LD treatment, shared 11 DE genes, as did all three treatment groups (LD, ED, HD) together, when compared to MD conditions. In contrast to the kidney, in maraena whitefish liver tissue, only one gene was affected by LD, not a single one by ED conditions, and no overlaps were calculated for the three treatment groups (LD, ED, HD) compared to MD, as to be seen in figure 3.9.B. Nevertheless, 65 DE genes were identified for HD compared to MD in the liver. For kidney and liver, only the HD vs. MD data sets were compared to each other, since in the liver for the comparison of LD and ED to MD conditions, only one or no DE gene was identified, as to be seen in figure 3.9.C. Here, besides 157 DE genes in the kidney and a significantly lower number of 58 DE genes in the liver, only six DE genes were shared by both tissues.

Agilent ID	Gene symbol	Function	FC Kid	FC Liv
A_05_P477247	*SAA* (serum amyloid A)	Acute phase response	13.3	8.8
A_05_P364387	*LYZ* (lysozyme)	Antibacterial activity	8.6	3.5
A_05_P266429	*CEBPB* (CCAAT enhancer binding protein beta)	Immune gene expression	3.9	2.4
A_05_P370212	*CFD* (complement factor D)	Complement activation	2.5	3.6
A_05_P382942	*LOC106585697* (Rieske domain-containing protein-like)	Electron transfer	-2.0	2.6
A_05_P279352	*CD86* (CD86 molecule)	T-cell stimulation	-2.1	2.8

(a) **DE genes**

Canonical pathway	p-value	z-score	Involved DE genes
LXR/RXR activation	1.8E-04	n.a.	*LYZ, SAA* (121)
IL-12 signaling & production in macrophages	2.61E-04	n.a.	*LYZ, CEBPB* (146)
Acute phase response signaling	3.54E-04	n.a.	*SAA, CEBPB* (170)
IL-17a signaling in fibroblasts	6.36E-03	n.a.	*CEBPB* (35)
Complement system	6.73E-03	n.a.	*CFD* (37)

(b) **IPA pathways**

Figure 3.10: **DE genes shared by kidney and liver after short-term exposure to HD and the resulting IPA pathways**
In figure 3.10a the six genes and their respective features (function; expression FC) are listed, that were commonly differentially expressed in kidney and liver at HD compared to MD conditions (see also 3.9.C). In figure 3.10b, Ingenuity® pathways are given resulting from an IPA analysis based on the six DE genes in figure 3.10a, shared by liver and kidney. The two DE genes *LOC106585697* and *CD86* were excluded from the IPA analysis as explained in section 3.4.3. For the listed pathways, no z-scores were available (n.a.), i.e., IPA software could not predict whether the respective pathways were induced or silenced in maraena whitefish kept at HD (compared to MD treatment). The examined tissues were abbreviated as "Kid" for kidney and "Liv" for liver.

Except from *LOC106585697*, the five remaining DE genes shared by kidney and liver (at HD vs. MD conditions), are involved in the immune response as indicated by their specific functions given in figure 3.10a.Taken together, from the overall six shared DE genes, the acute-phase-protein-encoding gene *SAA* revealed the overall highest expression fold changes of 13.3 in the kidney and of 8.8 in the liver for fish kept at HD conditions (relative to MD). To a lower level even the lysozyme-encoding gene *LYZ*, the transcription factor-encoding gene *CEBPB*, the complement factor-encoding gene *CFD*, the predicted non-heme iron oxygenase-encoding gene *LOC106585697*, and the immunoglobulin-encoding gene *CD86* were induced by the HD conditions compared to the MD control.

The subsequent IPA analysis is based on the six DE genes shared by kidney and liver, identified by the comparison of HD to MD conditions in maraena whitefish. Indeed, the two genes *LOC106585697* and *CD86*, were not taken into account for the IPA analysis, since the first did not match a corresponding object in the Ingenuity Knowledge Base, and the second did not meet the criteria of a total average

FC > 2. Thus, within the IPA analysis, the remaining four immune-related genes have been assigned to the top five pathways listed in figure 3.10b, which in turn are related to the immune response.

In maraena whitefish held at HD conditions, the altered expression of *LYZ* and *SAA* (relative to MD conditions) affected the immune-related *LXR/RXR-activation pathway*. Further, the *acute phase response-signaling pathway*, which belongs to the innate immune response, was influenced by the differential expression of *SAA* and *CEBPB*. The altered expression of *LYZ* and *CEBPB, of CEBPB* alone, and of *CFD*, was associated with pathways, that act as a link between innate and acquired immunity, namely *IL12 signaling and production in macrophages*, *IL17a signaling in fibroblasts*, and the *complement system*.

Except for the allocation of pathways, the four DE genes *SAA, LYZ*, *CEBPB*, and *CFD* were subjected to an IPA upstream-regulator analysis, to predict which genes may have led to the altered expression of those four genes. As shown in figure 3.11, the genes *SAA, CEBPB*, and *CFD* were directly activated by the nuclear receptor PPARG, whilst *LYZ* was only indirectly regulated by the cytokine IL6. Besides PPARG, the cytokines IL1B, IL6 and TNF might have had a direct and IL1A an indirect activating effect on *CEBPB* gene expression in maraena whitefish kept at HD (relative to MD). Also *SAA* up-regulation at HD compared to MD conditions, was probably not only restricted to PPARG, but was additionally, indirectly induced by the cytokines IL1B, IL6 and TNF. Within this analysis, the tumor necrosis factor (TNF) was found to be a key player, since it is connected with every other factor of the network, depart from *LYZ*.

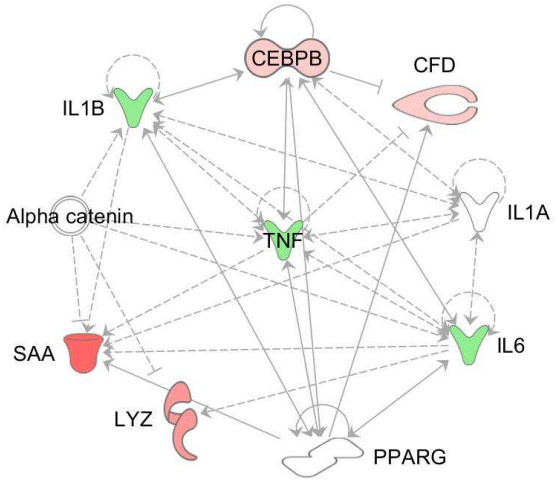

Figure 3.11: **IPA network based on upstream-regulator analysis for the DE-gene set shared by kidney and liver at short-term HD vs. MD conditions** The IPA software was used to predict upstream regulators that may have led to the altered expression of *SAA*, *LYZ*, *CEBPB* and *CFD* at HD vs. MD conditions in mareana whitefish. Different shades of red of the respective symbols, represent up-regulated genes according to FC values given in figure 3.10a. Green-coloured symbols indicate unregulated, but known candidate genes examined in the course of this study. Full and broken lines indicate a direct or indirect interaction between two factors. The arrows represent the direction of interaction, and activation, whereas horizontal lines at the end indicate an inhibition. The grey colouring of the arrows indicates that no prediction could be made, whether the regulator itself was activated or inhibited, and therefore led to an activation or inhibition of the related factors.

3.4.4. Modulation of plasma cortisol and glucose levels due to different stocking densities

The plasma cortisol and glucose levels were analysed after exposure of maraena whitefish to different stocking densities as shown in figure 3.12a and figure 3.12b. For the acute density experiment there was a tendency of a cortisol increase at HD, nevertheless no significant difference was calculated. This is particularly indicated by the ranges of the first to third quartile, reaching from 49.36 ng/ml to 85.02 ng/ml for acute HD and the comparable lower range of 33.6 ng/ml to 68.71 ng/ml for acute MD. Moreover, the median cortisol value of 56.05 ng/ml at acute HD was increased compared to the median cortisol value of 47.68 ng/ml at acute MD.

For the short-term density stress experiment, the average cortisol values were almost on the same level

for all treatments. The median values of the different density categories ranged from 31.86 ng/ml for MD (36.99 ng/ml for ED; 40.00 ng/ml for HD) to 44.36 ng/ml at LD.

The plasma glucose levels were not affected by this experiment, and no correlation to the different tested stocking densities was apparent, since the variation between individuals of the same group was higher than between the different treatments. Consequently, the median values of the different density categories are relatively constant. Thus, the median glucose concentrations were 10.04 nmol/µl (MD) and 9.45 nmol/µl (HD) for the acute stressed fish, and 8.48 nmol/µl (MD), 8.26 nmol/µl (HD), 9.23 nmol/µl (ED) and 7.49 nmol/µl (LD) for the fish in the short-term density experiment.

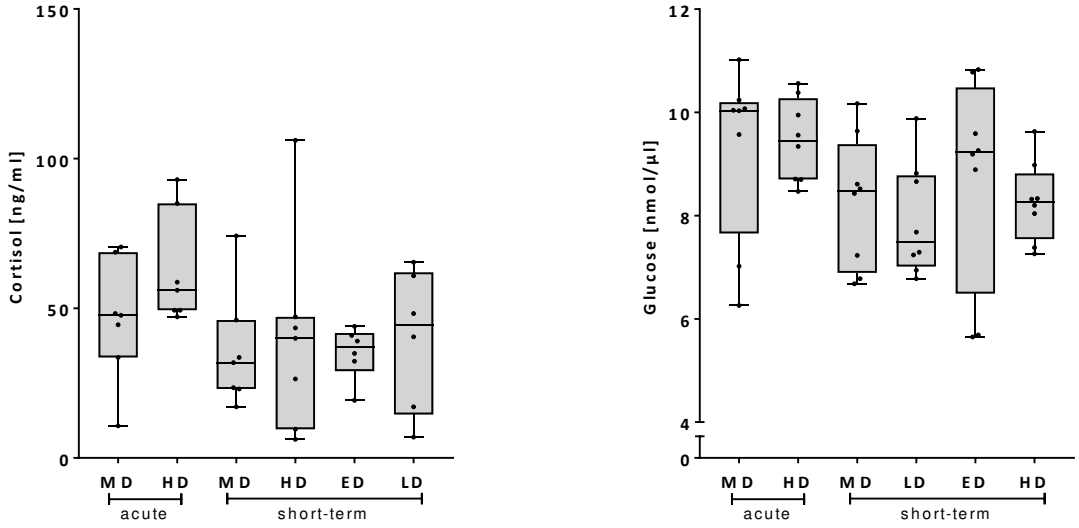

(a) Plasma cortisol levels

(b) Plasma glucose levels

Figure 3.12: **Influence of different stocking densities on plasma cortisol and glucose levels**
The box whisker diagrams show plasma cortisol levels [ng/ml] 3.12a and plasma glucose levels [nmol/µl] 3.12b on the ordinate, subjected to the different experimental conditions that are listed along the abscissa. The whiskers at top and bottom of the box plots display the minimum and maximum, whereas the frame of the boxes mark the first and third quartile (i.e., 50% of the observations) of the given data. The median is given as a horizontal line in each box, respectively. Additionally, seven individual measuring points for acute and short-term moderate density (MD) and high density (HD), as well as six measuring points for short-term enhanced density (ED) and low density (LD) are indicated in the diagram as black dots.

3.5. Influence of temperature stress on maraena whitefish mRNA levels and physiology

To get a fist insight of mareana whitefish's capability to cope with increasing water temperatures, an experiment was performed, in which the fish were exposed to a gradual and an acute temperature rise (see details in section 2.1.5). In brief, for the gradual rise (GR) treatment, fish were kept at water temperatures increasing from 18°C to 24°C within 12 d, whilst for the acute rise (AR) treatment fish were directly transferred from 18°C to 24°C aquaria and sampled after 1 h. In addition, a transfer-control group as handling reference (HR) and a temperature reference (TR) — fish kept at 18°C constantly — were sampled. The tissue (kidney, liver, spleen) and blood samples taken during the experiment, were subsequently analysed either by qPCR and microarray technique, or glucose and cortisol assays as described below.

3.5.1. Modulation of immune gene mRNA levels due to temperature stress

After exposure of maraena whitefish to GR, AR, HR, and TR treatment, the immune target gene mRNA levels were analysed two times independently (7 individuals in each case (n = 14), except for HR (n = 7)) in kidney, liver and spleen by qPCR using the BioMark™ HD-System (2.2.4.8.2). Based on the qPCR measurements, individual target-gene copy numbers were calculated (for details see 2.2.4.8) and subsequently converted to ratios of GR, AR, and HR conditions relative to TR conditions. The resulting data were used to construct heat maps using the RStudio software (see section 2.7.4). Additionally, individual copy numbers of the overall top three regulated genes were plotted as box-whisker plots showing the median, the 25 and 75 percentiles (box), and the 10 to 90 percentiles (whiskers).

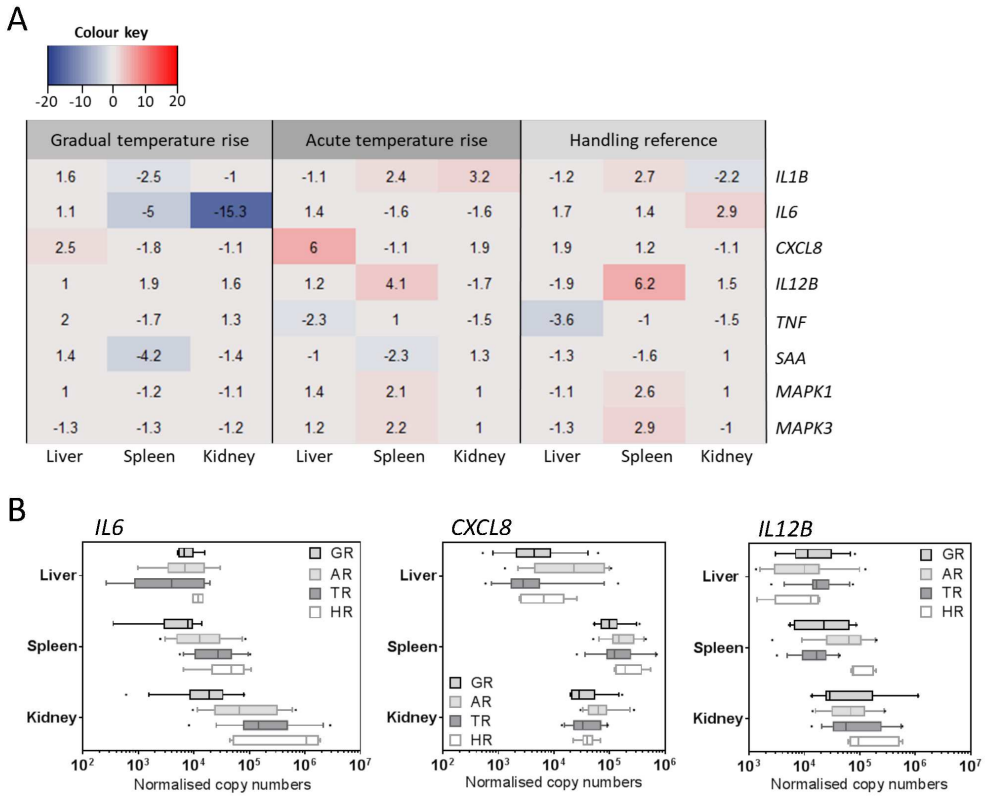

Figure 3.13: **Influence of rising temperature on maraena whitefish immune genes**
The heat map (**A**) illustrates average expression ratios as fold changes of the gradual and the acute temperature rise, and the handling reference relative to the temperature reference for the immune genes *IL1B*, *IL6*, *CXCL8*, *IL12B*, *TNF*, *SAA*, *MAPK1* and *MAPK3* (listed in rows) measured by qPCR (n = 14; except from handling reference: n = 7). The different tested tissues are given in columns. The bar above the heat map indicates the two treatment categories and a colour key is given on top of the scheme. The box-whisker plots (**B**) depict the individual copy numbers (abscissa) of the target genes (indicated above the plot) in the different tissues (ordinate), normalised by the reference genes *RPL9*, *RPL32*, and *EEF1A1B*. The different treatment categories given in the plot are gradual rise (GR), acute rise (AR), temperature reference (TR), and handling reference (HR), each indicated by a different shade of grey.

As shown in figure 3.13.A, after GR treatment of maraena whitefish, most immune target genes were not affected (i.e., absolute FC $\leq$ 2) or down-regulated, like *IL6* that revealed a 15.3-fold and a 5-fold down-regulation in the kidney and the spleen. Besides *IL6*, also *SAA* was slightly down-regulated in the spleen (-4.2-fold). Additionally, *CXCL8* (2.5-fold up) and *IL1B* (2.5-fold down) were marginally regulated at GR compared to TR conditions. After AR treatment of fish, expression fold changes of most immune target genes ranged between -2.3 to 2.4 relative to the temperature control (TR) and,

thus was only slightly regulated. The overall highest regulation for AR compared to TR treatment was found for *CXCL8* in the liver (6.0-fold up), for *IL12B* in the spleen (4.1-fold up), and for *IL1B* in the kidney (3.2-fold up). For the comparison of HR to TR conditions *CXCL8* was not affected, whereas *IL6* was up-regulated 2.9-fold in the kidney, but tended to be down-regulated at AR treatment. Moreover, *IL12B* showed a little higher transcript level at HR than at AR conditions, relative to TR. This trend towards greater regulation after HR, than after AR treatment, albeit to a very limited extent, was also evident for the genes *TNF*, *MAPK1*, and *MAPK3*.

From the box plots in figure 3.13.B, it becomes clear, that within this experiment, although the expression values for some genes and treatments show relatively wide variances, the box-whisker plots mostly overlap from one treatment group to another for the same tissue and gene. However, it should be mentioned that for *IL6,* in all three tissues examined and for *IL12B* in splenic and kidney tissue, copy numbers for HR conditions were amongst the overall highest, indicated by the right-sided boxes (also for *IL1B*, *MAPK1*, and *MAPK3* for some tissues, as to be seen in figure B.22).

3.5.2. Modulation of stress gene mRNA levels due to temperature stress

For the stress target genes, the respective expression values discussed in the following, were measured, calculated, and plotted exactly in the same way as previously described for the immune genes in section

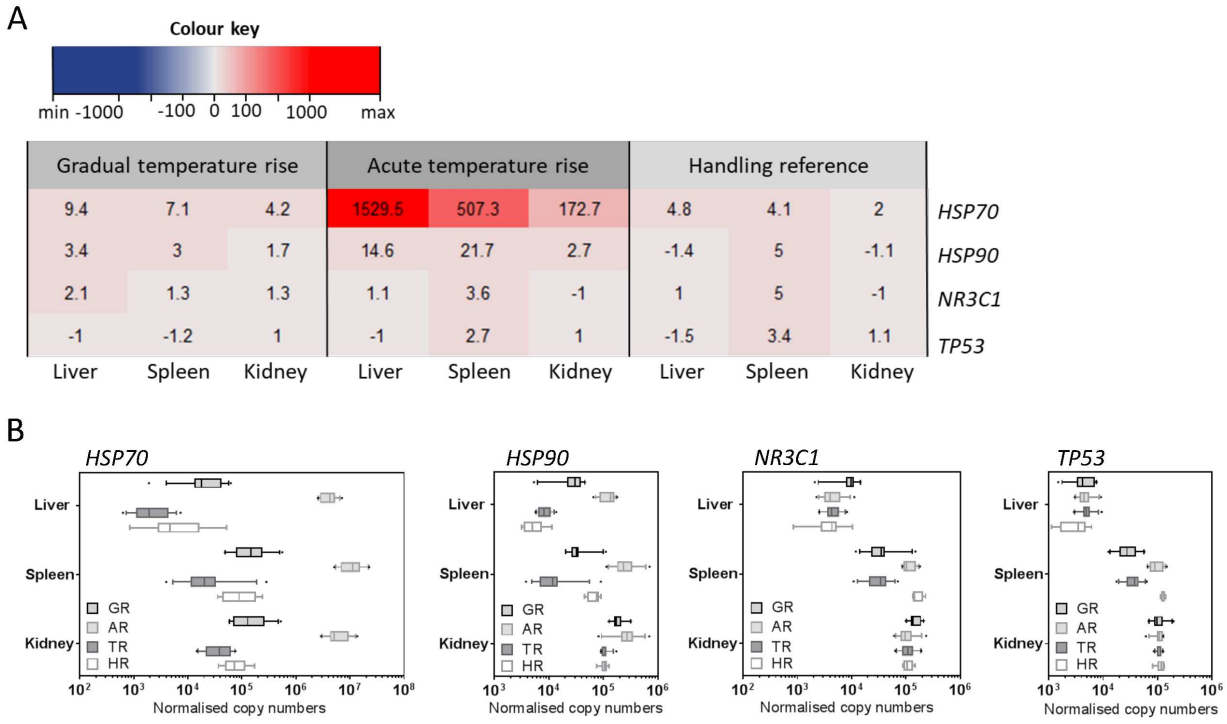

Figure 3.14: **Influence of rising temperature on maraena whitefish stress genes**
The heat map (**A**) illustrates average expression ratios as fold changes of the gradual and the acute temperature rise relative to the temperature and the handling reference for the stress genes *HSP70*, *HSP90*, *NR3C1*, and *TP53* (listed in rows) measured by qPCR (n = 14; except from handling reference: n = 7). The different tested tissues are given in columns. The bar above the heat map indicates the two treatment categories. A colour key is indicated on top of the scheme. The box-whisker plots (**B**) depict the individual copy numbers (abscissa) of the target genes (indicated above the plot) in the different tissues (ordinate), normalised by the reference genes *RPL9*, *RPL32*, and *EEF1A1B*. The different treatment categories given in the plot are gradual rise (GR), acute rise (AR), temperature reference (TR), and handling reference (HR), each indicated by a different shade of grey.

3.5.1, but all four target genes were presented as box plots. As shown by the heat-map in figure 3.14.A, maraena whitefish revealed a clear up-regulation of *HSP70* at GR conditions, especially in the liver (9.4-fold up), and also in the spleen (7.1-fold up) and in the kidney (4.2-fold). Additionally, *HSP90* was slightly induced at GR compared to TR, revealing values of FC = 3.4 in the liver and FC = 3.0 in the spleen, whilst *NR3C1* and *TP53* remained mostly unaffected. However, the AR treatment caused a massive up-regulation of *HSP70* in all tissues examined, compared to the TR conditions, as shown by a fold change of $\approx$ 1530 in the liver, together with a fold change of $\approx$ 510 in the spleen, and a fold change of $\approx$ 170 in the kidney. Like *HSP70*, *HSP90* was also more up-regulated after AR, than after GR treatment, compared to the control group (TR), but to a much lesser extent, since the values ranged between a maximum of 21.7 in the spleen (14.6 in the liver) and a minimum of 2.7 in the kidney. Moreover, the two genes *NR3C1* (3.6-fold up) and *TP53* (2.7-fold up) were slightly up-regulated in splenic tissue after AR treatment, relative to TR. Interestingly, as previously described for the immune target genes, also for the less regulated stress target genes *NR3C1* and *TP53*, in case of an up-regulation, the FC values were higher after HR treatment than after AR treatment if both were compared to TR. Although, at HR conditions *HSP70* (FC = 4.8 in liver, FC = 4.1 in spleen) and *HSP90* (FC = 5.0) were up-regulated as well, the FC values were much lower than for the AR conditions.

The box-plots in figure 3.14.B, clearly unveil the massive induction of *HSP70* (in all three tissues tested) and the clear up-regulation of *HSP90*, since the respective AR boxes were significantly shifted to the right, compared to the three other treatment categories. The higher effect of the HR over the AR treatment for *NR3C1* and *TP53* becomes clear by the right-sided position of the boxes for HR in splenic tissue. Within the liver and the kidney, the tissue-specific copy numbers for *NR3C1* and *TP53* were comparably uniformly distributed between the treatment categories and show relatively small variances.

3.5.3. Holistic analysis of gene expression at rising temperature

Besides the previously described qPCR analyses of the two target gene sets, tissue samples from the temperature experiment were additionally examined by the more comprehensive microarray technique. To confirm results from the qPCR measurements and, on the other hand, to identify further candidate genes that might interact with the target genes in a functional pathway. Thus, microarray data were analysed in the same way as previously described for the density stress experiment in section 3.4.3, based on comparisons of the GR, AR, and HR data sets to the TR data set, for kidney, liver, and spleen, respectively.

Evaluation of microarray data from the temperature experiment using Venn diagrams (see figure 3.15.A-C) revealed the overall highest numbers of 775 DE genes for GR, followed by 146 DE genes for AR, and 102 DE genes for HR treatment, each time compared to the temperature-control group (TR). Moreover, the tissue-specific distribution of DE genes showed that in case of GR and HR conditions, most genes were differentially expressed in the liver ($\approx$ 57% of all DE genes for GR are liver-specific; $\approx$ 55% of all DE genes for HR are liver-specific). However, for AR treatment, the spleen was the main tissue of altered gene expression, having a proportion of around 45% of all regulated genes (relative to TR conditions). Considering the intersections of the GR diagram (3.15.A), the highest number of 45 DE genes were shared by the liver and the kidney and all in all 13 genes exhibited an altered expression in all the three tissues analysed.

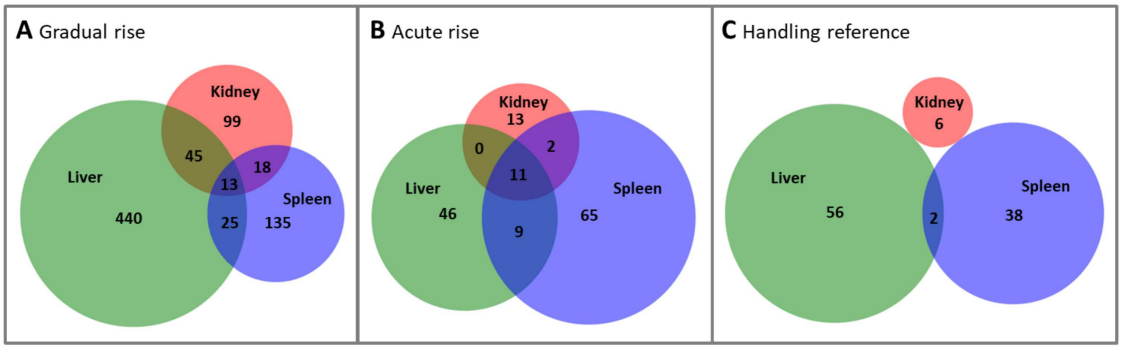

Figure 3.15: **Venn diagrams showing DE genes of maraena whitefish after exposure to rising temperature** The Venn Diagrams show the overlap of DE genes of the three different treatment categories (**A**) gradual temperature rise, (**B**) acute temperature rise, and (**C**) handling reference, each time compared to the temperature reference. Whilst numbers in the pure-colour areas indicate DE genes for one specific tissue (as labelled individually), the numbers in the mixed-colour intersections indicate DE genes that were shared between the respective tissues. This analysis is based on Agilent-IDs and only DE genes with an absolute FC > 2, and a corrected p-value < 0.05 were considered.

The mixed-colour areas for AR treatment in 3.15.B indicate that the highest proportion of 11 DE genes was shared by all three tissues, whereas only two DE genes were found to be shared between kidney and spleen, and even none between kidney and liver. As shown in the Venn diagram in 3.15.C, for the HR conditions (relative to TR), only two genes were commonly differentially expressed by liver and spleen (for details see table B.3), whereas not a single DE gene could be identified, that was shared between kidney. Consequently, the HR treatment was not taken into account for the subsequent analyses.

From the overall 13 DE genes at GR and the 11 DE genes at AR treatment, that were shared by all the three tissues examined, the top five regulated genes for each treatment category are given in figure 3.16a. Several of these top five regulated genes belong to the heat-shock response for both GR and AR conditions. For example, *SERPINH1* and *CLU*, which are both chaperone-encoding genes and belong to the top up-regulated genes for GR conditions (relative to TR), but exhibited relatively low maximum values of FC $= 5.2$ for *SERPINH1* in the spleen and of FC $= 2.9$ for *CLU* in the kidney. Additionally, the third top up-regulated gene for GR vs. TR treatment, a putative Jumonji-like-protein encoding gene *LOC110505518* , that is probably involved in the DNA damage response, was at maximum 3.4-fold up-regulated in the liver. The translation-regulator-encoding genes *EEF1A1a* and *EEF1A1b* were also up-regulated after GR treatment compared to TR, having maximum FC values of 5.6 and 5.1 in liver tissue, respectively.

For the comparison of the AR- to the TR- data set, three of the five top regulated genes were clearly involved in the heat-shock response, since they encode chaperones, as to be seen in the lower panel of figure 3.16a. These three genes altogether yielded maximum expression ratios in the liver, indicated by a very high value of FC $= 143.6$ for *HSPA1A*, besides the much lower values of FC $= 12.2$ for *HSP90*, and FC $= 10.6$ for *DNAJA2*. Likewise, for all three genes in kidney and spleen tissue, the FC values were reduced by about half, except from the still very high value of FC $= 109.4$ for *HSPA1A* in the spleen. The two protein encoding genes *DDIT4* and *DUSP1*, which are involved in different cellular stress responses, as indicated in figure 3.16a, were also up-regulated at AR compared to TR conditions. *DDIT4* was nearly 8-fold up-regulated in splenic and liver tissue, and 6-fold in the kidney, whereas *DUSP1* showed the highest up-regulation of around 7-fold in the spleen, and little lower FC values of 4.9 and 3.6 in the kidney and the liver, respectively.

Treatment category	Agilent ID	Gene symbol	Function	FC Kid	FC Liv	FC Spl
Gradual rise	A_05_P322977	*SERPINH1*	Chaperone of collagen	3.9	3.3	5.2
	A_05_P366617	*CLU*	Molecular chaperone	2.9	2.6	2.3
	A_05_P466547	*LOC110505518*	DNA-damage response	2.6	3.4	2.1
	A_05_P255059	*EEF1A1a*	Translation regulator	2.5	5.6	2.5
	A_05_P266979	*EEF1A1b*	Translation regulator	2.3	5.1	2.4
Acute rise	A_05_P252849	*HSP70*	Molecular chaperone	72.5	143.6	109.4
	A_05_P485612	*HSP90*	Molecular chaperone	6.8	12.2	6.2
	A_05_P410467	*DDIT4*	Involved in response to hypoxia and DNA damage	6.2	7.9	8.1
	A_05_P319052	*DNAJA2*	Cochaperone of Hsp70	5.2	10.6	5.3
	A_05_P424327	*DUSP1*	Regulation of cellular stress response and proliferation	4.9	3.6	7.3

(a) DE genes

Treatment category	Canonical pathway	p-value	z-score	Involved DE genes
Gradual rise	LXR/RXR activation	1.61E-03	n.a.	CLU, AGT (121)
	FXR/RXR activation	1.74E-03	n.a.	CLU, AGT (126)
	Glucocorticoid receptor signaling	1.19E-02	n.a.	FKBP5, AGT (339)
	IL-12 signaling & production in macrophages	7.08E-2	n.a.	CLU (146)
	Acute phase response signaling	8.02E-02	n.a.	AGT (170)
Acute rise	Aldosterone signaling in epithelial cells	1.05E-06	n.a.	*DUSP1, HSP70, HSP90, DNAJB1* (168)
	Unfolded protein response	2.42E-06	n.a.	*PPP1R15A, HSP70, DNAJA2* (55)
	Protein ubiquitination pathway	2.67E-04	n.a.	*HSP70, HSP90, DNAJB1* (265)
	Glucocorticoid receptor signaling	5.50E-04	n.a.	*DUSP1, HSP70, HSP90* (339)
	eNOS signaling	3.21E-03	n.a.	*HSP70, HSP90* (172)

(b) IPA pathways

Figure 3.16: **Selected DE genes after GR and AR treatment and the resulting IPA pathways**
In figure 3.16a the top five DE genes and their respective features (function; expression FC) are listed that were commonly differentially expressed in kidney, liver, and spleen after GR and AR treatment of maraena whitefish, compared to TR. In figure 3.16b the top five functional pathways are given, resulting from an IPA analysis based on the DE genes shared by kidney, liver, and spleen after GR and AR conditions, respectively (see DE-gene lists B.4and B.5). For the listed pathways, no z-scores were available (n.a.), i.e., IPA software could not predict wether the respective pathways were induced or silenced in maraena whitefish after GR, or AR treatment. Pathways, whose assignments to the indicated DE genes were statistically not significant (p-value ≥ 0.05) are shown in grey lettering. The examined tissues were abbreviated as "Kid" for kidney, "Liv" for liver, and "Spl" for spleen.

For the subsequent IPA analysis, only those DE genes were taken into account, that were shared by kidney, liver, and spleen and which matched a corresponding object in the Ingenuity Knowledge Base. Since the gene *LOC110505518* did not fit to an IPA object, for GR only 12 from the 13 DE genes could be taken into account, whereas all 11 DE genes for AR could be uploaded to be assessed by the IPA software. Therefore, averages were calculated for the gene-specific fold changes over all three tissues. Complete lists of the DE genes analysed by IPA software and their tissue-specific fold changes are found in the appendix in table B.4 for the GR-gene set and in table B.5 for the AR-gene set.

Within the IPA analysis only the three genes *CLU*, *AGT* and *FKBP5* of the overall 12 genes that were differentially expressed in maraena whitefish at GR conditions, compared to TR contol, could be assigned to functional pathways. Further, only the assignment of the upper three of the top five pathways given in the upper panel of figure 3.16b, was statistically significant (pathways whose assignment was statistically not significant are shown in grey lettering). The IPA analysis predicted the *LXR/RXR* and the *FXR/RXR activation pathways* to be affected by the two genes *CLU* and *AGT* after GR treatment, relative to TR control. Further, the IPA analysis predicted *AGT* and *FKBP5* to have affected the *glucocorticoid receptor signaling pathway* in maraena whitefish at GR conditions (relative to TR). Additionally, *CLU* has been assigned to the pathway of *IL12 signaling and production in macrophages* and *AGT* to the *acute phase response signaling*, but this was statistically not significant, as already mentioned before.

The IPA analysis of the AR-data set resulted in the top five pathways given in the lower panel of figure 3.16b, which were all influenced by the altered expression of the gene *HSP70* in combination with up to three other DE genes of the AR-data set. The highest number of overall four DE genes (*DUSP1*,

HSP70, *HSP90*, *DNAJB1*) of the AR treatment (relative to TR), were associated with the *aldosterone signaling pathway in epithelial cells*. According to the IPA based predictions, besides *HSP70*, also the two genes *PPP1R15A* and *DNAJA2* affected the pathway of the *unfolded protein response*. Moreover, *HSP70*, together with *HSP90* and *DNAJB1* were assigned to the *protein ubiquitination pathway*. As previously described for the comparison of the GR to the TR treatment, also for the AR-data set the IPA analysis predicted the *glucocorticoid receptor signaling pathway* as affected, unless the involved DE genes (*DUSP1*, *HSP70*, *HSP90*) differed completely from the GR-data set. The altered gene expression of *HSP70* and *HSP90* after AR treatment of maraena whitefish (compared to TR conditions), was very likely associated with the *eNOS signaling pathway*.

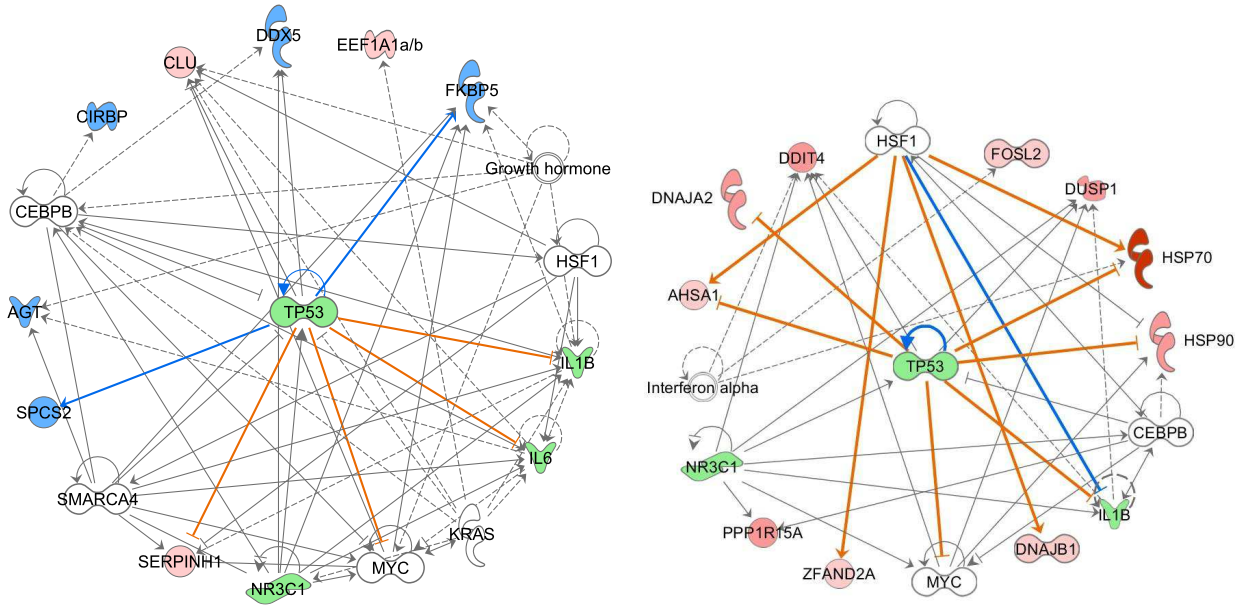

(a) Gradual temperature rise

(b) Acute temperature rise

Figure 3.17: **IPA networks based on upstream-regulator analyses for the DE-gene sets shared by kidney, liver, and spleen after GR or AR treatment**
IPA-based prediction of upstream regulators that may have led to the altered expression of DE genes from the GR- and the AR-data set. Different shades of red and blue of the respective symbols, represent up- and down-regulated genes according to FC values given in table B.4 for GR-data and table B.5 for AR data. Green-coloured symbols indicate known candidate genes examined in the course of this study. Full and broken lines indicate a direct or indirect interaction between two factors. The arrows represent the direction of interaction, and activation, whereas horizontal lines at the end indicate an inhibition. Relationships between the predicted regulators and other factors are displayed by orange (activation), blue (inhibition), and grey (uncertainty due to lack of knowledge, or state of the downstream molecule) colouring of the arrows.

In addition to the allocation of pathways to the two DE gene lists, IPA software was used to perform upstream-regulator analyses based on the 12 DE genes from the GR-data set (B.4), as well as for the 11 genes of the AR-data set (B.5). The network given in figure 3.17a predicts TP53 as a central regulator, that might have led to the differential expression of five (*SERPINH1*, *SPCS2*, *CLU*, *DDX5*, *FKBP5*) of the eleven DE genes found for GR vs. TR treatment within the microarray analysis. The IPA upstream regulator analysis predicted TP53 itself to be down-regulated (indicated by a blue arrow), which consequently led to the inhibition (blue arrows) of FKBP5 and SPCS2, since they are positively regulated by TP53. However, the factors SERPINH1, MYC, IL6 and IL1B were activated (orange arrows) due to low levels of TP53, since this factor has an inhibitory effect on these factors. According to the given network, TP53 also regulated the factors NR3C1, IL6 and IL1B, which were also predicted to be

regulators within this network and are target molecules within this study. NR3C1 might have influenced the altered expression of *DDX5*, whereas IL6 most likely regulated *AGT* expression, and IL1B might have had a regulatory effect on *SERPINH1*. Moreover, six other potential regulators have been identified by the IPA-software, which are CEBPB (acting exclusively on *CIRBP*), SMARCA4, also a well networked factor, as well as MYC, KRAS (solely regulated *EEF1A1a/b*), HSF1, and Growth hormone.

Just as before, for the analysis of the GR-data set, TP53 (again inhibited) was identified as the central regulator after AR treatment of maraena whitefish, as to be seen in figure 3.17b. Within the given network, the IPA analysis predicted TP53 to have probably caused the altered expression of six of the 11 DE genes of the AR-data set (compared to the TR-data set). Additionally, the down-regulated TP53 might have had mostly activating regulatory effects, since nearly all of the regulated genes (*HSP90*, *HSPA1a/b*, *DNAJA2*, *AHSA1*) were inhibited by TP53, except from *DUSP1* and *DDIT4*. Moreover, the network predicts the two factors NR3C1 and IL1B, to be regulated by TP53 and to act as upstream regulators on *DDIT4*, *DUSP1* and *PPP1R15A* (the latter was only regulated by NR3C1). Besides the potential regulators TP53, NR3C1 and IL1B, which are already known as target genes from this study, the IPA-software identified four additional regulators, named Interferon alpha (solely regulating *FOSL2*), MYC, CEBPB, and the as well highly networking factor HSF1, which also has activating effects on four (*AHSA1*, *HSP70*, *DNAJB1*, exclusively *ZFAND2A*) of the 11 DE genes after AR treatment of maraena whitefish (relative to TR treatment).

3.5.4. Modulation of plasma cortisol and glucose levels due to temperature stress

After exposure of maraena whitefish to an acute and a gradual temperature rise from 18°C to 24°C the plasma cortisol and glucose levels were analysed. Respective data for cortisol are shown in figure 3.18a and for glucose in figure 3.18b. The cortisol level for the AR treatment reached relatively high median

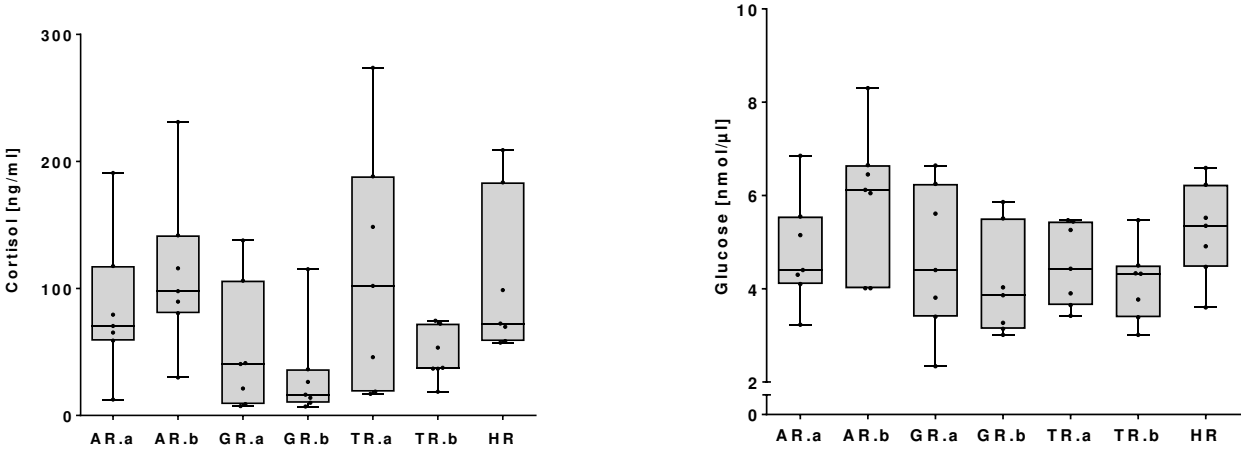

(a) Plasma cortisol levels

(b) Plasma glucose levels

Figure 3.18: **Influence of a temperature rise on plasma cortisol and glucose levels**
The box and whisker diagrams show plasma cortisol levels [ng/ml] (in figure 3.18a) and plasma glucose levels [nmol/µl] (in figure 3.18b) on the ordinate, subjected to the different experimental conditions that are listed along the abscissa.The whiskers at top and bottom of the box plots display the minimum and maximum, whereas the frame of the boxes mark the first and third quartile (i.e., 50% of the observations) of the given data. The median value is given as a horizontal line in each box respectively. Additionally, the seven individual measuring points of every treatment group are indicated in the diagrams as black dots. Within the experiment two independent replicates (referred to as "a" and "b") were performed for acute rise (AR), gradual rise (GR) and temperature reference (TR), whereas the handling reference (HR) was tested only once.

values of 70.4 ng/ml for AR.a and 97.9 ng/ml for AR.b, and both replicates show one clear up- and downward outlier. For the GR, median cortisol concentrations were considerably low for GR.a (40.5 ng/ml), and overall lowest for GR.b (16.4 ng/ ml), nonetheless there was one clear upward outlier of 115.1 ng/ml cortisol for GR.b. The median cortisol level of 102 ng/ml for TR.a was the overall highest. Additionally, TR.a revealed the highest variance of all tested individuals ranging from a minimum of 17 ng/ml to a maximum of 273.7 ng/ml. In contrast to that, the median value (37.5 ng/ml) and the variance of the cortisol concentrations for TR.b were comparably low. The median cortisol value of 72.4 ng/ml for the HR was, compared to all other groups, at a medium level, but the individuals of the HR group showed a high variance, too (minimum at 57.3 ng/ml, maximum at 208.9 ng/ml). All in all, there were no significant differences in plasma cortisol levels for the different treatments, since variations of the cortisol values between individuals of the same group were higher than between the four different treatments tested.

The plasma glucose concentrations of temperature stress groups were relatively close together, indicated by median values of 4.4 nmol/µl for AR.a and GR.a, as well as 3.86 nmol/µl for GR.b. Only for AR.b, the glucose concentration was slightly increased up to a median value of 6.1 nmol/µl. The median glucose values of the TR groups were in the same range as for the temperature stress groups, namely 4.4 nmol/µl for TR.a and 4.3 nmol/µl for TR.b. Even for the HR group, the calculated median value of 5.4 nmol/µl differed only marginally from the other treatment groups. Thus, there were no significant differences in the plasma glucose values for the tested treatment categories, since the individuals of the same group show higher variations than the different treatment groups of the experiment among one another.

3.6. Stimulation of maraena whitefish with *A. salmonicida*

Within this experiment, maraena whitefish was challenged with an inactivated suspension of the pathogenic bacterium *A. salmonicida* to study this fish's early immune response. Therefore, an *i.p.* injection was administered in form of an inactivated bacterial suspension to fish of the stimulated group (*A. sal*-S), or a PBS suspension to fish of the negative-control group (PBS-C). Subsequently, tissue samples were taken after 24 h, 48 h, and 72 h for each time six (*A. sal*-S) or five (PBS-C) individuals per time-point, as described in detail in section 2.1.6. The samples obtained from this experiment, were used to determine individual copy numbers (for details see 2.2.4.8), exclusively for the immune target-gene set, by qPCR using the BioMark™ HD-System (2.2.4.8.2). Based on the resulting copy numbers, expression ratios were calculated of stimulated fish (*A. sal*-S) relative to the unstimulated control (PBS-C) and plotted as heat maps using the RStudio software (see section 2.7.4). Further, as an overview, box-whisker-plots were constructed, representing the individual copy numbers for the three time-points summarised in one box, for each group and tissue.

3.6.1. Modulation of immune gene mRNA levels due to stimulation of maraena whitefish with *A. salmonicida*

As to be seen in figure 3.19.A, all immune genes were clearly regulated after *A. sal* stimulation, compared to the PBS negative control, albeit only in specific tissues, except from the gene *MAPK3*, which was only slightly affected at one time point in the liver (FC = -3.2 at 72 h). For example, in the head kidney, the genes *IL1B, IL6, IL12B, TNF*, and *MAPK1* showed the same expression pattern across the three sampling time points, starting with no or a slight up-regulation at 24 h, which then turned into a strong up-regulation at 48 h, especially for *IL1B* (122-fold up), *IL12B* (30.7-fold up) and *IL6* (27.2-fold up), and finally at 72 h, the expression ratios turned into minimum values, ranging from FC = -2.7 for *TNF*

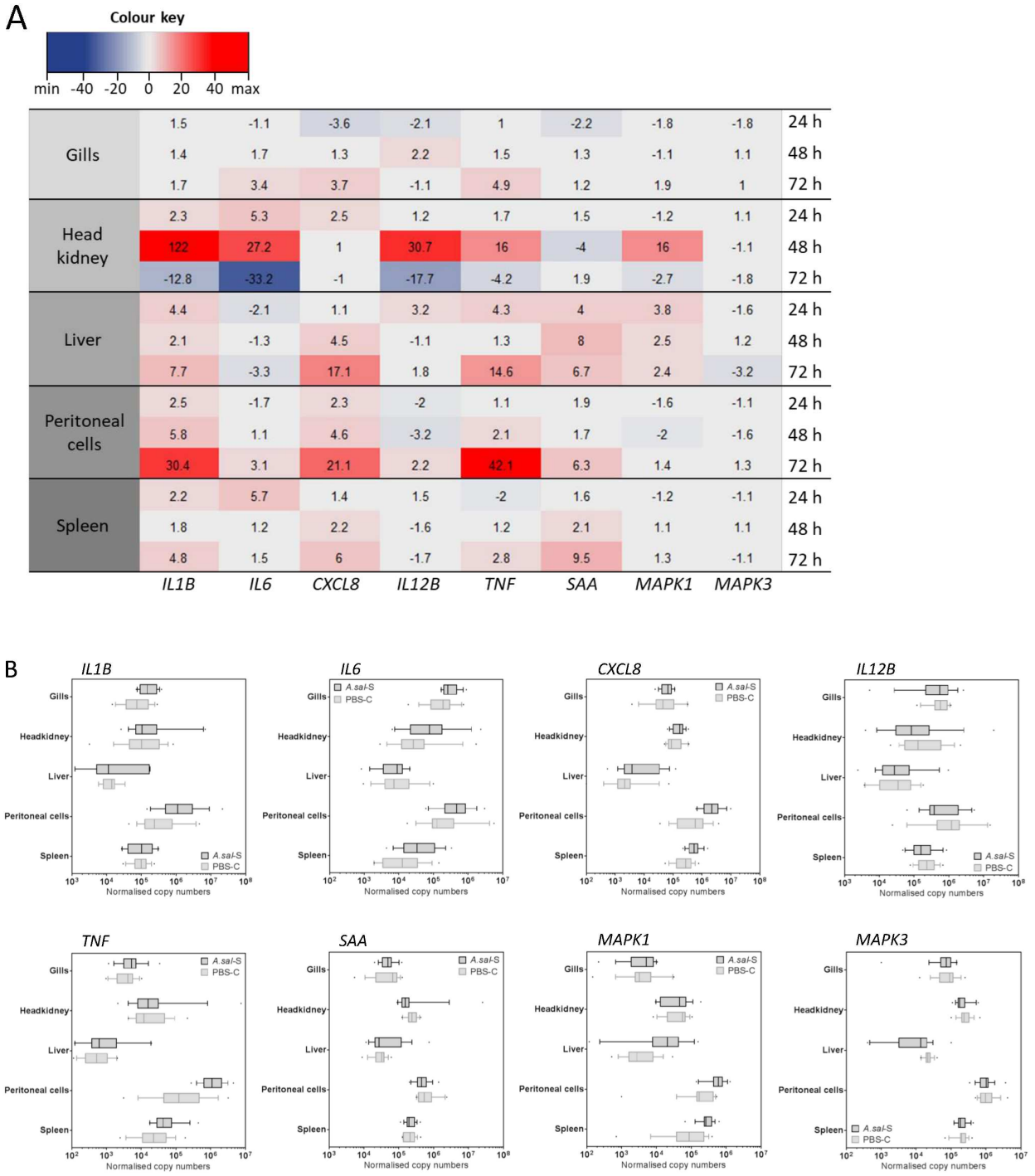

Figure 3.19: **Modulation of immune genes after stimulation of maraena whitefish with *A. salmonicida***
The heat map (**A**) illustrates average expression ratios as fold changes of the *A. salmonicida*-stimulated group (*A. sal*-S) relative to the negative control (PBS-C) for the immune genes *IL1B*, *IL6*, *CXCL8*, *IL12B*, *TNF*, *SAA*, *MAPK1* and *MAPK3* (listed in columns) measured by qPCR (n = 6 for *A. sal*-S; n = 5 for PBS-C). The different tested tissues are given in rows on the left, whereas the respective sampling time points are given on the right. A colour key is indicated on top. The box-whisker plots (**B**) depict the individual copy numbers (abscissa) of the target genes (indicated above the plot) in the different tissues (ordinate), summarised for all three sampling time-points together in one box. The different treatment categories given in the plot are *the A. salmonicida*-stimulated group (*A. sal*-S) and the negative-control group (PBS-C), each indicated by a different shade of grey. The copy numbers were normalised by the reference genes *RPL9*, *RPL32*, and *EEF1A1B*.

to FC = -33.2 for *IL6*. Within the peritoneal cells, located directly at the site of injection the genes

IL1B, *CXCL8,* and *TNF*, revealed a stepwise up-regulation from one sampling time point to another, resulting in maximum values of FC = 42.1, FC = 30.4, and FC = 21.1 at 72 h for *TNF*, *IL1B*, and *CXCL8*, respectively. Additionally, *SAA* was up-regulated 6.3-fold after 72 h in the peritoneal cells. However, in splenic tissue, *SAA* was the most up-regulated gene, which exhibited the highest FC value of 9.5 72 h after stimulation of maraena whitefish. Also for the genes *IL1B* (FC = 4.8), *CXCL8* (FC = 6.0), and *TNF* (FC = 2.8) the expression ratios were highest after 72 h in the spleen, whilst *IL6* reached a maximum induction of 5.7-fold already after 24 h within this tissue. In the liver, the genes *IL1B*, *CXCL8*, *TNF*, *SAA,* and *MAPK1* were particularly noticeable regulated, showing diverse expression patterns for each gene. Thus, *IL1B* and *TNF* revealed a medium up-regulation of around 4-fold at 24 h, then at 48 h the expression ratios were lowest, followed by maximum values of FC = 7.7 for *IL1B* and 14.6 for *TNF*. However, *CXCL8* was stepwise up-regulated in the liver, from 4.5- fold at 48 h to 17.1-fold at 72 h, whereas *MAPK1* was stepwise down-regulated in this tissue, from a maximum value of FC = 3.8 after 24 h to a minimum of FC = 2.4 after 72 h. Again another expression pattern was found for *SAA*, reaching an initial value of FC = 4.0 24 h post stimulation, this ratio doubled to a peak value of 8.0-fold up-regulation after 48 h and then again felt down to a little lower FC value of 6.7 after 72 h. Compared to the PBS-negative control, the *A. sal* stimulation caused only little effects on the immune target genes in the gills of maraena whitefish, since only slight up-regulations were recorded for *IL6* (3.4-fold), *CXCL8* (3.7-fold), and *TNF* (4.9-fold).

The box whisker plots in figure 3.19.B clearly display that for all immune target genes and both treatments (*A. sal*-S and PBS-C), highest relative copy numbers were determined in the peritoneal cells (except from PBS-C in *MAPK1*), whilst for both treatments and all genes, the lowest relative copy numbers were found in the liver, as well as in the gills for *SAA* and *MAPK1*. However, the genes *IL6* and *IL12B* revealed comparably high relative copy numbers in the gills, approximately on the same level as for the peritoneal cells. Further, it should be noted that for nearly all genes, the copy numbers varied similarly for both treatments in most tissues. Notable differences in variations of the copy numbers between the two treatment groups were mainly recorded for measurements in the liver (*IL1B*, *MAPK1*, *MAPK3*) and the head kidney (*TNF*, *SAA*).

3.7. Stimulation of head kidney primary cells with cortisol and PAMP reagents

Based on the results from the previous stimulation experiment with *A. salmonicida* (see section 3.6), the experimental design of the in vitro cell stimulation was developed. Since the overall highest range of regulation for the immune target genes was measured in the head kidney, and since it integrates hematopoietic and endocrine functions, this tissue was chosen for a further, more detailed analysis of maraena whitefish's early immune response. Therefore, primary cells from maraena whitefish head kidney, were stimulated using a mixture of six different PAMP reagents, comprising or mimicking features of Gram-negative and Gram-positive bacteria, as well as from dsRNA viruses, as indicated in detail in table 2.2. Additionally, primary cells were challenged with the steroid hormone cortisol (hydrocortisone), as well as with a mixture of cortisol and six PAMP reagents (further details in section 2.1.7). The sampling of the challenged head kidney cells was carried out 1 h, 3 h, 6 h, 12 h, 24 h and 48 h post stimulation, and once after 48 h for untreated cells, which served as negative control. The cells were subsequently subjected to the isolation of total RNA (2.2.1), which was finally used for qPCR measurements.

Depart from the stimulation experiment, morphology of head kidney cells was analysed by microscopy, and the cell composition was characterised using flow cytometry. Moreover, isolated RNA from untreated

cells was used to quantify expression of cell-specific transcription markers by qPCR, as described in the following.

3.7.1. Morphology of head kidney primary cells in inverted laser scanning microscopy

Prior to the cell-stimulation experiment, untreated head kidney primary cells were observed after in-vitro cultivation for 24 h, 48 h, and 72 h, using inverted laser scanning microscopy, to check when the cells start changing their morphology. This has been an important criterion to develop the experimental design, since the cells should not undergo spontaneous differentiation during the experimental period, to minimise effects on gene expression, apart from the stimulation. Microscopy of head kidney cells at a 200-fold magnification showed the characteristic morphology of individual cells with a circular to slightly oval shape and a size of around 7-45 µm, as to be seen in figure 3.20.A-B for 24 h and 48 h of cultivation. For the applied cultivation conditions (2.5), a morphological stability was observed for around 60 h, afterwards the cells began to elongate, forming bifurcated extensions (pseudopodia) and again began to connect with each other, as shown in figure 3.20.C at 72 h. Therefore, the experimental design has been adjusted to a maximum of 48 h of incubation after adding the respective stimulating reagents.

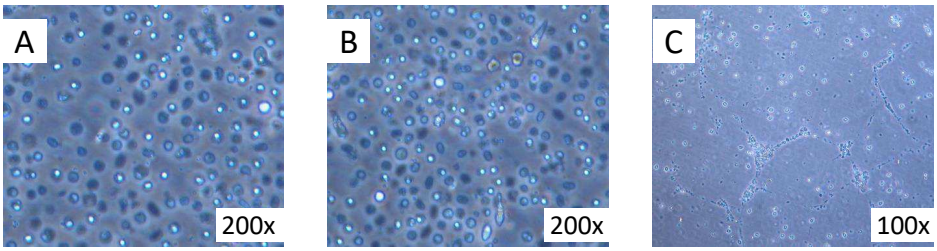

Figure 3.20: **Morphology of maraena whitefish head kidney cells observed by inverted laser scanning microscopy**
Head kidney cells after in vitro cultivation for 24 h (A), 48 h (B), and 72 h (C) in CCM at 19°C and 5% CO_2-atmosphere. The magnification was setted as indicated in figures A-C.

3.7.2. Composition of head kidney primary cells

The composition of head kidney cells, was analysed immediately after isolation from maraena whitefish, using flow cytometry as described in detail in section 2.5.2. As to be seen by the blue and yellow cloud of the dot plot in figure 3.21, two heterogeneous cell populations have been identified based on their cell volume by the forward scatter (FS INT) and their cell granularity by the side scatter (SS INT). The blue marked population, on the lower left corner, was mainly characterised by a highly varying cell size and a low cell granularity, which most likely corresponds to lymphocytes and precursor cells. However, the orange marked population was positioned a little more in the centre of the dot plot and therefore contained larger, but in size still highly varying and more granular cells, which most likely corresponds to monocytes and granulocyte-like cells.

3.7.3. Modulation of immune genes after stimulation of head kidney primary cells with cortisol and PAMP reagents

After challenging the head kidney cells with PAMP reagents and cortisol, the immune gene mRNA levels were analysed by qPCR using the BioMark™ HD-System (2.2.4.8.2). Based on the qPCR measurements,

individual gene copy numbers were calculated (for details see 2.2.4.8) and subsequently converted to ratios of stimulated cells relative to the untreated control. The resulting data were illustrated as heat map using the RStudio software (see section 2.7.4). As an overview, the box-whisker plots display individual copy numbers of each gene and treatment category, summarised for all six measured time points in one box.

The immune genes were clearly affected by the stimulation in the head kidney cells, as to be seen in the heat map in figure 3.22.A, since each target gene showed an individual cyclic up- and down-regulation for each treatment, considering the expression ratios over the whole experimental period from 1 h to 48 h post stimulation. Regarding the most noticeable expression values for each gene and treatment, the cortisol treatment led to a clear down-regulation of *IL1B* (-11.5-fold;1 h), *IL6* (-39.7-fold; 1 h), *CXCL8* (-18.4-fold; 12 h), and *TNF* (-130.5-fold; 12 h), while *SAA* (17.7-fold) and *MAPK3* (12.8-fold) were clearly up-regulated 48 h post cortisol treatment, compared to the untreated control.

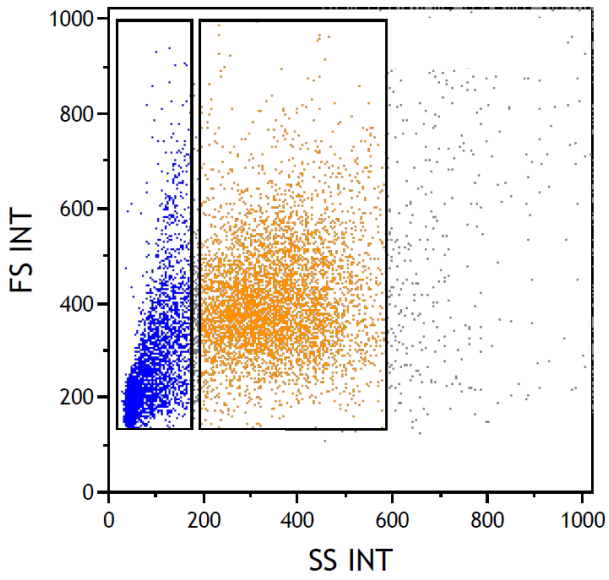

Figure 3.21: **Composition of head kidney cells of mareana whitefish analysed by flow cytometry**
The dot plot in figure 3.21 displays results from the flow cytometric analysis of head kidney cells, which were analysed regarding cell volume by the forward scatter given on the ordinate (FS INT) and cell granularity by the side scatter given on the abscissa (SS INT). The two different cell populations identified during flow cytometry, by which the cells were subsequently sorted are indicated by blue and orange dots, respectively.

Further, after 6 h of incubation of head kidney cells with the combination of cortisol and PAMP reagents, all target genes were up-regulated ranging from a slight up-regulation of FC = 2.3 for *TNF*, to a significant up-regulation of FC = 41 for *IL6*, which then reduced stepwise until 48 h of incubation. However, the genes *SAA*, *MAPK3, CXCL8*, and *MAPK1* revealed a second peak in transcript levels 48 h post treatment.

The stimulation of head kidney cells with PAMP reagents alone, led to a first increase in expression ratios for all immune target genes 3 h post treatment, whereby *SAA* reached the maximum FC of 26.2-fold of all genes, followed by little lower FC values ranging from 13.9 to 15.5 for *IL1B*, *CXCL8*, and *MAPK3*. Subsequently, 6 h post stimulation with PAMP reagents, expression ratios for all genes were reduced compared to the previous time point, whereas 12 h post stimulation the transcript levels increased again for the whole set of immune target genes, and even to maximum values for *SAA* (FC = 75.3) and *IL12B* (FC = 13.0). Whilst most genes exhibited a decrease in expression from 12 h to 48 h post PAMP treatment, for *CXCL8* and *SAA* transcript levels still increased gradually, reaching again a peak value of 47.5 for *SAA* and of 13.4 for *CXCL8*, respectively. An exception was found for *TNF*, this gene showed a delayed peak expression ratio of FC = 10.7 at 24 h post PAMP stimulation, compared to the 12 h peak FC values measured for all other genes. Overall, *SAA* revealed the constantly highest up-regulation over all six time points, while the highest values of down-regulation were recorded for *IL6*.

Additionally, the box-whisker plots in figure 3.22.B, give an overview of the average transcript values over all three treatments and for the negative control, since the individual copy numbers were plotted for all sampling time points together in one box. Thus, it becomes clear that *SAA* in particular, and as well

TNF, MAPK3, *CXCL8*, and to a lesser extent *IL1B* revealed a similar expression pattern for the three treatments, which was characterised by lowest average copy numbers following stimulation with cortisol alone, medium average transcript levels after stimulation with a mixture of cortisol and the PAMP

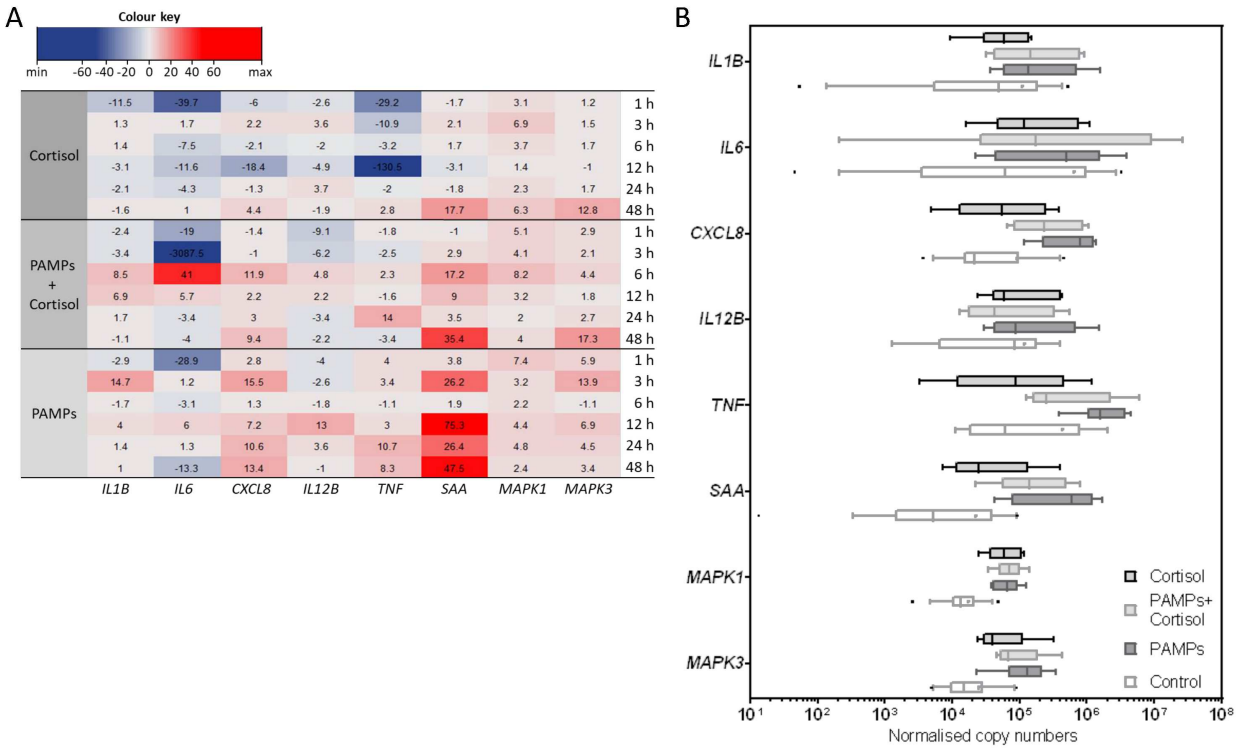

Figure 3.22: **Modulation of immune genes after in vitro stimulation of head kidney cells with cortisol and PAMP reagents**
The heat map (**A**) illustrates average expression ratios as fold changes of stimulated cells relative to the untreated control for the immune genes *IL1B*, *IL6*, *CXCL8*, *IL12B*, *TNF*, *SAA*, *MAPK1* and *MAPK3* (listed in columns) measured by qPCR (n = 9). The different sampling time points are given in rows on the right hand and the three treatment categories: PAMPs, cortisol, and PAMPs + cortisol, indicated by the grey-shaded boxes, are given on the left hand. A colour key is indicated on top. The box-whisker plots (**B**) depict the individual copy numbers (abscissa) for each treatment category and target gene (ordinate) summarised for all six measured time points in one box. The copy numbers were normalised by the reference genes *RPL9*, *RPL32*, and *EEF1A1B*. The different treatment categories given in the plot are PAMPs, cortisol, cortisol + PAMPs, and untreated cells as control, each indicated by a different shade of grey.

reagents, and finally highest average copy numbers after the treatment with PAMP reagents alone, as to be seen by the stepwise switch of the respective boxes to the right, compared to the control. However, for the genes *IL6*, and *MAPK1*, highest mean copy numbers were determined after stimulation with the mixture of cortisol and PAMP reagents, indicated by the shift to the right of the respective boxes. All in all, the box-whisker plots clearly show low variances in copy numbers for all four treatment categories, determined for *MAPK1* and *MAPK3*, moderately variances for transcription levels of *SAA*, *TNF*, *CXCL8* and *IL1B*, whilst the latter revealed a high variance for copy numbers of the negative control, but according to the position of the median the half of all transcript values calculated are still within the range of the values for the stimulation treatments. Moreover, for *IL6* the copy numbers determined for all treatment groups varied a lot, particularly for the stimulation with cortisol + PAMPs and the negative control, nonetheless all boxes showed similar ranges, and boxes representing the stimulation treatments were still slightly shifted to the right, compared to the control. Taken together, the box-whisker-plots clearly unveil for all genes, sampling time points, and treatment groups, on average a slight to very clear

up-regulation of the stimulated cells compared to the untreated control, since the boxes representing copy numbers for the control, were always in the lowest range.

3.7.4. Modulation of stress genes after stimulation of head kidney primary cells with cortisol and PAMP reagents

For the stress target genes, the respective copy numbers and the resulting expression ratios, were measured, calculated, and plotted exactly in the same way as already described for the immune genes in section 3.7.3.

The stimulation of head kidney cells affected expression ratios of the whole set of stress target genes, particularly *HSP70* and *TP53* for all three stimulation treatments, as illustrated by the heat map in figure 3.23.A, while HSP90 was mainly regulated due to PAMP treatment and *NR3C1* due to the combined treatment with cortisol and PAMP reagents. Moreover, *HSP70* was exclusively up-regulated, during the whole experiment, for all tested treatments and sampling time points and also the genes *HSP90* and *TP53* were up-regulated or not affected. Solely the gene *NR3C1* showed a slight down-regulation post cortisol (-3.5-fold, 1 h) and cortisol + PAMPs (-2.1-fold, 3 h) treatment. Additionally, for all four target

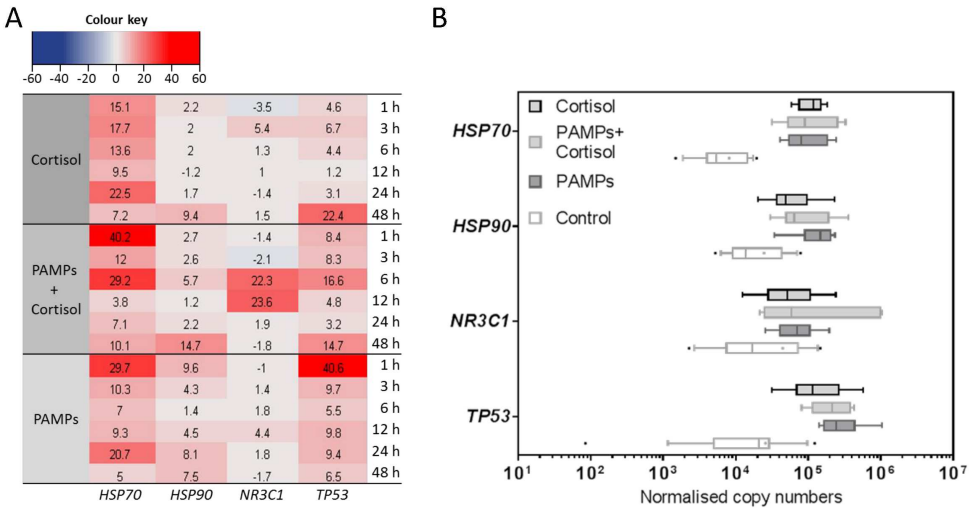

Figure 3.23: **Modulation of stress genes after in vitro stimulation of head kidney cells with cortisol and PAMP reagents**
The heat map (**A**) illustrates average expression ratios as fold changes of stimulated cells relative to the untreated control for the stress genes *HSP70*, *HSP90*, *NR3C1*, and *TP53* (listed in columns) measured by qPCR (n = 9). The different sampling time points are given in rows on the right hand and the three treatment categories: PAMPs, cortisol, and PAMPs + cortisol, indicated by the grey-shaded boxes, are given on the left hand. A colour key is indicated above the scheme. The box-whisker plots (**B**) depict the individual copy numbers (abscissa) for each treatment category and target gene (ordinate) summarised for all six measured time points in one box. The copy numbers were normalised by the reference genes *RPL9*, *RPL32*, and *EEF1A1B*. The different treatment categories given in the plot are PAMPs, cortisol, and cortisol + PAMPs, and untreated cells as control, each indicated by a different shade of grey.

genes a cyclic up- and down-regulation was recorded, as already described for the immune target genes, although not that obvious for some genes and treatments. Thus, after stimulation with cortisol, two peak values were determined for *HSP70* at 3 h (17.7-fold) and 24 h (22.5-fold) and for *TP53* at 3 h (6.7-fold) and 48 h (22.4-fold) of incubation. Except from one peak value of FC = 9.4 (48 h) for *HSP90* and of FC = 5.4 (3 h) for *NR3C1*, both genes showed no noticeable regulation after cortisol treatment.

The stimulation of head kidney cells with a mixture of cortisol and PAMP reagents caused three peaks of up-regulation for HSP70, which became each time lower (FC = 40.2 after 1 h; FC = 29.2 after 6 h; FC = 10.1 after 48 h). The same treatment led to two, gradually increasing peak values, for *HSP90* and *TP53* at 6 h and 48 h. However, for the gene *NR3C1* only one, sharply increasing peak expression from 6 h (22.3-fold up) to 12 h (23.6-fold up) post stimulation was calculated, that finally sharply dropped again.

When head kidney cells were treated with PAMP reagents alone, this caused a fast induction of the genes *TP53*, *HSP70*, and *HSP90*, which were clearly up-regulated as fast as 1 h post stimulation. This initial, sharp up-regulation was followed by a gradual down-regulation, which then turned into a second, but lower peak value for *HSP70* (FC = 20.7), *TP53* (FC = 9.8), and *HSP90* (FC = 8.1). A completely different expression pattern was found for the gene *NR3C1*, which remained completely unaffected after stimulation with PAMP reagents, except from one slightly elevated FC value of 4.4 after 12 h of incubation.

In addition to the heat map, the box-whisker plots in figure 3.23.B, display the individual copy numbers of all sampling time points summarised in one box, for each gene and treatment, including the negative control. The diagram clearly unveils the much higher transcript levels of the stimulated cells, compared to the negative control, for all stress target genes, indicated by the left-side shifted boxes representing the copy numbers of the negative control. Moreover, the box-whisker plots unveil the comparably low variances in copy numbers for all four treatment categories and genes, except from little higher variances for the transcript numbers of the *TP53* and *NR3C1* negative control. Except for *NR3C1* after stimulation with PAMP + cortisol, for this gene copy numbers varied more than for the other two stimulation assays, since solely this treatment led to a rapid and significant up-regulation for two sampling time points (6-12 h).

3.8. Maraena whitefish's ontogenetic development

The *IGF* gene expression, during mareana whitefish's ontogenetic development, was examined by two different experiments. On the one hand, gene expression profiles were assessed for *IGF1* and *IGF2*, during the development from unfertilised egg to fingerling by qPCR measurements, on the other hand, the influence of incubation temperature on maraena whitefish development pre- and post-hatch was surveyed. For this reason, *IGF1* and *IGF2* expression were determined over the whole experimental period, and additionally morphological parameters were recorded at specific stages of embryonic development, as well as after hatch.

3.8.1. Expression profile of *IGF*s during maraena whitefish's ontogeny from egg to fingerling

The gene expression profiles of *IGF1* and *IGF2* were analysed at stated intervals from shortly before fertilisation until 60 days post-hatching by qPCR using a LightCycler®96 system (2.2.4.8) as described in detail in section 2.1.8.1. Therefore, qPCR measurements served to calculate individual target-gene copy numbers (for details see 2.2.4.8), which were always related to 1 µg of total RNA., and additionally, the *IGF2/IGF1* gene expression ratio was determined, for direct comparison.

As shown by the bar graphs in figure 3.24.A and 3.24B, during the development of maraena whitefish from egg to fingerling, *IGF1* and *IGF2* exhibited mainly the same expression pattern, characterised by high variations. The unfertilised eggs revealed high numbers of maternally transferred transcripts for *IGF1* (≈ 165,000 copies/µg RNA), as well as for *IGF2* (≈ 395,000 copies/µg RNA), which were both nearly depleted within the following 24 h. Consequently, at 1 dpf, minimum transcript levels of ≈ 248 copies/µg

RNA for *IGF1* and ≈614 copies/µg RNA for *IGF2* were detected. Subsequently, the *IGF* transcript levels gradually rose to a peak within the egg stage at 66 dpf (≈139,000 copies/µg RNA for IGF1; ≈664,000 copies/µg RNA for *IGF2*). Solely for *IGF2*, a notable increase in expression was measured at the transition from the eyeless egg (45A dpf) to the eyed egg stage (45B dpf), which was not detectable for *IGF1*. After hatch, gene copy numbers reduced slightly for *IGF1* (4-fold down) and *IGF2* (2-fold down), but they subsequently increased again with the onset of feeding at the fry stage. Hence, the transcript values for both genes were on medium levels and finally soared sharply when fry were developing into fingerlings. Therefore, the overall highest transcript numbers were recorded at dph 60 with ≈243,000 copies/µg RNA for IGF1 and ≈672,000 copies/µg RNA for *IGF2*. In addition to that, the ratio of *IGF2*/*IGF1*, given in figure 3.24.C, indicates that *IGF2* transcript levels were higher than those for *IGF1* at every stage analysed, pre- and post-hatch. Particularly at life stages before the egg reaches the eyed-egg stage (8 dpf-45A dpf) and shortly after hatch (4 dph), *IGF2* copy numbers were clearly higher (> 14-fold up to > 75-fold) than those for *IGF1*, but they became nearly the same after onset of feeding and the transition of maraena whitefish fry to fingerling.

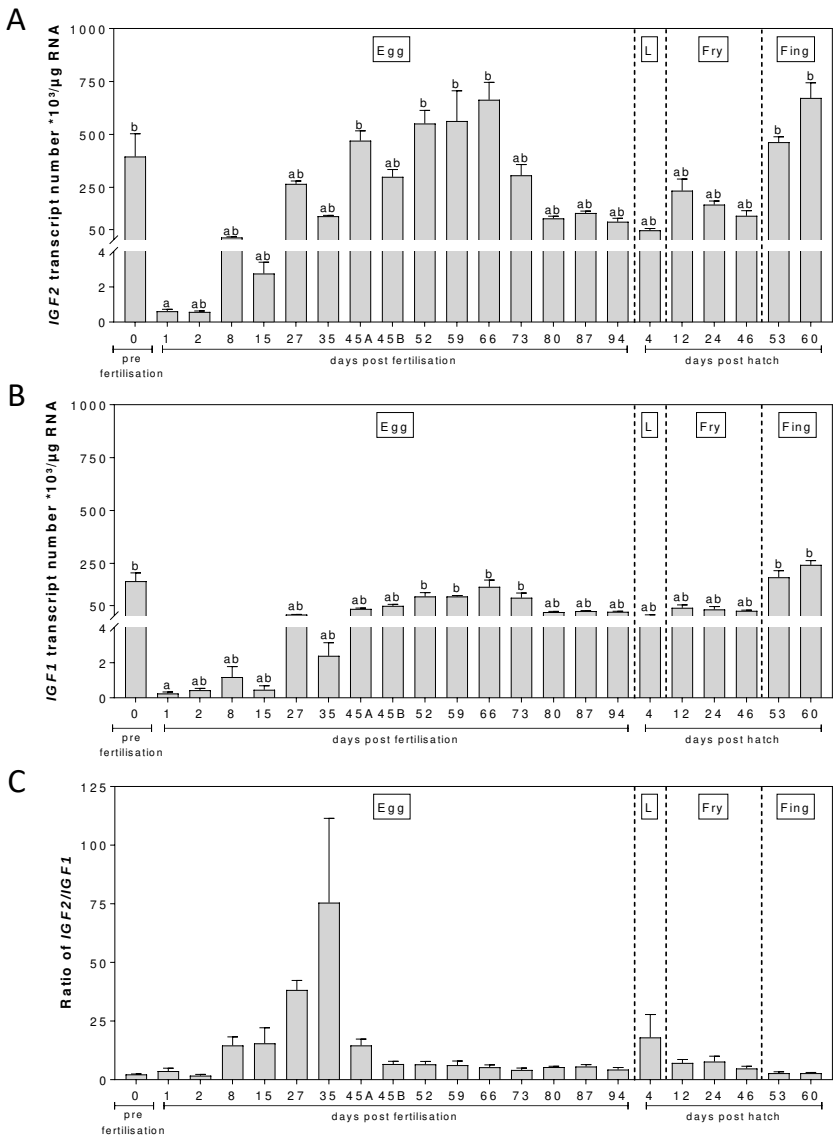

Figure 3.24: ***IGF1* and *IGF2* expression rates during maraena whitefish ontogeny from egg to fingerling**
The figure represents expression levels of *IGF1* (A) and *IGF2* (B) normalised to 1 µg RNA and the ratio of *IGF2*/*IGF1* gene expression (C). The bar graphs display the mean transcript numbers per µg RNA +SEM (n = 4). The sampling time point 1 dpf was set as the overall reference value to calculate significance levels that are indicated with letters above the bars. Different letters at least indicate $p < 0.05$. The 45A labelling on the x-axis represents eyeless eggs and 45B eyed eggs at the same time point. The dashed lines indicate the border between the morphological stages that are given in the boxes on the upper margin. The morphological stage "L" corresponds to larvae and "Fing" to fingerling, respectively.

3.8.2. Influence of incubation temperature on developing larvae pre- and post-hatch

The influence of incubation temperature on the development of maraena whitefish pre- and post-hatch was examined by measuring the *IGF1* and *IGF2* mRNA levels of fertilised eggs and larvae in three different temperature groups (4°C, 6°C, and 9°C) using qPCR (2.2.4.8) on the the BioMark™ HD-System, as described in detail in section 2.1.8.2. In addition to that, parameters of embryonic development like time point of eyed egg stage, hatching time and rate, and length increase of larvae after hatch were recorded.

3.8.2.1. Influence of incubation temperature on maraena whitefish morphology pre- and post-hatch Table 3.1 summarises all morphological parameters measured according to the development of maraena whitefish at the three different incubation temperatures analysed. The given values clearly demonstrate the shortened embryonic development with increasing incubation temperature, since the eyed-egg stage was reached already at 27 dpf (9°C group) and 30 dpf (6°C group), compared to 41 dpf for eggs incubated at 4°C. In line with this data, hatching set in already 49 dpf at 9°C and 62 dpf at 6°C, whereas the 4°C group hatched much later at 83 dpf. Moreover, length determination clearly unveiled

Table 3.1: **Influence of incubation temperature on development pre- and post-hatch**
In the table, the parameters are listed, which indicate the varying development of maraena whitefish pre- and post-hatch due to different incubation temperatures. The different analysed parameters are abbreviated as follows: incubation temperature (IncTemp), eyed egg stage (EES), hatching time (HT), hatching rate (HR), total length (TL), and average length increase (LI). Data for hatching rate and total length (n = 5) are indicated as mean values ± SD (standard deviation). Data for EES, HT, HR were adapted from Luft *et al.* (2015).

IncTemp	EES [dpf]	HT [dpf]	HR [%] ±SD	Time [weeks post hatch]						Ø LI [mm]
					0	1	2	3	4	
4°C	41	83	70.1	TL [mm]	11.2	14.6	18.6	21.6	28.6	4.35
			1.4	±SD	0.84	1.14	1.67	2.07	2.70	
6°C	30	62	74.7	TL [mm]	12.6	17.6	20.8	24.8	30.0	4.35
			2.4	±SD	0.89	1.14	1.30	2.28	2.55	
9°C	27	49	66.8	TL [mm]	9.2	12.6	17.0	21.4	25.4	4.05
			1.5	±SD	0.84	1.14	1.22	1.52	1.14	

that the early hatched larvae in the 9°C group were significantly smaller than the larvae in the 6°C group at all surveyed life stages, and even significantly smaller than larvae of the 4°C group at 1 wph, 3 wph, and 4 wph. This is also shown by the comparison of the average weekly length increase of larvae, which was 4.35 mm for the 4°C and the 6°C groups, but only 4.05 mm for the 9°C group. Altogether, 6°C seemed to be an optimal incubation temperature, since it led to accelerated embryonic development and the highest hatching rate (≈75%), the largest larvae size at hatch, and the best larval growth.

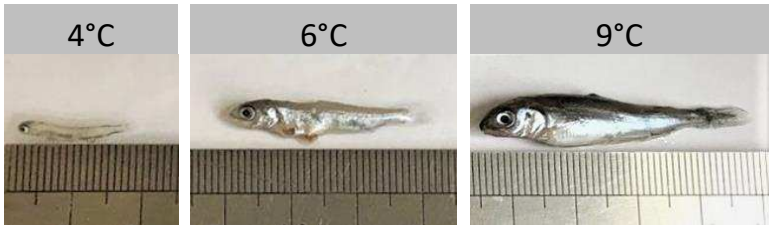

Figure 3.25: **Varying ontogenetic development of maraena whitefish due to different incubation temperatures**
Representative presentation of the different ontogenetic development of maraena whitefish at 97 dpf due to different incubation temperatures (4°C, 6°C, 9°C) as indicated above the figures. The total length was 19 mm, 33 mm, and 45 mm for the three displayed fish belonging to the 4°C, 6°C, and 9°C group, respectively. The vertical lines on top of the ruler indicate millimetre distances, whereas the vertical lines below indicate centimetre distances.

In comparison, at 9°C, embryonic development was accelerated as well, but hatching rate (≈67%), larvae size at hatch, and larval growth were even smaller than for the 4°C reference group.

If maraena whitefish development was not compared relative to each other, but for an absolute time span, as exemplarily displayed in figure 3.25 for fish aged 97 dpf, the massive differences in ontogenetic development become clear. At around 100 days post fertilisation (97 dpf), fish of the 4°C temperature group were still larvae, whilst fish of the 6°C group were already in the fry stage and moreover, the fish of the 9°C group even reached the stage of fingerlings.

3.8.2.2. Influence of incubation temperature on *IGF* expression The copy numbers of *IGF1* and *IGF2* for the three different temperature groups were displayed as relative values, in form of percentages, whereby the 4°C group was set as 100% and the 6°C and the 9°C group relative to the 4°C group.

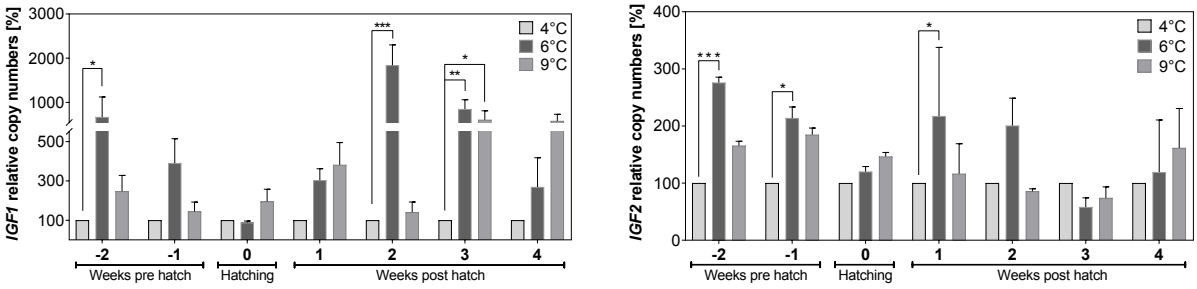

(a) *IGF1* (b) *IGF2*

Figure 3.26: **Modulation of *IGF1* and *IGF2* gene expression due to different incubation temperatures** Effect of incubation temperature on early development of maraena whitefish, represented by relative mRNA levels of *IGF1* (a) and *IGF2* (b) given in percentage. The bar graphs display the ratios of mean transcript numbers +SEM (n = 4) related to the 4°C-group that was set as 100% at all analysed stages. The respective 4°C sample was also set as reference to calculate significance levels for each developmental stage analysed. Significant differences in gene expression are marked by black asterisks (*, $p \leq 0.05$; **, p 0.01, ***, $p \leq 0.001$). After hatch, larvae were kept in previous groups, but transferred to 15°C aquaria.

As shown in figure 3.26.A and 3.26.B, the *IGF* gene expression was highly variable during the investigation period, but in general, for both *IGF1* and *IGF2* the lowest transcript numbers were found in eggs kept at the lowest incubation temperature of 4°C, except for hatching (0) for *IGF1* at 2 wph, as well as at 3 wph for *IGF2*. Accordingly, before hatch, both *IGF1* and *IGF2* gene expression was lowest for the 4°C group and highest for the 6°C group, whereas transcript numbers of the 9°C group were in between. These expression profiles suggest a temperature-related *IGF* expression and fit the observations that were made regarding embryonic development, hatching period and rate. At hatch, *IGF1* transcripts of the 6°C group reduced to a minimum value of only 88% relative to the 4°C group, whereas transcripts increased by nearly 50% in the 9°C group. Hence, *IGF1* expression rates seemed to be inversely proportional to larvae size at hatch. For *IGF2*, the copy numbers reduced at hatch as well but were staggered according to the respective incubation temperature (lowest at 4°C, highest at 9°C). After hatching, larvae of every group were reared at the same temperature (15°C; see 2.1.8.2), nevertheless, *IGF* expression remained highly variable from 1 wph to 4 wph. For *IGF1*, a staggered expression pattern was found at 1 wph, when feeding of larvae set in; here, transcript numbers exceeded those of the 4°C group by 200% (6°C) to 280% (9°C). For *IGF2* at 1 wph, a significant up-regulation of transcripts of the 6°C group were detected, whereas for the 9°C group, *IGF2* transcripts decreased gradually to an overall minimum of 70% relative to the 4°C group at 3 wph. However, *IGF1* transcript numbers were particularly high for the 6°C group at 2 wph

(> 18-fold up) and 3 wph (> 8-fold up), as well as for the 9°C group at 3 wph (> 6-fold up) and 4 wph (≈ 6-fold up). At four weeks post-hatch, again a staggered expression pattern for *IGF1* and *IGF2* has been observed. In most cases, *IGF* gene expression was highest within the 6°C group, which seemed to improve conditions for embryonic development. Consequently, in most life stages analysed, the transcript numbers of the 9°C group were in between those of the 4°C and the 6°C groups; this is in line with the fact that this temperature shortened the hatching period but resulted in reduced larval growth. Overall, first indications for a correlation of temperature with *IGF* expression during embryonic development could be detected, and it seemed that optimal conditions cause significantly higher expression rates of both *IGF1* and *IGF2* at specific life stages pre- and post-hatch of maraena whitefish.

4. Discussion

4.1. Glucose colorimetric assay

In order to determine glucose concentrations of plasma samples, obtained from the density stress (2.1.4) and the temperature stress (2.1.5) experiment, the Glucose Colorimetric Assay Kit II (BioVision) was used according to the manufacturer's instructions. Prior to the test procedure blood samples were centrifuged (4°C and 1700 rcf) and the supernatant was kept on ice until the measurement. The kit provides a dye that reacts with glucose to generate a colour. The intensity of the emerging colour is proportional to the glucose concentration of the samples and can be measured in a micro-titre plate reader ($\lambda = 450$ nm). The samples were analysed at the Beckman Coulter DTX 800/880 Series Multimode Detector (Beckman Coulter) and measured two times independently. Then, mean values were calculated for each sample and the resulting data were analysed using the GraphPadPrism®software (version 7.03).

4.2. Maraena whitefish was reared according to economic and sustainable requirements in a recirculation system

In the course of this study, maraena whitefish was comparatively reared in a cold-water flow-through and a warm-water recirculation system and growth was assessed by analysing different phenotypic parameters, above all weight and length. The rearing and analysing of both cohorts for 48 weeks showed that, in principle, maraena whitefish can be successfully cultured in both aquaculture systems. However, the phenotypic data clearly unveiled an overall much higher growth performance of maraena whitefish in the recirculation system, indicated by a clearly higher condition factor and a one third higher total length and a two third higher total weight compared to fish in the flow-through system. Hence, within one season of culturing in a recirculation system, maraena whitefish reached a marketable total body mass (> 330 g) and length (> 30 cm), which corresponds to the growth performance of rainbow trout in the same aquaculture facility, as reported by Borchel (2015) and was even higher compared to European whitefish (*Coregonus lavaretus*) cultured in a comparable aquaculture system at 10°C constantly (Siikavuopio *et al.*, 2012). By contrast, the average length (20 cm) and weight (< 80 g) maraena whitefish reached within the same culturing period in the flow-through system, was far below the typically marketed < 500 g "pan-size" of salmonids (Kenney PB, 2014). This means, using this culturing method, a second season is needed to obtain a marketable product, which is economically less attractive. The reasons for these clear differences in growth performance might be diverse, covering aspects like feed, photoperiod, pond shape and water quality. But above all, the temperature is very likely to have a major impact on growth performance, as it is generally regarded as one of the main factors influencing fish growth (Siikavuopio *et al.*, 2013; Szczepkowski *et al.*, 2006; Boltaña *et al.*, 2017; Viadero, 2005). Particularly salmonids are found to have a relatively small and highly species-specific range between preferable and harmful temperatures, as reviewed by Stien *et al.* (2013). Likewise, in their study on European whitefish Goebel *et al.* (2017) demonstrated the high impact of water temperature on the fish's growth, indicating that temperatures around 10°C are less advantageous, whereas 14°C seemed to be preferable. This is in line with observations made in this study, since maraena whitefish growth remained static from around the second half of the culturing period when water temperatures fell below 10°C in the flow-through system. On the other hand, Szczepkowski *et al.* (2006) and Matousek *et al.* (2017) showed that for the growth of juvenile coregonids, water temperatures from 19 - 22°C were beneficial, whilst at 24°C growth of *Coregonus lavaretus* (L.) was significantly decreased and mortality of *Coregonus peled* increased from

25°C upwards. Hence, the average temperature of 20.0°C, never exceeding a maximum of 22°C, in the recirculation system have most likely contributed to the higher growth performance of maraena whitefish in the recirculation compared to flow-through system, recorded in this work.

Further, Roque d'Orbcastel *et al.* (2009) reported a higher mass increase of rainbow trout for the cultivation in a recirculation compared to a flow-through system, despite similar rearing temperatures in both systems. This supports the assumption of a multifactorial cause for the different growth performances of maraena whitefish in the two tested systems analysed in this study. Since maraena whitefish is often described as sensitive, having high demands regarding water quality (Lorenz, 2012; Arndt, 2001; Luft *et al.*, 2015), the recirculation system might be beneficial because it ensures — besides consistent water temperatures — a constantly high water quality.

However, the well controllable conditions in recirculation systems not only allow more efficient fish growth but have further important benefits. Thus, compared to conventional flow-through systems, the fully or partially enclosed recirculation systems are more environmentally friendly in terms of water consumption (Roque d'Orbcastel *et al.*, 2009; Tal *et al.*, 2009; Martins *et al.*, 2010) and antibiotic treatment (Watts *et al.*, 2017), since the included purification and disinfection mechanisms enable a constant water recycling and a significant decrease of the microbial load. D'Orbcastel *et al.* (2009) found in their comparative study about sustainable aquaculture that recirculation systems have a lower overall environmental impact, compared to flow-through systems, which can be reduced to a minimum by technical improvements, as reported by Tal *et al.* (2009).

From the economic point of view, despite very high investment and energy costs, recirculation systems are advantageous, as they allow higher stocking densities and are independent from weather conditions, which makes a year-round production possible and thus contributes to yield improvement (Roque d'Orbcastel *et al.*, 2009; Martins *et al.*, 2010). An off-season breeding was already successfully tested in a small-scale for maraena whitefish (Bochert, 2014; Luft *et al.*, 2015). Additionally, Martins *et al.* (2010) and Badiola *et al.* (2012) illustrate the importance of recirculation systems for a seminal, constantly developing European aquaculture industry and the high potential of this technology for an economically efficient fish production, which simultaneously has a minimum environmental impact and secures fish welfare.

Taken together, the data collected within this work for the initial cultivation trials of maraena whitefish clearly showed that it is a promising species for local, economic and sustainable aquaculture if reared in recirculation systems, which is additionally strenghtened since a year-round production and a off-season reproduction of this species has been realised (Luft *et al.*, 2015; Bochert, 2014). Unless the importance of coregonids is steadily increasing for European aquaculture (Szczepkowski *et al.*, 2006; Siikavuopio *et al.*, 2012; Bochert, 2014; Goebel *et al.*, 2017), there is still a huge lack of knowledge concerning optimal rearing conditions, e.g., in terms of feed and temperature. Moreover recent studies revealed that for salmonids, suitable rearing conditions are highly species-specific, indicating that still a lot of research is needed to exploit the entire growth potential of maraena whitefish in aquaculture.

4.3. For all target genes full-length or partial ORF sequences were isolated and confirmed by structural and evolutionary analysis

In the course of this study, full-length or partial ORF sequences were isolated for all selected immune, stress, and growth genes. Regarding the immune gene set, the isolated maraena whitefish *IL1B* transcript encodes for a putative IL1B protein of 260 aa residues, which contains the teleost-specific IL1B aa-sequence structure, lacking a clear IL1B cut site (Secombes *et al.*, 1999; Zou *et al.*, 1999; Fujiki *et al.*,

2000), but having the typical IL1-family signature, that was previously identified for other fish species, and which is highly conserved within the family of salmonids (Husain *et al.*, 2012; Ho *et al.*, 2016; Xu *et al.*, 2016). The protein could be assigned to type II IL1B proteins, indicated by the short sequence length, compared to the longer aa sequence of type I IL1B molecules (> 275 aa) and the low degree of aa-sequence conservation (< 34%) within teleost species, as reported by Husain *et al.* (2012). Additionally the assignment to the type II IL1B molecules was confirmed by phylogenetic analysis.

For the maraena whitefish *IL6* transcript, the deduced protein was well conserved within the family of salmonids, but all in all revealed a low sequence identity to non-teleostean vertebrates, as expected from literature (Iliev *et al.*, 2007; Varela *et al.*, 2012; Castellana *et al.*, 2008). However the predicted IL6 homologue is structurally well conserved, showing the characteristic IL6 aa-sequence features (signal-peptide, IL6-family signature, four α-helices) that were previously reported for the closely related rainbow trout (Iliev *et al.*, 2007) but for several other teleost species, as well (Varela *et al.*, 2012; Bird *et al.*, 2005; Castellana *et al.*, 2008).

Similar results were found for the isolated maraena whitefish *CXCL8* transcript, whose deduced aa sequence has the typical CXCL8 structure, containing the indicative C-x-C motif, that was previously described for several putative piscine CXCL8 peptides (Lee *et al.*, 2001; Laing *et al.*, 2002; Chen *et al.*, 2005; Seppola *et al.*, 2008). Moreover, based on findings of Abdelkhalek *et al.* (2009) and van der Aa *et al.* (2010) about two possible CXCL8 lineages in teleost fish, which is contradictory to the single CXCL8 copy known from mammals, an evolutionary analysis was conducted. The putative maraena whitefish CXCL8, was assigned to the fish-specific CXCL8 lineage 1, with a high bootstrap support of 99%, since it showed higher sequence identity to its homologues in other fish species than to mammals. In contrast, the teleostean CXCL8 lineage 2 peptides are characterised by their slightly higher relation to mammalian than to piscine counterparts (Abdelkhalek *et al.*, 2009; van der Aa *et al.*, 2010).

The transcript isolated for the *IL12B* gene, one of two genes coding for the IL12 hetero-dimer, was encoding for a potential IL12p40c subunit, as was indicated by evolutionary analysis of the predicted protein sequence. As previously reported for common carp, amberjack and salmonids, fish possess at least three genes coding for the IL12p40 subunit, in contrast to mammals encoding only one IL12p40 protein (Huising *et al.*, 2006; Matsumoto *et al.*, 2016; Wang & Husain, 2014). Further, the different piscine IL12p40 isoforms share low intra- and inter-species sequence identity with each other (Huising *et al.*, 2006; Matsumoto *et al.*, 2016; Wang & Husain, 2014). This was true for the maraena whitefish IL12p40c as well, since it was only highly homologue to other potential salmonid IL12p40c isoforms, but not to other species IL12p40c and also not, compared to salmonid IL12p40a and IL12p40b, the sequence identity was as low as with higher vertebrates. Despite the low sequence similarity, the potential maraena whitefish IL12p40c protein was conserved for several cystein residues, participating in intra-chain disulphide bonds, the C-terminal WSxWS motif, and for the aa residues that are crucial for the formation of the IL12p70 heterodimer, which is in line with previous studies of several putative fish IL12p40 peptides (Huising *et al.*, 2006; Nascimento *et al.*, 2007a; Tsai *et al.*, 2014; Wang & Husain, 2014; Matsumoto *et al.*, 2016). The one cystein residue, which is missing in teleost IL12p40c, forms the inter-chain disulphide bridge between IL12p40 and IL12p35 and though has a stabilising function but is not necessary for the IL12p70 formation, as reported by Yoon *et al.* (2000). Consequently, it can be assumed that the predicted maraena whitefish IL12p40c protein is capable of forming a hetero-dimer with the IL12p35 subunit, as was previously found for common carp IL12p40c (Huising *et al.*, 2006).

Based on the isolated maraena whitefish *TNF* transcript, the TNF aa sequence was predicted, whose structure is characteristic for a vertebrate and especially for a teleost TNF member, since it contained

a transmembrane domain, a TNF-family signature motif, two highly conserved cystein residues, and a TACE cut site, as was previously described in literature (Saeij *et al.*, 2003b; Savan *et al.*, 2005; Glenney & Wiens, 2007; Roher *et al.*, 2010; Hong *et al.*, 2013; Zou & Secombes, 2016). Further, evolutionary analysis showed that the maraena whitefish TNF protein was clustered together with salmonid TNF-α1 and TNF-α2 isoforms and was clearly separated from salmonid TNF-α3 and other TNF proteins from teleosts, reptiles and mammals. Consequently, the putative, partial maraena whitefish TNF can not clearly be classified as a TNF-α1 or TNF-α2, but according to Hong *et al.* (2013) it can be assigned to the fish-specific type-I TNFs, whilst the salmonid TNF-α3 belongs to the fish-specific type-II TNFs. The two isoforms most likely emerged within the teleostean whole genome duplication event and Hong *et al.* (2013) further hypothesised that type-II TNF precursors, due to structural differences of their aa sequence, reside in the transmembrane-bound form, whereas type-I TNF molecules can be processed by TACE into the mature, soluble and extracellular form.

The maraena whitefish *SAA* transcript obtained within this study, coded for a protein, that was predicted to have a signal-peptide and hydrophobic region within the N-terminal domain, as well as a highly conserved SAA protein signature motif and a molecular weight of approximately 12 kDa, which is altogether indicative for SAA proteins, as it was previously reported for several vertebrate SAA molecules (Uhlar & Whitehead, 1999; Rebl *et al.*, 2009; Wei *et al.*, 2013; Jayasinghe *et al.*, 2015). Further, the putative maraena whitefish SAA aa-sequence revealed a comparably high degree of conservation among vertebrates, which agrees with previous publications about predicted teleostean (Fujiki *et al.*, 2000; Rebl *et al.*, 2009; Wei *et al.*, 2013; Jayasinghe *et al.*, 2015; Kovacevic & Belosevic, 2015) or even invertebrate (Qu *et al.*, 2014) SAA proteins. Regarding its evolutionary relationship, the maraena whitefish SAA protein was shown to be closely related to its homologues in other salmonids. Additionally, it was found, that the piscine SAA proteins and the mammalian A-SAA molecules emerged from a common ancestral gene, whereas the mammalian C-SAA proteins constitute a distinct clade, which is in line with evolutionary studies of SAA protein sequences conducted by Uhlar *et al.* (1994).

Like tetrapods, teleost fish are known to possess two closely related *MAPK* genes sharing high similarity in sequence, structure, and function among each other, as well as among vertebrates (Li *et al.*, 2011; Buscà *et al.*, 2015). Accordingly, the partial protein sequence, deduced from the maraena whitefish *MAPK1* transcript obtained within this work, was extraordinarily high conserved from fish to mammals, as well as the partial protein, encoded by the transcript isolated for the *MAPK3* gene. Regarding their structure, both deduced maraena whitefish MAPK aa sequences coded for a catalytic loop motif, which is thought to be crucial for the substrate turnover and therefore highly conserved (Roskoski, 2012). Moreover, for both predicted aa sequences the characteristic protein-serine/threonine kinase signature pattern was identified, which is located within the active-site of these enzymes (Roskoski, 2012). Additionally, for the predicted maraena whitefish MAPK3 protein, the highly conserved kinase insert domain, which is suggested to be involved into the nuclear uptake of the enzyme (Roskoski, 2012), was identified. Despite their high level of similarity and the relatively short ORF region isolated for the *MAPK1* gene, the phylogenetic analysis of the maraena whitefish *MAPK1* and *MAPK3* transcript clearly separated the sequences into two clades together with their respective homologues of other vertebrate species, as was previously reported by Li *et al.* (2011).

In this study, for the stress-target gene set, partial maraena whitefish *HSP70* and *HSP90* transcripts were isolated, that revealed high inter-species homology for the deduced amino acid sequences. The predicted, partial proteins contained HSP70 or HSP90 signature motifs, as already reported for other putative fish HSP70 and HSP90 proteins (Ming *et al.*, 2010; Zhang *et al.*, 2011a; Mu *et al.*, 2013;

Poompoung *et al.*, 2014; Xu *et al.*, 2014; Wang *et al.*, 2014a; Yan *et al.*, 2017; Pu *et al.*, 2016). For maraena whitefish HSP70, phylogenetic analysis confirmed the high grade of conservation of the tested amino acid sequences within teleosts, whereas mammalian homologues were clustered together in an own major branch. In case of maraena whitefish HSP90, for the resulting phylogenetic tree all tested amino acid sequences were clustered into two separate groups for HSP90A and HSP90B, respectively. However, the putative maraena whitefish HSP90 protein built an out-group, since sequence information was insufficient to assign it to the HSP90A or HSP90B group, respectively.

Based on structural analysis of the isolated maraena whitefish *NR3C1* transcript, the typical GCR aa-sequence structure, containing the two zinc finger motifs within the DBD, were identified. Additionally, evolutionary analysis confirmed that the isolated maraena whitefish *NR3C1* codes for a putative GCR and not for the closely related GCR2 or MR. As was previously shown for several other fish GCRs, the functional domains (DBD, LBD) of the putative GCR are characterised by a high inter-species homology, apart from a nine aa insert between the two zinc fingers of the DBD that was found to be exclusively present in rainbow trout and maraena whitefish (Ducouret *et al.*, 1995; Takeo *et al.*, 1996; Bury *et al.*, 2003; Stolte *et al.*, 2006; Acerete *et al.*, 2007; Arterbery *et al.*, 2010).

The partial maraena whitefish *TP53* transcript obtained within this study showed complete homology to the GenBank entry for *Coregonus lavaretus* TP53 transcript (EU978857), thus it is very likely to be the same species. Further, it was shown that the isolated, partial protein contains two indicative TP53-family sequences, namely a TP53 DBD and a tetramerisation motif, that were both highly conserved between vertebrates, as reported in literature (Sun *et al.*, 2016; Joerger *et al.*, 2014). However, phylogenetic analysis clearly unveiled that TP53 aa sequence identity was highest within the family of salmonids and that the putative piscine TP53 proteins are more distantly related to their homologues in higher vertebrates.

The deduced aa sequences of the maraena whitefish *IGF1* and *IGF2* transcripts both comprise the signal peptide and the A-, B, C-, D- and E-domains that are distinctive for IGFs and well known from literature (Rinderknecht & Humbel, 1978b; Humbel, 1990; Reinecke & Collet, 1998; Reinecke *et al.*, 2005). Moreover, the A- and B-domains of maraena whitefish IGF-1 and IGF-2 are highly conserved compared to other vertebrate species (e.g., humans and mice) and showed a perfect consensus with salmonid orthologues. Further, phylogenetic analysis clearly unveiled a high degree of conservation for both IGFs within teleosts.

4.4. In healthy juvenile maraena whitefish more than half of the target genes seem to interfere with reproductive functions

The analysis of the tissue-specific expression of target genes from healthy juvenile maraena whitefish (48 wph) showed that transcripts were detected for all selected genes (immune-, stress-, and growth-specific genes) in all tested tissues, albeit the individual genes revealed considerable variations regarding their tissue-specific mRNA levels, as discussed in the following.

The ubiquitous expression of the maraena whitefish *IL1B* transcript is in line with reports from several *IL1B* homologues in teleost fish, such as common carp (Engelsma *et al.*, 2001, 2003), Atlantic halibut (Øvergård *et al.*, 2012), channel catfish (Wang *et al.*, 2006), Asian swamp eel (Xu *et al.*, 2016), and rainbow trout (Husain *et al.*, 2012). The comparably high *IL1B* expression in gonads, gills and spleen, determined in maraena whitefish, was also observed for rainbow trout type I *IL1B3* (Husain *et al.*, 2012), which is interesting, since the isolated maraena whitefish *IL1B* sequence was more similar to type II *IL1B*

genes. Taken together, this expression pattern mainly confirms the known function of IL6 in immunity.

The *IL6* expression in most teleost tissues analysed so far was not detectable or very low, except from some species-specific tissues with remarkably high copy numbers, as was shown for thymus and brain of Atlantic halibut (Øvergård *et al.*, 2012), kidney and spleen of zebrafish (Varela *et al.*, 2012), and white muscle and skin of gilthead seabream (Castellana *et al.*, 2008). However for maraena whitefish, notably high mRNA levels were determined in gonads, which was also reported for rainbow trout ovarian tissue (Iliev *et al.*, 2007).

A constitutive expression of *TNF-α*, as found for maraena whitefish, was previously reported in literature for a number of teleosts (Savan *et al.*, 2005; Nascimento *et al.*, 2007b; Hong *et al.*, 2013). Similar to *TNF-α1* and *TNF-α2* of the closely related rainbow trout (Hong *et al.*, 2013), maraena whitefish *TNF* exhibited highest expression values in gills, emphasising its importance in the early immune response, since this organs are constantly and directly exposed to the environment and hence to pathogens, as well. But different from the situation in rainbow trout, the maraena whitefish *TNF* gene exhibited notably high mRNA values in gonads.

The two closely related *MAPK1* and *MAPK3* genes are known to be ubiquitously expressed in mammals, as was also shown for orange-spotted grouper and within this study for maraena whitefish (Buscà *et al.*, 2015; Sun *et al.*, 2018). In mammals and in zebrafish the highest *MAPK1* and *MAPK3* expression values were found in the brain (Buscà *et al.*, 2015; Krens *et al.*, 2006), whilst in maraena whitefish peak mRNA levels were determined in gonads but in the brain *MAPK1* and *MAPK3* expression was still comparably high reaching second highest transcript levels. In general, the *MAPK1* and *MAPK3* expression pattern of maraena whitefish seems to be very similar to that of its mammalian counterparts. This is not self-evident, because regardless of their high structural and functional conservation, alternating *MAPK1* and *MAPK3* expression profiles have been proven, as shown for reptiles by Buscà *et al.* (2015), where only one of the two genes seems to be expressed in the brain.

Besides their ubiquitous abundance, the very high transcript levels of maraena whitefish *CXCL8* in spleen, gills, and kidney were also reported for rainbow trout *CXCL8*, as well as for common carp *CXCL8* paralogues (Huising *et al.*, 2003, 2004; Abdelkhalek *et al.*, 2009; Laing *et al.*, 2002). The predominant expression of *CXCL8* homologues in immune-related organs underlines the high relevance of this chemokine in immune functions. Moreover, the constitutive *CXCL8* expression in fish might have beneficial effects for teleost immunity, since it is in total contradiction to the situation in humans where *CXCL8* expression in non-pathological tissue is not detectable, due to a strict repression of its promoter (Jundi & Greene, 2015).

Similar to *IL12p40* homologues of other teleost fish, maraena whitefish *IL12p40c* was ubiquitously expressed (Huising *et al.*, 2006; Yoshiura *et al.*, 2003; Øvergård *et al.*, 2012), which is contradictory to the situation in mammals where *IL12p40* expression is known to be highly inducible (Weinmann *et al.*, 1999; Liu *et al.*, 2003). Moreover, for Atlantic halibut, *IL12p40c* transcript levels were reported to be highest in gills and spleen, as was found for maraena whitefish as well, whilst e.g., for common carp *IL12p40c* transcript levels were uniformly high in immune and not-immune organs (Huising *et al.*, 2006), thus different species-specific roles of this gene might be possible.

A notably high splenic mRNA expression of *SAA*, together with a comparable low hepatic expression, as found in unstimulated healthy maraena whitefish, was only reported for goldfish so far (Kovacevic & Belosevic, 2015). In contrast, the tissue distribution of SAA transcripts was analysed in healthy rainbow trout, orange-spotted grouper (*Epinephelus coioides*), and black rockfish (*Sebastes schlegeli*) and for all

three species the *SAA* expression levels were highest in liver, as known from the multiple *SAA* genes in mammals, as well (Villarroel *et al.*, 2008; Wei *et al.*, 2013; Jayasinghe *et al.*, 2015; Uhlar & Whitehead, 1999). Moreover, compared to all other target genes, SAA revealed, by far, the highest transcript levels in all tissues tested, except from *HSP90* mRNA in the heart, muscle, and skin. In accordance with these findings, Urieli-Shoval *et al.* (1998) reported about strong signals they found in several healthy human tissues using the in-situ hybridisation technique with a SAA RNA probe. The authors therefore hypothesised that SAA might be important for tissue-specific defence mechanisms, to protect the host from pathogens and injuries, since this molecule might communicate with the external tissue environment and is able to prevent oxidative tissue damage (Urieli-Shoval *et al.*, 1998). Such functions of SAA might have been preserved in maraena whitefish, as well.

The constitutive expression of the maraena whitefish *HSP70* and *HSP90* genes is consistent with results previously reported from various fish species (Zhang *et al.*, 2011a; Mu *et al.*, 2013; Qin *et al.*, 2016; Peng *et al.*, 2016; Eid *et al.*, 2016; Wang *et al.*, 2017; Yan *et al.*, 2017). Moreover, maraena whitefish revealed a peak expression of *HSP70* in gonads, followed by still very high mRNA values in spleen, which is similar to that found by Mu *et al.* (2013) in the Korean rockfish (*Sebastes schlegeli*), who concluded that this chaperone might have functions in reproduction and immunity in fish, as is already discussed in literature (Domingos *et al.*, 2013; Mu *et al.*, 2013; Han *et al.*, 2016; Liang *et al.*, 2016; Roberts *et al.*, 2010). Similarly to the cardiac-specific expression pattern of *HSP70* and *HSP90* that Liang *et al.* (2016) observed in marbled eel (*Anguilla marmorata*), *HSP70* showed very high and *HSP90* even higher transcript levels in maraena whitefish cardiac tissue, indicating a role of HSP's for the function or development of this organ. This assumption is supported by previous studies of Sass *et al.* (1996) and (Bornman *et al.*, 1996), who found evidence for a function of *HSP90* in the myogenesis of developing zebrafish and humans, respectively. Moreover, *in vitro* experiments on rat myocytes performed by Heads *et al.* (1994) confirmed that a constitutive and high *HSP70* expression protects heart-derived muscle cells from thermal stress.

As in maraena whitefish, the GCR encoding gene *NR3C1* was observed to be ubiquitously expressed in other teleost fish, like rainbow trout (Takeo *et al.*, 1996; Bury *et al.*, 2003), gilthead seabream by Acerete *et al.* (2007), European bass (*Dicentrarchus labrax*) by Vazzana *et al.* (2008), and Burton's mouthbrooder (*Astatotilapia burtoni*) by Greenwood *et al.* (2003). Interestingly, in healthy maraena whitefish, the GCR transcript numbers were by far highest in gonads.

For the *TP53* gene, highest mRNA levels were determined in maraena whitefish gonadal and splenic tissue. However, for the closely related rainbow trout an expression of the TP53 protein in splenic tissue was not detectable (Liu *et al.*, 2011). Interestingly, in mice the same phenomenon was observed by Rogel *et al.* (1985) and the authors proved that the considerably high splenic *TP53* mRNA levels were not reflected on protein level because of a very fast TP53 degradation (< 6 min versus 20-30 min in other healthy tissues) that was solely detectable in the spleen. Generally, the ubiquitous *TP53* mRNA abundance found for maraena whitefish, was observed in several other animals as well (Hoever *et al.*, 1994; Cachot *et al.*, 1998; Qi *et al.*, 2013; Sun *et al.*, 2016).

Despite their ubiquitous abundance in the different tested tissues, the liver is the major site of *IGF* expression in maraena whitefish, as already known from other vertebrate species like humans, mice, and chickens (Reinecke & Collet, 1998; Roith *et al.*, 2001; Puche & Castilla-Cortázar, 2012; Mathews *et al.*, 1986). Whereas whitefish *IGF1* mRNA levels were highly variable in different tissues, *IGF2* levels appeared to be more consistent, which was also observed for other teleost fishes (Ayson *et al.*, 2002; Greene & Chen, 1997; Vong *et al.*, 2003; Mathews *et al.*, 1986). Further, Ayson *et al.* (2002) and Vong

et al. (2003) observed a relatively high general and hepatic *IGF2* transcript abundance, but not higher than the liver-specific *IGF1* mRNA levels in adult rabbitfish (*Siganus guttatus*) and juvenile common carp (*Cyprinus carpio*). In contrast to that, in maraena whitefish, *IGF2* gene expression exceeds *IGF1* transcript numbers even in advanced juvenile life-stages, in all tissues examined, including the liver. Similar results were reported only for the closely related rainbow trout (Greene & Chen, 1999).

On the level of proteins, in the liver and gill, but not in muscle tissue, several high-molecular weight IGF-1 precursor forms have been detected, indicating a tissue-specific expression of IGF pro-peptides. It is known that the *IGF1* gene locus encodes multiple precursors, including signal peptides and extension peptides, that are post-translationally modified to generate mature IGF proteins (Humbel, 1990; Zou *et al.*, 2009). The presence of four pro-peptide forms in the liver supports the findings of high *IGF1* gene expression in the liver compared to other tissues. Consequently, it seems that in maraena whitefish, similar to mammals, IGF-1 is synthesized predominantly in the liver and transported via the blood to target tissues (Argente *et al.*, 2017; Puche & Castilla-Cortázar, 2012; Sjögren *et al.*, 1999). The signals above 10 kDa that were detected for the recombinant IGF-1 and IGF-2 proteins are not necessarily precursor forms of mature IGF proteins, but might rather represent IGF-multimers.

Interestingly, more than half of all target genes exhibited highest expression levels in the gonads, suggesting a role of the genes *IL1B*, *IL6*, *TNF*, *MAPK1*, *MAPK3*, *NR3C1*, *TP53*, and *HSP70* for maraena whitefish reproductive functions. This assumption is supported by a variety of mammalian and piscine studies found in literature. For example, Bornstein *et al.* (2004) described that IL6 "exerts adverse effects on the male reproductive function" and that IL1B and TNF influence steroidogenesis in mammalian gonads, which was confirmed for TNF in the goldfish (*Carassius auratus*) via *in vitro* studies carried out by Lister & Van Kraak (2002). Moreover, from a high *IL6* expression in rainbow trout ovaries, Iliev *et al.* (2007) suggested a function of this cytokine in ovulation and steroidogenesis, as was previously reported for mammals (Machelon *et al.*, 1994; Van der Hoek *et al.*, 1998; Bornstein *et al.*, 2004) and which might be possible for maraena whitefish IL6, as well. In case of the MAPKs, Ponza *et al.* (2011) previously reported that MAPK1 has a function in the development and maturation of oocytes and ovaries of the giant tiger shrimp (*Penaeus monodon*). Moreover, the pivotal importance of MAPK3 but also of MAPK1 for female fertility is already known in mammals (Hatano *et al.*, 2003; Fan *et al.*, 2009). For the GCR, an interaction with the hypothalamic-pituitary-gonad axis is reported in mammals and in fish, as reviewed by Whirledge & Cidlowski (2010) and Milla *et al.* (2009). The reviews of Hu (2009) and d'Avila Paskulin *et al.* (2012) summarise the multiple functions of the *TP53* gene for spermatogenesis and female fertility in mammals, which are partly even found in lowe vertebrates (*Xenopus laevis*) and invertebrates (*Drosophila melanogaster*) and thus might be well conserved in the animal kingdom (Hu, 2009; Belyi *et al.*, 2010). Further, even for the chaperone HSP70, similar to its mammalian counterpart, a role for reproductive functions in fish is already discussed in literature (Domingos *et al.*, 2013; Mu *et al.*, 2013; Han *et al.*, 2016; Liang *et al.*, 2016; Roberts *et al.*, 2010).

In summary, the analysis of the tissue distribution showed that several of the immune and stress target genes, namely *IL1B*, *IL6*, *TNF*, *MAPK1*, *MAPK3*, *NR3C1, TP53* and *HSP70* seem to assume functions in reproductive organs of healthy maraena whitefish. As members of the immune-gene-set, the genes *CXCL8*, *IL12B*, and *SAA* showed highest transcript values in immune-related organs, whereas the generally notably high values of the *SAA* mRNA indicate a special role of this molecule in the pathogen defence of maraena whitefish. The *IGF* genes were expectedly highly expressed in the liver, the main metabolic organ. However, particularly *HSP90*, but *HSP70* as well, revealed to play a role in the development and protection of cardiac tissue from unstressed maraena whitefish.

4.5. High stocking density mainly induced immune genes — particularly *SAA* — and related pathways

One major criterion in aquaculture is the stocking density, which on the one hand has to be as high as possible to meet commercial production requirements but, on the other hand should be carefully adjusted to the fish's biology to gain a high quality product at a maximum yield within the range of animal welfare demands. Ellis *et al.* (2002) fittingly summarised that optimal growth performance and welfare aspects go hand in hand if appropriate SDs are applied in aquaculture. Nonetheless, the authors noted that in aquaculture practice SDs are rather determined by economic criteria (Ellis *et al.*, 2002). Consequently, several studies report on the negative effects of high SDs on growth performance that are mainly caused by an increased energy demand and a reduced immune competence of farmed fish due to the onset of chronic stress (Iguchi *et al.*, 2003; Ni *et al.*, 2016; Liu *et al.*, 2015, 2016b; Yarahmadi *et al.*, 2016; Ren *et al.*, 2017; Feshalami *et al.*, 2017). Another striking aspect is that the susceptibility to stress is highly species-specific even among the closely related salmonids as reviewed by Barton (2002) and therefore recommendations on stocking densities of one species can not simply be transferred to another.

Since SDs between 15 to 60 kg/m^{3}are often applied in commercial scale aquaculture (Ellis *et al.*, 2002) and SDs of 90 kg/m^3 or even higher are not unusual for salmonid farming in recirculation systems (Murray *et al.*, 2014), within this study maraena whitefish was exposed to SDs between 10 and 100 kg/m^3. To determine this fish's capability to cope with these aquaculture-specific conditions, the influence of density stress on physiological parameters and on pre-selected gene sets was examined and additionally via holistic analyses genes were identified that revealed to be differentially expressed in a more general manner, i.e., in both tested tissues, the liver and the kidney. On the other hand, the tissue-specific and cellular responses of maraena whitefish to density stress were presented by Korytár *et al.* (2016).

The elevation of plasma cortisol and glucose levels are characteristic for the acute stress response and lead to metabolic and transcriptomic adjustments (Mommsen *et al.*, 1999; Barton, 2002; Caipang *et al.*, 2008, 2009; Aluru & Vijayan, 2009). Although, no significant differences were recorded for the plasma cortisol and glucose levels in maraena whitefish, it is obvious that the cortisol values were generally notably high, especially in the HD group after acute density stress and for some individuals of the HD group after short-term density stress. According to Barton (2002), physiological plasma cortisol levels of various fish species ranged between 1-11 ng/ml, which increased 1 h after exposure to acute stress to values between 43-129 ng/ml for several salmonid species. Keeping in mind that the maraena whitefish cohort used for this experiment was obtained from wild-caught fish that have never before experienced any breeding influence, the cultivation within this anthropogenic environment seems to cause generally highly elevated cortisol levels, ranging at average levels of 32-56 ng/ml in all tested groups. However, the plasma glucose levels are within the physiological ranges, as previously reported for salmonids (Wright *et al.*, 1989; Bucking *et al.*, 2005).

Nevertheless, the expression of several target genes was affected following the stocking density experiment, mainly by HD but also by ED conditions, whereas potential adverse effects of LD treatment, as previously reported by North *et al.* (2006), were reflected neither in transcription profiles nor in physiological parameters. The exposure of maraena whitefish to acute (24 h) HD conditions (100 kg/m^3) led to the modulation of the immune genes *IL1B*, *IL6*, *SAA* and *CXCL8*, while the expression of the stress-target-genes remained virtually unaffected. A clear up-regulation of *IL1B* was determined in the kidney, besides a slight induction in the spleen, as was also found for *IL6* (kidney) and *SAA* (gills, liver, spleen, kidney), whereas *CXCL8* was marginally down-regulated in the liver. This up-regulation of factors of the

innate immune system found for maraena whitefish is in line with previous studies that demonstrated the beneficial effect of acute stress on the immune response, as summarised by Nardocci *et al.* (2014). In case of *SAA,* various studies proved the induction of this gene by immune-relevant stressors, like infectious or immune-stimulatory agents in hepatic and extra-hepatic tissues of teleosts (Fujiki *et al.*, 2000; Jørgensen *et al.*, 2000; Bayne & Gerwick, 2001; Saeij *et al.*, 2003c; Villarroel *et al.*, 2008; Wei *et al.*, 2013; Kania *et al.*, 2014; Kovacevic & Belosevic, 2015), but few information is available about the modulation of this gene due to crowding stress. Whereas Cairns *et al.* (2008) found an up-regulation of several acute-phase-related genes, but not *SAA*, in rainbow trout liver after 24 h of acute confinement stress, Talbot *et al.* (2009) determined a slight induction of *SAA* expression in hepatic tissue of rainbow trout in a similar experiment, as was determined in this study for maraena whitefish, as well. Moreover, for the *IL6* gene, there is rather evidence for a stress-dependent down-regulation, as has been demonstrated by several *in vitro* experiments (Castro *et al.*, 2011; Philip & Vijayan, 2015; Zou & Secombes, 2016; Khansari *et al.*, 2017b,a). Nonetheless, an acute stress induced up-regulation of *IL6,* as found in maraena whitefish, was also observed by Castillo *et al.* (2009) following *in vitro* administration of ACTH to head kidney cells of gilthead seabream. In line with this, Khansari *et al.* (2017b) noted that in teleost fish, stress hormones cause a diverse and species-specific expression of cytokine-encoding genes, like *IL6*, *IL1B* and *TNF*. Accordingly, in contrast to the unaffected *TNF* expression observed in maraena whitefish, Wiseman *et al.* (2007) found *TNF*, to be significantly up-regulated only 1 h after exposure of rainbow trout to acute handling stress. Further, Fast *et al.* (2008) reported on the enhanced *IL1B* expression in response to acute stress in head kidney macrophages of Atlantic salmon and Caipang (2012) showed a significant and sharp up-regulation of *IL1B* 2 h but even for *CXCL8* 24 to 72 h after an acute crowding stress in Atlantic cod. Moreover, Sun *et al.* (2017) found peak expression values of *CXCL8* 96 h after exposure to acute crowding stress in large yellow croaker (*Larimichthys crocea*). Consequently, it might be possible that the sampling as early as 1 h post acute crowding stress, was not the most appropriate time point to record stress-induced peak expression levels for all the genes examined in maraena whitefish.

Similarly to acute density stress, the exposure of maraena whitefish to short-term (8 d) density stress rather modulated the expression of immune-related genes than of stress genes. However, it should be noted that solely the up-regulation of the *SAA* gene determined by qPCR was confirmed by the microarray analysis and both techniques resulted in almost exactly identical values for the liver and the kidney, respectively. However, the altered expression of the genes *IL1B*, *CXCL8* , *HSP70*, and *HSP90* determined by qPCR were not confirmed by the comparably less sensitive but yet reliable microarray-technique, most likely because of their relatively low induction (FC <5) and hence this questions their relevance for the search for potential robust marker genes (Allanach *et al.*, 2008).

For *SAA*, the expression values increased again in all tested tissues at HD conditions compared to the acute density stress experiment and additionally, for ED conditions, an up-regulation of the *SAA* expression has been recorded in liver, spleen, and kidney, as well. A similar transient up-regulation of the *SAA* gene expression to fold-change values of about 10 within several days of exposure to confinement stress were determined by Talbot *et al.* (2009) in rainbow trout.

The holistic analysis of maraena whitefish gene expression in liver and kidney tissue after exposure to different stocking densities clearly unveiled that, (i) the gene expression was mainly altered in the kidney and, (ii) the highest density of 100 kg/m^{3}had the overall highest impact on gene expression in maraena whitefish. This is completely in contrast to the results reported for rainbow trout, in which indeed a comparably high stocking density also led to the strongest regulation of genes, but in this species the number of DE genes was significantly higher in the liver than in the kidney (Rebl *et al.*, 2017).

Consequently, based on the primarily liver-specific alterations of gene expression in rainbow trout, mainly metabolic pathways were affected by crowding stress (Rebl *et al.*, 2017), whereas in maraena whitefish the majority of genes showed alterations in the kidney and therefore mainly immune-related pathways were affected due to crowding stress. Nonetheless, Korytár *et al.* (2016) also found several typical stress-related pathways to be induced in the liver, but interestingly glucose-related metabolic pathways were mainly affected in the kidney of maraena whitefish. This is interesting, since previously published transcriptome studies uniformly stressed the importance of the liver — as the main metabolic organ — for metabolic adjustments, particularly those that supply glucose, due to an enhanced energy demand of fish during acute stress (Wiseman *et al.*, 2007; Aluru & Vijayan, 2009; Liu *et al.*, 2014). However, microarray-based gene expression profiling set out by Krasnov *et al.* (2005) and Verleih *et al.* (2015), reported on relevant metabolic changes in the kidney of rainbow trout post handling or thermal stress, respectively. This indicates that the tissue-specific stress response is not only modulated in a species-specific manner but is also individually adjusted to the given stressor within the same species, as was previously suggested by Barton (2002) and Ellis *et al.* (2002).

Aiming at the identification of global and robust marker genes for crowding stress, within this study solely the shared DE genes of liver and kidney after exposure of maraena whitefish to different stocking densities were considered. This revealed that crowding stress affected several pro-inflammatory genes and related pathways. Thus, besides *SAA*, the holistic expression analysis identified the DE genes *LYZ*, *CEBPB* and *CFD* that were not as strongly induced as *SAA* but influenced several immune-related pathways. The *LYZ* gene codes for lysozyme, an enzyme of the innate immunity having antibacterial activity, that is well studied in salmonids and broadly discussed in literature regarding its induction and role within the acute stress response (Fevolden *et al.*, 1994; Demers & Bayne, 1997; Fevolden *et al.*, 1999, 2002; North *et al.*, 2006; Caipang, 2012).Thus, in maraena whitefish held at HD conditions, the up-regulation of *LYZ* and *SAA* (relative to MD conditions) affected the *LXR/RXR-activation pathway*, which is involved in the regulation of lipid metabolism, inflammation, and cholesterol metabolism. The *LXR/RXR-activation pathway* was also found to be significantly activated in common carp after exposure to toxic nanoparticles (Chupani *et al.*, 2017) and due to the acclimation to cold and warm temperatures (Dietrich *et al.*, 2018), indicating the role of this pathway for the maintenance of homoeostasis in different health-threatening situations. This is also true for the *acute phase response-signaling pathway*, which belongs to the innate immune response, and was affected due to stress exposure of common carp (Chupani *et al.*, 2017; Dietrich *et al.*, 2018) and rainbow trout (Cairns *et al.*, 2008), as well as due to crowding-stress in maraena whitefish, where it was affected, as expected, by the differential expression of *SAA* and also by *CEBPB.* The *CEBPB* gene codes for a transcription factor that is known to regulate the expression of genes involved in the acute phase response, such as *SAA*, which possesses a CEBPB binding site within its promoter region (Burgess-Beusse & Darlington, 1998). But *CEBPB* seems to interfere with additional pathways, since the altered expression of *CEBPB* and *LYZ* and of *CEBPB* alone was associated with *IL12 signaling and production in macrophages* and *IL17a signaling in fibroblasts*, respectively. Both pathways represent the bridge between innate and adaptive immune responses, whilst the first exerts its activating effect on adaptive immunity via *CEBPB* (Ma *et al.*, 2015) and the second rather has a suppressive effects on pro-inflammatory genes through the inhibition of *CEBPB* (Shen *et al.*, 2009). Beyond that, other studies on teleost species also found that *CEBPB* was regulated in response to various stressors, such as temperature (Buckley & Somero, 2009; Verleih *et al.*, 2015), hyperosmolarity (Wong *et al.*, 2014), and hyperoxia (Huang *et al.*, 2009).

The gene *CFD* encodes a serine peptidase, that is elementary for the initiation of the alternative *com-*

plement cascade, a pathway that is elementary for the innate immune response (Noris & Remuzzi, 2013) and which is known to be present in salmonid fish (Köbis *et al.*, 2015). The alternative *complement cascade* is not only activated by PAMPs but also by DAMPs released from stressed or apoptotic cells, which unveils the importance of this pathway for the maintenance of homoeostasis, despite its role for the clearance of pathogens (Ricklin *et al.*, 2010). Therefore the up-regulation of *CFD* after short-term high density stress indicates a role of the alternative complement pathway within the acute stress response of maraena whitefish, as was previously stated by Sun *et al.* (2018) for the large yellow croaker.

Finally, *TNF* was predicted to play a key role within the regulation of the various immune-related processes that were altered during maraena whitefish's stress response to short-term HD conditions. These pleiotropic functions of TNF in homoeostasis and immunity were proved in numerous studies, in mammals as well as in fish, as summarised in literature (Baud & Karin, 2001; Hong *et al.*, 2013; Sedger & McDermott, 2014; Brenner *et al.*, 2015; Zou & Secombes, 2016; Kalliolias & Ivashkiv, 2016). Thus, similar to its mammalian counterpart, the piscine TNF is known to play a central role for the regulation of a variety of immune genes and exerts its stimulatory effects, e.g., via NF-κB and CEBPB signaling pathways (Zou & Secombes, 2016; Talbot *et al.*, 2009), of which the latter were found to be affected in maraena whitefish. Further, TNF is involved in leukocyte proliferation, has activating effects on macrophages and enhances the phagocytic activity of leukocytes (Zou & Secombes, 2016). This is in line with observations made by Korytár *et al.* (2016), who found "elevated numbers of myeloid cells together with increased phagocytic activity of peripheral blood leukocytes" in mareana whitefish exposed to HD conditions.

In conclusion, the data obtained in this study for maraena whitefish after acute and short-term density stress are typical changes that were previously described for a secondary stress response (Barton, 2002). This is characterised by up-regulated immune genes together with a systemic induction of immune-related pathways in parallel with metabolic changes, mainly concerning glucose metabolism pathways, such as glycolysis, glycogenolysis, and gluconeogenesis, as was found in maraena whitefish kidney (Korytár *et al.*, 2016). The cytokine TNF, suggestively plays a major role in regulating the aforementioned processes, whilst the APP encoding gene *SAA*, revealed to be valuable for maraena whitefish in coping with short-term crowding stress. Further, the transcription factor CEBPB seems to have an important function in the crowding-stress-related regulation of *SAA* and other factors of innate immunity, making it an interesting candidate for further studies. In contrast to the data found within this experiment, Yarahmadi *et al.* (2016) reported on the suppression of immune related genes, like *IL1B*, *TNF*, and *IL8*, in parallel with a significant up-regulation of the stress gene *HSP70* in rainbow trout under long-term crowding stress conditions (30 d). Similarly, several reviews described the suppressive effects of chronic stress on immune functions (Barton, 2002; Tort, 2011b; Nardocci *et al.*, 2014; Dhabhar, 2014; Zwollo, 2018). Therefore, taken together, the density stress experiment clearly showed that, at least after eight days of crowding stress, maraena whitefish exerts hallmarks of a prolonged acute and not a chronic stress response, indicating the fish's adaptation capability (Barton, 2002; Dhabhar, 2014; Nardocci *et al.*, 2014). Whether and when a chronic stress response to high stocking densities is induced in maraena whitefish, as well, must be clarified in future long-term studies.

4.6. Acute and gradual temperature stress caused patterns of an acute or chronic stress response

Previous work has shown that temperature has a major impact on fish growth, which increases with temperature until an optimal level is reached (Viadero, 2005; Besson *et al.*, 2016; Boltaña *et al.*, 2017). Particularly salmonids have highly species-specific and comparable small temperature tolerance ranges, which should be taken into account for successful aquaculture (Stien *et al.*, 2013). Accordingly, in literature there are varying and, in part, contradictory data about the optimal rearing temperatures of coregonids, whilst the upper temperature limit was reported to be at around 24 - 25°C (Szczepkowski *et al.*, 2006; Siikavuopio *et al.*, 2012, 2013; Goebel *et al.*, 2017; Matousek *et al.*, 2017). In the course of this study, a well growth performance was observed for maraena whitefish in a recirculation system at temperatures ranging between 18 - 22°C (see sections 3.1, 4.2). Based on these results, the temperature stress experiment was performed to examine potential harmful effects of a gradual or an acute temperature rise to 24°C on mareana whitefish.

After exposure of mareana whitefish to GR and AR conditions the selected immune genes show contradictory expression profiles, i.e., they were mainly down-regulated in response to GR and mostly up-regulated at AR conditions. However, the stress-target-genes revealed a staggered induction from GR to AR treatment. Moreover, the comprehensive microarray-based expression analysis supported this finding of different responses to GR and AR conditions, since there were no overlaps within the DE genes that were top-regulated in an apparently systemic manner, i.e., within all three tissues analysed.

Thus, after 12 d of GR treatment, the expression profiles of maraena whitefish target genes revealed hallmarks of chronic stress, indicated by suppressed immune genes (*IL1B*, *IL6*, *SAA*) and simultaneously up-regulated stress genes (*HSP70*, *HSP90, NR3C1*), as previously described in literature for other (fish) species (Barton, 2002; Tort, 2011b,a; Dhabhar, 2014; Nardocci *et al.*, 2014; Zwollo, 2018). In general, the effect of chronic stress on gene expression in fish was rather analysed for crowding and not for temperature stress. Nonetheless, Yarahmadi *et al.* (2016) reported expression profiles for stress- and immune-related genes in response to long-term crowding stress in rainbow trout that were similar to those found for GR treatment in maraena whitefish. Moreover, suppressed immune functions (Pickering & Pottinger, 1989; Gil Barcellos *et al.*, 2004; Fast *et al.*, 2008) and an activation of stress factors, mainly HSP70 and HSP90 (Deane *et al.*, 2002; van der Meer, 2005; Feidantsis *et al.*, 2009; Roberts *et al.*, 2010), after long-term exposure of various fish species to several stress conditions has been proven in many cases. In contrast to the GR data in maraena whitefish, Rebl *et al.* (2013) and Verleih *et al.* (2015) determined elevated transcript numbers for several genes of innate immunity, even after two weeks exposure of rainbow trout to mild temperature stress (max. 23°C). Thus, the prolonged temperature challenge unveiled an enhanced immune capacity of the selected rainbow trout strains, which might be a result of several decades of breeding selection during aquaculture, particularly the Born trout seems to have well adapted to local aquaculture conditions (Rebl *et al.*, 2012, 2013). However, the first-time cultured maraena whitefish, used in this study, have not yet undergone any adaptation to an anthropogenic environment and consequently can be regarded as sensitive as wild fish.

Surprisingly, in contrast to the other pro-inflammatory cytokines, the *CXCL8* transcript levels were not reduced but slightly elevated in hepatic tissue of maranea whitefish due to GR conditions, indicating that this individual lineage 1 *CXCL8* variant, or the cytokine in general, might be differentially regulated in response to prolonged stress. This assumption is supported by a study of Philip & Vijayan (2015), who observed a similar phenomenon for *CXCL8* transcripts in rainbow trout liver *in vitro*. Accordingly,

the authors concluded that in fish, *CXCL8*, other than *IL6*, is not regulated by the *Janus kinase/signal transducer and activator of transcription* (JAK/STAT) pathway, which in case of stress is inhibited by the *suppressors of cytokine signaling* (SOCS) (Zou & Secombes, 2016; Rebl & Goldammer, 2018). Thus Philip & Vijayan (2015) suggested that in fish, *CXCL8* expression is not affected by the cortisol-driven SOCS induction that leads to cytokine suppression during severe or prolonged stress. Moreover, van der Aa *et al.* (2010) found that transcripts of the different piscine *CXCL8* lineages show different and partly opposing expression patterns following a stress exposure, which might be another explanation for the observed maraena whitefish *CXCL8* expression pattern.

Unlike the GR treatment, the exposure to AR conditions led to an up-regulation of several immune target genes, as well as to an enhanced induction of the stress target genes, above all, *HSP70* revealed a systemic, massive increase in transcript numbers. The strong induction of HSPs is characteristic for a heat-shock response as known from literature (Lindquist & Craig, 1988; Barton, 2002; Basu *et al.*, 2002; Yamashita *et al.*, 2010; Roberts *et al.*, 2010; Tort, 2011b). Accordingly, various studies reported the considerable up-regulation of HSPs, mainly of HSP70 and HSP90, in several fish species that were subjected to acute hyperthermic stress (Ojima *et al.*, 2005a,b; Healy *et al.*, 2010; Quinn *et al.*, 2011; Peng *et al.*, 2016). Moreover, the massive induction of *HSP70* after acute heat stress, as was found in this study for maraena whitefish, was also reported for individual *HSP70* paralogues of rainbow trout (Ojima *et al.*, 2005a), killifish (*Fundulus heteroclitus*) (Healy *et al.*, 2010), and stickleback (*Gasterosteus aculeatus*) (Metzger *et al.*, 2016). Consequently, due to its significant regulation HSP70 was even suggested to be a potent biomarker for thermal and other types of environmental stress, as concluded from several studies on various vertebrate and invertebrate species (de Pomerai, 1996; Vijayan *et al.*, 1997; Lewis *et al.*, 1999; Manjari *et al.*, 2015).

Reports about immune gene expression in response to acute hyperthermic stress are few and contradictory across teleosts, since stimulatory (Ruis & Bayne, 1997; Wendelaar Bonga, 1997) as well as suppressive effects (Le Morvan *et al.*, 1998; Magnadóttir *et al.*, 1999) were evenly reported. This, on the one hand, indicates the high complexity of these processes (Wendelaar Bonga, 1997) and, on the other hand, reflects the high dependence of the results to the experimental design and the selected tissues or cells. However, in their reviews Barton (2002), Tort (2011b), and Nardocci *et al.* (2014) noted, that acute stress usually has stimulatory effects on immune functions in fish, which is in line with findings in other vertebrates (Dhabhar & McEwen, 1997; Edwards *et al.*, 2007; Dhabhar, 2014). Corresponding to this Thorne *et al.* (2010), Dittmar *et al.* (2014), and Tomalty *et al.* (2015) found increased activities of innate and/or acquired immune functions in Antarctic plunderfish (*Harpagifer antarcticus*), stickleback (*Gasterosteus aculeatus*), and Chinook salmon (*Oncorhynchus tshawytscha*) after exposure to a sharp temperature increase. Notably, similar to the results in the given study, in Chinook salmon *IL1B* and *CXCL8* were found to be up-regulated after acute heat stress (Tomalty *et al.*, 2015). However, other immune-related genes remained unaffected (IL6), or were slightly down-regulated *(TNF, SAA)* at AR conditions in maraena whitefish, which is interesting particularly in case of the *SAA* gene, since it was found to be clearly up-regulated at density stress conditions. Several *in vitro* studies on different mammalian cells reported a decrease in *TNF* expression in response to heat shock, most likely mediated by HSP70 or its co-chaperone HSF1, to prevent — besides heat-induced tissue damage — additional adverse effects of this highly potent pro-inflammatory cytokine on tissue integrity (Meng *et al.*, 1999; Yoo *et al.*, 2000; Singh *et al.*, 2000; Ferat-Osorio *et al.*, 2014).

Expression profiles of the selected gene sets determined after HR and AR treatment, revealed to be very much alike, indicating that an acute stressor, regardless whether temperature or handling, similarly

induces the target genes in maraena whitefish. Nonetheless, the immune genes *IL6*, *IL12B* and *TNF*, as well as the stress genes *NR3C1* and *TP53*, seem to be slightly more induced in response to the handling procedure than to the acute temperature rise. Further, regarding the stress genes, the AR treatment seems to cause more systemic alterations in gene expression, while HR conditions led to DE genes mainly in splenic tissue. Matching these results, the increase of GCR in response to handling stress in splenic leukocytes, is already described in literature (Tort, 2011a). Overall, these data clearly unveil that the two sets of target genes were equally affected by the handling procedure and by the temperature rise in maraena whitefish. Further, the holistic analysis showed that the AR treatment affected overall just a little more genes than the handling control, however the latter provoked a higher DE gene count in hepatic tissue. Nonetheless, the sets of top-regulated and most-likely systemically DE genes determined within the microarray-based analysis for AR and HR treatment were completely distinct, thus there has been no conflict in interpretation.

The comprehensive assessment of temperature-related gene expression revealed that the GR treatment led to a massive amount of DE genes, mainly in the liver, whilst at AR conditions the overall count of DE genes was significantly lower and the spleen was the main site of altered expression. Within this study, the focus should be on those genes, that exhibited systemically alterations in their expression, i.e., across all three tissues analysed, whereas the distinct tissue-specific expression profiles were discussed in Rebl *et al.* (2018).

For the GR experiment, despite the overall comparably high number of 775 DE genes, only 12 (annotated) genes were found to be commonly differentially expressed in a systemic manner. Further, the alterations in transcript levels, that were determined by qPCR for the immune and the stress gene sets, were not confirmed within the microarray-based expression analysis. Instead of the pre-defined genes, the two chaperones, *SERPINH1* (HSP47) and *CLU*, were identified as top up-regulated genes, as well as the two translation regulator encoding genes *EEF1A1a* and *EEF1A1b*, which all together revealed moderate expression ratios. Moreover, several genes, that are known to play a role within the cold-shock response, such as *CIRBP* (Phadtare *et al.*, 1999; Rebl *et al.*, 2013; Verleih *et al.*, 2015), *YBX2* (Lindquist *et al.*, 2014; Xu *et al.*, 2017) and *AGT* (Hiramatsu *et al.*, 1984; Cassis *et al.*, 1998; Sun *et al.*, 2003), were found to be down-regulated in mareana whitefish due to the prolonged exposure to elevated temperature. Additionally, also the immune-related genes *CEACAM20* and *FKBP5* revealed decreased transcript numbers at GR conditions, similarly to some members of the immune-gene set (*IL1B, IL6, SAA*), as already discussed above.

However, within the IPA analysis only the three genes *CLU*, *AGT* and *FKBP5* of the overall 12 DE genes could be assigned to functional pathways and the assignment of only three of the top five pathways was statistically significant. The IPA analysis predicted the *LXR/RXR* and the *FXR/RXR activation pathways* to be affected by the two genes *CLU* and *AGT* after GR treatment. Whereas the *LXR/RXR activation pathway* is involved in the regulation of lipid metabolism, inflammation, and cholesterol metabolism, the *FXR/RXR activation pathway* connects the bile acid regulation with lipoprotein, lipid and glucose metabolism. Accordingly, the apolipoprotein "clusterin", encoded by the *CLU* gene, is known to have diverse regulatory and protective functions in basic cellular processes, as it is a master regulator of distinct lipid metabolism pathways and has chaperone-like functions in response to heat (Matukumalli *et al.*, 2017). Moreover, clusterin was found to regulate the expression of *AGT* and *vice versa* (Yoo *et al.*, 1998; Jung *et al.*, 2014). The gene *AGT*, codes for the glycoprotein "angiotensinogen" that induces the expression of proteins involved in cellular growth and matrix formation, as well as in inflammatory processes, since it recruits inflammatory cells and increases the expression of chemokines, adhesion

molecules, and cytokines (Mezzano *et al.*, 2001; Ruiz-Ortega *et al.*, 2002; Jung *et al.*, 2014). Additionally, angiotensinogen is part of the renin-angiotensin system (RAS) that is involved in the regulation of blood pressure and fluid homoeostasis and which is activated due to chronic exposure to cold, causing an increase in blood pressure (Sun *et al.*, 2003; Wu *et al.*, 2011). Consequently this factor is found to be down-regulated in response to prolonged heat stress in mareana whitefish. Further, several studies reported that the *AGT* expression is regulated by the GCR (Dostal *et al.*, 2000; Wu *et al.*, 2011; Pandey, 2013). Hence, the IPA analysis supposed that down-regulation of *AGT*, as well as of *FKBP5,* interferes with the *glucocorticoid receptor signaling pathway* in maraena whitefish at GR conditions. This pathway mainly regulates the cortisol-driven stress-response, but also a multitude of anti-inflammatory actions, metabolic functions, and the cell differentiation. The *FKBP5* gene codes for the FKBP51 protein that negatively regulates the action of the GCR by binding to HSP90 within the GCR hetero-complex and therefore reduces the cortisol affinity to the latter (Binder, 2009; Galigniana *et al.*, 2012). Interestingly, the interplay of *FKBP5* and the GCR hetero-complex has major functions during chronic stress and in the regulation of anxiety and depression in mammals (Binder, 2009; Pérez-Ortiz *et al.*, 2013; Guidotti *et al.*, 2013). Further, the suppressed *FKBP5* expression found for maranea whitefish, could have caused an increased activity of the *GCR*, resulting in a more efficient "stress-coping behaviour" and an "increased tolerance to chronic stress", as was recently observed in mice *(Hartmann* et al.*, 2012; Zheng* et al.*, 2016).* Consequently, the down-regulation of the two genes *AGT* and *FKBP5* in maraena whitefish due to GR treatment might be indicative for a highly potent stress-response, induced by its major regulator the GCR that leads to the suppression of immune and growth functions, which in turn are hallmarks of chronic stress (Barton, 2002).

After exposure to AR conditions, 11 exclusively up-regulated genes, that were shared by liver, spleen, and kidney, were identified by comprehensive gene expression analysis. Further, among these DE genes, that are all associated with an acute heat-shock response, the stress target genes *HSP70* and *HSP90* were the top-two up-regulated genes, with highest transcript levels in the liver, as was previously found using qPCR analysis. Although the fold changes determined by qPCR are much higher than those resulting from the microarray-based analysis, the tendency of a strong to massive up-regulation for *HSP90* and *HSP70* is evenly reflected by both data sets. The differences found in the magnitude of transcript values, especially for HSP70, suggestively resulting from different paralogues that were measured on the microarray chip and by qPCR, respectively. Several studies elucidated the existence of multiple *HSP70* and *HSP90* paralogues providing highly distinct transcript numbers in response to stress in teleost fish (Basu *et al.*, 2002; Ojima *et al.*, 2005a; Garcia de la serrana & Johnston, 2013; Wang *et al.*, 2014a; Yan *et al.*, 2017).

The IPA analysis of the AR-data set resulted in five top-regulated pathways, which were all influenced by the altered expression of *HSP70* in combination with up to three other DE genes. The highest number of overall four DE genes (*DUSP1*, *HSP70*, *HSP90*, *DNAJB1*), were associated with the *aldosterone signaling pathway* in epithelial cells, which plays a major role in cation homeostasis and thus also in the control of the blood pressure. The inducible, early-response gene *DUSP1* encodes the "dual specificity phosphatase 1" that regulates MAPKs and thus related signaling cascades, which are involved in various physiological processes, such as the regulation of the cardiovascular system (Patterson *et al.*, 2009; Li *et al.*, 2015). The blood-pressure and -flow control, are crucial physiologic processes, as with raising temperature the oxygen saturation of water decreases, but simultaneously the oxygen demand in fish increases due to higher metabolic rates (Wendelaar Bonga, 1997; Mommsen *et al.*, 1999; Wiseman *et al.*, 2007). Therefore, at higher ambient temperatures fish have to increase the blood flow to ensure

a sufficient oxygen supply and to prevent hypoxia (Pörtner, 2002). Indicating the importance of these physiological adjustments, the IPA analysis predicted that also the *eNOS signaling pathway*, which also serves the regulation of blood vessel vasodilation and blood pressure, was affected by alterations in *HSP70* and *HSP90* transcript numbers. Both chaperones are known to have direct positive (HSP90) or indirect negative (HSP70) regulatory effects on the activity of the eNOS enzyme (Sessa, 2004; Jiang *et al.*, 2003).

Moreover, as previously described for the GR treatment, also for the AR-data set the IPA analysis predicted the *glucocorticoid receptor signaling pathway* as affected, unless the involved DE genes (*DUSP1*, *HSP70*, *HSP90*) differed completely from the GR-data set. This indicates that, depending on the stressor, different gene sets are responsible for similar responses.

According to the IPA based predictions, besides *HSP70*, also its co-chaperone encoding gene *DNAJA2* and the gene *PPP1R15A* affected the pathway of the *unfolded protein response*. This pathway is activated in case of an accumulation of unfolded proteins in the lumen of the endoplasmic reticulum — as in case of heat-stress — and comprises multiple mechanisms to regain homoeostasis (Walter & Ron, 2005). Besides the HSPs, the stress-inducible gene *PPP1R15A* (alias *GADD34*), encoding the "protein phosphatase 1 regulatory subunit 15A" was up-regulated in maraena whitefish, as well. As already discussed by Rebl *et al.* (2018), this protein plays a role in cellular recovery from the *unfolded protein response* (UPR), since it dampens the translational repression exerted by factors of the UPR as was found in mammals (Novoa *et al.*, 2001; Brush *et al.*, 2003; Kojima *et al.*, 2003).

Moreover, *HSP90* and *HSP70* together with its co-chaperone *DNAJB1* were assigned to the *protein ubiquitination pathway*, which, just like the previous pathway, plays a major role in the degradation of proteins (Ciechanover, 1998). These two pathways are representative for the typical chaperone activity of HSP70 and HSP90, which serve the protection and refolding of proteins (Iwama *et al.*, 1998; Basu *et al.*, 2002; Roberts *et al.*, 2010).

Further, based on the given data, the transcription regulator TP53 most likely had a role as master regulator within both stress responses, i.e., for acute as well as for gradual temperature stress. It is well known from literature that TP53 possesses major regulatory functions during stress responses, since it is activated by a plethora of stress stimuli and mediates protective functions, such as cell cycle arrest, apoptosis and senescence, DNA repair and control of mitochondrial respiration (Horn & Vousden, 2007; Belyi *et al.*, 2010; Lazo, 2017). Besides a vast amount of *in vivo* and *in vitro* studies in mammals, several fish species served as a model to elucidate regulatory mechanisms of TP53, however mainly with regard to oncogenetic issues (Krause *et al.*, 1997; Cachot *et al.*, 1998; Storer & Zon, 2010). Owing to its outstanding role in sensing environmental stress stimuli, TP53 is now also in the focus of biomarker research and hence isolated and characterised in aquaculture-relevant species like orange-spotted grouper (*Epinephelus coioides*) (Qi *et al.*, 2013) and rainbow trout (Liu *et al.*, 2011).

Despite clear signs of stress-induced alterations in gene expression for the pre-defined target genes measured by qPCR as well as within the comprehensive microarray-based analysis, the "classical" plasma parameters cortisol and glucose showed no significant differences, neither at GR nor at AR conditions. Nonetheless, the plasma cortisol levels found in maraena whitefish are comparably high (16-274 ng/ml), considering that basal plasma cortisol levels are reported to be lower than 2-10 ng/ml in salmonids (Barton, 2002; Talbot *et al.*, 2009; Zwollo, 2018) and that a 10- to 100-fold increase of these values is indicative for a HPI-based stress response (Barton, 2002; Gesto *et al.*, 2008; Talbot *et al.*, 2009; Zwollo, 2018). Notably, the peak cortisol concentrations determined within this experiment were much higher than for the density stress experiment. Despite a slight tendency of overall higher cortisol levels at AR

conditions compared to GR conditions, the data indicate that maraena whitefish is highly sensitive to the experimental and sampling procedure, although there are high inter-individual differences for each group. This high sensitivity might be due to the fact that the individuals of this experiment derived from wild-caught fish and thus represent the first generation of maraena whitefish in aquaculture, which consequently has not yet passed an adaptation process to this anthropogenic environment. Apart from that, the reliability of plasma cortisol levels as stress indicators is partly controversial due to numerous contradictory studies and hence is under discussion in literature (Mommsen *et al.*, 1999; Martinez-Porchas *et al.*, 2009; Roberts *et al.*, 2010; Rebl *et al.*, 2017, 2018). In contrast to cortisol, the plasma glucose levels of mareana whitefish are obviously unaffected by the temperature rise and the sampling procedure, since the values determined in the different groups are all within physiological ranges (Wright *et al.*, 1989; Bucking *et al.*, 2005).

In conclusion, this experiment clearly unveiled that the AR treatment led to completely distinct expression profiles than the GR treatment, whereas the latter led to a much higher DE gene count. The differences were indicated by the non-overlapping sets of top-regulated genes identified by the comprehensive transcript profiling, as well as by the opposing or highly varying transcript numbers of the target genes determined by qPCR. Nonetheless, particularly *HSP70*, but also *HSP90*, as well as the *glucocorticoid receptor signaling pathway* were found to play important roles in response to acute and prolonged temperature stress in maraena whitefish. Additionally, *TP53* might have major regulatory functions in coping with acute and prolonged thermal stress within this species. Under GR conditions, hallmarks of a tertiary, i.e., chronic stress response were found, such as the suppression of immune genes, whilst several protective genes (*HSP70, HSP90*, *SERPINH1, CLU*) were moderately induced. Moreover, metabolic processes (*LXR/RXR* and the *FXR/RXR activation pathways*) seem to be affected and signs of a prolonged induction of the GCR, through the suppression of its antagonist *FKBP5* were found. Altogether, this indicates that maraena whitefish has severe difficulties in adapting to the prolonged temperature stress and thus initiates mechanisms of a chronic stress response (Barton, 2002).

However, under AR conditions maraena whitefish gene expression profiles reveal clear hallmarks of an acute heat-shock response, characterised by a massive or at least strong induction of the genes *HSP70* and *HSP90,* accompanied by the activation of various other stress-related genes and pathways and of the pro-inflammatory genes *IL1B* and *CXCL8.* Hence, these data illustrate that mareana whitefish is able to overcome a short heat exposure, yet the strong reactions might also reflect that AR conditions pose a serious threat to the fish's health and homoeostasis.

Consequently, it can be concluded that the acute and the gradual temperature rise had adverse effects on maraena whitefish and in accordance with previous studies on other coregonids (Szczepkowski *et al.*, 2006; Siikavuopio *et al.*, 2012, 2013; Goebel *et al.*, 2017; Matousek *et al.*, 2017), a temperature of 24°C can be regarded as critical for this species, as well.

Moreover, this experiment clearly showed that maraena whitefish is not only very sensible to temperature but to handling stress, too. This is indicative for the missing adaptation of these first-time reared animals to the anthropogenic environment, which can be improved by selective breeding and further domestication processes, as previously reported for the rainbow-trout (Rebl *et al.*, 2012, 2013).

4.7. Stimulation with *A. salmonicida* induced patterns of an inflammatory response

As reported by Luft *et al.* (2015), based on microbiological examinations, *A. salmonicida* was found to have a high prevalence in the aquaculture facility used in this study and moreover maraena whitefish

exhibited a high susceptibility to infections with this pathogen, resulting in very high mortalities of about 60%. Owing to its crucial role for infections, especially for farmed salmonids, *A. salmonicida* was used in the course of this study, as similarly in a vast amount of studies to analyse the immune responses of aquaculture-relevant species to this important fish pathogen. Even though this bacterium suggestively invades its host mainly through lesions, but also via skin, gills or gastrointestinal tract (Svendsen & Bøgwald, 1997; Ferguson *et al.*, 1998; Svendsen *et al.*, 1999; Mulder *et al.*, 2007), within this study the peritoneal cavity served for the controlled administration of an *A. salmonicida* suspension, since this is a well established experimental method (Yaffe & Yoffey, 1982; Melnicoff *et al.*, 1989; Meseguer *et al.*, 1993; Afonso *et al.*, 1997; Do Vale *et al.*, 2002; Chadzinska *et al.*, 2008; Korytár *et al.*, 2013). Moreover, within this experiment the fish were administered inactivated *A. salmonicida*, as this bacterium is known to survive in macrophages and is able to evade and modulate the host's defence mechanisms, due to its A-layer and various virulence factors, and therefore suppresses the inflammatory response (Daly *et al.*, 1996; Fehr *et al.*, 2006; Vanden Bergh & Frey, 2014; Menanteau-Ledouble *et al.*, 2016).

Thus within the given experiment, the immune-gene set was used to examine mechanisms and intensity of the inflammatory response of mareana whitefish to *A. salmonicida*, since it comprises genes encoding major pro-inflammatory cytokines and other factors related to innate immunity. Indeed, the data showed altered expressions for all immune target genes and all of them showed highest transcript numbers in the peritoneal cells. Here, mainly the pro-inflammatory cytokines *IL1B*, *TNF* and *CXCL8*, revealed a strong increase in transcript levels, which is indicative for the initiation of an inflammatory response (Mulder *et al.*, 2007; Seppola *et al.*, 2008; Zou & Secombes, 2016) and therefore for a successful stimulation of maraena whitefish. This is not self-evident, since inactivated *A. salmonicida* in rainbow trout in vitro experiments failed to trigger the expression of pro-inflammatory cytokines (Komatsu *et al.*, 2009). Moreover, alterations in the gene expression ratios were recorded not only at the infection site, but also in several tissues of maraena whitefish, confirming a systemic effect of this stimulation trial, despite the usage of inactivated bacteria.

Notably, maximum expression values for the induced immune genes were recorded not before 72 h post stimulation in peritoneal cells, as well as in the spleen (apart from *IL6* in this tissue), liver and gills. A similar pattern of gradually increasing transcripts from 24 h to 72 h post infection for *IL1B*, *TNF,* and *CXCL8* was reported for the liver and the thymus by Brietzke *et al.* (2015) after infection of rainbow trout with live *A. salmonicida*. However, the authors recorded much higher and systemic peak expressions for all three pro-inflammatory cytokines already 6 h to 12 h post infection (Brietzke *et al.*, 2015). A similarly fast and very strong induction of *IL1B* and *CXCL8* even with inactivated *A. salmonicida* was observed after stimulation of Atlantic cod, as well (Feng *et al.*, 2009). Therefore, it is highly likely that also maraena whitefish exerted such a fast and effective cytokine activation in response to the bacterial stimuli, which is indicated by the dramatic influx of granulated myeloid cells to the infection site, as observed for this experiment (Altmann *et al.*, 2016). Indeed, this granulocyte trafficking is based on the previous actions of pro-inflammatory cytokines, here mainly the chemokine CXCL8 promotes the movement of neutrophils, the first-line effector cells of innate immune response, that arrive at first and in large quantities at the infection site, a process that was equally observed in mammals and teleosts (Cole *et al.*, 2014; Havixbeck *et al.*, 2016)

This assumption is further supported by the recorded peak expression of the genes *IL1B*, *IL6*, *IL12B* and *TNF* in the head kidney, that was followed by a significant down-regulation. This could be explained by the comparably high proportion of myeloid cells that are stored in the head kidney, whereas the other immune-related tissues rather provide lymphoid cells, as was previously reported for rainbow trout

by Korytár *et al.* (2013). Upon bacterial stimulation, these myeloid cells were activated, resulting in the secretion of pro-inflammatory cytokines, as observed in maraena whitefish 48 h post stimulation. Subsequently, the chemokine-induced massive emigration of granular myeloid cells to the infection site started, which most likely caused the down-regulation of several immune genes 72 h post stimulation in the head kidney of maraena whitefish and simultaneous led to up-regulation of the same genes in peritoneal cells, where the arrival of granulocytes peaks at this time point (Altmann *et al.*, 2016; Korytár *et al.*, 2013).

The given experiment successfully demonstrated the high capability of maraena whitefish in combating the bacterial insult. This is reflected by remarkably high expression ratios even three days after stimulation in several tissues, whilst similar studies on other teleost species reported a decline of the cytokine expression to basal levels within several days post treatment (Feng *et al.*, 2009; Seppola *et al.*, 2008; Chadzinska *et al.*, 2008). Likewise, Zhang *et al.* (2011b) observed that in Atlantic salmon a high expression of pro-inflammatory genes and other factors of innate immunity benefit the survival of an *A. salmonicida* infection.

Besides the mobilisation of granulocytes, mainly the cytokines *IL1B*, *TNF,* and particularly *IL6* lead to the activation of the APR, of which a major APP is encoded by the gene *SAA*. Indeed, in parallel with the sharp increase in *IL6* expression in the head kidney at 48 h post stimulation, a moderate peak expression of *SAA* was recorded in the liver of maraena whitefish, known as the main site of SAA synthesis in mammals and fish (Uhlar & Whitehead, 1999; Villarroel *et al.*, 2008). Further, maraena whitefish revealed a strong *SAA* up-regulation in the spleen and a moderately induced *SAA* expression at the infection site. This comparably belated induction of the SAA expression at around 24 h to 96 h post exposure to a stimuli is well known from literature (Jensen *et al.*, 1997; Uhlar & Whitehead, 1999; Jørgensen *et al.*, 2000; Wei *et al.*, 2013) and moreover even the medium to strong up-regulation of *SAA*, as determined in this experiment for maraena whitefish, was previously found in several infection studies (Ewart *et al.*, 2005; Villarroel *et al.*, 2008; Starliper, 2011; Kania *et al.*, 2014), however Lin *et al.* (2007) even recorded a massive induction of *SAA,* comparable to those in mammals (Uhlar & Whitehead, 1999; Gruys *et al.*, 2005; Grover *et al.*, 2016; De Buck *et al.*, 2016), in zebrafish after infection with *A. salmonicida*. Moreover, besides SAA, several studies found that plasma proteins of the complement system play an important role during *A. salmonicida* infection in teleosts (Secombes & Olivier, 1997; Ewart *et al.*, 2005; Overturf & LaPatra, 2006; Skugor *et al.*, 2009; Millán *et al.*, 2011; Rebl *et al.*, 2013), another defence mechanism of innate immunity that is still largely unexplored in maraena whitefish.

Interestingly, it was found that maraena whitefish *IL12B*, encoding a subunit of the hetero-dimeric cytokine that *inter alia* is responsible for the initiation and modulation of the adaptive immune response (Trinchieri, 2003; Wang *et al.*, 2014b; Wang & Husain, 2014; Zou & Secombes, 2016), showed a strong increase in transcript numbers in the head kidney, which is contradictory to previous reports in teleosts, where IL12p40c (which is most likely the IL12B paralog identified in maraena whitefish), was found to be barely inducible by LPS or bacterial stimuli and more characterised by a high constitutive expression ((Huising *et al.*, 2006; Wang & Husain, 2014; Matsumoto *et al.*, 2016)). This might indicate a special role of this paralog in maraena whitefish, probably within the activation of acquired immunity, a well-known function of the IL12 cytokine (Weinmann *et al.*, 1999; Trinchieri, 2003; Wang *et al.*, 2014b; Wang & Husain, 2014), since the head kidney is a major lymphoid tissue in teleosts.

Another noteworthy finding is the different expression of the two sister genes *MAPK1* and *MAPK3*, encoding kinases which are involved in a plethora of cellular processes, e.g., in the signal transduction of IL1B, TNF, and IL6 signaling cascades (Tibbles & Woodgett, 1999; Schlaepfer *et al.*, 2007; Roher *et al.*,

2010; Radtke *et al.*, 2010; Scheller *et al.*, 2011). Whilst *MAPK1* transcript levels reveal notable increases in the head kidney and the liver, *MAPK3* expression remains virtually unaffected. Since both kinases are functional homologues it might be possible that in maraena whitefish only *MAPK1* was involved in the observed inflammatory processes, likewise Sun *et al.* (2018) found distinct expression patterns of *MAPK1* and *MAPK3* in orange spotted grouper in response to a parasite infection. However, it should be taken into account that both kinases are mainly regulated by phosphorylation and less on transcript level (Roher *et al.*, 2010).

In summary, the given experiment unveiled a clear effect of the stimulation with inactivated *A. salmonicida* on maraena whitefish gene expression, which resulted in expression profiles that were characteristic for an inflammatory response. Accordingly, a strong induction, mainly of pro-inflammatory cytokines, such as *IL1B*, *IL6*, and *IL12B* in the head kidney and of *IL1B*, *CXCL8*, and *TNF* in the peritoneal cells, was observed. Whereas, the typical, immediate and sharp up-regulation of the pro-inflammatory cytokines was not recorded in this study, since the earliest sampling was possible only 24 h post treatment, it is very likely to be present in maraena whitefish, as well. This assumption is supported by the massive influx of granulocytes into the peritoneal cavity that most likely was induced by an initial and sharp increase in cytokine abundance. Further, the APP encoding gene, *SAA*, was found to be moderately to strongly induced in response to the bacterial stimuli in the liver and in the spleen.

4.8. The primary cell stimulation assay gave insight into mechanisms of the joint immune-endocrine regulation within the teleost head kidney

The stimulation of the head kidney primary cells, as intended, offered further insights in the early regulation of the immune genes in response to a pathogen-like stimuli in addition to the data from the *in vivo* stimulation of maraena whitefish with the bacterium *A. salmonicida*. Moreover, the experiment enlightened mechanisms of the combined immune-endocrine regulation within the head kidney.

The head kidney primary cells isolated from maraena whitefish were in size and morphology similar to those of other teleosts, which were described by the use of microscopy, as well (Blüm *et al.*, 1989; Mackenzie *et al.*, 2003; Arnold, 2009; Goetz *et al.*, 2012). Further the flow-cytometric analysis of the head kidney cell composition revealed that there were two main populations of cells, i.e., one that contains mainly less granular and smaller cells — small lymphocytes — and another comprising more granular and larger cells — granulocytes. This confirms the successful enrichment of head kidney leukocytes within the analysed primary cell culture and further the presence of two main leukocyte populations is in line with previously published data about head kidney primary cultures in rainbow trout (Korytár *et al.*, 2013) and common carp (Joerink *et al.*, 2006), whereas even three main populations of leukocytes have been identified in brook trout (*Salvelinus fontinalis*) (Mackenzie *et al.*, 2003). Based on previous findings that morphologic differentiation — mainly of monocytes to macrophages or dendritic cells — is accompanied by tremendous changes in gene expression (Tamayo, 1999; Mackenzie *et al.*, 2003; Lehtonen *et al.*, 2007), the experiment was restricted to the period of morphological stability of the isolated cells, i.e., to 48 h of incubation after stimulation.

In teleost fish, the head kidney is the major immune organ that additionally possesses interrenal tissue and thus integrates immune-endocrine functions (Press & Evensen, 1999; Tort *et al.*, 2003; Uribe *et al.*, 2011; Nardocci *et al.*, 2014; Rebl & Goldammer, 2018). Therefore, the given experiment served to demonstrate the effect of immune- or stress-stimulatory agents, as well as the combination of both, on the expression of the immune- and the stress-gene sets.

The stimulation with PAMP reagents induced a very fast and strong up-regulation of the "immediate early" pro-inflammatory cytokines *IL1B* and *CXCL8* in maraena whitefish, which matches well with results found in literature about *in vitro* PAMP- or pathogen-stimulated head kidney cells, as reported for several fish species (Huising *et al.*, 2003; Iliev *et al.*, 2005; van der Aa *et al.*, 2010; Xu *et al.*, 2016). However, other expression patterns of both genes were found (Seppola *et al.*, 2008) , which suggests that they might be regulated in a species-specific manner, or even more likely that the several *IL1B* and *CXCL8* homologues that are thought to exist in some teleost fish, like salmonids, are differentially expressed in response to immune stimuli, as already discussed in literature (Secombes *et al.*, 2011; Husain *et al.*, 2012; van der Aa *et al.*, 2010; Bird & Tafalla, 2015).

In addition to *IL1B* and *CXCL8*, the genes *SAA*, *MAPK1*, and *MAPK3* were also immediately and significantly up-regulated within the first three hours post treatment with PAMP reagents. A fast activation of the APP encoding gene *SAA* within several hours post *in vitro* stimulation with different pathogens or pathogen-like reagents is documented in literature for rainbow trout (Villarroel *et al.*, 2008) and the mollusc *Crassostrea hongkongensis* (Qu *et al.*, 2014). However, Jørgensen *et al.* (2000) recorded a notable increase in *SAA* transcript levels only 48 h post *in vitro* treatment of Atlantic salmon hepatocytes with LPS. Moreover, similar to the oscillating *SAA* transcript levels in head kidney cells of maraena whitefish, Jayasinghe *et al.* (2015) and Wei *et al.* (2013) recorded a fast increase in hepatic *SAA* gene expression, showing multiple peaks for black rockfish and orange-spotted grouper following *in vivo* stimulation with several pathogens.

The two serine/threonine protein kinases MAPK1 and MAPK3 are well-known regulators of the immune response and in presence of pathogenic or pathogen-like stimuli these kinases are activated (Kyriakis & Avruch, 2012; Soares-Silva *et al.*, 2016). Nevertheless MAPK1 and MAPK3 are mainly regulated by phosphorylation and dephosphorylation, in case of activation the constitutively expressed genes *MAPK1* and *MAPK3* are induced as well, resulting in elevated mRNA levels, as shown for mammals (Goral & Kovacs, 2005; Garcia-Rodriguez *et al.*, 2012; Jiang & Tang, 2018). Therefore, the up-regulation of *MAPK1* and *MAPK3* observed within all three head kidney cell stimulation assays in maraena whitefish, most likely indicates an increased need of both protein kinases to overcome a homoeostatic disbalance.

The slightly delayed but still fast up-regulation of *IL6* and *IL12B* to peak values at 12 h post stimulation found in maraena whitefish is in line with findings of Øvergård *et al.* (2012), who stimulated head kidney leukocytes in Atlantic halibut. Additionally, solely for *IL6*, a strong down-regulation in response to all three stimulation assays was observed in maraena whitefish, indicating that this cytokine, which itself exerts pro- and anti-inflammatory functions, is tightly regulated in this species. The suppression of *IL6* transcription might has been mediated by TP53 and/or the GCR, two known repressors of the *IL6* gene (Tanaka *et al.*, 2014), since one or both genes (*TP53*, *NR3C1*) were found to be induced at respective time points. Further, the oscillating *IL6* expression pattern matches well with the three peaks of up-regulation of the *SAA* gene, whose expression is mainly induced by IL6 (Tanaka *et al.*, 2014) and thus is directly dependent from *IL6* transcript numbers, as was shown for mammals (Gervois *et al.*, 2004).

Interestingly, for another immediate early cytokine, the maraena whitefish type I *TNF,* a peak expression was determined only 24 h post stimulation, which is comparably late. In contrast, in similar experiments on rainbow trout head kidney cells, Iliev *et al.* (2005) found a massive LPS-induced *TNF* up-regulation (within 12 h) and Hong *et al.* (2013) reported a sharp increase of type I and type II TNF gene expression (only 4 h) post stimulation with LPS or Poly I:C. However, Zou *et al.* (2002) determined a differential *in vitro* expression of two *TNF* genes in rainbow trout macrophages of which one was highly and the other barely inducible by LPS. Thus, it is very likely that even maraena whitefish, like other salmonids

(Hong *et al.*, 2013) and teleosts (Polinski *et al.*, 2013), possesses several *TNF* paralogues with distinct expression patterns.

In addition to the immune genes, even the four maraena whitefish stress genes (*HSP70*, *HSP90*, *NR3C1*, *TP53*) showed significant variations in transcript numbers following the treatment with PAMP reagents. Particularly the transcription of *TP53* and *HSP70*, but of *HSP90*, as well, was rapidly and strongly induced, whereas *NR3C1* showed a delayed and slight rise in transcript numbers. In a similar *in vitro* study on common carp head kidney phagocytes Stolte *et al.* (2009) however recorded a very fast but only slight increase of *HSP70*, *HSP90*, and *NR3C1* transcript levels after LPS stimulation. Interestingly, following *in vivo* stimulation of common carp with zymosan A, Stolte *et al.* (2009) found a similar fast and strong induction of the *HSP70* gene, revealing two peak values, as was recorded for maraena whitefish *HSP70* in head kidney leukocytes *in vitro*. Several studies in fish elucidated the interactions of HSP70 with the immune response and that it is inducible by LPS (Zhang *et al.*, 2011a) and various pathogens (Elibol-Flemming *et al.*, 2009; Dang *et al.*, 2010; Ming *et al.*, 2010; Zhang *et al.*, 2014; Liang *et al.*, 2016). Further, the *HSP90* gene was shown to be inducible by bacterial challenge, as well, which was proven by a study from Liang *et al.* (2016) in marbled eel (*Anguilla marmorata*) and by Pu *et al.* (2016) in *Schizothorax prenanti*. In mammals, both HSPs are known to interfere with immune functions, since HSP70, e.g., stimulates monocytes and macrophages to release cytokines and HSP90, e.g., promotes the maturation of dendritic cells (Gaston, 2002). Indeed, as reviewed by Roberts *et al.* (2010), the various immune-stimulatory functions of HSP70 and HSP90 are just about to be enlightened in fish, as well. Besides their immune-modulatory functions, under stressful conditions, like a pathogenic challenge, both HSPs also act in their "classical" role as chaperones to stabilise important regulators of the immune response, such as TP53 (Wang & Chen, 2003; Müller *et al.*, 2004; Walerych *et al.*, 2009) and the GCR (Stolte *et al.*, 2006; Castro *et al.*, 2011; Nardocci *et al.*, 2014; Rebl & Goldammer, 2018). Therefore, the first peak in *HSP70* and *HSP90* transcript numbers might partly be related to the rapid increase in *TP53* transcripts and the second to the up-regulation of the GCR encoding gene *NR3C1*.

In case of TP53, there are a plethora of publications elucidating the immune-modulatory functions of this protein that is suggested, at least in mammals, to interact with the complete set of innate TLR genes (Menendez *et al.*, 2013) and moreover seems to play a role in innate antiviral immunity (Rivas *et al.*, 2010). However, to date only few studies on the immune-related functions of TP53 in fish are available. For example, Guo *et al.* (2017) reported on significantly increased *TP53* mRNA levels following viral *in vitro* stimulation of a mandarin fish (*Siniperca chuatsi*) cell line and in their comprehensive study on channel catfish, Mu *et al.* (2015) identified several *TP53* paralogues that revealed a tissue-specific, significant up-regulation after bacterial challenge. Moreover, Liu *et al.* (2009) reported on the dampening effect of TP53 on the LPS induced secretion of cytokines through a negative regulatory effect on the transcription factor NFκB to prevent an overshooting inflammatory response. The balancing reciprocal inhibitory actions of TP53, the major sensor and mediator of intrinsic stress, and NF-κB, the major sensor and mediator of extrinsic stress (Lane & Levine, 2010; Gudkov *et al.*, 2011), seems to be evolutionarily well conserved from mammals to invertebrates (Li *et al.*, 2017) and thus could be an explanation for the rapid and high increase in maraena whitefish *TP53* transcript levels following PAMP treatment.

In contrast to the immune-stimulating PAMPs, cortisol, the major stress hormone in fish, is well known for its anti-inflammatory but also immune-modulatory effects, as has often been documented in literature (Barnes & Adcock, 1993; Carlson *et al.*, 1993; Espelid *et al.*, 1996; Stolte *et al.*, 2006; Tokarz *et al.*, 2015; Nardocci *et al.*, 2014; Rebl & Goldammer, 2018). Accordingly, within the present work, the stimulation of head kidney primary cells with cortisol resulted in a significant down-regulation of genes,

which code for pro-inflammatory cytokines (*IL1B*, *IL6*, *CXCL8*, *IL12B*, *TNF*), as was previously reported for several *in vitro* studies on head kidney primary cultures from various fish species (MacKenzie *et al.*, 2006; Castillo *et al.*, 2009; Castro *et al.*, 2011; Khansari *et al.*, 2017a). Unlike the cytokines, the stress genes were clearly induced following cortisol treatment, which is in line with literature (Bury *et al.*, 2003; Stolte *et al.*, 2006, 2009; Vazzana *et al.*, 2010). Particularly *HSP70* showed an instantaneous, strong up-regulation and also *TP53* and the GCR encoding gene *NR3C1* were rapidly and significantly induced. Notably, in parallel with the peak expression of *NR3C1* three hours post treatment, the genes *HSP70*, *TP53* and *MAPK1* showed a first peak in up-regulation, whereas shortly before, the cytokines were significantly down-regulated. Indeed, there is evidence in literature for the interaction of the GCR with *HSP70*, *TP53* and *MAPK1* to exert its anti-inflammatory actions via NFκB and CREB (cAMP response element binding protein) (Mommsen *et al.*, 1999; Kirschke *et al.*, 2014; Petta *et al.*, 2016). However, the genes *HSP70*, *HSP90*, and *TP53* showed a second and even higher peak expression at 24 to 48 h post stimulation, which was recorded again shortly after the strong down-regulation of the cytokine encoding genes and thus it seems that the regulation of these genes is interrelated. This might be mediated by the action of TP53 on NF-κB, as mentioned before, or maybe by SOCS, which were found to be negative regulators of cytokines (Philip *et al.*, 2012; Philip & Vijayan, 2015) as well as positive regulators of TP53 (Calabrese *et al.*, 2009), whereas the latter information is mainly based on mammalian cancer studies and not investigated in fish so far.

In accordance with the results from maraena whitefish, Celi *et al.* (2012) observed a strong induction of *HSP70* and *HSP90* transcripts in sea bass head kidney post i.p. injection of cortisol. On the other hand, several studies stated that cortisol alone has no effect on HSP expression, as reviewed by Iwama *et al.* (1999) and Basu *et al.* (2002), however these studies mainly concentrated on protein levels in hepatic or gill tissue. Strikingly, simultaneous to the second peak in *HSP70*, *HSP90*, and *TP53* transcript levels, the immune-related genes *SAA*, *MAPK1*, and *MAPK3* were found to be up-regulated, as well. Besides their regulatory function within the immune response, *MAPK1*, and *MAPK3,* as known from mammals, are also activated in response to environmental stress (Kyriakis & Avruch, 2012), a state that was apparently successfully mimicked via cortisol stimulation within the given experiment. On the contrary, glucocorticoids are well-known repressors of the APR, since they negatively regulate the cytokine production via the GCR (Uhlar & Whitehead, 1999; Tort, 2011b), as e.g., shown by reduced *SAA* transcript levels in rainbow trout hepatocytes following cortisol stimulation (Philip *et al.*, 2012). However, there is evidence for the up-regulation of *SAA* expression in response to various acute stressors in mammals and fish as well (Kim *et al.*, 2011; Talbot *et al.*, 2009; Gadan *et al.*, 2012), complying with the enhanced *SAA* transcription found within the present experiment.

Interestingly, compared to the other two treatments, the co-stimulation of head kidney leukocytes with PAMPs and cortisol led to the overall most significant regulation of several immune- and stress-related genes, i.e., highest up- and down-regulation of *IL6*, the strongest suppression of IL12B and induction of *TNF*, *MAPK3*, *HSP70*, *HSP90*, and *NR3C1* transcription. However, the transcript numbers for the genes *IL1B*, *CXCL8*, *SAA*, and *TP53* were lower compared to the stimulation with PAMP reagents but higher than post cortisol treatment. Therefore, these results represent the suppressive effect of cortisol on PAMP-stimulated immune-related genes like *IL6, IL1B*, *CXCL8*, IL12B, and *SAA*, as is well-documented in literature for various fish species, tissues, and cell types *(Fast* et al.*, 2008; Stolte* et al.*, 2008; Saeij* et al.*, 2003a; Gadan* et al.*, 2012; Philip & Vijayan, 2015; Philip* et al.*, 2012; Khansari* et al.*, 2017b).* Despite their initial down-regulation, all cytokines revealed a peak of moderate up-regulation at around 6 to 24 h post treatment. Here, the multifunctional cytokines IL6 and TNF were temporarily

strongly induced, which is in line with previous reports (Castillo *et al.*, 2009; Khansari *et al.*, 2017b) in which Khansari *et al.* (2017b) fittingly stated that stress hormones provoke distinct and species-specific expression patterns of these two cytokines in teleost fish.

A suppressive effect of cortisol was also reported for the heat- or pathogen-stimulated *HSP70* and *HSP90* transcription (Iwama *et al.*, 1999; Basu *et al.*, 2001, 2002; Stolte *et al.*, 2009). However, similar to the HSP expression in head kidney leukocytes of maraena whitefish, Stolte *et al.* (2009) recorded significantly elevated *HSP70* and *HSP90* transcript numbers in response to the co-stimulation of head kidney phagocytes with cortisol and LPS in common carp, whereas the GCR encoding gene was barely affected. Particularly the high abundance of *NR3C1* transcripts in maraena whitefish after the co-stimulation assay is interesting, since it might indicate an increased need of GCR molecules to "increase the sensitivity for cortisol to facilitate its feedback control" as was concluded by Stolte *et al.* (2008) after a similar observation for a GCR encoding gene in common carp. Further, it is highly likely that the recorded up-regulation of *HSP70* and *HSP90* gene expression is related to the very high *NR3C1* transcript levels. Moreover, TP53, that was comparably low but still strongly up-regulated within this stimulation assay, was shown to be essential for the GCR mediated inhibition of its antagonist NF-κB, to negatively regulate the immune response and thus to avert harmful effects and to regain homoeostasis (Petta *et al.*, 2016). All in all, the data suggest that in case of a combined stress- and immune-related stimulation of head kidney leukocytes, the GCR plays a central role in maraena whitefish to balance the partly opposing mechanisms of the stress- and the immune-response.

In conclusion, the three different stimulation assays applied to head kidney leukocytes from maraena whitefish provoked highly different gene expression patterns for both, the immune- and the stress-gene set and therefore this experiment gave insight into the close interdigitation of endocrine and immune functions in maraena whitefish head kidney. Particularly the genes *HSP70*, *TP53*, *IL6* and *SAA* revealed to be highly regulated in response to the different tested stimuli.

The discussed partial deviating from literature results, as well as the contradictory findings documented in literature, might be due to the fact that the head kidney primary culture is a complex composition of leukocytes that exert highly cell type- and moreover species-specific stress- and immune-responses as was already discussed by several authors (Weyts *et al.*, 1999; Stolte *et al.*, 2006; Aluru & Vijayan, 2009; Nardocci *et al.*, 2014). Thus, in future work it would be of high interest to analyse the immune-endocrine regulation of the distinct leukocyte populations present in the head kidney. Nonetheless, within this experiment the primary culture has been a useful tool to study regulatory mechanisms within the head kidney, since primary cell cultures are generally characterised by the high integrity of the original biologial activity compared to cell lines (Goetz *et al.*, 2012).

Moreover, the results provide additional information about the early regulation of the immune genes in response to a pathogenic stimuli, which complements and confirms the data from the *in vivo* stimulation of maraena whitefish with *A. salmonicida.* In this regard, a rapid, moderate to strong increase in the gene expression was recorded for all cytokines, but particularly for IL1B and CXCL8, within the first 24 h post PAMP stimulation, indicating that maraena whitefish similar to other salmonid species (Feng *et al.*, 2009; Brietzke *et al.*, 2015) is able to exert a fast and effective cytokine activation.

4.9. Temperature significantly affected maraena whitefish's early ontogenetic development during which *IGF2* was predominantly expressed

In poikilothermic vertebrates like teleost fish, growth is strongly influenced by different extrinsic factors such as temperature, photoperiod, and food availability (Picha *et al.*, 2008). Thus, growth is controlled by the interaction of a variety of hormones, which integrate the different external and internal stimuli. The GH-IGF axis is key to the interplay of environment and hormones and primarily controls vertebrate growth but is also involved in the regulation of embryonic development (Forbes, 2016; Reinecke *et al.*, 2005; Picha *et al.*, 2008; Gabillard *et al.*, 2003a; Wen *et al.*, 2015; Wood *et al.*, 2005). Therefore, *IGF1* and *IGF2* seemed to be suitable target genes to investigate fish development at initial life stages, which are critical for successful aquaculture. Thus, the expression of the two genes was characterised throughout the development of maraena whitefish from egg to fingerling.

It is known that IGF-2 acts particularly as an embryonic growth factor, whereas IGF-1 plays a more important role during postnatal growth (Pimentel, 1994). Nonetheless, many studies in mammals and even some in fish showed the vital importance of IGF-1 and IGF-2 for pre- and postnatal growth and development (Rotwein *et al.*, 1987; Baker *et al.*, 1993; Powell-Braxton *et al.*, 1993; Greene & Chen, 1997; Agrogiannis *et al.*, 2014; Begemann *et al.*, 2015). Most studies reported that *IGF2* mRNA abundance is higher in embryonic life stages, while *IGF1* expression is higher within postnatal development in mammals and also in teleost fish (Reinecke & Collet, 1998; Duguay *et al.*, 1994; Beck *et al.*, 1987; Daughaday & Rotwein, 1989; Lund *et al.*, 1986). In line with these reports, a much higher expression of *IGF2* than of *IGF1* was measured throughout embryonic and larval development, especially before the eyed-egg stage, and shortly after hatch. This supports the idea of a predominant role of IGF-2 for embryonic development but also underlines its function at life stages post-hatch for maraena whitefish. Similar results have been detected by Greene & Chen (1997), Perrot *et al.* (1999), and Ayson *et al.* (2002) in several other fish species. Even in humans, *IGF2* expression is maintained postnatally, leading to high amounts of serum IGF-2 levels, whereas in mice, the *IGF2* gene is significantly downregulated after birth, although substantial amounts of IGF-2 were also detected in this species (Wolf *et al.*, 1998; Rotwein, 2018).

Further, it might be noteworthy that high numbers of *IGF1* transcripts and even more of *IGF2,* were found to be maternally transferred to the unfertilised egg. As shown for zebrafish, the transfer of maternal factors in the egg is vital for the earliest stages of egg development, when the embryo relies on maternal gene products until the zygotic genome is activated (Pelegri, 2003). In maraena whitefish, 24 h post-fertilisation it already seemed that maternal *IGF* mRNAs were depleted and the synthesis of zygotic factors had begun, since there was a dramatic drop in *IGF1* and *IGF2* transcripts between eggs pre-fertilisation (0) and 1 dpf. Also, Perrot *et al.* (1999) demonstrated that *IGF2* levels dropped to a minimum four to eight hours post-fertilisation of gilthead seabream eggs and recovered again after 12 hpf. However, Zou *et al.* (2009) did not report such a substantial drop in *IGF* transcripts for zebrafish, although they detected maternally deposited transcripts (*IGF1B* and *IGF2A*) that were constantly expressed throughout embryogenesis, whereas *IGF1A* and *IGF2B* transcripts were produced subsequently by the activated zygotic genome. For comparison, Heinecke *et al.* (2014) analysed adaptive and innate immune molecules and found, e.g., first zygotic IgM transcripts (by qPCR) only four days post fertilisation in developing rainbow trout. The vital importance of IGFs for embryonic development of fish seems thus to be reflected by their presence in zygotes as early as 12-24 hpf.

Regarding the influence of temperature on maraena whitefish development, the morphological data ob-

tained in this work, show a clear relation of increasing rearing temperatures to accelerated embryonic growth and shortened hatching periods. This is in accordance with previous reports from many other fish species (Schirone & Gross, 1968; Blaxter, 1992; Rombough, 1997; Gabillard *et al.*, 2003a; Soundarapandian *et al.*, 2014; Thépot & Jerry, 2015; Perrichon *et al.*, 2017). Moreover, we detected a reduction of hatching rate and a length increase of larvae incubated at 9°C. These effects have been explained earlier by a higher metabolic rate at elevated temperatures, which causes a premature depletion of the yolk sac, together with an enhanced production of nitrogenous waste in the form of ammonia (Blaxter, 1992; Perrichon *et al.*, 2017). Taken together, this indicates that 6°C could be a preferable incubation temperature for maraena whitefish in aquaculture, since it resulted in a shortened hatching period together with a high hatching rate and fast larval growth.

Further, the *IGF* gene expression data provide indications for a temperature-dependent modulation of the *IGF1* and *IGF2* expression during maraena whitefish embryonic development, since both genes were up-regulated in the elevated temperature groups 6°C and 9°C compared to the 4°C reference group. In a similar study, Gabillard *et al.* (2003a) also found a temperature effect on *IGF2* gene expression during the development of rainbow trout, but not for *IGF1*. However, at advanced life stages, the positive correlation of increased temperature with growth and IGF-1 plasma levels is already published for several salmonid species (Beckman *et al.*, 1998; Gabillard *et al.*, 2003b; Larsen *et al.*, 2001; McCormick *et al.*, 2000). Nevertheless, to the author's knowledge, a temperature-dependent increase of *IGF1* expression has not been reported for embryonic development of fish so far. The positive effects of an improved incubation temperature seemed to be mirrored in significantly high *IGF1* and *IGF2* expression rates at specific life stages of maraena whitefish even post-hatch, as was observed for the 6°C group within this study.

In conclusion, these results clearly demonstrate a high-level expression of *IGF2* at all tested life stages, tissues, and temperatures, indicating a substantial role of this particular factor for the development of maraena whitefish pre- and post-hatch. Moreover, it was observed a correlation of incubation temperature with accelerated egg development and larval growth after hatch and that elevated incubation temperatures resulted in increased *IGF1* and *IGF2* expression during embryonic development. Even post-hatch *IGF* expression was significantly higher for the best-developing larvae (6°C group) at specific life stages of maraena whitefish.

5. Outlook

In the course of this study the potential of maraena whitefish for local aquaculture was assessed and first guidelines for suitable cultivation conditions of this species were derived. Therefore, this work set a basis and on the same time offers several starting points for future research on this species. In this regard, it would be highly useful to conduct additional sequencing effort to identify gene duplicates for the 14 candidate genes, which are most likely present in maraena whitefish, since this species is thought to have experienced a fish-specific (Taylor *et al.*, 2003; Meyer & Van De Peer, 2005) and additionally a salmonid-specific (Koop & Davidson, 2008) whole genome duplication event. This is of high interest, since the different gene duplicates, that have not been eliminated by natural selection processes often code for distinct, e.g., tissue-specific, functions as observed in several other fish species (Koop & Davidson, 2008).

Further, it would be interesting to check whether the results found for the most promising candidate genes *SAA* and *HSP70* are restricted to the mRNA level or whether the high induction of these genes following aquaculture-specific stressors, like density and temperature stress or pathogenic factors, are also reflected on protein level. In general, fish-specific antibodies are barely provided, however for SAA (Kania *et al.*, 2014), as well as for HSP70 (LeBlanc *et al.*, 2011) salmonid-specific antibodies are available and thus it would be possible to determine the tissue-specific concentration of these proteins in maraena whitefish in response to several stressors by Western blot technique.

For future work, no matter whether mRNA or protein expression measurements, it would be highly valuable to expand the focus on such tissues that are easily accessible during aquaculture practice, like the skin mucus, which seems to be very promising in the search for stress markers (Pérez-Sánchez *et al.*, 2017), since this could pave the way for the development of a marker tool to determine stressful states in fish during cultivation in aquaculture.

Moreover, based on the data obtained in this study, further experiments could be performed with narrowed parameter ranges and/or extended trial periods to determine optimal husbandry conditions regarding egg incubation and cultivation temperature and stocking density.

In addition to this, a selective breeding program must be performed to promote traits of commercial interest, like an efficient growth and pathogen defence and a low stress susceptibility. These selection processes could be simultaneously monitored by gene expression analyses (Lamaze *et al.*, 2013), e.g., based on knowledge obtained within this study for the 14 candidate genes, to verify a targeted breeding of maraena whitefish.

Not least because of the contradictory data found in literature, regarding gene expression patterns in the teleost head kidney, it would be reasonable to deepen the investigations of the immune-endocrine interactions in this organ. Therefore, it would be useful to analyse the candidate gene expression profiles of the distinct cell populations individually after separation by flow-cytometry and additionally to investigate the effect of catecholamines, a second group of hormones produced in the head kidney (chromaffin cells).

6. Summary

The present study provides a first overview of the developmental, physiological, and molecular mechanisms occurring in maraena whitefish in response to culturing procedures and to aquaculture related stressors. Moreover, the data confirm the central hypothesis of this study that maraena whitefish as a native fish species provides a good capability of adaptation to local brackish water conditions, although the lack of breeding selection might cause a high stress susceptibility of this sensitive fish species during cultivation.

As to that, initial cultivation trials clearly showed that if reared in tempered recirculation systems ($\approx$20°C), maraena whitefish is a suitable fish species for the establishment of a local, economic and sustainable aquaculture. However, there is still a lot of research needed to exploit the entire growth potential of this fish in aquaculture. Particularly the early life stages from egg to fry are critical for a successful aquaculture. Accordingly, within this study egg incubation at 6°C was found to be favourable, compared to usually applied 4°C.

For the molecular analyses, a set of 14 genes was selected covering the following three main topics: (i) innate immune response (*IL1B*, *IL6*, *IL8*, *IL12B*, *TNF*, *SAA*, *MAPK1*, *MAPK3*), (ii) stress response (*HSP70*, *HSP90*, *NR3C1*, *TP53*), and (iii) growth and development (*IGF1*, *IGF2*). For all selected genes, partial mRNA sequences were identified and published. Tissue profiling experiments revealed that all genes were constitutively expressed and interestingly, several of the immune- and stress-target genes (*IL1B*, *IL6*, *TNF*, *MAPK1*, *MAPK3*, *NR3C1, TP53* and *HSP70*) showed considerably high transcript levels in the gonads and thus might interfere with reproductive functions in healthy maraena whitefish.

The three different gene sets were individually applied to several experiments to analyse the fish's response to aquaculture-related stressors, such as temperature stress, crowding stress, and pathogens.

Following the density stress experiment, the gene expression profiles showed that an acute but particularly a short-term exposure to HD conditions provoked a secondary stress response, indicating that a stocking density of 100 kg/m^3 is a serious threat to the homeostasis of maraena whitefish. In this regard, it seems that the genes *TNF*, *CEBPB,* and particularly *SAA* play an important role for this fish while coping with crowding stress, as was additionally confirmed by a holistic gene expression analysis.

Regarding the temperature stress experiment, it was shown that the AR treatment led to hallmarks of an acute heat-shock response, whilst the GR treatment induced hallmarks of a tertiary, i.e., chronic stress response, as determined by individual and comprehensive gene expression analyses. Hence, both treatments had adverse effects on maraena whitefish health status and therefore a temperature of 24°C can be regarded as critical for this species. Notably, particularly *HSP70*, but also *HSP90* and *TP53*, as well as the *glucocorticoid receptor signaling pathway* were found to play an important role in response to acute and prolonged temperature stress in maraena whitefish. Moreover, this experiment clearly showed that maraena whitefish is not only very sensible to temperature but to handling stress, too.

The stimulation of maraena whitefish with inactivated *A. salmonicida* induced expression profiles that were characteristic for an inflammatory response. Here, mainly the pro-inflammatory cytokines were strongly induced in the head kidney and in the peritoneal cells, which most likely led to the observed massive influx of granulocytes into the peritoneal cavity and to an APR, indicated by the strong induction of the APP encoding gene, *SAA*. Thus, the pathogenic stimuli induced a strong inflammatory response, which is on the one hand beneficial for the health status of the fish but on the other hand it consumes energy that is needed for an optimal growth.

In the course of this study, a primary cell culture of head kidney leukocytes from mareana whitefish was established, which served as an *in vitro* model to study the mechanisms of the combined immune-

endocrine regulation that is unique for the teleost head kidney. Accordingly, it was found that endocrine- as well as immune-related stimuli and the combination of both similarly led to a considerable regulation of stress- and immune-related genes of head kidney leukocytes. However the genes *HSP70*, *TP53*, *IL6* and *SAA* showed the highest alterations in transcript numbers for all three stimulation assays.

Furthermore, within this work, a high-level expression of *IGF2* at all tested life stages, tissues, and temperatures was recorded, which indicates a substantial role of this particular factor for the development of maraena whitefish pre- and post-hatch. Additionally, it was observed that elevated incubation temperatures resulted in increased *IGF1* and *IGF2* expression during embryonic development and that even post-hatch *IGF* expression was significantly higher for the best-developing larvae (6°C group) at specific life stages of maraena whitefish.

In conclusion, this study demonstrates the general potential of maraena whitefish for local aquaculture. However, it was shown that the stocking density, the temperature, and the water quality (reagarding pathogenic contaminations) must be carefully adjusted within optimal ranges, to avoid adverse effects on this sensitive species that moreover needs to undergo several generations of breeding selection to adapt to the artificial environment. Moreover, the data indicate that particularly *SAA* and *HSP70* are promising candidate genes for the search for molecular markers that could support the development of a highly productive and robust maraena whitefish population for local aquaculture.

References

Abdelkhalek, Nevien K., Komiya, Asuka, Kato-Unoki, Yoko, Somamoto, Tomonori, & Nakao, Miki. 2009. Molecular evidence for the existence of two distinct IL-8 lineages of teleost CXC-chemokines. *Fish and Shellfish Immunology*, **27**, 763–767.

Abram, Quinn H, Dixon, Brian, & Katzenback, Barbara A. 2017. Impacts of Low Temperature on the Teleost Immune System. *Biology*, **6**(4), 39.

Acerete, L., Balasch, J.C., Castellana, B., Redruello, B., Roher, N., Canario, A.V., Planas, J.V., MacKenzie, S., & Tort, L. 2007. Cloning of the glucocorticoid receptor (GR) in gilthead seabream (Sparus aurata): Differential expression of GR and immune genes in gilthead seabream after an immune challenge. *Comparative Biochemistry and Physiology Part B*, **148**, 32–43.

Afonso, António, Ellis, Anthony E., & Silva, Manuel T. 1997. The leucocyte population of the unstimulated peritoneal cavity of rainbow trout (Oncorhynchus mykiss). *Fish and Shellfish Immunology*, **7**, 335–348.

Agrogiannis, Georgios D., Sifakis, Stavros, Patsouris, Efstratios S., & Konstantinidou, Anastasia E. 2014. Insulin-like growth factors in embryonic and fetal growth and skeletal development. *Molecular Medicine Reports*, **10**(2), 579–584.

Akira, Shizuo, Uematsu, Satoshi, & Takeuchi, Osamu. 2006 (feb). *Pathogen recognition and innate immunity*.

Allanach, K., Mengel, M., Einecke, G., Sis, B., Hidalgo, L. G., Mueller, T., & Halloran, P. F. 2008. Comparing microarray versus RT-PCR assessment of renal allograft biopsies: Similar performance despite different dynamic ranges. *American Journal of Transplantation*, **8**, 1006–1015.

Altmann, Simone, Rebl, Alexander, Kühn, Carsten, & Goldammer, Tom. 2014. Identification and de novo sequencing of housekeeping genes appropriate for gene expression analyses in farmed maraena whitefish (Coregonus maraena) during crowding stress. *Fish physiology and biochemistry*, **41**(2), 397–412.

Altmann, Simone, Korytár, Tomáš, Kaczmarzyk, Danuta, Nipkow, Mareen, Kühn, Carsten, Goldammer, Tom, & Rebl, Alexander. 2016. Toll-like receptors in maraena whitefish: Evolutionary relationship among salmonid fishes and patterns of response to Aeromonas salmonicida. *Fish & Shellfish Immunology*, **54**, 391–401.

Aluru, Neelakanteswar, & Vijayan, Mathilakath M. 2009. Stress transcriptomics in fish: A role for genomic cortisol signaling. *General and Comparative Endocrinology*, **164**(nov), 142–150.

Argente, Jesús, Chowen, Julie A, Pérez-Jurado, Luis A, Frystyk, Jan, & Oxvig, Claus. 2017. One level up: abnormal proteolytic regulation of IGF activity plays a role in human pathophysiology. *EMBO Molecular Medicine*, **9**(10), e201707950.

Arndt, Gerd-Michael. 2001. Wiederansiedlung, Bestandserhöhung und Bestandsmanagement der Großen Maräne (Coregonus lavaretus) sowie Bestandseinschätzung und -stabilisierung der Kleinen Maräne (Coregonus albula) in Mecklenburg-Vorpommern. *FISCH UND UMWELT Mecklenburg-Vorpommern e.V.*, 71–80.

Arndt, Gerd-Michael, & Jansen, Wolfgang. 2008. Erste Ergebnisse zur Aufzucht von Ostseeschnäpeln (Coregonus lavaretus) in einer Teichwirtschaft in Mecklenburg-Vorpommern. *FISCH UND UMWELT Mecklenburg-Vorpommern e.V.*, 5–14.

Arndt, Gerd-Michael, & Jansen, Wolfgang. 2010. Aquakultur von Ostseeschnäpeln (Coregonus lavaretus balticus) in der Teichwirtschaft Frauenmark in Mecklenburg - Vorpommern. *Fisch und Umwelt Mecklenburg-Vorpommern e.V.*, 9–18.

Arnold, J E. 2009. Hematology of Fish : WBC and RBC Cell Morphology. *Proceding of the ACVP/ASVCP Concurrent Annual Meetings*, 9–12.

Arterbery, Adam S, Deitcher, David L, & Bass, Andrew H. 2010. Corticosteroid receptor expression in a teleost fish that displays alternative male reproductive tactics. *General and comparative endocrinology*, **165**(1), 83–90.

Austin, Brian, & Austin, Dawn A. 2012. *Bacterial Fish Pathogens: Disease of Farmed and Wild Fish*. Springer Science & Business Media.

Ayson, Felix G, de Jesus, Evelyn Grace T, Moriyama, Shunsuke, Hyodo, Susumu, Funkenstein, Bruria, Gertler, Arieh, & Kawauchi, Hiroshi. 2002. Differential expression of insulin-like growth factor I and II mRNAs during embryogenesis and early larval development in rabbitfish, Siganus guttatus. *General and comparative endocrinology*, **126**(2), 165–74.

Badiola, Maddi, Mendiola, Diego, & Bostock, John. 2012. Recirculating Aquaculture Systems (RAS) analysis: Main issues on management and future challenges. *Aquacultural Engineering*, **51**(nov), 26–35.

Badolato, R, Wang, J M, Stornello, S L, Ponzi, A N, Duse, M, & Musso, T. 2000. Serum amyloid A is an activator of PMN antimicrobial functions: Induction of degranulation, phagocytosis, and enhancement of anti-Candida activity. *Journal of Leukocyte Biology*, **67**(3), 381–386.

Badolato, Raffaele, Wang, Ji Ming, Murphy, William J, Lloyd, Andrew R, Michiel, Dennis F, Bausserman, Linda L, Kelvin, David J, & Oppenheim, Joost J. 1994. Serum amyloid A is a chemoattractant: induction of migration, adhesion, and tissue infiltration of monocytes and polymorphonuclear leukocytes. *The Journal of experimental medicine*, **180**(1), 203–9.

Baker, Julie, Liu, Jeh-Ping, Robertson, Elizabeth J., & Efstratiadis, Argiris. 1993. Role of insulin-like growth factors in embryonic and postnatal growth. *Cell*, **75**(1), 73–82.

Barnes, Peter J., & Adcock, Ian. 1993 (dec). *Anti-inflammatory actions of steroids: molecular mechanisms*.

Barton, B. A. 2002. Stress in Fishes: A Diversity of Responses with Particular Reference to Changes in Circulating Corticosteroids. *Integrative and Comparative Biology*, **42**(3), 517–525.

Basu, N., Nakano, T., Grau, E. G., & Iwama, G. K. 2001. The effects of cortisol on heat shock protein 70 levels in two fish species. *General and Comparative Endocrinology*, **124**, 97–105.

Basu, N., Todgham, A.E., Ackerman, P.A., Bibeau, M.R., Nakano, K., Schulte, P.M., & Iwama, George K. 2002. Heat shock protein genes and their functional significance in fish. *Gene*, **295**(2), 173–183.

Baud, Véronique, & Karin, Michael. 2001. Signal transduction by tumor necrosis factor and its relatives. *Trends in Cell Biology*, **11**(9), 372–377.

Bayne, Christopher J, & Gerwick, Lena. 2001. The acute phase response and innate immunity of fish. *Developmental & Comparative Immunology*, **25**(8-9), 725–743.

Beck, F, Samani, N J, Penschow, J D, Thorley, B, Tregear, G W, & Coghlan, J P. 1987. Histochemical localization of IGF-I and -II mRNA in the developing rat embryo. *Development (Cambridge, England)*, **101**(1), 175–184.

Beckman, Brian R., Larsen, Donald A., Moriyama, Shunsuke, Lee-Pawlak, Beeda, & Dickhoff, Walton W. 1998. Insulin-like growth factor-I and environmental modulation of growth during smoltification of spring chinook salmon (Oncorhynchus tshawystscha). *General and Comparative Endocrinology*, **109**(3), 325–335.

Begemann, Matthias, Zirn, Birgit, Santen, Gijs, Wirthgen, Elisa, Soellner, Lukas, Büttel, Hans-Martin, Schweizer, Roland, van Workum, Wilbert, Binder, Gerhard, & Eggermann, Thomas. 2015. Paternally Inherited IGF2 Mutation and Growth Restriction. *The Newe England Journal of Medicine*, **373**(4), 349–356.

Belyi, Vladimir A, Ak, Prashanth, Markert, Elke, Wang, Haijian, Hu, Wenwei, Puzio-Kuter, Anna, & Levine, Arnold J. 2010. The origins and evolution of the p53 family of genes. *Cold Spring Harbor perspectives in biology*, **2**(jun), a001198.

Besson, M., Vandeputte, M., van Arendonk, J. A.M., Aubin, J., de Boer, I. J.M., Quillet, E., & Komen, H. 2016. Influence of water temperature on the economic value of growth rate in fish farming: The case of sea bass (Dicentrarchus labrax) cage farming in the Mediterranean. *Aquaculture*, **462**, 47–55.

Bielohuby, Maximilian, Zarkesh-Esfahani, Sayyed Hamid, Manolopoulou, Jenny, Wirthgen, Elisa, Walpurgis, Katja, Toghiany Khorasgani, Mohaddeseh, Aghili, Zahra Sadat, Wilkinson, Ian Robert, Hoeflich, Andreas, Thevis, Mario, Ross, Richard J., & Bidlingmaier, Martin. 2014. Validation of serum IGF-I as a biomarker to monitor the bioactivity of exogenous growth hormone agonists and antagonists in rabbits. *Disease Models & Mechanisms*, **7**(11), 1263–1273.

Bienert, Stefan, Waterhouse, Andrew, De Beer, Tjaart A.P., Tauriello, Gerardo, Studer, Gabriel, Bordoli, Lorenza, & Schwede, Torsten. 2017. The SWISS-MODEL Repository-new features and functionality. *Nucleic Acids Research*, **45**(jan), D313–D319.

Bimboim, H.C., Doly, J., Birnboim, H. C., & Doly, J. 1979. A rapid alkaline extraction procedure for screening recombinant plasmid DNA. *Nucleic Acids Research*, **7**(6), 1513–1523.

Binder, Elisabeth B. 2009. *The role of FKBP5, a co-chaperone of the glucocorticoid receptor in the pathogenesis and therapy of affective and anxiety disorders*.

Bird, Steve, & Tafalla, Carolina. 2015. Teleost Chemokines and Their Receptors. *Biology*, **4**(4), 756–784.

Bird, Steve, Zou, Jun, Savan, Ram, Kono, Tomoya, Sakai, Masahiro, Woo, Janet, & Secombes, Chris. 2005. Characterisation and expression analysis of an interleukin 6 homologue in the Japanese pufferfish, Fugu rubripes. *Developmental & Comparative Immunology*, **29**(jan), 775–789.

Blaxter, J. H. S. 1992. The effect of temperature on larval fishes. *Netherlands Journal of Zoology*, **42**(2-3), 336–357.

Blüm, Volker, Casado, Juan, Lehmann, Jens, & Mehring, Eva. 1989. *Farbatlas der Histologie der Regenbogenforelle*. Bochum: Springer Verlag.

Bochert, Ralf. 2014. Neue Ergebnisse zur Aufzucht von Ostseeschnäpeln (Coregonus maraena) (Bloch, 1779) unter Brackwasserbedingungen. *Fisch & Fischmarkt in M-V*, **1**, 18–21.

Bochert, Ralf, Horn, Theresa, & Luft, Peter. 2017. Maraena whitefish (Coregonus maraena) larvae reveal enhanced growth during first feeding with live Artemia nauplii. *Archives of Polish Fisheries*, **25**(1), 3–10.

Boltaña, Sebastián, Sanhueza, Nataly, Aguilar, Andrea, Gallardo-Escarate, Cristian, Arriagada, Gabriel, Valdes, Juan Antonio, Soto, Doris, & Quiñones, Renato A. 2017. Influences of thermal environment on fish growth. *Ecology and evolution*, **7**(sep), 6814–6825.

Borchel, Andreas. 2015. *Charakterisierung von Transkriptom und Phänotyp different robuster Zuchtlinien der Regenbogenforelle mit Fokus auf das Kreatin-System der Fische Inhaltsverzeichnis*. Ph.D. thesis, University of Rostock.

Bornman, L, Polla, B S, & Gericke, G S. 1996. Heat-shock protein 90 and ubiquitin: developmental regulation during myogenesis. *Muscle & nerve*, **19**(may), 574–80.

Bornstein, S. R., Rutkowski, H, & Vrezas, I. 2004. Cytokines and steroidogenesis. *Molecular and Cellular Endocrinology*, **215**(feb), 135–141.

Brenner, Dirk, Blaser, Heiko, & Mak, Tak W. 2015. Regulation of tumour necrosis factor signalling: live or let die. *Nature Reviews Immunology*, **15**(jun), 362–374.

Brietzke, Andreas, Korytár, Thomáš, Jaros, Joanna, Köllner, Bernd, Goldammer, Tom, Seyfert, Hans Martin, & Rebl, Alexander. 2015. Aeromonas salmonicida Infection Only Moderately Regulates Expression of Factors Contributing to Toll-Like Receptor Signaling but Massively Activates the Cellular and Humoral Branches of Innate Immunity in Rainbow Trout (Oncorhynchus mykiss). *Journal of Immunology Research*, **2015**, 901015.

Brietzke, Andreas, Borchel, Andreas, Altmann, Simone, Nipkow, Mareen, Rebl, Alexander, Brunner, Ronald M., & Goldammer, Tom. 2016. Transcriptome sequencing of maraena whitefish (Coregonus maraena). *Marine Genomics*, **29**(oct), 27–29.

Brocchieri, Luciano, Conway De Macario, Everly, & Macario, Alberto J L. 2008. Hsp70 genes in the human genome: Conservation and differentiation patterns predict a wide array of overlapping and specialized functions. *BMC Evolutionary Biology*, **8**(1), 19.

Brown, Christopher L, Vera Cruz, Emmanuel M, Bolivar, Remedios B, & Borski, Russell J. 2012. Production, Growth, and Insulin-Like Growth Factor-I (IGF-I) Gene Expression as an Instantaneous Growth Indicator in Nile Tilapia Oreochromis Niloticus. *Chap. 3, pages 79–89 of:* Saroglia, Marco, & Liu, Zhanjiang (eds), *Functional Genomics in Aquaculture*. Oxford, UK: Wiley-Blackwell.

Brush, Matthew H, Weiser, Douglas C, & Shenolikar, Shirish. 2003. Growth arrest and DNA damage-inducible protein GADD34 targets protein phosphatase 1 alpha to the endoplasmic reticulum and promotes dephosphorylation of the alpha subunit of eukaryotic translation initiation factor 2. *Molecular and cellular biology*, **23**(4), 1292–303.

Bucking, Carol, Wood, Chris M, & Moon, T W. 2005. Renal regulation of plasma glucose in the freshwater rainbow trout. *The Journal of experimental biology*, **208**(jul), 2731–9.

Buckley, Bradley A., & Somero, George N. 2009. cDNA microarray analysis reveals the capacity of the cold-adapted Antarctic fish Trematomus bernacchii to alter gene expression in response to heat stress. *Polar Biology*, **32**(mar), 403–415.

Bukau, Bernd, & Horwich, Arthur L. 1998. The Hsp70 and Hsp60 chaperone machines. *Cell*, **92**(3), 351–366.

Burgess-Beusse, B L, & Darlington, G J. 1998. C/EBPalpha is critical for the neonatal acute-phase response to inflammation. *Molecular and cellular biology*, **18**(12), 7269–77.

Bury, N R, Sturm, A, Le Rouzic, P, Lethimonier, C, Ducouret, B, Guiguen, Y, Robinson-Rechavi, M, Laudet, V, Rafestin-Oblin, M E, & Prunet, P. 2003. Evidence for two distinct functional glucocorticoid receptors in teleost fish. *Journal of Molecular Endocrinology*, **31**(1), 141–156.

Buscà, Roser, Christen, Richard, Lovern, Matthew, Clifford, Alexander M, Yue, Jia Xing, Goss, Greg G, Pouysségur, Jacques, & Lenormand, Philippe. 2015. ERK1 and ERK2 present functional redundancy in tetrapods despite higher evolution rate of ERK1. *BMC Evolutionary Biology*, **15**(1), 179.

Cachot, Jérôme, Galgani, François, & Vincent, Françoise. 1998. cDNA cloning and expression analysis of flounder p53 tumour suppressor gene. *Comparative Biochemistry and Physiology Part B*, **121**(nov), 235–242.

Cai, Zhonghua, Gao, Chunping, Zhang, Yong, & Xing, Kezhi. 2009. Functional characterization of the ELR motif in piscine ELR +CXC-like chemokine. *Marine Biotechnology*, **11**(jul), 505–512.

Caipang, Christopher Marlowe A. 2012. Potential molecular biomarkers of crowding stress in Atlantic cod, Gadus morhua and their importance in health management. *Animal Biology & Animal Husbandry International Journal of the Bioflux Society*, **4**(2), 79–83.

Caipang, Christopher Marlowe A., Brinchmann, Monica F., & Kiron, Viswanath. 2008. Short-term overcrowding of Atlantic cod, Gadus morhua: Effects on serum-mediated antibacterial activity and transcription of glucose transport and antioxidant defense related genes. *Comparative Biochemistry and Physiology Part A*, **151**(dec), 560–565.

Caipang, Christopher Marlowe A., Berg, Ingvild, Brinchmann, Monica F., & Kiron, Viswanath. 2009. Short-term crowding stress in Atlantic cod, Gadus morhua L. modulates the humoral immune response. *Aquaculture*, **295**(oct), 110–115.

Cairns, M.T., Johnson, M.C., Talbot, A.T., Pemmasani, J.K., McNeill, R.E., Houeix, B., Sangrador-Vegas, A., & Pottinger, T.G. 2008. A cDNA microarray assessment of gene expression in the liver of rainbow trout (Oncorhynchus mykiss) in response to a handling and confinement stressor. *Comparative Biochemistry and Physiology Part D*, **3**(mar), 51–66.

Calabrese, Viviane, Mallette, Frédérick A., Deschênes-Simard, Xavier, Ramanathan, Sheela, Gagnon, Julien, Moores, Adrian, Ilangumaran, Subburaj, & Ferbeyre, Gerardo. 2009. SOCS1 Links Cytokine Signaling to p53 and Senescence. *Molecular Cell*, **36**, 754–767.

Carlson, R.E., Anderson, D.P., & Bodammer, J.E. 1993. In vivo cortisol administration suppresses the in vitro primary immune response of winter flounder lymphocytes. *Fish & Shellfish Immunology*, **3**(jul), 299–312.

Cassis, L, Laughter, A, Fettinger, M, Akers, S, Speth, R, Burke, G, King, V, & Dwoskin, L. 1998. Cold exposure regulates the renin-angiotensin system. *J Pharmacol Exp Ther*, **286**(2), 718–726.

Castellana, Barbara, Iliev, Dimitar B., Sepulcre, M. Pilar, MacKenzie, Simon, Goetz, Frederick W., Mulero, Victoriano, & Planas, Josep V. 2008. Molecular characterization of interleukin-6 in the gilthead seabream (Sparus aurata). *Molecular Immunology*, **45**(jul), 3363–3370.

Castillo, Juan, Teles, Mariana, Mackenzie, Simon, & Tort, Lluis. 2009. Stress-related hormones modulate cytokine expression in the head kidney of gilthead seabream (Sparus aurata). *Fish & Shellfish Immunology*, **27**(sep), 493–499.

Castro, Rosario, Zou, Jun, Secombes, Christopher J., & Martin, Samuel A M. 2011. Cortisol modulates the induction of inflammatory gene expression in a rainbow trout macrophage cell line. *Fish and Shellfish Immunology*, **30**(1), 215–223.

Celi, Monica, Vazzana, Mirella, Sanfratello, Maria Antonietta, & Parrinello, Nicolò. 2012. Elevated cortisol modulates hsp70 and hsp90 gene expression and protein in sea bass head kidney and isolated leukocytes. *General and Comparative Endocrinology*, **175**, 424–431.

Chadzinska, Magdalena, Leon-Kloosterziel, Karen M., Plytycz, Barbara, & Lidy Verburg-van Kemenade, B.M. 2008. In vivo kinetics of cytokine expression during peritonitis in carp: Evidence for innate and alternative macrophage polarization. *Developmental & Comparative Immunology*, **32**(jan), 509–518.

Chen, Liqiao, He, Chongbo, Baoprasertkul, Puttharat, Xu, Peng, Li, Ping, Serapion, Jerry, Waldbieser, Geoff, Wolters, William, & Liu, Zhanjiang. 2005. Analysis of a catfish gene resembling interleukin-8: cDNA cloning, gene structure, and expression after infection with Edwardsiella ictaluri. *Developmental & Comparative Immunology*, **29**(jan), 135–142.

Chomczynski, P, & Sacchi, N. 1987. Single-step method of RNA isolation by acid guanidinium thiocyanate-. *Anal Biochem*, **162**(1), 156–159.

Chupani, Latifeh, Zusková, Eliška, Niksirat, Hamid, Panáček, Aleš, Lünsmann, Vanessa, Haange, Sven-Bastiaan, von Bergen, Martin, & Jehmlich, Nico. 2017. Effects of chronic dietary exposure of zinc oxide nanoparticles on the serum protein profile of juvenile common carp (Cyprinus carpio L.). *Science of The Total Environment*, **579**(feb), 1504–1511.

Ciechanover, Aaron. 1998. The ubiquitin-proteasome pathway: on protein death and cell life. *The EMBO Journal*, **17**(24), 7151– 7160.

Clemmons, David R. 2007. Value of Insulin-like Growth Factor System Markers in the Assessment of Growth Hormone Status. *Endocrinology and Metabolism Clinics of North America*, **36**(1), 109–129.

Cole, Joby, Aberdein, Jody, Jubrail, Jamil, & Dockrell, David H. 2014. *The Role of Macrophages in the Innate Immune Response to Streptococcus pneumoniae and Staphylococcus aureus. Mechanisms and Contrasts*. 1 edn. Vol. 65. Elsevier Ltd.

Combet, C, Blanchet, C, Geourjon, C, & Deléage, G. 2000 (mar). *NPS@: Network protein sequence analysis*.

Cornish-Bowden, A. 1985. Nomenclature for incompletely specified bases in nucleic acid sequences: recommendations 1984. *Nucleic acids research*, **13**(9), 3021–30.

Cray, Carolyn, Zaias, Julia, & Altman, Norman H. 2009. Acute phase response in animals: a review. *Comparative medicine*, **59**(6), 517–26.

Crippen, Tawni L., Bootland, Linda M., Leong, Jo Ann C., Fitzpatrick, Martin S., Schreck, Carl B., & Vella, Anthony T. 2001. Analysis of salmonid leukocytes purified by hypotonic lysis of erythrocytes. *Journal of Aquatic Animal Health*, **13**(3), 234–245.

Crowhurst, Meredith O, Layton, Judith E, & Lieschke, Graham J. 2002. Developmental biology of zebrafish myeloid cells. *The International journal of developmental biology*, **46**(4), 483–92.

Cruz, Shelly Abad, Lin, Chia-Hao, Chao, Pei-Lin, & Hwang, Pung-Pung. 2013. Glucocorticoid Receptor, but Not Mineralocorticoid Receptor, Mediates Cortisol Regulation of Epidermal Ionocyte Development and Ion Transport in Zebrafish (Danio Rerio). *PLoS ONE*, **8**(10), e77997.

Daly, J.G., Kew, A.K., Moore, A.R., & Olivier, G. 1996. The cell surface of Aeromonas salmonicida determines in vitro survival in cultivated brook trout (Salvelinus fontinalis) peritoneal macrophages. *Microbial Pathogenesis*, **21**, 447–461.

Dang, Wei, hua Hu, Yong, Zhang, Min, & Sun, Li. 2010. Identification and molecular analysis of a stress-inducible Hsp70 from Sciaenops ocellatus. *Fish and Shellfish Immunology*, **29**, 600–607.

Daughaday, W H, & Rotwein, P. 1989. Insulin-like growth factors I and II. Peptide, messenger ribonucleic acid and gene structures, serum, and tissue concentrations. *Endocrine reviews*, **10**(1), 68–91.

d'Avila Paskulin, Diego, Rodrigues Paixão-Côrtes, Vanessa, Hainaut, Pierre, Cátira Bortolini, Maria, & Ashton-Prolla, Patricia. 2012. The TP53 fertility network. *Genetics and Molecular Biology*, **35**(4), 939–946.

De Buck, Mieke, Gouwy, Mieke, Wang, Ji Ming, Snick, Jacques Van, Opdenakker, Ghislain, Struyf, Sofie, & Van Damme, Jo. 2016. Structure and expression of different serum amyloid A (SAA) variants and their concentration-dependent functions during host insults. *Current Medicinal Chemistry*, **23**(17), 1725–55.

de Castro, Edouard, Sigrist, Christian J. A., Gattiker, Alexandre, Bulliard, Virginie, Langendijk-Genevaux, Petra S., Gasteiger, Elisabeth, Bairoch, Amos, & Hulo, Nicolas. 2006. ScanProsite: Detection of PROSITE signature matches and ProRule-associated functional and structural residues in proteins. *Nucleic Acids Research*, **34**(jul).

de Pablo, F, Scott, Laurie A, Roth, Jesse, Pablo, FDE Flora D E, Scott, Laurie A, & Roth, Jesse. 1990. Insulin and insulin-like growth factor I in early development: peptides, receptors and biological events. *Endocrine reviews*, **11**(4), 558–77.

de Pomerai, DI. 1996. Review : Heat-shock proteins as biomarkers of pollution. *Human & Experimental Toxicology*, **15**(apr), 279–285.

Deane, Eddie E, Kelly, Scott P, Luk, James C Y, & Woo, Norman Y S. 2002. Chronic salinity adaptation modulates hepatic heat shock protein and insulin-like growth factor I expression in black sea bream. *Marine biotechnology (New York, N.Y.)*, **4**(2), 193–205.

Demers, Nora E., & Bayne, Christopher J. 1997. The immediate effects of stress on hormones and plasma lysozyme in rainbow trout. *Developmental & Comparative Immunology*, **21**(4), 363–373.

Dhabhar, Firdaus S. 2014. Effects of stress on immune function: the good, the bad, and the beautiful. *Immunologic Research*, **58**(may), 193–210.

Dhabhar, Firdaus S., & McEwen, Bruce S. 1997. Acute Stress Enhances while Chronic Stress Suppresses Cell-Mediated Immunityin Vivo:A Potential Role for Leukocyte Trafficking. *Brain, Behavior, and Immunity*, **11**(dec), 286–306.

Dietrich, Mariola A., Hliwa, Piotr, Adamek, Mikołaj, Steinhagen, Dieter, Karol, Halina, & Ciereszko, Andrzej. 2018. Acclimation to cold and warm temperatures is associated with differential expression of male carp blood proteins involved in acute phase and stress responses, and lipid metabolism. *Fish and Shellfish Immunology*, **76**, 305–315.

Dittmar, Janine, Janssen, Hannah, Kuske, Andra, Kurtz, Joachim, & Scharsack, Jörn P. 2014. Heat and immunity: An experimental heat wave alters immune functions in three-spined sticklebacks (Gasterosteus aculeatus). *Journal of Animal Ecology*, **83**, 744–757.

Do Vale, Ana, Afonso, António, & Silva, Manuel T. 2002. The professional phagocytes of sea bass (DicDo Vale, A., Afonso, A., & Silva, M. T. (2002). The professional phagocytes of sea bass (Dicentrarchus labrax L.): cytochemical characterisation of neutrophils and macrophages in the normal and inflamed peritone. *Fish & Shellfish Immunology*, **13**, 183–198.

Domingos, Fabricio F.T., Thomé, Ralph G., Martinelli, Patrícia M., Sato, Yoshimi, Bazzoli, Nilo, & Rizzo, Elizete. 2013. Role of HSP70 in the regulation of the testicular apoptosis in a seasonal breeding teleost Prochilodus argenteus from the São Francisco river, Brazil. *Microscopy Research and Technique*, **76**(apr), 350–356.

D'Orbcastel, Emmanuelle Roque, Blancheton, Jean-Paul, & Aubin, Joël. 2009. Towards environmentally sustainable aquaculture: Comparison between two trout farming systems using Life Cycle Assessment. *Aquacultural Engineering*, **40**(may), 113–119.

Dostal, David E., Booz, George W., & Baker, Kenneth M. 2000. Regulation of angiotensinogen gene expression and protein in neonatal rat cardiac fibroblasts by glucocorticoid and β-adrenergic stimulation. *Basic Research in Cardiology*, **95**(dec), 485–491.

Duan, Cunming. 1997. The Insulin-like Growth Factor System and Its Biological Actions in Fish. *Integrative and Comparative Biology*, **37**(6), 491–503.

Duan, Cunming. 1998. Nutritional and Developmental Regulation of Insulin-like Growth Factors in Fish. *The Journal of Nutrition*, **128**(2), 306–314.

Ducouret, B., Tujague, M., Ashraf, J, Mouchel, N, Servel, N, Valotaire, Y, & Thompson, E B. 1995. Cloning of a teleost fish glucocorticoid receptor shows that it contains a deoxyribonucleic acid-binding domain different from that of mammals. *Endocrinology*, **136**(9), 3774–3783.

Duguay, S J, Swanson, P, & Dickhoff, W W. 1994. Differential expression and hormonal regulation of alternatively spliced IGF-I mRNA transcripts in salmon. *Journal of Molecular Endocrinology*, **12**(1), 25–37.

Dyer, Anthony R., Upton, Zee, Stone, David, Thomas, Philip M., Soole, Kathleen L., Higgs, Naomi, Quinn, Kirsty, & Carragher, John F. 2004. Development and validation of a radioimmunoassay for fish insulin-like growth factor I (IGF-I) and the effect of aquaculture related stressors on circulating IGF-I levels. *General and Comparative Endocrinology*, **135**, 268–275.

Edwards, Kate M., Burns, Victoria E., Carroll, Douglas, Drayson, Mark, & Ring, Christopher. 2007. The acute stress-induced immunoenhancement hypothesis. *Exercise and Sport Sciences Reviews*, **35**(3), 150–155.

Eid, Ihlam Ibrahim, Bhassu, Subha, Goh, Zee Hong, Khoo, Li Teng, & Tan, Geok Yuan Annie. 2016. Molecular characterization and gene evolution of the heat shock protein 70 gene in snakehead fish with different tolerances to temperature. *Biochemical Systematics and Ecology*, **66**(jun), 137–144.

Elibol-Flemming, Banu, Waldbieser, Geoffrey C., Wolters, William R., Boyle, Carolyn R., & Hanson, Larry A. 2009. Expression analysis of selected immune-relevant genes in channel catfish during Edwardsiella ictaluri infection. *Journal of Aquatic Animal Health*, **21**(1), 23–35.

Ellis, A. E. 1977. The leucocytes of fish: A review. *Journal of Fish Biology*, **11**(nov), 453–491.

Ellis, T., North, B., Scott, A. P., Bromage, N. R., Porter, M., & Gadd, D. 2002. The relationships between stocking density and welfare in farmed rainbow trout. *Journal of Fish Biology*, **61**(3), 493–531.

Engelsma, Marc Y., Stet, René J.M., Saeij, Jeroen P., & Verburg-van Kemenade, B.M. Lidy. 2003. Differential expression and haplotypic variation of two interleukin-1β genes in the common carp (Cyprinus carpio L.). *Cytokine*, **22**(apr), 21–32.

Engelsma, M.Y., Stet, R.J.M., Schipper, H., & Verburg-van Kemenade, B.M.L. 2001. Regulation of interleukin 1 beta RNA expression in the common carp, Cyprinus carpio L. *Developmental & Comparative Immunology*, **25**(apr), 195–203.

Ericsson, Lowell H., Eriksen, Nils, Walsh, Kenneth A., & Benditt, Earl P. 1987. Primary structure of duck amyloid protein A The form deposited in tissues may be identical to its serum precursor. *FEBS Letters*, **218**(1), 11–16.

Espelid, Sigrun, Løkken, Gunn Berit, Steiro, Kari, & Bøgwald, Jarl. 1996. Effects of cortisol and stress on the immune system in Atlantic salmon (Salmo salar L.). *Fish and Shellfish Immunology*, **6**(2), 95–110.

Ewart, Vanaya K., Belanger, Jasmine C., Williams, Jason, Karakach, Tobias, Penny, Susanne, Tsoi, Stephen C.M., Richards, Robert C., & Douglas, Susan E. 2005. Identification of genes differentially expressed in Atlantic salmon (Salmo salar) in response to infection by Aeromonas salmonicida using cDNA microarray technology. *Developmental & Comparative Immunology*, **29**(jan), 333–347.

Fan, Heng-Yu, Liu, Zhilin, Shimada, Masayuki, Sterneck, Esta, Johnson, Peter F, Hedrick, Stephen M, & Richards, Joanne S. 2009. MAPK3/1 (ERK1/2) in ovarian granulosa cells are essential for female fertility. *Science*, **324**(may), 938–41.

Fänge, R, & Nilsson, S. 1985. The fish spleen: structure and function. *Experientia*, **41**(2), 152–158.

Fast, Mark D., Hosoya, Sho, Johnson, Stewart C., & Afonso, Luis O.B. 2008. Cortisol response and immune-related effects of Atlantic salmon (Salmo salar Linnaeus) subjected to short- and long-term stress. *Fish & Shellfish Immunology*, **24**(feb), 194–204.

Fehr, D., Casanova, Carlo, Liverman, Amy, Blazkova, Hana, Orth, Kim, Dobbelaere, Dirk, Frey, Joachim, & Burr, Sarah E. 2006. AopP, a type III effector protein of Aeromonas salmonicida, inhibits the NF- B signalling pathway. *Microbiology*, **152**(9), 2809–2818.

Feidantsis, Konstantinos, Pörtner, Hans O., Lazou, Antigoni, Kostoglou, Basile, & Michaelidis, Basile. 2009. Metabolic and molecular stress responses of the gilthead seabream Sparus aurata during long-term exposure to increasing temperatures. *Marine Biology*, **156**(mar), 797–809.

Felsenstein, Joseph. 1985. Confidence limits on phylogenies: An approach using the bootstrap. *Evolution*, **39**(4), 783–791.

Feng, C Y, Johnson, S C, Hori, T S, Rise, M, Hall, J R, Gamperl, A K, Hubert, S, Kimball, J, Bowman, S, & Rise, M L. 2009. Identification and analysis of differentially expressed genes in immune tissues of Atlantic cod stimulated with formalin-killed, atypical Aeromonas salmonicida. *Physiol Genomics*, **37**, 149–163.

Ferat-Osorio, Eduardo, Sánchez-Anaya, Aldair, Gutiérrez-Mendoza, Mireille, Boscó-Gárate, Ilka, Wong-Baeza, Isabel, Pastelin-Palacios, Rodolfo, Pedraza-Alva, Gustavo, Bonifaz, Laura C, Cortés-Reynosa, Pedro, Pérez-Salazar, Eduardo, Arriaga-Pizano, Lourdes, López-Macías, Constantino, Rosenstein, Yvonne, & Isibasi, Armando. 2014. Heat shock protein 70 down-regulates the production of toll-like receptor-induced pro-inflammatory cytokines by a heat shock factor-1/constitutive heat shock element-binding factor-dependent mechanism. *Journal of Inflammation*, **11**(19), 1–12.

Ferguson, Yvonne, Bricknell, Ian R, Glover, L.Anne, MacGregor, Doreen M, & Prosser, Jim I. 1998. Colonisation and transmission of lux-marked and wild-type Aeromonas salmonicida strains in Atlantic salmon (Salmo salar L.). *FEMS Microbiology Ecology*, **27**(3), 251–260.

Feshalami, Mohammad Yooneszadeh, Amiri, Farokh, Nikpey, Mansour, Mortazavizadeh, Seyed Abdolsaheb, Gisbert, Enric, & Mozanzadeh, Mansour Torfi. 2017. Influence of Stocking Density on Growth and Physiological Responses of Beluga, Huso huso (Brandt, 1869), and Ship Sturgeon, Acipenser nudiventis (Lovetsky, 1828), Juveniles in a Flow-through System. *Journal of the World Aquaculture Society*, **48**(4), 611–622.

Fevolden, S.-E., Roed, K. H., Fjalestad, K. T., & Stien, J. 1999. Poststress levels of lysozyme and cortisol in adult rainbow trout: heritabilities and genetic correlations. *Journal of Fish Biology*, **54**(apr), 900–910.

Fevolden, S.E., Røed, K.H., & Gjerde, B. 1994. Genetic components of post-stress cortisol and lysozyme activity in Atlantic salmon; correlations to disease resistance. *Fish & Shellfish Immunology*, **4**, 507–519.

Fevolden, Svein-Erik, Røed, Knut H., & Fjalestad, Kjersti T. 2002. Selection response of cortisol and lysozyme in rainbow trout and correlation to growth. *Aquaculture*, **205**(feb), 61–75.

Forbes, Briony E. 2016. Two years in IGF research. *Growth Hormone & IGF Research*, **30-31**(oct), 70–74.

Franz, Anne-Constance, Faass, Oliver, Köllner, Bernd, Shved, Natallia, Link, Karl, Casanova, Ayako, Wenger, Michael, D'Cotta, Helena, Baroiller, Jean-François, Ullrich, Oliver, Reinecke, Manfred, & Eppler, Elisabeth. 2016. Endocrine and Local IGF-I in the Bony Fish Immune System. *Biology*, **5**(1), 9.

Fujiki, Kazuhiro, Shin, Dong-Ho, Nakao, Miki, & Yano, Tomoki. 2000. Molecular cloning and expression analysis of carp (Cyprinus carpio) interleukin-1β, high affinity immunoglobulin E Fc receptor γ subunit and serum amyloid A. *Fish & Shellfish Immunology*, **10**(apr), 229–242.

Gabillard, Jean-Charles, Rescan, Pierre-Yves, Fauconneau, Benoit, Weil, Claudine, & Le Bail, Pierre-Yves. 2003a. Effect of temperature on gene expression of the Gh/Igf system during embryonic development in rainbow trout (Oncorhynchus mykiss). *Journal of experimental zoology. Part A, Comparative experimental biology*, **298**(2), 134–42.

Gabillard, Jean-Charles, Weil, Claudine, Rescan, Pierre-Yves, Navarro, Isabel, Gutiérrez, Joaquim, & Le Bail, Pierre-Yves. 2003b. Effects of environmental temperature on IGF1, IGF2, and IGF type I receptor expression in rainbow trout (Oncorhynchus mykiss). *General and Comparative Endocrinology*, **133**(2), 233–242.

Gadan, K., Marjara, I. Singh, Sundh, H., Sundell, K., & Evensen, O. 2012. Slow release cortisol implants result in impaired innate immune responses and higher infection prevalence following experimental challenge with infectious pancreatic necrosis virus in Atlantic salmon (Salmo salar) parr. *Fish and Shellfish Immunology*, **32**(5), 637–644.

Gadberry, Michael D, Malcomber, Simon T, Doust, Andrew N, & Kellogg, Elizabeth a. 2005. Primaclade–a flexible tool to find conserved PCR primers across multiple species. *Bioinformatics (Oxford, England)*, **21**(7), 1263–4.

Galigniana, Natalia M., Ballmer, Luzia T., Toneatto, Judith, Erlejman, Alejandra G., Lagadari, Mariana, & Galigniana, Mario D. 2012. Regulation of the glucocorticoid response to stress-related disorders by the Hsp90-binding immunophilin FKBP51. *Journal of Neurochemistry*, **122**, 4–18.

Garcia de la serrana, Daniel, & Johnston, Ian A. 2013. Expression of Heat Shock Protein (Hsp90) Paralogues Is Regulated by Amino Acids in Skeletal Muscle of Atlantic Salmon. *PLoS ONE*, **8**(9), e74295.

Garcia-Rodriguez, Sonia, Callejas-Rubio, Jose-Luis, Ortego-Centeno, Norberto, Zumaquero, Esther, Ríos-Fernandez, Raquel, Arias-Santiago, Salvador, Navarro, Pilar, Sancho, Jaime, & Zubiaur, Mercedes. 2012. Altered AKT1 and MAPK1 Gene Expression on Peripheral Blood Mononuclear Cells and Correlation with T-Helper-Transcription Factors in Systemic Lupus Erythematosus Patients. *Mediators of Inflammation*, **2012**, 1–14.

Gaston, J S H. 2002. Heat shock proteins and innate immunity. *Clinical and Experimental Immunology*, **127**, 1–3.

Gervois, Philippe, Kleemann, Robert, Pilon, Antoine, Percevault, Frédéric, Koenig, Wolfgang, Staels, Bart, & Kooistra, Teake. 2004. Global suppression of IL-6-induced acute phase response gene expression after chronic in vivo treatment

with the peroxisome proliferator-activated receptor-alpha activator fenofibrate. *The Journal of Biological Chemistry*, **279**(16), 16154–60.

Gesto, Manuel, Soengas, José L., & Míguez, Jesús M. 2008. Acute and prolonged stress responses of brain monoaminergic activity and plasma cortisol levels in rainbow trout are modified by PAHs (naphthalene, β-naphthoflavone and benzo(a)pyrene) treatment. *Aquatic Toxicology*, **86**(feb), 341–351.

Geven, Edwin J.W., & Klaren, Peter H.M. 2017. The teleost head kidney: Integrating thyroid and immune signalling. *Developmental and Comparative Immunology*, **66**(jan), 73–83.

Gil Barcellos, Leonardo José, Kreutz, Luiz Carlos, De Souza, Cleverson, Rodrigues, Laura Beatriz, Fioreze, Irineo, Quevedo, Rosmari Mezzalira, Cericato, Leonardo, Soso, Auren Benck, Fagundes, Michele, Conrad, Jaqueline, Lacerda, Luciana de Almeida, & Terra, Silvia. 2004. Hematological changes in jundiá (Rhamdia quelen Quoy and Gaimard Pimelodidae) after acute and chronic stress caused by usual aquacultural management, with emphasis on immunosuppressive effects. *Aquaculture*, **237**(aug), 229–236.

Glenney, Gavin W, & Wiens, Gregory D. 2007. Early diversification of the TNF superfamily in teleosts: genomic characterization and expression analysis. *Journal of immunology*, **178**(12), 7955–7973.

Goebel, SusanneE., Baer, Jan, & Geist, Juergen. 2017. Effects of temperature and rearing density on growth of juvenile European whitefish (Coregonus macrophthalmus) in aquaculture. *Fundamental and Applied Limnology*, **189**(3), 257–266.

Goetz, Frederick W., Planas, Josep V., Díaz, Mònica, Iliev, Dimitar B., & MacKenzie, Simon. 2012. Culture of Fish Head Kidney Mononuclear Phagocytes and Muscle Satellite Cells: Valuable Models for Aquaculture Biotechnology Research. *Chap. Goetz2012, pages 207–221 of:* Fletcher, Garth L., & Rise, Matthew L. (eds), *Aquaculture Biotechnology*, 1 edn. Wiley-Blackwell.

Gonzaga, J., Anderson, A., Richardson, N., Nocillado, J., & Elizur, A. 2010. Cloning of IGF-I, IGF-II and IGF-IR cDNAs in Mullet (Mugil cephalus) and Grouper (Epinephelus coioides): Molecular Markers for Egg Quality in Marine Fish. *Asian Journal of Biological Sciences*, **3**, 55–67.

Goral, J., & Kovacs, E. J. 2005. In Vivo Ethanol Exposure Down-Regulates TLR2-, TLR4-, and TLR9-Mediated Macrophage Inflammatory Response by Limiting p38 and ERK1/2 Activation. *The Journal of Immunology*, **174**(1), 456–463.

Greene, M W, & Chen, T T. 1997. Temporal expression pattern of insulin-like growth factor mRNA during embryonic development in a teleost, rainbow trout (Onchorynchus mykiss). *Molecular marine biology and biotechnology*, **6**(2), 144–51.

Greene, Michael W., & Chen, Thomas T. 1999. Quantitation of IGF-I, IGF-II, and multiple insulin receptor family member messenger RNAs during embryonic development in rainbow trout. *Molecular Reproduction and Development*, **54**(4), 348–361.

Greenwood, Anna K., Butler, Paul C., White, Richard B., DeMarco, Ulrike, Pearce, David, & Fernald, Russell D. 2003. Multiple Corticosteroid Receptors in a Teleost Fish: Distinct Sequences, Expression Patterns, and Transcriptional Activities. *Endocrinology*, **144**(10), 4226–4236.

Grover, Saini, Rohit, Bhardwaj, Pearl, & Bhardwaj, Amit. 2016. Acute-phase reactants. *Journal of Oral Research and Review*, **8**(1), 32.

Gruys, E, Toussaint, M J M, Niewold, T A, & Koopmans, S J. 2005. Acute phase reaction and acute phase proteins. *Journal of Zhejiang University. Science. B*, **6B**(11), 1045–56.

Gudkov, Andrei V, Gurova, Katerina V, & Komarova, Elena A. 2011. Inflammation and p53: A Tale of Two Stresses. *Genes & cancer*, **2**(4), 503–16.

Guex, Nicolas, Peitsch, Manuel C., & Schwede, Torsten. 2009. Automated comparative protein structure modeling with SWISS-MODEL and Swiss-PdbViewer: A historical perspective. *Electrophoresis*, **30**(jun), 162–173.

Guidotti, Gianluigi, Calabrese, Francesca, Anacker, Christoph, Racagni, Giorgio, Pariante, Carmine M, & Riva, Marco A. 2013. Glucocorticoid receptor and FKBP5 expression is altered following exposure to chronic stress: modulation by antidepressant treatment. *Neuropsychopharmacology : official publication of the American College of Neuropsychopharmacology*, **38**(mar), 616–27.

Guo, Huizhi, Fu, Xiaozhe, Lin, Qiang, Liu, Lihui, Liang, Hongru, Huang, Zhibin, Li, Ningqiu, & Su, Jianguo. 2017. Mandarin fish p53: Genomic structure, alternatively spliced variant and its mRNA expression after virus challenge. *Fish and Shellfish Immunology*, **70**, 536–544.

Han, Ying-Li, Yang, Wan-Xi, Long, Ling-Li, Sheng, Zhang, Zhou, Yang, Zhao, Yong-Qiang, Wang, You-Fa, & Zhu, Jun-Quan. 2016. Molecular cloning, expression pattern, and chemical analysis of heat shock protein 70 (HSP70) in the mudskipper Boleophthalmus pectinirostris: Evidence for its role in regulating spermatogenesis. *Gene*, **575**(jan), 331–338.

Hanahan, D. 1983. Studies on transformation of Escherichia coli with plasmids. *Journal of molecular biology*, **166**(4), 557–580.

Hari-Dass, Ranjeeta, Shah, Chandrabala, Meyer, David J, & Raynes, John G. 2005. Serum amyloid A protein binds to outer membrane protein A of gram-negative bacteria. *Journal of Biological Chemistry*, **280**(19), 18562–18567.

Hartmann, Jakob, Wagner, Klaus V., Liebl, Claudia, Scharf, Sebastian H., Wang, Xiao-Dong, Wolf, Miriam, Hausch, Felix, Rein, Theo, Schmidt, Ulrike, Touma, Chadi, Cheung-Flynn, Joyce, Cox, Marc B., Smith, David F., Holsboer, Florian, Müller, Marianne B., & Schmidt, Mathias V. 2012. The involvement of FK506-binding protein 51 (FKBP5) in the behavioral and neuroendocrine effects of chronic social defeat stress. *Neuropharmacology*, **62**(jan), 332–339.

Harun, Nor Omaima, Zou, Jun, Zhang, Yang-An, Nie, Pin, & Secombes, Chris J. 2008. The biological effects of rainbow trout (Oncorhynchus mykiss) recombinant interleukin-8. *Developmental and comparative immunology*, **32**(jan), 673–81.

Hatano, Naoya, Mori, Yoshiko, Oh-hora, Masatsugu, Kosugi, Atsushi, Fujikawa, Takahiko, Nakai, Naoya, Niwa, Hitoshi, Miyazaki, Jun-ichi, Hamaoka, Toshiyuki, & Ogata, Masato. 2003. Essential role for ERK2 mitogen-activated protein kinase in placental development. *Genes to Cells*, **8**(nov), 847–856.

Havixbeck, Jeffrey J., Rieger, Aja M., Wong, Michael E., Hodgkinson, Jordan W., & Barreda, Daniel R. 2016. Neutrophil contributions to the induction and regulation of the acute inflammatory response in teleost fish. *Journal of Leukocyte Biology*, **99**(feb), 241–252.

He, Rong, Sang, Hairong, & Ye, Richard D. 2003. Serum amyloid A induces IL-8 secretion through a G protein-coupled receptor, FPRL1/LXA4R. *Blood*, **101**(4), 1572–1581.

He, Rong, Shepard, Larry W, Chen, Jia, Pan, Zhixing K, & Ye, Richard D. 2006. Serum amyloid A is an endogenous ligand that differentially induces IL-12 and IL-23. *Journal of immunology*, **177**(6), 4072–9.

Heads, R J, Latchman, D S, & Yellon, D M. 1994. Stable high level expression of a transfected human HSP70 gene protects a heart-derived muscle cell line against thermal stress. *Journal of molecular and cellular cardiology*, **26**(jun), 695–9.

Healy, Timothy M., Tymchuk, Wendy E., Osborne, Edward J., & Schulte, Patricia M. 2010. Heat shock response of killifish (Fundulus heteroclitus): candidate gene and heterologous microarray approaches. *Physiological Genomics*, **41**(apr), 171–184.

Heinecke, Rasmus D, Chettri, Jiwan K, & Buchmann, Kurt. 2014. Adaptive and innate immune molecules in developing rainbow trout, Oncorhynchus mykiss eggs and larvae: expression of genes and occurrence of effector molecules. *Fish & shellfish immunology*, **38**(1), 25–33.

Hiramatsu, Kunihide, Yamada, Takashi, & Katakura, Masafumi. 1984. Acute effects of cold on blood pressure, renin-angiotensin-aldosterone system, catecholamines and adrenal steroids in man. *Clinical and Experimental Pharmacology and Physiology*, **11**(apr), 171–179.

Ho, Ping Yueh, Byadgi, Omkar, Wang, Pei Chyi, Tsai, Ming An, Liaw, Li Ling, & Chen, Shih Chu. 2016. Identification, molecular cloning of IL-1β and its expression profile during Nocardia seriolae infection in largemouth bass, Micropterus salmoides. *International Journal of Molecular Sciences*, **17**(1670).

Hochleithner, Martin. 2001. *Lachsfische Biologie und Aquakultur*. 1 edn. Aqua Tech Publications.

Hoever, M, Clement, J H, Wedlich, D, Montenarh, M, & Knochel, W. 1994. Overexpression of wild-type p53 interferes with normal development in Xenopus laevis embryos. *Oncogene*, **9**(jan), 109–120.

Hong, Suhee, Li, Ronggai, Xu, Qiaoqing, Secombes, Chris J, & Wang, Tiehui. 2013. Two Types of TNF- Exist in Teleost Fish: Phylogeny, Expression, and Bioactivity Analysis of Type-II TNF-3 in Rainbow Trout Oncorhynchus mykiss. *The Journal of Immunology*, **191**(12), 5959–5972.

Horn, H F, & Vousden, K H. 2007. Coping with stress: multiple ways to activate p53. *Oncogene*, **26**(feb), 1306–1316.

Horváth, Ibolya, Multhoff, Gabriele, Sonnleitner, Alois, & Vígh, László. 2008. Membrane-associated stress proteins: More than simply chaperones. *Biochimica et Biophysica Acta - Biomembranes*, **1778**(7-8), 1653–1664.

Hu, Wenwei. 2009. The role of p53 gene family in reproduction. *Cold Spring Harbor Perspectives in biology*, dec, 00:a001073.

Huang, Tien-sheng, Olsvik, Pål A., Krøvel, Anne, Tung, Hui-shan, & Torstensen, Bente E. 2009. Stress-induced expression of protein disulfide isomerase associated 3 (PDIA3) in Atlantic salmon (Salmo salar L.). *Comparative Biochemistry and Physiology Part B*, **154**(dec), 435–442.

Huising, Mark O., Stolte, Ellen, Flik, Gert, Savelkoul, Huub F.J., & Verburg-van Kemenade, B.M.Lidy. 2003. CXC chemokines and leukocyte chemotaxis in common carp (Cyprinus carpio L.). *Developmental & Comparative Immunology*, **27**(dec), 875–888.

Huising, Mark O., Van Der Meulen, Talitha, Flik, Gert, & Verburg-Van Kemenade, B. M Lidy. 2004. Three novel carp CXC chemokines are expressed early in ontogeny and at nonimmune sites. *European Journal of Biochemistry*, **271**(20), 4094–4106.

Huising, Mark O., van Schijndel, Jessica E., Kruiswijk, Corine P., Nabuurs, Sander B., Savelkoul, Huub F.J., Flik, Gert, & Lidy Verburg-van Kemenade, B.M. 2006. The presence of multiple and differentially regulated interleukin-12p40 genes in bony fishes signifies an expansion of the vertebrate heterodimeric cytokine family. *Molecular Immunology*, **43**(apr), 1519–1533.

Hulsen, Tim, de Vlieg, Jacob, & Alkema, Wynand. 2008. BioVenn - A web application for the comparison and visualization of biological lists using area-proportional Venn diagrams. *BMC Genomics*, **9**(1), 488.

Humbel, Rene E. 1990. Insulin-like growth factors I and II. *European Journal of Biochemistry*, **190**(3), 445–462.

Husain, Mansourah, Bird, Steve, van Zwieten, Ruthger, Secombes, Christopher J., & Wang, Tiehui. 2012. Cloning of the IL-1β3 gene and IL-1β4 pseudogene in salmonids uncovers a second type of IL-1β gene in teleost fish. *Developmental and Comparative Immunology*, **38**(nov), 431–446.

Hwa, Vivian, Youngman, Oh, Rosenfeld, Ron G, Oh, Y, & Rosenfeld, Ron G. 1999. The insulin-like growth factor-binding protein (IGFBP) superfamily. *Endocrine reviews*, **20**(6), 761–787.

Iguchi, Kei'ichiro, Ogawa, Kogi, Nagae, Masaki, & Ito, Fuminari. 2003. The influence of rearing density on stress response and disease susceptibility of ayu (Plecoglossus altivelis). *Aquaculture*, **220**(apr), 515–523.

Iliev, Dimitar B., Liarte, Cristina Q., MacKenzie, Simon, & Goetz, Frederick W. 2005. Activation of rainbow trout (Oncorhynchus mykiss) mononuclear phagocytes by different pathogen associated molecular pattern (PAMP) bearing agents. *Molecular Immunology*, **42**(10), 1215–1223.

Iliev, Dimitar B., Castellana, Barbara, MacKenzie, Simon, Planas, Josep V., & Goetz, Frederick W. 2007. Cloning and expression analysis of an IL-6 homolog in rainbow trout (Oncorhynchus mykiss). *Molecular Immunology*, **44**(mar), 1814–1818.

Inaba, Hiroto, & Pui, Ching-Hon. 2010. Glucocorticoid use in acute lymphoblastic leukaemia. *Lancet Oncology*, **11**(11), 1096–1106.

Iwama, George K., Thomas, Philip T., Forsyth, Robert B., & Vijayan, Mathilakath M. 1998. Heat shock protein expression in fish. *Reviews in Fish Biology and Fisheries*, **8**(1), 35–56.

Iwama, G.K., Mathilakath, M.V., Forsyth, R.B., & Ackerman, P.A. 1999. Heat shock proteins and physiological stress in fish. *American Zoologist*, **39**, 901–909.

Janeway, Charles, Travers, Paul, Walport, Mark, & Shlomchik, Mark. 2001. *Immunobiology 5 : the immune system in health and disease*. 5th edn. Garland Pub.

Jansen, Wolfgang, Jennerich, Hans-joachim, Wenzel, Hans-joachim, & Schulz, Steffen. 2008. Zur Haltung von Ostseeschnäpeln in einem Kaltwasserkreislauf in Hohen Wangelin Material und Methoden Ergebnisse und Diskussion. *Fischerei & Fischmarkt in M-V*, **4**, 36–39.

Jayasinghe, J.D.H.E., Elvitigala, Don Anushka Sandaruwan, Whang, Ilson, Nam, Bo-Hye, & Lee, Jehee. 2015. Molecular characterization of two immunity-related acute-phase proteins: Haptoglobin and serum amyloid A from black rockfish (Sebastes schlegeli). *Fish and Shellfish Immunology*, **45**(aug), 680–688.

Jennerich, Hans-Joachim, & Arndt, Gerd-Michael. 2012a. Aquakulturgestütztes Fischereimanagement der Maränenbestände, Große Maräne (Coregonus lavaretus L.) und Ostseeschnäpel (Coregonus lavaretus balticus, Thienemann 1921) in Binnenseen und Küstengewässern des Landes Mecklenburg-Vorpommern 2009 bis 2012. *Mitteilungen der Landesforschungsanstalt für Landwirtschaft und Fischerei*, **48**, 48.

Jennerich, Hans-Joachim, & Arndt, Gerd-Michael. 2012b. Aufbau und Entwicklung einer Ostseeschnäpelaquakultur (Coregonus lavaretus balticus) in Mecklenburg-Vorpommern. *Mitteilungen der Landesforschungsanstalt für Landwirtschaft und Fischerei*, **48**, 53.

Jennerich, Hans-Joachim, & Schulz, Norbert. 2011. Zur Situation des Ostseeschnäpels (Coregonus lavaretus balticus, Thienemann, 1922) in Mecklenburg-Vorpommern. *Mitteilungen der Landesforschungsanstalt für Landwirtschaft und Fischerei*, **45**, 12–20.

Jensen, L E, Hiney, M P, Shields, D C, Uhlar, C M, Lindsay, A J, & Whitehead, A S. 1997. Acute phase proteins in salmonids: evolutionary analyses and acute phase response. *Journal of immunology*, **158**(1), 384–392.

Jiang, Jihong, Cyr, Douglas, Babbitt, Roger W, Sessa, William C, & Patterson, Cam. 2003. Chaperone-dependent regulation of endothelial nitric-oxide synthase intracellular trafficking by the co-chaperone/ubiquitin ligase CHIP. *The Journal of biological chemistry*, **278**(49), 49332–41.

Jiang, Liping, & Tang, Zhen. 2018. Expression and regulation of the ERK1/2 and p38 MAPK signaling pathways in periodontal tissue remodeling of orthodontic tooth movement. *Molecular medicine reports*, **17**(jan), 1499–1506.

Joerger, Andreas C, Wilcken, Rainer, & Andreeva, Antonina. 2014. Tracing the evolution of the p53 tetramerization domain. *Structure*, **22**(sep), 1301–1310.

Joerink, Maaike, Ribeiro, CMS Carla M S, Stet, René J M, Hermsen, Trudi, Savelkoul, Huub F J, & Wiegertjes, Geert F. 2006. Head kidney-derived macrophages of common carp (Cyprinus carpio L.) show plasticity and functional polarization upon differential stimulation. *The Journal of Immunology*, **177**(1), 61–69.

Jørgensen, J B, Lunde, H, Jensen, L, Whitehead, A S, & Robertsen, B. 2000. Serum amyloid A transcription in Atlantic salmon (Salmo salar L.) hepatocytes is enhanced by stimulation with macrophage factors, recombinant human IL-1 beta, IL-6 and TNF alpha or bacterial lipopolysaccharide. *Developmental and comparative immunology*, **24**(6-7), 553–63.

Jundi, Karim, & Greene, Catherine M. 2015. Transcription of Interleukin-8: How Altered Regulation Can Affect Cystic Fibrosis Lung Disease. *Biomolecules*, **5**(jul), 1386–98.

Jung, Gwon-Soo, Jeon, Jae-Han, Jung, Yun-A, Choi, Yeon-Kyung, Kim, Hye-Soon, Kim, Jung-Guk, Park, Keun-Gyu, Kim, Mi-Kyung, & Lee, In-Kyu. 2014. Clusterin/apolipoprotein J attenuates angiotensin II-induced renal fibrosis. *PloS one*, **9**(8), e105635.

Kalliolias, George D., & Ivashkiv, Lionel B. 2016. TNF biology, pathogenic mechanisms and emerging therapeutic strategies. *Nature Reviews Rheumatology*, **12**(jan), 49–62.

Kania, Per W., Chettri, Jiwan K., & Buchmann, Kurt. 2014. Characterization of serum amyloid A (SAA) in rainbow trout using a new monoclonal antibody. *Fish & Shellfish Immunology*, **40**(oct), 648–658.

Kelley, Kevin M., Oh, Youngman, Gargosky, Sharron E., Gucev, Zoran, Matsumoto, Tomoko, Hwa, Vivian, Ng, Lilly, Simpson, Diane M., & Rosenfeld, Ron G. 1996. Insulin-like growth factor-binding proteins (IGFBPs) and their regulatory dynamics. *The International Journal of Biochemistry & Cell Biology*, **28**(6), 619–637.

Kenney PB, Davidson JW. 2014. Growth Performance, Fillet Quality, and Reproductive Maturity of Rainbow Trout (Oncorhynchus mykiss) Cultured to 5 Kilograms within Freshwater Recirculating Systems. *Journal of Aquaculture Research & Development*, **5**(4).

Khansari, Ali Reza, Parra, David, Reyes-López, Felipe E., & Tort, Lluís. 2017a. Cytokine modulation by stress hormones and antagonist specific hormonal inhibition in rainbow trout (Oncorhynchus mykiss) and gilthead sea bream (Sparus aurata) head kidney primary cell culture. *General and Comparative Endocrinology*, **250**(sep), 122–135.

Khansari, Ali Reza, Parra, David, Reyes-López, Felipe E., & Tort, Lluís. 2017b. Modulatory inÂ vitro effect of stress hormones on the cytokine response of rainbow trout and gilthead sea bream head kidney stimulated with Vibrio anguillarum bacterin. *Fish & Shellfish Immunology*, **70**(nov), 736–749.

Kim, Myung-Hoo, Yang, Ji-Young, Upadhaya, Santi Devi, Lee, Hyun-Jun, Yun, Cheol-Heui, & Ha, Jong K. 2011. The stress of weaning influences serum levels of acute-phase proteins, iron-binding proteins, inflammatory cytokines, cortisol, and leukocyte subsets in Holstein calves. *Journal of veterinary science*, **12**(2), 151–157.

Kirschke, Elaine, Goswami, Devrishi, Southworth, Daniel, Griffin, Patrick R, & Agard, David A. 2014. Glucocorticoid receptor function regulated by coordinated action of the Hsp90 and Hsp70 chaperone cycles. *Cell*, **157**(7), 1685–1697.

Köbis, Judith M., Rebl, Alexander, Kühn, Carsten, Korytár, Tomáš, Köllner, Bernd, & Goldammer, Tom. 2015. Comprehensive and comparative transcription analyses of the complement pathway in rainbow trout. *Fish & shellfish immunology*, **42**(1), 98–107.

Kojima, Eiji, Takeuchi, Akihide, Haneda, Masataka, Yagi, Ayako, Hasegawa, Tadao, ichi Yamaki, Ken, Takeda, Kiyoshi, Akira, Shizuo, Shimokata, Kaoru, & ichi Isobe, Ken. 2003. The function of GADD34 is a recovery from a shutoff of protein synthesis induced by ER stress: elucidation by GADD34-deficient mice. *The FASEB journal*, **17**(11), 1573–1575.

Komatsu, Koichiro, Tsutsui, Shigeyuki, Hino, Kazuyoshi, Araki, Kyosuke, Yoshiura, Yasutoshi, Yamamoto, Atsushi, Nakamura, Osamu, & Watanabe, Tasuku. 2009. Expression profiles of cytokines released in intestinal epithelial cells of the rainbow trout, Oncorhynchus mykiss, in response to bacterial infection. *Developmental & Comparative Immunology*, **33**(apr), 499–506.

Koop, Ben F, & Davidson, William S. 2008. Genomics and the Genome Duplication in Salmonids. *Fisheries for Gloval Welfare and Environment*, 77–86.

Korytár, Tomáš, Jaros, Joanna, Verleih, Marieke, Rebl, Alexander, Kotterba, Günter, Kühn, Carsten, Goldammer, Tom, & Köllner, Bernd. 2013. Novel insights into the peritoneal inflammation of rainbow trout (Oncorhynchus mykiss). *Fish & shellfish immunology*, **35**(4), 1192–9.

Korytár, Tomáš, Nipkow, Mareen, Altmann, Simone, Goldammer, Tom, Köllner, Bernd, & Rebl, Alexander. 2016. Adverse husbandry of maraena whitefish directs the immune system to increase mobilization of myeloid cells and proinflammatory responses. *Frontiers in Immunology*, **7**(DEC).

Kottelat, Maurice, & Freyhof, Jörg. 2007. Family Coregonidae. *Pages 349–394 of: Handbook of European freshwater fishes*, 1 edn.

Kovacevic, Nikolina, & Belosevic, Miodrag. 2015. Molecular and functional characterization of goldfish (Carassius auratus L.) Serum Amyloid A. *Fish and Shellfish Immunology*, **47**(dec), 942–953.

Krämer, Andreas, Green, Jeff, Pollard, Jack, Tugendreich, Stuart, Kramer, A., Green, Jeff, Pollard, Jack, & Tugendreich, Stuart. 2014. Causal analysis approaches in Ingenuity Pathway Analysis. *Bioinformatics*, **30**(4), 523–530.

Krasnov, Aleksei, Koskinen, Heikki, Pehkonen, Petri, Rexroad, Caird E, Afanasyev, Sergey, Mölsä, Hannu, & Mölsä, Hannu. 2005. Gene expression in the brain and kidney of rainbow trout in response to handling stress. *BMC genomics*, **6**(3), 1–11.

Krause, Maureen K, Rhodes, Linda D, & Van Beneden, Rebecca J. 1997. Cloning of the p53 tumor suppressor gene from the Japanese medaka (Oryzias latipes) and evaluation of mutational hotspots in MNNG-exposed fish. *Gene*, **189**(apr), 101–106.

Krens, S.F. Gabby, He, Shuning, Spaink, Herman P., & Snaar-Jagalska, B. Ewa. 2006. Characterization and expression patterns of the MAPK family in zebrafish. *Gene Expression Patterns*, **6**(oct), 1019–1026.

Krumm, Brian, Xiang, Yan, & Deng, Junpeng. 2014. Structural biology of the IL-1 superfamily: Key cytokines in the regulation of immune and inflammatory responses. *Protein Science*, **23**(5), 526–538.

Kum, Cavit, & Sekkin, Selim. 2011. The Immune System Drugs in Fish: Immune Function, Immunoassay, Drugs. *Chap. 11, pages 169–216 of:* Aral, Faruk (ed), *Recent Advances in Fish Farms*. Rijeka: InTech.

Kyriakis, J. M., & Avruch, J. 2012. Mammalian MAPK Signal Transduction Pathways Activated by Stress and Inflammation: A 10-Year Update. *Physiological Reviews*, **92**, 689–737.

Laing, Kerry J., Zou, Jun J., Wang, Tiehui, Bols, Niels, Hirono, Ikuo, Aoki, Takashi, & Secombes, Christopher J. 2002. Identification and analysis of an interleukin 8-like molecule in rainbow trout Oncorhynchus mykiss. *Developmental and Comparative Immunology*, **26**(jun), 433–444.

Lamaze, Fabien C., Garant, Dany, & Bernatchez, Louis. 2013. Stocking impacts the expression of candidate genes and physiological condition in introgressed brook charr (Salvelinus fontinalis) populations. *Evolutionary Applications*, **6**(feb), 393–407.

Lane, David, & Levine, Arnold. 2010. p53 Research : The Past Thirty Years and the Next Thirty Years p53 Research : The Past Thirty Years and. *Cold Spring Harbor Perspectives in Biology*, **2**:**a000893**, 1–11.

Larsen, D A, Beckman, B R, & Dickhoff, W W. 2001. The effect of low temperature and fasting during the winter on metabolic stores and endocrine physiology (insulin, insulin-like growth factor-I, and thyroxine) of coho salmon, Oncorhynchus kisutch. *General and comparative endocrinology*, **123**(3), 308–23.

Lazo, Pedro A. 2017. Reverting p53 activation after recovery of cellular stress to resume with cell cycle progression. *Cellular Signalling*, **33**(may), 49–58.

Le Morvan, C, Troutaud, D, & Deschaux, P. 1998. Differential effects of temperature on specific and nonspecific immune defences in fish. *Journal of Experimental Biology*, **201**, 165–168.

LeBlanc, S., Middleton, S., Gilmour, K. M., & Currie, S. 2011. Chronic social stress impairs thermal tolerance in the rainbow trout (Oncorhynchus mykiss). *Journal of Experimental Biology*, **214**, 1721–1731.

Lee, Eun Young, Park, Hyoun Hyang, Kim, Young Tae, Chung, Jong Kyeong, & Choi, Tae Jin. 2001. Cloning and sequence analysis of the interleukin-8 gene from flounder (Paralichthys olivaceous). *Gene*, **274**(aug), 237–243.

Lehtonen, Anne, Ahlfors, Helena, Veckman, Ville, Miettinen, Minja, Lahesmaa, Riitta, & Julkunen, Ilkka. 2007. Gene expression profiling during differentiation of human monocytes to macrophages or dendritic cells. *Journal of Leukocyte Biology*, **82**(sep), 710–720.

Lewis, S., Handy, R. D., Cordi, B., Billinghurst, Z., & Depledge, M. H. 1999. Stress proteins (HSP's): Methods of Detection and Their Use as an Environmental Biomarker. *Ecotoxicology*, **8**, 351–368.

Li, Chang-Yi, Yang, Ling-Chao, Guo, Kai, Wang, Yue-Peng, & Li, Yi-Gang. 2015. Mitogen-activated protein kinase phosphatase-1: A critical phosphatase manipulating mitogen-activated protein kinase signaling in cardiovascular disease (Review). *International Journal of Molecular Medicine*, **35**(apr), 1095–1102.

Li, Haoyang, Wang, Sheng, Chen, Yonggui, Lü, Kai, Yin, Bin, Li, Sedong, He, Jianguo, & Li, Chaozheng. 2017. Identification of two p53 isoforms from Litopenaeus vannamei and their interaction with NF-κB to induce distinct immune response. *Scientific Reports*, **7**(dec), 45821.

Li, Meng, Liu, Jun, & Zhang, Chiyu. 2011. Evolutionary History of the Vertebrate Mitogen Activated Protein Kinases Family. *PLoS ONE*, **6**(10), e26999.

Liang, Fenfei, Zhang, Guosong, Yin, Shaowu, & Wang, Li. 2016. The role of three heat shock protein genes in the immune response to Aeromonas hydrophila challenge in marbled eel, Anguilla marmorata. *Royal Society open science*, **3**(oct), 160375.

Lin, Bin, Chen, Shangwu, Cao, Zhen, Lin, Yiqun, Mo, Dunzhou, Zhang, Haibo, Gu, Juda, Dong, Meiling, Liu, Zehuan, & Xu, Anlong. 2007. Acute phase response in zebrafish upon Aeromonas salmonicida and Staphylococcus aureus infection: Striking similarities and obvious differences with mammals. *Molecular Immunology*, **44**(jan), 295–301.

Lindquist, Jonathan A., Brandt, Sabine, Bernhardt, Anja, Zhu, Cheng, & Mertens, Peter R. 2014. The role of cold shock domain proteins in inflammatory diseases. *Journal of Molecular Medicine*, **92**(mar), 207–216.

Lindquist, S, & Craig, E A. 1988. The Heat-Shock Proteins. *Annual Review of Genetics*, **22**(1), 631–677.

Lister, Andrea, & Van Kraak, Glen Der. 2002. Modulation of goldfish testicular testosterone production in vitro by tumor necrosis factor α, interleukin-1β, and macrophage conditioned media. *Journal of Experimental Zoology*, **292**, 477–486.

Liu, Baoliang, Liu, Ying, & Wang, Xianping. 2015. The effect of stocking density on growth and seven physiological parameters with assessment of their potential as stress response indicators for the Atlantic salmon (Salmo salar). *Marine and Freshwater Behaviour and Physiology*, **48**(may), 177–192.

Liu, Gang, Park, Young-Jun, Tsuruta, Yuko, Lorne, Emmanuel, & Abraham, Edward. 2009. p53 Attenuates lipopolysaccharide-induced NF-kappaB activation and acute lung injury. *The Journal of immunology*, **182**(8), 5063–71.

Liu, Jianguo, Cao, Shanjin, Herman, Lisa M, & Ma, Xiaojing. 2003. Differential regulation of interleukin (IL)-12 p35 and p40 gene expression and interferon (IFN)-gamma-primed IL-12 production by IFN regulatory factor 1. *The Journal of experimental medicine*, **198**(8), 1265–76.

Liu, Michelle, Tee, Catherine, Zeng, Fanxing, Sherry, James P., Dixon, Brian, Bols, Niels C., & Duncker, Bernard P. 2011. Characterization of p53 expression in rainbow trout. *Comparative Biochemistry and Physiology - Part C*, **154**(nov), 326–332.

Liu, Qian, Li, Anping, Tian, Yijun, Wu, Jennifer D., Liu, Yu, Li, Tengfei, Chen, Yuan, Han, Xinwei, & Wu, Kongming. 2016a. The CXCL8-CXCR1/2 pathways in cancer. *Cytokine and Growth Factor Reviews*, **31**(oct), 61–71.

Liu, Qun, Hou, Zhishuai, Wen, Haishen, Li, Jifang, He, Feng, Wang, Jinhuan, Guan, Biao, & Wang, Qinglong. 2016b. Effect of stocking density on water quality and (Growth, Body Composition and Plasma Cortisol Content) performance of pen-reared rainbow trout (Oncorhynchus mykiss). *Journal of Ocean University of China*, **15**(aug), 667–675.

Liu, Sixin, Gao, Guangtu, Palti, Yniv, Cleveland, Beth M, Weber, Gregory M, & Rexroad, Caird E. 2014. RNA-seq analysis of early hepatic response to handling and confinement stress in rainbow trout. *PloS one*, **9**(2), e88492.

Lodhia, Kunal Amratlal, Tienchaiananda, Piyawan, & Haluska, Paul. 2015. Understanding the Key to Targeting the IGF Axis in Cancer: A Biomarker Assessment. *Frontiers in Oncology*, **5**, 142.

Lorenz, Thomas. 2012. *Zusammenfassender Bericht Maränenprojekt 2009-2012: Aufkommen und Verteilung des Ostseeschnäpels (Coregonus lavaretus balticus) in Stettiner Haff, Peenestrom und Darß-Zingster Boddenkette sowie Untersuchung des Vorkommens der Großen Maräne (Coregonus lava.* Tech. rept.

Luft, Peter, Bochert, Ralf, Horn, Theresa, Schumacher, Carolin, & Bissa, Karl. 2015. *Die Etablierung von Nutzfischmodellen am Standort Born zur Entwicklung robuster Zuchtlinien für die regionale Aquakultur am Beispiel des Schnäpels (Coregonus maraena (Bloch, 1779)) in Mecklenburg-Vorpommern in den Jahren 2013 bis 2015.* Tech. rept. Landesforschungsanstalt für Landwirtschaft und Fischerei, Born a. Darß.

Lund, P K, Moats-Staats, B M, Hynes, M A, Simmons, J G, Jansen, M, D'Ercole, A J, & Van Wyk, J J. 1986. Somatomedin-C/insulin-like growth factor-I and insulin-like growth factor-II mRNAs in rat fetal and adult tissues. *The Journal of biological chemistry*, **261**(31), 14539–44.

Ma, Xiaojing, Yan, Wenjun, Zheng, Hua, Du, Qinglin, Zhang, Lixing, Ban, Yi, Li, Na, & Wei, Fang. 2015. Regulation of IL-10 and IL-12 production and function in macrophages and dendritic cells. *F1000Research*, **4**, 1–13.

Machelon, Véronique, Emilie, Dominique, Lefevre, Anick, Nome, Franqoise, Durand-Gasselin, Ingrid, & Testart, Jacques. 1994. Interleukin-6 biosynthesis in human preovulatory follicles: Some of its potential roles at ovulation. *Journal of Clinical Endocrinology and Metabolism*, **79**(2), 633–642.

MacKenzie, S, Iliev, D, Liarte, C, Koskinen, H, Planas, J V, Goetz, F W, Mölsä, H, Krasnov, a, & Tort, L. 2006. Transcriptional analysis of LPS-stimulated activation of trout (Oncorhynchus mykiss) monocyte/macrophage cells in primary culture treated with cortisol. *Molecular immunology*, **43**(9), 1340–8.

Mackenzie, Simon, Planas, Josep V, & Goetz, Frederick W. 2003. LPS-stimulated expression of a tumor necrosis factor-alpha mRNA in primary trout monocytes and in vitro differentiated macrophages. *Developmental & Comparative Immunology*, **27**, 393–400.

Macqueen, Daniel J, & Johnston, Ian A. 2014. A well-constrained estimate for the timing of the salmonid whole genome duplication reveals major decoupling from species diversification. *Proceedings of the Royal Society B*, **281**(20132881).

Magnadóttir, Bergljót. 2006. Innate immunity of fish (overview). *Fish & Shellfish Immunology*, **20**(feb), 137–151.

Magnadóttir, Bergljót, Jónsdóttir, Halla, Helgason, SigurÃ°ur, Björnsson, Björn, Jørgensen, Trond Ø, & Pilström, Lars. 1999. Humoral immune parameters in Atlantic cod (Gadus morhua L.): I. The effects of environmental temperature. *Comparative Biochemistry and Physiology Part B: Biochemistry and Molecular Biology*, **122**, 173–180.

Mancera, Juan Miguel, & McCormick, Stephen D. 1998. Osmoregulatory actions of the GH/IGF axis in non-salmonid teleosts. *Comparative Biochemistry and Physiology Part B: Biochemistry and Molecular Biology*, **121**(1), 43–48.

Mandriani, Barbara, Castellana, Stefano, Rinaldi, Carmela, Manzoni, Marta, Venuto, Santina, Rodriguez-Aznar, Eva, Galceran, Juan, Nieto, M. Angela, Borsani, Giuseppe, Monti, Eugenio, Mazza, Tommaso, Merla, Giuseppe, & Micale, Lucia. 2016. Identification of p53-target genes in Danio rerio. *Scientific Reports*, **6**(oct), 32474.

Manjari, Rao, Yadav, Mrigakshi, Ramesh, Kandasamy, Uniyal, Sarveshwa, Rastogi, Sunil Kumar, Sejian, Veerasamy, & Hyder, Iqbal. 2015. HSP70 as a marker of heat and humidity stress in Tarai buffalo. *Tropical Animal Health and Production*, **47**(jan), 111–116.

Marchler-Bauer, Aron, Bo, Yu, Han, Lianyi, He, Jane, Lanczycki, Christopher J, Lu, Shennan, Chitsaz, Farideh, Derbyshire, Myra K, Geer, Renata C., Gonzales, Noreen R, Gwadz, Marc, Hurwitz, David I, Lu, Fu, Marchler, Gabriele H, Song, James S, Thanki, Narmada, Wang, Zhouxi, Yamashita, Roxanne A, Zhang, Dachuan, Zheng, Chanjuan, Geer, Lewis Y, & Bryant, Stephen H. 2017. CDD/SPARCLE: Functional classification of proteins via subfamily domain architectures. *Nucleic Acids Research*, **45**(jan).

Martinez-Porchas, Marcel, Martinez-Cordova, Luis T., & Ramos-Enriquez, Rogelio. 2009. Cortisol and Glucose : Reliable indicators of fish stress ? *Journal of Aquatic Sciences*, **4**, 158–178.

Martins, C.I.M., Eding, E.H., Verdegem, M.C.J., Heinsbroek, L.T.N., Schneider, O., Blancheton, J.P., D'Orbcastel, E. Roque, & Verreth, J.A.J. 2010. New developments in recirculating aquaculture systems in Europe: A perspective on environmental sustainability. *Aquacultural Engineering*, **43**(nov), 83–93.

Mathews, L. S., Norstedt, G., & Palmiter, R. D. 1986. Regulation of insulin-like growth factor I gene expression by growth hormone. *Proceedings of the National Academy of Sciences*, **83**(24), 9343–9347.

Matousek, Jan, Stejskal, Vlastimil, Prokesova, Marketa, & Kouril, Jan. 2017. The effect of water temperature on growth parameters of intensively reared juvenile peled Coregonus peled. *Aquaculture Research*, **48**(apr), 1877–1884.

Matsumoto, Megumi, Hayashi, Kazuma, Suetake, Hiroaki, Yamamoto, Atsushi, & Araki, Kyosuke. 2016. Identification and functional characterization of multiple interleukin 12 in amberjack (Seriola dumerili). *Fish and Shellfish Immunology*, **55**(aug), 281–292.

Matukumalli, Suvarsha Rao, Tangirala, Ramakrishna, & Rao, C M. 2017. Clusterin: full-length protein and one of its chains show opposing effects on cellular lipid accumulation. *Scientific reports*, **7**, 41235.

McCormick, S D, Moriyama, S, & Björnsson, B T. 2000. Low temperature limits photoperiod control of smolting in atlantic salmon through endocrine mechanisms. *American journal of physiology. Regulatory, integrative and comparative physiology*, **278**(5), R1352–R1361.

Melnicoff, Meryle J., Horan, Paul K., & Morahan, Page S. 1989. Kinetics of changes in peritoneal cell populations following acute inflammation. *Cellular Immunology*, **118**(jan), 178–191.

Menanteau-Ledouble, Simon, Kumar, Gokhlesh, Saleh, Mona, & El-Matbouli, Mansour. 2016 (jun). *Aeromonas salmonicida: Updates on an old acquaintance*.

Menendez, Daniel, Shatz, Maria, & Resnick, Michael A. 2013. Interactions between the tumor suppressor p53 and immune responses. *Current Opinion in Oncology*, **25**(1), 85–92.

Meng, Xianzhong, Banerjee, Anirban, Ao, Lihua, Meldrum, Daniel R., Cain, Brian S., Shames, Brian D., & Harken, Alden H. 1999. Inhibition of myocardial TNF-α production by heat shock. A potential mechanism of stress-induced cardioprotection against postischemic dysfunction. *Pages 69–82 of: Annals of the New York Academy of Sciences*, vol. 874. Wiley/Blackwell (10.1111).

Meseguer, J., Esteban, M. A., Muñoz, J., & López-Ruiz, A. 1993. Ultrastructure of the peritoneal exudate cells of seawater teleosts, seabream (Sparus aurata) and sea bass (Dicentrarchus labrax). *Cell & Tissue Research*, **273**(2), 301–307.

Metzger, David C.H., Hemmer-Hansen, Jakob, & Schulte, Patricia M. 2016. Conserved structure and expression of hsp70 paralogs in teleost fishes. *Comparative Biochemistry and Physiology Part D: Genomics and Proteomics*, **18**(jun), 10–20.

Meyer, Axel, & Van De Peer, Yves. 2005. From 2R to 3R: Evidence for a fish-specific genome duplication (FSGD). *BioEssays*, **27**(9), 937–945.

Mezzano, Sergio A, Ruiz-Ortega, Marta, & Egido, Jesús. 2001. Angiotensin II and Renal Fibrosis. *Hypertension*, **38**(3), 635–638.

Milla, S., Wang, N., Mandiki, S. N.M., & Kestemont, P. 2009. Corticosteroids: Friends or foes of teleost fish reproduction? *Comparative Biochemistry and Physiology - Part A*, **153**, 242–251.

Millán, Adrián, Gómez-Tato, Antonio, Pardo, Belén G., Fernández, Carlos, Bouza, Carmen, Vera, Manuel, Alvarez-Dios, J. Antonio, Cabaleiro, Santiago, Lamas, Jesús, Lemos, Manuel L., & Martínez, Paulino. 2011. Gene Expression Profiles of the Spleen, Liver, and Head Kidney in Turbot (Scophthalmus maximus) Along the Infection Process with Aeromonas salmonicida Using an Immune-Enriched Oligo-microarray. *Marine Biotechnology*, **13**(6), 1099–1114.

Ming, Jianhua, Xie, Jun, Xu, Pao, Liu, Wenbin, Ge, Xianping, Liu, Bo, He, Yijin, Cheng, Yanfen, Zhou, Qunlan, & Pan, Liangkun. 2010. Molecular cloning and expression of two HSP70 genes in the Wuchang bream (Megalobrama amblycephala Yih). *Fish & Shellfish Immunology*, **28**(mar), 407–418.

Mommsen, Thomas P., Vijayan, Mathilakath M., & Moon, Thomas W. 1999. Cortisol in teleosts: Dynamics, mechanisms of action, and metabolic regulation. *Reviews in Fish Biology and Fisheries*, **9**(3), 211–268.

Moreira, P. S.A., & Volpato, G. L. 2004. Conditioning of stress in Nile tilapia. *Journal of Fish Biology*, **64**(4), 961–969.

Moriyama, Shunsuke, Ayson, Felix G., & Kawauchi, Hiroshi. 2000. Growth Regulation by Insulin-like Growth Factor-I in Fish. *Bioscience, Biotechnology, and Biochemistry*, **64**(8), 1553–1562.

Mu, Weijie, Wen, Haishen, Li, Jifang, & He, Feng. 2013. Cloning and expression analysis of a HSP70 gene from Korean rockfish (Sebastes schlegeli). *Fish & Shellfish Immunology*, **35**(oct), 1111–1121.

Mu, Weijie, Yao, Jun, Zhang, Jiaren, Liu, Shikai, Wen, Haishen, Feng, Jianbin, & Liu, Zhanjiang. 2015. Expression of tumor suppressor genes in channel catfish after bacterial infections. *Developmental and Comparative Immunology*, **48**, 171–177.

Mulder, I.E., Wadsworth, S., & Secombes, C.J. 2007. Cytokine expression in the intestine of rainbow trout (Oncorhynchus mykiss) during infection with Aeromonas salmonicida. *Fish & Shellfish Immunology*, **23**(oct), 747–759.

Müller, Lin, Schaupp, Andreas, Walerych, Dawid, Wegele, Harald, & Buchner, Johannes. 2004. Hsp90 regulates the activity of wild type p53 under physiological and elevated temperatures. *The Journal of biological chemistry*, **279**(47), 48846–54.

Murray, Francis, Bostock, John, & Fletcher, David. 2014. *Review of Recirculation Aquaculture System Technologies and their Commercial Application*. Tech. rept. Highlands and Islands Enterprise.

Nardocci, Gino, Navarro, Cristina, Cortés, Paula P., Imarai, Mónica, Montoya, Margarita, Valenzuela, Beatriz, Jara, Pablo, Acuña-Castillo, Claudio, & Fernández, Ricardo. 2014. Neuroendocrine mechanisms for immune system regulation during stress in fish. *Fish & Shellfish Immunology*, **40**(2), 531–538.

Nascimento, Diana S., do Vale, Ana, Tomás, Ana M., Zou, Jun, Secombes, Christopher J., & dos Santos, Nuno M.S. 2007a. Cloning, promoter analysis and expression in response to bacterial exposure of sea bass (Dicentrarchus labrax L.) interleukin-12 p40 and p35 subunits. *Molecular Immunology*, **44**(mar), 2277–2291.

Nascimento, Diana S., Pereira, Pedro J.B., Reis, Marta I.R., do Vale, Ana, Zou, Jun, Silva, Manuel T., Secombes, Christopher J., & dos Santos, Nuno M.S. 2007b. Molecular cloning and expression analysis of sea bass (Dicentrarchus labrax L.) tumor necrosis factor-α (TNF-α). *Fish & Shellfish Immunology*, **23**(sep), 701–710.

Nedić, Olgica, Malenković, Vesna, Nikolić, Judith Anna, & Baricević, Ivona. 2007. Insulin-like growth factor I (IGF-I) as a sensitive biomarker of catabolism in patients with gastrointestinal diseases. *Journal of clinical laboratory analysis*, **21**(5), 335–9.

Ni, Meng, Wen, Haishen, Li, Jifang, Chi, Meili, Bu, Yan, Ren, Yuanyuan, Zhang, Mo, Song, Zhifei, & Ding, Houmeng. 2016. Effects of stocking density on mortality, growth and physiology of juvenile Amur sturgeon (Acipenser schrenckii). *Aquaculture Research*, **47**(may), 1596–1604.

Nielsen, Henrik. 2017. Predicting Secretory Proteins with SignalP. *Pages 59–73 of: Protein Function Prediction (Methods in Molecular Biology vol. 1611)*. Springer.

Nipkow, Mareen, Wirthgen, Elisa, Luft, Peter, Rebl, Alexander, Hoeflich, Andreas, & Goldammer, Tom. 2018. Characterization of igf1 and igf2 genes during maraena whitefish (Coregonus maraena) ontogeny and the effect of temperature on embryogenesis and igf expression. *Growth Hormone & IGF Research*, **40**(jun), 32–43.

Noris, Marina, & Remuzzi, Giuseppe. 2013. Overview of complement activation and regulation. *Seminars in Nephrology*, **33**(6), 479–92.

North, B.P., Turnbull, J.F., Ellis, T., Porter, M.J., Migaud, H., Bron, J., & Bromage, N.R. 2006. The impact of stocking density on the welfare of rainbow trout (Oncorhynchus mykiss). *Aquaculture*, **255**(may), 466–479.

Novoa, I, Zeng, H, Harding, H P, & Ron, D. 2001. Feedback inhibition of the unfolded protein response by GADD34-mediated dephosphorylation of eIF2alpha. *The Journal of cell biology*, **153**(5), 1011–22.

Ojima, Nobuhiko, Yamashita, Michiaki, & Watabe, Shugo. 2005a. Comparative expression analysis of two paralogous Hsp70s in rainbow trout cells exposed to heat stress. *Biochimica et Biophysica Acta - Gene Structure and Expression*, **1681**(2-3), 99–106.

Ojima, Nobuhiko, Yamashita, Michiaki, & Watabe, Shugo. 2005b. Quantitative mRNA expression profiling of heat-shock protein families in rainbow trout cells. *Biochemical and Biophysical Research Communications*, **329**(1), 51–57.

Okonechnikov, Konstantin, Golosova, Olga, & Fursov, Mikhail. 2012. Unipro UGENE: a unified bioinformatics toolkit. *Bioinformatics (Oxford, England)*, **28**(8), 1166–7.

Øvergård, Aina-Cathrine, Nerland, Audun Helge, & Patel, Sonal. 2012. Characterisation and expression analysis of the Atlantic halibut (Hippoglossus hippoglossus L.) cytokines: IL-1β, IL-6, IL-11, IL-12β and IFNγ. *Molecular Biology Reports*, **39**(mar), 2201–2213.

Overturf, K., & LaPatra, S. 2006. Quantitative expression (Walbaum) of immunological factors in rainbow trout, Oncorhynchus mykiss (Walbaum), after infection with either Flavobacterium psychrophilum, Aeromonas salmonicida, or infectious haematopoietic necrosis virus. *Journal of Fish Diseases*, **29**, 215–224.

Pandey, Varunkumar Girijaprasad. 2013. *The Effect of Glucocorticoids on Regulation of the Human Angiotensinogen Gene and Blood Pressure*. Ph.D. thesis, University of Toledo.

Parra, David, Reyes-Lopez, Felipe E, & Tort, Lluis. 2015. Mucosal immunity and B cells in teleosts: Effect of vaccination and stress. *Frontiers in Immunology*, **6**(JUL), 1–12.

Patterson, Kate I, Brummer, Tilman, O'Brien, Philippa M, & Daly, Roger J. 2009. Dual-specificity phosphatases: critical regulators with diverse cellular targets. *The Biochemical journal*, **418**(mar), 475–89.

Pelegri, Francisco. 2003. Maternal factors in zebrafish development. *Developmental dynamics : an official publication of the American Association of Anatomists*, **228**(3), 535–54.

Peng, Guogan, Zhao, Wen, Shi, Zhenguang, Chen, Huirong, Liu, Yang, Wei, Jie, & Gao, Fengying. 2016. Cloning HSP70 and HSP90 genes of kaluga (Huso dauricus) and the effects of temperature and salinity stress on their gene expression. *Cell stress & chaperones*, **21**(mar), 349–59.

Pérez-Ortiz, José M., García-Gutiérrez, María S., Navarrete, Francisco, Giner, Salvador, & Manzanares, Jorge. 2013. Gene and protein alterations of FKBP5 and glucocorticoid receptor in the amygdala of suicide victims. *Psychoneuroendocrinology*, **38**(aug), 1251–1258.

Pérez-Sánchez, Jaume, Terova, Genciana, Simó-Mirabet, Paula, Rimoldi, Simona, Folkedal, Ole, Calduch-Giner, Josep A, Olsen, Rolf E, & Sitjà-Bobadilla, Ariadna. 2017. Skin Mucus of Gilthead Sea Bream (Sparus aurata L.). Protein Mapping and Regulation in Chronically Stressed Fish. *Frontiers in physiology*, **8**, 34.

Perrichon, Prescilla, Pasparakis, Christina, Mager, Edward M, Stieglitz, John D, Benetti, Daniel D, Grosell, Martin, & Burggren, Warren W. 2017. Morphology and cardiac physiology are differentially affected by temperature in developing larvae of the marine fish mahi-mahi (Coryphaena hippurus). *Biology open*, **6**(jun), 800–809.

Perrot, V, Moiseeva, E B, Gozes, Y, Chan, S J, Ingleton, P, & Funkenstein, B. 1999. Ontogeny of the insulin-like growth factor system (IGF-I, IGF-II, and IGF-1R) in gilthead seabream (Sparus aurata): expression and cellular localization. *General and comparative endocrinology*, **116**, 445–460.

Peters, Gerrit, Gongoll, Silvia, Langner, Cord, Mengel, Michael, Piso, Pompiliu, Klempnauer, Jürgen, Rüschoff, Josef, Kreipe, Hans, & von Wasielewski, Reinhard. 2003. IGF-1R, IGF-1 and IGF-2 expression as potential prognostic and predictive markers in colorectal-cancer. *Virchows Archiv*, **443**(aug), 139–145.

Petersen, Thomas Nordahl, Brunak, Søren, Von Heijne, Gunnar, & Nielsen, Henrik. 2011 (oct). *SignalP 4.0: Discriminating signal peptides from transmembrane regions*.

Petta, Ioanna, Dejager, Lien, Ballegeer, Marlies, Lievens, Sam, Tavernier, Jan, De Bosscher, Karolien, & Libert, Claude. 2016. The Interactome of the Glucocorticoid Receptor and Its Influence on the Actions of Glucocorticoids in Combatting Inflammatory and Infectious Diseases. *Microbiology and Molecular Biology Reviews*, **80**(jun), 495–522.

Phadtare, Sangita, Alsina, Janivette, & Inouye, Masayori. 1999. Cold-shock response and cold-shock proteins. *Current Opinion in Microbiology*, **2**(apr), 175–180.

Philip, Anju M., & Vijayan, Mathilakath M. 2015. Stress-immune-growth interactions: Cortisol modulates suppressors of cytokine signaling and JAK/STAT pathway in rainbow trout liver. *PLoS ONE*, **10**(6), 1–18.

Philip, Anju M., Daniel Kim, S., & Vijayan, Mathilakath M. 2012. Cortisol modulates the expression of cytokines and suppressors of cytokine signaling (SOCS) in rainbow trout hepatocytes. *Developmental and Comparative Immunology*, **38**(2), 360–367.

Phipson, Belinda, Lee, Stanley, Majewski, Ian J., Alexander, Warren S., & Smyth, Gordon K. 2016. Robust hyperparameter estimation protects against hypervariable genes and improves power to detect differential expression. *Annals of Applied Statistics*, **10**(2), 946–963.

Picha, Matthew E., Turano, Marc J., Beckman, Brian R., & Borski, Russell J. 2008. Endocrine Biomarkers of Growth and Applications to Aquaculture: A Minireview of Growth Hormone, Insulin- Like Growth Factor (IGF)-I, and IGFBinding Proteins as Potential Growth Indicators in Fish. *North American Journal of Aquaculture*, **70**, 196–211.

Pickering, A. D., & Pottinger, T. G. 1989. Stress responses and disease resistance in salmonid fish: Effects of chronic elevation of plasma cortisol. *Fish Physiology and Biochemistry*, **7**(1-4), 253–258.

Pimentel, Enrique. 1994. Insulin-like Growth Factors. *Chap. 2, pages 55–96 of: Handbook of Growth Factors Volume II: Peptide Growth Factors*. CRC Press.

Polinski, Mark, Bridle, Andrew, & Nowak, Barbara. 2013. Temperature-induced transcription of inflammatory mediators and the influence of Hsp70 following LPS stimulation of southern bluefin tuna peripheral blood leukocytes and kidney homogenates. *Fish and Shellfish Immunology*, **34**(5), 1147–1157.

Ponza, Pattareeya, Yocawibun, Patchari, Sittikankaew, Kanchana, Hiransuchalert, Rachanimuk, Yamano, Keisuke, & Klinbunga, Sirawut. 2011. Molecular cloning and expression analysis of the Mitogen-activating protein kinase 1 (MAPK1) gene and protein during ovarian development of the giant tiger shrimp Penaeus monodon. *Molecular Reproduction and Development*, **78**(5), 347–360.

Poompoung, Pornpun, Panprommin, Dutrudi, Srisapoome, Prapansak, & Poompuang, Supawadee. 2014. Cloning and expression of two HSC70 genes in walking catfish Clarias macrocephalus (Günther, 1864) challenged with Aeromonas hydrophila. *Aquaculture Research*, **45**(jul), 1319–1331.

Pörtner, H.O. 2002. Climate variations and the physiological basis of temperature dependent biogeography: systemic to molecular hierarchy of thermal tolerance in animals. *Comparative Biochemistry and Physiology Part A*, **132**(aug), 739–761.

Pottinger, T. G., Moran, T. A., & Morgan, J. A.W. 1994. Primary and secondary indices of stress in the progeny of rainbow trout (Oncorhynchus mykiss) selected for high and low responsiveness to stress. *Journal of Fish Biology*, **44**(1), 149–163.

Powell-Braxton, L, Hollingshead, P, Warburton, C, Dowd, M, Pitts-Meek, S, Dalton, D, Gillett, N, & Stewart, T A. 1993. IGF-I is required for normal embryonic growth in mice. *Genes & development*, **7**(12B), 2609–17.

Press, C. Mc L., & Evensen, O. 1999. The morphology of the immune system in teleost fishes. *Fish and Shellfish Immunology*, **9**(4), 309–318.

Pu, Yundan, Zhu, Jieyao, Wang, Hong, Zhang, Xin, Hao, Jin, Wu, Yuanbin, Geng, Yi, Wang, Kaiyu, Li, Zhiqiong, Zhou, Jian, & Chen, Defang. 2016. Molecular characterization and expression analysis of Hsp90 in Schizothorax prenanti. *Cell Stress and Chaperones*, **21**, 983–991.

Puche, Juan E, & Castilla-Cortázar, Inma. 2012 (nov). *Human conditions of insulin-like growth factor-I (IGF-I) deficiency*.

Qi, Zeng-Hua, Liu, Yu-Feng, Luo, Sheng-Wei, Chen, Chu-Xian, Liu, Yuan, & Wang, Wei-Na. 2013. Molecular cloning, characterization and expression analysis of tumor suppressor protein p53 from orange-spotted grouper, Epinephelus coioides in response to temperature stress. *Fish & Shellfish Immunology*, **35**(nov), 1466–1476.

Qin, Chuanjie, Shao, Ting, & Duan, Huiguo. 2016. The cloning of a heat shock protein 90β gene and expression analysis in Botia reevesae after ammonia-N exposure and Aeromonas hydrophila challenge. *Aquaculture Reports*, **3**(may), 159–165.

Qu, Fufa, Xiang, Zhiming, & Yu, Ziniu. 2014. The first molluscan acute phase serum amyloid A (A-SAA) identified from oyster Crassostrea hongkongensis: molecular cloning and functional characterization. *Fish & shellfish immunology*, **39**(2), 145–51.

Quinn, Nicole L., McGowan, Colin R., Cooper, Glenn A., Koop, Ben F., & Davidson, William S. 2011. Identification of genes associated with heat tolerance in Arctic charr exposed to acute thermal stress. *Physiological Genomics*, **43**(jun), 685–696.

Radtke, Simone, Wüller, Stefan, Yang, Xiang-ping, Lippok, Barbara E, Mütze, Barbara, Mais, Christine, de Leur, Hildegard Schmitz-Van, Bode, Johannes G, Gaestel, Matthias, Heinrich, Peter C, Behrmann, Iris, Schaper, Fred, & Hermanns, Heike M. 2010. Cross-regulation of cytokine signalling: pro-inflammatory cytokines restrict IL-6 signalling through receptor internalisation and degradation. *Journal of cell science*, **123**(Pt 6), 947–959.

Rebl, Alexander, & Goldammer, Tom. 2018. Under control: The innate immunity of fish from the inhibitors' perspective. *Fish and Shellfish Immunology*, **77**(jun), 328–349.

Rebl, Alexander, Goldammer, Tom, Fischer, Uwe, Köllner, Bernd, & Seyfert, Hans-Martin. 2009. Characterization of two key molecules of teleost innate immunity from rainbow trout (Oncorhynchus mykiss): MyD88 and SAA. *Veterinary Immunology and Immunopathology*, **131**(1-2), 122–126.

Rebl, Alexander, Rebl, Henrike, Liu, Shuzhen, Goldammer, Tom, & Seyfert, Hans-Martin. 2011. Salmonid Tollip and MyD88 factors can functionally replace their mammalian orthologues in TLR-mediated trout SAA promoter activation. *Developmental and comparative immunology*, **35**(1), 81–7.

Rebl, Alexander, Verleih, Marieke, Korytár, Thomáš, Kühn, Carsten, Wimmers, Klaus, Köllner, Bernd, & Goldammer, Tom. 2012. Identification of differentially expressed protective genes in liver of two rainbow trout strains. *Veterinary immunology and immunopathology*, **145**(1-2), 305–15.

Rebl, Alexander, Verleih, Marieke, Köbis, Judith M., Kühn, Carsten, Wimmers, Klaus, Köllner, Bernd, & Goldammer, Tom. 2013. Transcriptome profiling of gill tissue in regionally bred and globally farmed rainbow trout strains reveals different strategies for coping with thermal stress. *Marine biotechnology*, **15**(4), 445–60.

Rebl, Alexander, Rebl, Henrike, Korytár, Tomáš, Goldammer, Tom, & Seyfert, Hans-Martin. 2014. The proximal promoter of a novel interleukin-8-encoding gene in rainbow trout (Oncorhynchus mykiss) is strongly induced by CEBPA, but not NF-κB p65. *Developmental and comparative immunology*, **46**(2), 155–64.

Rebl, Alexander, Zebunke, Manuela, Borchel, Andreas, Bochert, Ralf, Verleih, Marieke, & Goldammer, Tom. 2017. Microarray-predicted marker genes and molecular pathways indicating crowding stress in rainbow trout (Oncorhynchus mykiss). *Aquaculture*, **473**(apr), 355–365.

Rebl, Alexander, Verleih, Marieke, Nipkow, Mareen, Altmann, Simone, Bochert, Ralf, & Goldammer, Tom. 2018. Gradual and acute temperature rise induces crossing endocrine, metabolic and immunological pathways in maraena whitefish (Coregonus maraena). *Frontiers in Genetics*, **9**, 241.

Reinecke, M, & Collet, C. 1998. The phylogeny of the insulin-like growth factors. *International review of cytology*, **183**(jan), 1–94.

Reinecke, Manfred. 2010. Insulin-like Growth Factors and Fish Reproduction. *Biology of Reproduction*, **82**(4), 656–661.

Reinecke, Manfred, Björnsson, Björn Thrandur, Dickhoff, Walton W, McCormick, Stephen D, Navarro, Isabel, Power, Deborah M, & Gutiérrez, Joaquim. 2005. Growth hormone and insulin-like growth factors in fish: where we are and where to go. *General and comparative endocrinology*, **142**(1-2), 20–4.

Ren, Yuanyuan, Wen, Haishen, Li, Yun, & Li, Jifang. 2017. Stocking density affects the growth performance and metabolism of Amur sturgeon by regulating expression of genes in the GH/IGF axis. *Chinese Journal of Oceanology and Limnology*, 1–17.

Richter, Hartmut, Lückstädt, Christian, Focken, Ulfert L., & Becker, Klaus. 2000. An improved procedure to assess fish condition on the basis of length-weight relationships. *Archive of Fishery and Marine Research*, **48**(3), 226–235.

Ricker, W. E. 1975. *Computation and interpretation of biological statistics of fish populations*. Tech. rept.

Ricklin, Daniel, Hajishengallis, George, Yang, Kun, & Lambris, John D. 2010. Complement: a key system for immune surveillance and homeostasis. *Nature immunology*, **11**(9), 785–97.

Riera Romo, Mario, Pérez-Martínez, Dayana, & Castillo Ferrer, Camila. 2016. Innate immunity in vertebrates: An overview. *Immunology*, **148**(2), 125–139.

Rinderknecht, Ernst, & Humbel, Rene E. 1978a. Primary Structure Of Human Insulin-Like Growth Factor II. *FEBS Letters*, **89**(2), 283–286.

Rinderknecht, Ernst, & Humbel, Rene E. 1978b. The Amino Acid Sequence of Human Insulin-like Growth Factor I and Its Structural Homology with Proinsulin *. *The Journal of biological chemistry*, **253**(April 25), 2769–2776.

Ritchie, Matthew E., Phipson, Belinda, Wu, Di, Hu, Yifang, Law, Charity W., Shi, Wei, & Smyth, Gordon K. 2015. limma powers differential expression analyses for RNA-sequencing and microarray studies. *Nucleic acids research*, **43**(7), e47.

Rivas, Carmen, Aaronson, Stuart A, & Munoz-Fontela, Cesar. 2010. Dual Role of p53 in Innate Antiviral Immunity. *Viruses*, **2**(jan), 298–313.

Roberts, R J, Agius, C, Saliba, C, Bossier, P, & Sung, Y Y. 2010. Heat shock proteins (chaperones) in fish and shellfish and their potential role in relation to fish health: A review. *Journal of Fish Diseases*, **33**(10), 789–801.

Rogel, A, Popliker, M, Webb, C G, & Oren, M. 1985. p53 cellular tumor antigen: analysis of mRNA levels in normal adult tissues, embryos, and tumors. *Molecular and cellular biology*, **5**(10), 2851–5.

Roher, Nerea, Callol, Agnes, Planas, Josep V., Goetz, Frederick W., & MacKenzie, Simon A. 2010. Endotoxin recognition in fish results in inflammatory cytokine secretion not gene expression. *Innate Immunity*, **17**(1), 16–28.

Roith, Derek Le, Scavo, Louis, & Butler, Andrew. 2001. What is the role of circulating IGF-I? *Trends in Endocrinology & Metabolism*, **12**(2), 48–52.

Romano, N, Ceccariglia, S, Mastrolia, L, & Mazzini, M. 2002. Cytology of lymphomyeloid head kidney of Antarctic fishes Trematomus bernacchii (Nototheniidae) and Chionodraco hamatus (Channicthyidae). *Tissue and Cell*, **34**(2), 63–72.

Rombough, P.J. 1997. The effect of temperature on embryonic and larval development. *Pages 177–223 of: Global Warming: Implications for Freshwater and Marine Fish*, vol. 59. Birkhäuser-Verlag.

Roque d'Orbcastel, Emmanuelle, Person-Le Ruyet, Jeanine, Le Bayon, Nicolas, & Blancheton, Jean Paul. 2009. Comparative growth and welfare in rainbow trout reared in recirculating and flow through rearing systems. *Aquacultural Engineering*, **40**(2), 79–86.

Rose-John, Stefan. 2018. Interleukin-6 family cytokines. *Cold Spring Harbor Perspectives in Biology*, **10**(2), a028415.

Roskoski, Robert. 2012. ERK1/2 MAP kinases: Structure, function, and regulation. *Pharmacological Research*, **66**(2), 105–143.

Rotwein, P., Pollock, K. M., Watson, M., & Milbrandt, J. D. 1987. Insulin-like growth factor gene expression during rat embryonic development. *Endocrinology*, **121**, 2141–2144.

Rotwein, Peter. 2018. The complex genetics of human insulin-like growth factor 2 are not reflected in public databases. *Journal of Biological Chemistry*, jbc.RA117.001573.

Ruis, Marco A.W., & Bayne, Christopher J. 1997. Effects of Acute Stress on Blood Clotting and Yeast Killing by Phagocytes of Rainbow Trout. *Journal of Aquatic Animal Health*, **9**(3), 279–290.

Ruiz-Ortega, Marta, Ruperez, Mónica, Lorenzo, Oscar, Esteban, Vanesa, Blanco, Julia, Mezzano, Sergio, & Egido, Jesus. 2002. Angiotensin II regulates the synthesis of proinflammatory cytokines and chemokines in the kidney. *Kidney International*, **62**(82), S12–S22.

Saeij, J P J, Verburg-van Kemenade, B M L, van Muiswinkel, W B, & Wiegertjes, G F. 2003a. Daily handling stress reduces carp disease resistance: modulatory effects of cortisol on apoptosis and in vitro leukocyte functions. *Developmental and Comparative Immunology*, **27**(3), 233–245.

Saeij, Jeroen P.J, Stet, René J.M, de Vries, Beja J, van Muiswinkel, Willem B, & Wiegertjes, Geert F. 2003b. Molecular and functional characterization of carp TNF: a link between TNF polymorphism and trypanotolerance? *Developmental & Comparative Immunology*, **27**(jan), 29–41.

Saeij, Jeroen P.J, Vries, Beitske J.de, & Wiegertjes, Geert F. 2003c. The immune response of carp to Trypanoplasma borreli: kinetics of immune gene expression and polyclonal lymphocyte activation. *Developmental & Comparative Immunology*, **27**(dec), 859–874.

Saiki, R K, Gelfand, D H, Stoffel, S, Scharf, S J, Higuchi, R, Horn, G T, Mullis, K B, & Erlich, H A. 1988. Primer-directed enzymatic amplification of DNA with a thermostable DNA polymerase. *Science (New York, N.Y.)*, **239**, 487–91.

Saitou, N, & Nei, M. 1987. The neighbor-joining method: a new method for reconstructing phylogenetic trees. *Molecular biology and evolution*, **4**(4), 406–25.

Sanger, F, Nicklen, S, & Coulson, A R. 1977. DNA sequencing with chain-terminating inhibitors. *Proceedings of the National Academy of Sciences of the United States of America*, **74**(12), 5463–7.

Santiago, Pedro, Roig-López, José Luis, Santiago, Carlos, & García-Arrarás, José E. 2000. Serum amyloid a protein in an echinoderm: Its primary structure and expression during intestinal regeneration in the sea cucumber Holothuria glaberrima. *Journal of Experimental Zoology*, **288**(4), 335–344.

Sass, Jennifer B., Weinberg, Eric S., & Krone, Patrick H. 1996. Specific localization of zebrafishhsp90α mRNA tomyoD-expressing cells suggests a role for hsp90α during normal muscle development. *Mechanisms of Development*, **54**(feb), 195–204.

Savan, Ram, Kono, Tomoya, Igawa, Daisuke, & Sakai, Masahiro. 2005. A novel tumor necrosis factor (TNF) gene present in tandem with the TNF-alpha gene on the same chromosome in teleosts. *Immunogenetics*, **57**(apr), 140–150.

Schachte, John H. 2002. Furunculosis. New York: New York Department of Environmental Conservatory. Rome. NY.

Scheller, Jürgen, Chalaris, Athena, Schmidt-Arras, Dirk, & Rose-John, Stefan. 2011. The pro- and anti-inflammatory properties of the cytokine interleukin-6. *Biochimica et Biophysica Acta - Molecular Cell Research*, **1813**(5), 878–888.

Schirone, Robert C., & Gross, Leo. 1968. Effect of temperature on early embryological development of the zebra fish, Brachydanio rerio. *Journal of Experimental Zoology*, **169**(sep), 43–52.

Schlaepfer, David D, Hou, Shihe, Lim, Ssang-Taek, Tomar, Alok, Yu, Honggang, Lim, Yangmi, Hanson, Dan a, Uryu, Sean a, Molina, John, & Mitra, Satyajit K. 2007. Tumor necrosis factor-alpha stimulates focal adhesion kinase activity required for mitogen-activated kinase-associated interleukin 6 expression. *The Journal of biological chemistry*, **282**(24), 17450–9.

Schulz, Norbert. 2000. Das Wiedereinbürgerungs- und Besatzprogramm des Ostseeschnäpels Coregonus lavaretus balticus (Thienemann) in der vorpommerschen Boddenlandschaft, Rückblick und Ausblick. *Fisch und Umwelt Mecklenburg-Vorpommern e.V.*, 45–59.

Schulz, Norbert. 2008. Zur fischereilichen Situation im Stettiner Haff, Chancen für ein besatzgestütztes Fischereimanagement am Beispiel des Ostseeschnäpels (Coregonus lavaretus balticus, Thienemann, 1992). *Fisch und Umwelt Mecklenburg-Vorpommern e.V.*, 81–103.

Schulz, Norbert. 2012. *Aquakulturgestütztes Fischereimanagement der Maränenbestände, Große Maräne (Coregonus lavaretus L.) und Ostseeschnäpel (Coregonus lavaretus balticus, Thienemann 1922) in Binnenseen und Küstengewässern des Landes Mecklenburg- Vorpommerns in den Jahren 2009*. Tech. rept. Fisch und Umwelt Mecklenburg-Vorpommern e.V., Rostock.

Schulz, Norbert, Haunschild, Gertraud, Lorenz, Thomas, Steinfurth, Peter, Plötz, Bernd, Koßmann, Martin, & Schurno, Mathias. 2012. Aquakulturgestütztes Fischereimanagement der Maränenbestände, Große Maräne (Coregonus lavaretus L.) und Ostseeschnäpel (Coregonus lavaretus balticus, Thienemann 1921) in Binnenseen und Küstengewässern des Landes Mecklenburg-Vorpommern 2009 bis 2012. *FISCH UND UMWELT Mecklenburg-Vorpommern e.V.*, 1–28.

Secombes, C. J., Wang, T., & Bird, S. 2011. The interleukins of fish. *Developmental and Comparative Immunology*, **35**(12), 1336–1345.

Secombes, Christopher J. 1996. The nonspecific immune system: cellular defenses. *Chap. 2, pages 63–101 of:* Iwama, George K., & Nakanashi, Teruyuki (eds), *The Fish Immune System: Organism, Pathogen, and Environment*. San Diego: Academic Press.

Secombes, Christopher J., & Olivier, Gilles. 1997. Host-Pathogen Interactions in Salmonids. *Chap. 10, pages 269–296 of:* Bernorth EM, Ellis AE, Midtlyng PJ, Olivier G, Smith P (ed), *Furunculosis: multidisciplinary fish disease research*.

Secombes, Christopher J, Bird, Steve, Cunningham, Charles, & Zou, Jun. 1999. Interleukin-1 in fish. *Fish and Shellfish Immunology*, **9**(may), 335–343.

Sedger, Lisa M., & McDermott, Michael F. 2014. TNF and TNF-receptors: From mediators of cell death and inflammation to therapeutic giants - past, present and future. *Cytokine & Growth Factor Reviews*, **25**(aug), 453–472.

Seppola, Marit, Larsen, Atle Noralf, Steiro, Kari, Robertsen, Børre, & Jensen, Ingvill. 2008. Characterisation and expression analysis of the interleukin genes, IL-1β, IL-8 and IL-10, in Atlantic cod (Gadus morhua L.). *Molecular Immunology*, **45**(feb), 887–897.

Sessa, William C. 2004. eNOS at a glance. *Journal of cell science*, **117**(12), 2427–9.

Shah, Chandrabala, Hari-Dass, Ranjeeta, & Raynes, John G. 2006. Serum amyloid A is an innate immune opsonin for Gram-negative bacteria. *Blood*, **108**(5), 1751–1757.

Shen, Fang, Li, Nan, Gade, Padmaja, Kalvakolanu, Dhananjaya V, Weibley, Timothy, Doble, Brad, Woodgett, James R, Wood, Troy D, & Gaffen, Sarah L. 2009. IL-17 receptor signaling inhibits C/EBPbeta by sequential phosphorylation of the regulatory 2 domain. *Science Signaling*, **2**(59), ra8.

Shimatsu, Akira, & Rotwein, Peter. 1987. Mosaic Evolution of the Insulin-like Growth Factors. *The Journal of biological chemistry*, **262**(June 5), 7894–7900.

Sievers, Fabian, Wilm, Andreas, Dineen, David, Gibson, Toby J, Karplus, Kevin, Li, Weizhong, Lopez, Rodrigo, McWilliam, Hamish, Remmert, Michael, Söding, Johannes, Thompson, Julie D, & Higgins, Desmond G. 2011. Fast, scalable generation of high-quality protein multiple sequence alignments using Clustal Omega. *Molecular systems biology*, **7**(539), 1–6.

Siikavuopio, Sten I., Knudsen, Rune, Amundsen, Per-Arne, & Saether, Bjørn Steinar. 2012. Growth performance of European whitefish (Coregonus lavaretus (L.)) under a constant light and temperature regime. *Aquaculture Research*, **43**(oct), 1592–1598.

Siikavuopio, Sten Ivar, Knudsen, Rune, Amundsen, Per Arne, Sæther, Bjørn Steinar, & James, Philip. 2013. Effects of high temperature on the growth of European whitefish (Coregonus lavaretus L.). *Aquaculture Research*, **44**(dec), 8–12.

Singh, I S, Viscardi, R M, Kalvakolanu, I, Calderwood, S, & Hasday, J D. 2000. Inhibition of tumor necrosis factor-alpha transcription in macrophages exposed to febrile range temperature. A possible role for heat shock factor-1 as a negative transcriptional regulator. *The Journal of biological chemistry*, **275**(13), 9841–8.

Sjögren, K, Liu, J L, Blad, K, Skrtic, S, Vidal, O, Wallenius, V, LeRoith, D, Törnell, J, Isaksson, O G, Jansson, J O, & Ohlsson, C. 1999. Liver-derived insulin-like growth factor I (IGF-I) is the principal source of IGF-I in blood but is not required for postnatal body growth in mice. *Proceedings of the National Academy of Sciences of the United States of America*, **96**(jun), 7088–92.

Skelton, Nicholas J, Quan, Cliff, Reilly, Dorothea, & Lowman, Henry. 1999. Structure of a CXC chemokine-receptor fragment in complex with interleukin-8. *Structure*, **7**(feb), 157–168.

Skugor, Stanko, Jørgensen, Sven Martin, Gjerde, Bjarne, & Krasnov, Aleksei. 2009. Hepatic gene expression profiling reveals protective responses in Atlantic salmon vaccinated against furunculosis. *BMC genomics*, **10**(503), 1–15.

Smyth, Gordon K. 2004. Linear models and empirical bayes methods for assessing differential expression in microarray experiments. *Statistical applications in genetics and molecular biology*, **3**(3).

Smyth, Gordon K, & Speed, Terry. 2003. Normalization of cDNA microarray data. *Methods (San Diego, Calif.)*, **31**(4), 265–73.

Soares-Silva, Mercedes, Diniz, Flavia F, Gomes, Gabriela N, & Bahia, Diana. 2016. The Mitogen-Activated Protein Kinase (MAPK) Pathway: Role in Immune Evasion by Trypanosomatids. *Frontiers in microbiology*, **7**, 183.

Soundarapandian, P, Dinakaran, GK, & Varadharajan, D. 2014. Effect of Temperatures on the Embryonic Development, Morphometrics and Survival of Macrobrachium Idella Idella (Hilgendorf, 1898). *Journal of Aquaculture Research & Development*, **5**(7), 280.

Sparre, Per, & Venema, Siebren C. 1998. Introduction to tropical fish stock assessment. *FAO fisheries technical paper*, **306/1**(Part I: Manual), 1–376.

Starliper, Clifford E. 2011. Bacterial coldwater disease of fishes caused by Flavobacterium psychrophilum. *Journal of Advanced Research*, **2**(apr), 97–108.

Steel, Diana M., & Whitehead, Alexander S. 1994. The major acute phase reactants: C-reactive protein, serum amyloid P component and serum amyloid A protein. *Immunology Today*, **15**(2), 81–88.

Steinel, Natalie C., & Bolnick, Daniel I. 2017. Melanomacrophage centers as a histological indicator of immune function in fish and other poikilotherms. *Frontiers in Immunology*, **8**(JUL), 1–8.

Stien, Lars H., Bracke, Marc B. M., Folkedal, Ole, Nilsson, Jonatan, Oppedal, Frode, Torgersen, Thomas, Kittilsen, Silje, Midtlyng, Paul J., Vindas, Marco A., Øverli, Øyvind, & Kristiansen, Tore S. 2013. Salmon Welfare Index Model (SWIM 1.0): a semantic model for overall welfare assessment of caged Atlantic salmon: review of the selected welfare indicators and model presentation. *Reviews in Aquaculture*, **5**(mar), 33–57.

Stolte, Ellen H, Verburg van Kemenade, B. M Lidy, Savelkoul, Huub F J, & Flik, Gert. 2006. Evolution of glucocorticoid receptors with different glucocorticoid sensitivity. *Journal of Endocrinology*, **190**(1), 17–28.

Stolte, Ellen H., Nabuurs, Sander B., Bury, Nic R., Sturm, Armin, Flik, Gert, Savelkoul, Huub F.J., & Lidy Verburg-van Kemenade, B. M. 2008. Stress and innate immunity in carp: Corticosteroid receptors and pro-inflammatory cytokines. *Molecular Immunology*, **46**, 70–79.

Stolte, Ellen H., Chadzinska, Magdalena, Przybylska, Dominika, Flik, Gert, Savelkoul, Huub F.J., & Verburg-van Kemenade, B.M. Lidy. 2009. The immune response differentially regulates Hsp70 and glucocorticoid receptor expression in vitro and in vivo in common carp (Cyprinus carpio L.). *Fish & Shellfish Immunology*, **27**(1), 9–16.

Storer, Narie Y, & Zon, Leonard I. 2010. Zebrafish models of p53 functions. *Cold Spring Harbor perspectives in biology*, **2**(aug), a001123.

Sun, Hong-Yan, Huang, Mian-Zhi, Mo, Ze-Quan, Chen, Liang-Shi, Chen, Guo, Yang, Man, Ni, Lu-Yun, Li, Yan-Wei, & Dan, Xue-Ming. 2018. Characterization and expression patterns of ERK1 and ERK2 from Epinephelus coioides against Cryptocaryon irritans infection. *Fish & Shellfish Immunology*, **74**(mar), 393–400.

Sun, Peng, Bao, Peibo, & Tang, Baojun. 2017. Transcriptome analysis and discovery of genes involved in immune pathways in large yellow croaker (Larimichthys crocea) under high stocking density stress. *Fish & Shellfish Immunology*, **68**(sep), 332–340.

Sun, Shengming, Gu, Zhimin, Fu, Hongtuo, Zhu, Jian, Ge, Xianping, & Xuan, Fujun. 2016. Molecular cloning, characterization, and expression analysis of p53 from the oriental river prawn, Macrobrachium nipponense, in response to hypoxia. *Fish and Shellfish Immunology*, **54**(jul), 68–76.

Sun, Zhongjie, Cade, Robert, Zhang, Zhonge, Alouidor, James, & Van, Huong. 2003. Angiotensinogen gene knockout delays and attenuates cold-induced hypertension. *Hypertension*, **41**(2), 322–7.

Svendsen, Y. S., Dalmo, R. A., & Bogwald, J. 1999. Tissue localization of Aeromonas salmonicida in Atlantic salmon, Salmo salar L., following experimental challenge. *Journal of Fish Diseases*, **22**(mar), 125–131.

Svendsen, Yngvar S., & Bøgwald, Jarl. 1997. Influence of artificial wound and non-intact mucus layer on mortality of Atlantic salmon (Salmo salar L.) following a bath challenge with Vibrio anguillarum and Aeromonas salmonicida. *Fish and Shellfish Immunology*, **7**(jul), 317–325.

Szczepkowski, Miroslaw, Szczepkowska, Bozena, & Krzywosz, Tadeusz. 2006. Indices of Juvenile Whitefish (Coregonus Lavaretus (L .)). *Archives of Polish Fisheries*, **14**, 95–104.

Takeo, Jiro, Hata, Jun-ichiro, Segawa, Chisako, Toyohara, Haruhiko, & Yamashita, Shinya. 1996. Fish glucocorticoid receptor with splicing variants in the DNA binding domain. *FEBS Letters*, **389**(3), 244–248.

Tal, Yossi, Schreier, Harold J., Sowers, Kevin R., Stubblefield, John D., Place, Allen R., & Zohar, Yonathan. 2009. Environmentally sustainable land-based marine aquaculture. *Aquaculture*, **286**(jan), 28–35.

Talbot, Anita T., Pottinger, Tom G., Smith, Terry J., & Cairns, Michael T. 2009. Acute phase gene expression in rainbow trout (Oncorhynchus mykiss) after exposure to a confinement stressor: A comparison of pooled and individual data. *Fish & Shellfish Immunology*, **27**(aug), 309–317.

Tam, Benita, Gough, William A., & Tsuji, Leonard. 2011. The Impact of Warming on The Appearance of Furunculosis in Fish of The James Bay Region, Quebec, Canada. *Regional Environmental Change*, **11**(1), 123–132.

Tamayo, P. 1999. Interpreting patterns of gene expression with self-organizing maps: methods and application to hematopoietic differentiation. *Proc. Natl. Acad. Sci. USA*, **96**(May), 2912.

Tamura, Koichiro, Stecher, Glen, Peterson, Daniel, Filipski, Alan, & Kumar, Sudhir. 2013. MEGA6: Molecular Evolutionary Genetics Analysis version 6.0. *Molecular biology and evolution*, **30**(12), 2725–9.

Tanaka, Toshio, Narazaki, Masashi, & Kishimoto, Tadamitsu. 2014. Il-6 in inflammation, Immunity, And disease. *Cold Spring Harbor Perspectives in Biology*, **6**(sep), a016295.

Taylor, John S, Braasch, Ingo, Frickey, Tancred, Meyer, Axel, & Van de Peer, Yves. 2003. Genome duplication, a trait shared by 22000 species of ray-finned fish. *Genome research*, **13**, 382–90.

Thépot, Valentin, & Jerry, Dean R. 2015. The effect of temperature on the embryonic development of barramundi, the Australian strain of Lates calcarifer (Bloch) using current hatchery practices. *Aquaculture Reports*, **2**(nov), 132–138.

Thorne, M.A.S., Burns, G., Fraser, K.P.P., Hillyard, G., & Clark, M.S. 2010. Transcription profiling of acute temperature stress in the Antarctic plunderfish Harpagifer antarcticus. *Marine Genomics*, **3**(mar), 35–44.

Tibbles, L a, & Woodgett, J R. 1999. The stress-activated protein kinase pathways. *Cellular and molecular life sciences : CMLS*, **55**(10), 1230–1254.

Tokarz, Janina, Möller, Gabriele, Hrabě De Angelis, Martin, & Adamski, Jerzy. 2015. Steroids in teleost fishes: A functional point of view. *Steroids*, **103**(nov), 123–144.

Tomalty, Katharine M H, Meek, Mariah H, Stephens, Molly R, Rincón, Gonzalo, Fangue, Nann A, May, Bernie P, & Baerwald, Melinda R. 2015. Transcriptional Response to Acute Thermal Exposure in Juvenile Chinook Salmon Determined by RNAseq. *G3*, **5**(apr), 1335–49.

Tort, L. 2011a. Hormonal responses to stress: Impact of Stress in Health and Reproduction. *Pages 1541–1552 of:* Farrell, Anthony P. (ed), *Encyclopedia of Fish Physiology*, vol. 2. Elsevier Inc.

Tort, L., Balasch, J. C., & Mackenzie, S. 2003. Fish immune system. A crossroads between innate and adaptive responses. *Immunologia*, **22**, 277–286.

Tort, Lluis. 2011b. Stress and immune modulation in fish. *Developmental & Comparative Immunology*, **35**(dec), 1366–1375.

Trinchieri, Giorgio. 2003. Interleukin-12 and the regulation of innate resistance and adaptive immunity. *Nature Reviews Immunology*, **3**(2), 133–146.

Tsai, Jui-Ling, Jose Priya, T.A., Hu, Kuang-Yu, Yan, Hong-Young, Shen, San-Tai, & Song, Yen-Ling. 2014. Grouper interleukin-12, linked by an ancient disulfide-bond architecture, exhibits cytokine and chemokine activities. *Fish & Shellfish Immunology*, **36**(jan), 27–37.

Uhlar, Clarissa M., & Whitehead, Alexander S. 1999. Serum amyloid A, the major vertebrate acute-phase reactant. *European Journal of Biochemistry*, **265**(2), 501–523.

Uhlar, Clarissa M., Burgess, Conal J., Sharp, Paul M., & Whitehead, Alexander S. 1994. Evolution of the Serum Amyloid A (SAA) Protein Superfamily. *Genomics*, **19**(jan), 228–235.

Untergasser, Andreas, Nijveen, Harm, Rao, Xiangyu, Bisseling, Ton, Geurts, René, & Leunissen, Jack A.M. 2007. Primer3Plus, an enhanced web interface to Primer3. *Nucleic Acids Research*, **35**, W71–W74.

Uribe, C., Folch, H., Enriquez, R., & Moran, G. 2011. Innate and adaptive immunity in teleost fish: a review. *Veterinární Medicína*, **56**(10), 486–503.

Urieli-Shoval, Simcha, Cohen, Patrizia, Eisenberg, Shlomit, & Matzner, Yaacov. 1998. Widespread Expression of Serum Amyloid A in Histologically Normal Human Tissues: Predominant Localization to the Epithelium. *Journal of Histochemistry & Cytochemistry*, **46**(12), 1377–1384.

Urieli-Shoval, Simcha, Linke, Reinhold P, & Matzner, Yaacov. 2000. Expression and function of serum amyloid A, a major acute-phase protein, in normal and disease states. *Current Opinion in Hematology*, **7**(1), 64–69.

Vallés, Patricia G., Lorenzo, Andrea Gil, Bocanegra, Victoria, & Vallés, Roberto. 2014. Acute kidney injury: What part do toll-like receptors play? *International Journal of Nephrology and Renovascular Disease*, **7**(June 2014), 241–251.

van der Aa, Lieke M., Chadzinska, Magdalena, Tijhaar, Edwin, Boudinot, Pierre, & Lidy verburg Van kemenade, B. M. 2010. CXCL8 chemokines in teleost fish: Two lineages with distinct expression profiles during early phases of inflammation. *PLoS ONE*, **5**(8), e12384.

Van der Hoek, K H, Woodhouse, C M, Brännström, M, & Norman, R J. 1998. Effects of interleukin (IL)-6 on luteinizing hormone- and IL-1beta-induced ovulation and steroidogenesis in the rat ovary. *Biology of reproduction*, **58**(5), 1266–1271.

van der Meer, David L.M. 2005. Gene expression profiling of the long-term adaptive response to hypoxia in the gills of adult zebrafish. *American Journal of Physiology-Regulatory, Integrative and Comparative Physiology*, **289**, 1512–1519.

Vanden Bergh, Philippe, & Frey, Joachim. 2014. Aeromonas salmonicida subsp. salmonicida in the light of its type-three secretion system. *Microbial Biotechnology*, **7**(5), 381–400.

Varela, M., Dios, S., Novoa, B., & Figueras, A. 2012. Characterisation, expression and ontogeny of interleukin-6 and its receptors in zebrafish (Danio rerio). *Developmental & Comparative Immunology*, **37**(may), 97–106.

Vazzana, M., Vizzini, A., Salerno, G., Di Bella, M.L., Celi, M., & Parrinello, N. 2008. Expression of a glucocorticoid receptor (DIGR1) in several tissues of the teleost fish Dicentrarchus labrax. *Tissue and Cell*, **40**(apr), 89–94.

Vazzana, Mirella, Vizzini, Aiti, Sanfratello, Maria Antonietta, Celi, Monica, Salerno, Giuseppina, & Parrinello, Nicolò. 2010. Differential expression of two glucocorticoid receptors in seabass (teleost fish) head kidney after exogeneous cortisol inoculation. *Comparative Biochemistry and Physiology Part A*, **157**(sep), 49–54.

Vera Cruz, Emmanuel M., Brown, Christopher L., Luckenbach, J. Adam, Picha, Matthew E., Bolivar, Remedios B., & Borski, Russell J. 2006. Insulin-like growth factor-I cDNA cloning, gene expression and potential use as a growth rate indicator in Nile tilapia, Oreochromis niloticus. *Aquaculture*, **251**, 585–595.

Verleih, Marieke, Borchel, Andreas, Krasnov, Aleksei, Rebl, Alexander, Korytár, Tomáš, Kühn, Carsten, & Goldammer, Tom. 2015. Impact of Thermal Stress on Kidney-Specific Gene Expression in Farmed Regional and Imported Rainbow Trout. *Marine Biotechnology*, **17**(5), 576–592.

Viadero, Roger C. 2005. Factors Affecting Fish Growth and Production. *Pages 129–133 of: Water Encyclopedia*. Hoboken, NJ, USA: John Wiley & Sons, Inc.

Vijayan, Mathilakath M., Pereira, Cristina, Forsyth, Robert B., Kennedy, Christopher J., & Iwama, George K. 1997. Handling stress does not affect the expression of hepatic heat shock protein 70 and conjugation enzymes in rainbow trout treated with β-naphthoflavone. *Life Sciences*, **61**(2), 117–127.

Villarroel, Franz, Casado, Alin, Vásquez, Jorge, Matamala, Ella, Araneda, Bruno, Amthauer, Rodolfo, Enriquez, Ricardo, & Concha, Margarita I. 2008. Serum amyloid A: A typical acute-phase reactant in rainbow trout? *Developmental and Comparative Immunology*, **32**(10), 1160–1169.

Vinay, D S, & Kwon, B S. 2011. The tumour necrosis factor/TNF receptor superfamily: Therapeutic targets in autoimmune diseases. *Clinical and Experimental Immunology*, **164**(2), 145–157.

Vong, Q P, Chan, K M, & Cheng, C H K. 2003. Quantification of common carp (Cyprinus carpio) IGF-I and IGF-II mRNA by real-time PCR: differential regulation of expression by GH. *The Journal of endocrinology*, **178**(3), 513–21.

Walerych, D, Olszewski, M B, Gutkowska, M, Helwak, A, Zylicz, M., & Zylicz, A. 2009. Hsp70 molecular chaperones are required to support p53 tumor suppressor activity under stress conditions. *Oncogene*, **28**(dec), 4284–4294.

Walter, Peter, & Ron, David. 2005. The Unfolded Protein Response: From Stress Pathway to Homeostatic Regulation. *Science*, **334**, 1081–1087.

Wang, Chuangui, & Chen, Jiandong. 2003. Phosphorylation and hsp90 binding mediate heat shock stabilization of p53. *Journal of Biological Chemistry*, **278**(3), 2066–2071.

Wang, Pengfei, Zeng, Shuang, Xu, Peng, Zhou, Lei, Zeng, Lei, Lu, Xue, Wang, Haifang, & Li, Guifeng. 2014a. Identification and expression analysis of two HSP70 isoforms in mandarin fish Siniperca chuatsi. *Fisheries Science*, **80**(jul), 803–817.

Wang, Qin, Wang, Junnan, Wang, Guiling, Wu, Congdi, & Li, Jiale. 2017. Molecular cloning, sequencing, and expression profiles of heat shock protein 90 (HSP90) in Hyriopsis cumingii exposed to different stressors: Temperature, cadmium and Aeromonas hydrophila. *Aquaculture and Fisheries*, **2**(mar), 59–66.

Wang, Tiehui, & Husain, Mansourah. 2014. The expanding repertoire of the IL-12 cytokine family in teleost fish: Identification of three paralogues each of the p35 and p40 genes in salmonids, and comparative analysis of their expression and modulation in Atlantic salmon Salmo salar. *Developmental and Comparative Immunology*, **46**(2), 194–207.

Wang, Tiehui, Husain, Mansourah, Hong, Suhee, & Holland, Jason W. 2014b. Differential expression, modulation and bioactivity of distinct fish IL-12 isoforms: Implication towards the evolution of Th1-like immune responses. *European Journal of Immunology*, **44**(5), 1541–1551.

Wang, Yaping, Wang, Qun, Baoprasertkul, Puttharat, Peatman, Eric, & Liu, Zhanjiang. 2006. Genomic organization, gene duplication, and expression analysis of interleukin-1β in channel catfish (Ictalurus punctatus). *Molecular Immunology*, **43**(apr), 1653–1664.

Waterhouse, Andrew, Bertoni, Martino, Bienert, Stefan, Studer, Gabriel, Tauriello, Gerardo, Gumienny, Rafal, Heer, Florian T, de Beer, Tjaart A P, Rempfer, Christine, Bordoli, Lorenza, Lepore, Rosalba, & Schwede, Torsten. 2018. SWISS-MODEL: homology modelling of protein structures and complexes. *Nucleic Acids Research*, **1**(may), 1–8.

Watts, Joy E M, Schreier, Harold J, Lanska, Lauma, & Hale, Michelle S. 2017. The Rising Tide of Antimicrobial Resistance in Aquaculture: Sources, Sinks and Solutions. *Marine drugs*, **15**(158), 1–16.

Wei, Jingguang, Guo, Minglan, Ji, Huasong, & Qin, Qiwei. 2013. Molecular cloning, characterization of one key molecule of teleost innate immunity from orange-spotted grouper (Epinephelus coioides): Serum amyloid A. *Fish and Shellfish Immunology*, **34**(jan), 296–304.

Weinmann, Amy S, Plevy, Scott E, & Smale, Stephen T. 1999. Rapid and Selective Remodeling of a Positioned Nucleosome during the Induction of IL-12 p40 Transcription. *Immunity*, **11**(dec), 665–675.

Wen, Haishen, Qi, Qian, Hu, Jian, Si, Yufeng, He, Feng, & Li, Jifang. 2015. Expression analysis of the insulin-like growth factors I and II during embryonic and early larval development of turbot (Scophthalmus maximus). *Journal of Ocean University of China*, **14**(2), 309–316.

Wendelaar Bonga, S. E. 1997. The stress response in fish. *Physiological Reviews*, **77**(3), 591–625.

Wenger, Michael, Shved, Natallia, Akgül, Gülfirde, Caelers, Antje, Casanova, Ayako, Segner, Helmut, & Eppler, Elisabeth. 2014. Developmental oestrogen exposure differentially modulates IGF-I and TNF-α expression levels in immune organs of Yersinia ruckeri-challenged young adult rainbow trout (Oncorhynchus mykiss). *General and Comparative Endocrinology*, **205**, 168–175.

Weyts, F. A.A., Cohen, N., Flik, G., & Verburg-van Kemenade, B. M.L. 1999. Interactions between the immune system and the hypothalamo-pituitary-interrenal axis in fish. *Fish and Shellfish Immunology*, **9**(1), 1–20.

Whirledge, S, & Cidlowski, J A. 2010. Glucocorticoids, stress, and fertility. *Minerva endocrinologica*, **35**(2), 109–25.

Wiseman, Steve, Osachoff, Heather, Bassett, Erin, Malhotra, Jana, Bruno, Joy, VanAggelen, Graham, Mommsen, Thomas P., & Vijayan, Mathilakath M. 2007. Gene expression pattern in the liver during recovery from an acute stressor in rainbow trout. *Comparative Biochemistry and Physiology - Part D*, **2**(sep), 234–244.

Wolf, Eckhard, Hoeflich, Andreas, & Lahm, Harald. 1998. What is the function of IGF-II in postnatal life? Answers from transgenic mouse models. *Growth Hormone & IGF Research*, **8**(3), 185–193.

Wong, Marty Kwok-Shing, Ozaki, Haruka, Suzuki, Yutaka, Iwasaki, Wataru, & Takei, Yoshio. 2014. Discovery of osmotic sensitive transcription factors in fish intestine via a transcriptomic approach. *BMC genomics*, **15**(dec), 1134.

Wood, Antony W., Duan, Cunming, & Bern, Howard A. 2005. Insulin-Like Growth Factor Signaling in Fish. *International Review of Cytology*, **243**, 215–285.

Wright, B Y Patricia A, Perry, Steve F, & Moon, Thomas W. 1989. Regulation of hepatic gluconeogenesis and glycogenolysis by catecholamines in rainbow trout during environmental hypoxia. *Experimental Biology*, **147**, 169–188.

Wu, Congqing, Lu, Hong, Cassis, Lisa A, & Daugherty, Alan. 2011. Molecular and Pathophysiological Features of Angiotensinogen: A Mini Review. *North American journal of medicine & science*, **4**(4), 183–190.

Xu, Dan, Xu, Shaohai, Kyaw, Aung Maung Maung, Lim, Yen Ching, Chia, Sook Yoong, Chee Siang, Diana Teh, Alvarez-Dominguez, Juan R, Chen, Peng, Leow, Melvin Khee-Shing, & Sun, Lei. 2017. RNA Binding Protein Ybx2 Regulates RNA Stability During Cold-Induced Brown Fat Activation. *Diabetes*, **66**(dec), 2987–3000.

Xu, Q. Q., Xu, P., Zhou, J. W., Pan, T. S., Tuo, R., Ai, K., & Yang, D. Q. 2016. Cloning and expression analysis of two pro-inflammatory cytokines, IL-1β and its receptor, IL-1R2, in the Asian swamp eel Monopterus albus. *Molecular Biology*, **50**(5), 671–683.

Xu, Yipeng, Zheng, Guowan, Dong, Shengzhang, Liu, Guangfu, & Yu, Xiaoping. 2014. Molecular cloning, characterization and expression analysis of HSP60, HSP70 and HSP90 in the golden apple snail, Pomacea canaliculata. *Fish & Shellfish Immunology*, **41**(dec), 643–653.

Yaffe, P, & Yoffey, J M. 1982. Phagocytic lymphoid cells and transitional cells in the peritoneal cavity. *Journal of anatomy*, **134**(4), 729–40.

Yamashita, Michiaki, Yabu, Takeshi, & Ojima, Nobuhiko. 2010. Stress Protein HSP70 in Fish. *Aqua-BioScience Monographs*, **3**(4), 111–141.

Yan, Jie, Liang, Xiao, Zhang, Yin, Li, Yang, Cao, Xiaojuan, & Gao, Jian. 2017. Cloning of three heat shock protein genes (HSP70, HSP90α and HSP90β) and their expressions in response to thermal stress in loach (Misgurnus anguillicaudatus) fed with different levels of vitamin C. *Fish and Shellfish Immunology*, **66**(jul), 103–111.

Yarahmadi, Peyman, Miandare, Hamed Kolangi, Fayaz, Sahel, & Caipang, Christopher Marlowe A. 2016. Increased stocking density causes changes in expression of selected stress- and immune-related genes, humoral innate immune parameters and stress responses of rainbow trout (Oncorhynchus mykiss). *Fish & Shellfish Immunology*, **48**(jan), 43–53.

Yoo, C.-G., Lee, S., Lee, C.-T., Kim, Y. W., Han, S. K., & Shim, Y.-S. 2000. Anti-Inflammatory Effect of Heat Shock Protein Induction Is Related to Stabilization of I B Through Preventing I B Kinase Activation in Respiratory Epithelial Cells. *The Journal of Immunology*, **164**(sep), 5416–5423.

Yoo, K H, Thornhill, B A, Wolstenholme, J T, & Chevalier, R L. 1998. Tissue-specific regulation of growth factors and clusterin by angiotensin II. *American journal of hypertension*, **11**(6 Pt 1), 715–22.

Yoon, C, Johnston, S C, Tang, J, Stahl, M, Tobin, J F, & Somers, W S. 2000. Charged residues dominate a unique interlocking topography in the heterodimeric cytokine interleukin-12. *The EMBO journal*, **19**(14), 3530–41.

Yoshiura, Yasutoshi, Kiryu, Ikunari, Fujiwara, Atsushi, Suetake, Hiroaki, Suzuki, Yuzuru, Nakanishi, Teruyuki, & Ototake, Mitsuru. 2003. Identification and characterization of Fugu orthologues of mammalian interleukin-12 subunits. *Immunogenetics*, **55**(aug), 296–306.

Zante, Merle D., Borchel, Andreas, Brunner, Ronald M., Goldammer, Tom, & Rebl, Alexander. 2015. Cloning and characterization of the proximal promoter region of rainbow trout (Oncorhynchus mykiss) interleukin-6 gene. *Fish & Shellfish Immunology*, **43**(1), 249–256.

Zhang, Anying, Zhou, Xiaofei, Wang, Xinyan, & Zhou, Hong. 2011a. Characterization of two heat shock proteins (Hsp70/Hsc70) from grass carp (Ctenopharyngodon idella): Evidence for their differential gene expression, protein

synthesis and secretion in LPS-challenged peripheral blood lymphocytes. *Comparative biochemistry and physiology. Part B*, **159**(jun), 109–114.

Zhang, Lili, Sun, Chengfei, Ye, Xing, Zou, Shuming, Lu, Maixin, Liu, Zhigang, & Tian, Yuanyuan. 2014. Characterization of four heat-shock protein genes from Nile tilapia (Oreochromis niloticus) and demonstration of the inducible transcriptional activity of Hsp70 promoter. *Fish Physiology and Biochemistry*, **40**, 221–233.

Zhang, Zuobing, Niu, Cuijuan, Storset, Arne, Bøgwald, Jarl, & Dalmo, Roy A. 2011b. Comparison of Aeromonas salmonicida resistant and susceptible salmon families: A high immune response is beneficial for the survival against Aeromonas salmonicida challenge. *Fish and Shellfish Immunology*, **31**, 1–9.

Zheng, Dali, Sabbagh, Jonathan J, Blair, Laura J, Darling, April L, Wen, Xiaoqi, & Dickey, Chad A. 2016. MicroRNA-511 Binds to FKBP5 mRNA, Which Encodes a Chaperone Protein, and Regulates Neuronal Differentiation. *The Journal of biological chemistry*, **291**(34), 17897–906.

Zhou, M. Y., & Gomez-Sanchez, C. E. 2000. Universal TA cloning. *Current issues in molecular biology*, **2**(1), 1–7.

Zhou, M Y, Clark, S E, & Gomez-Sanchez, C E. 1995. Universal cloning method by TA strategy. *BioTechniques*, **19**(1), 34–5.

Zou, J, Cunningham, C, & Secombes, C J. 1999. The rainbow trout Oncorhynchus mykiss interleukin-1 beta gene has a differ organization to mammals and undergoes incomplete splicing. *European Journal of Biochemistry*, **259**, 901–908.

Zou, J., Wang, T., Hirono, I., Aoki, T., Inagawa, H., Honda, T., Soma, G.-I., Ototake, M., Nakanishi, T., Ellis, A.E., & Secombes, C.J. 2002. Differential expression of two tumor necrosis factor genes in rainbow trout, Oncorhynchus mykiss. *Developmental & Comparative Immunology*, **26**(mar), 161–172.

Zou, Jun, & Secombes, Christopher. 2016. The Function of Fish Cytokines. *Biology*, **5**(2), 23.

Zou, Shuming, Kamei, Hiroyasu, Modi, Zubin, & Duan, Cunming. 2009. Zebrafish IGF Genes: Gene Duplication, Conservation and Divergence, and Novel Roles in Midline and Notochord Development. *PLoS ONE*, **4**(9), e7026.

Zwollo, Patty. 2018. The humoral immune system of anadromous fish. *Developmental & Comparative Immunology*, **80**(mar), 24–33.

Zylicz, Maciej, King, Frank W, & Wawrzynow, Alicja. 2001. Hsp70 interactions with the p53 tumour suppressor protein. *EMBO Journal*, **20**(17), 4634–4638.

Appendix

A. Additional Materials

A.1. Media, buffers, and protocols

A.1.1. Agarose gel electrophoresis

0.5 x TBE (Tris-borate-EDTA)	
Tris-borate	44.5 mM
boric acid	44.5 mM
EDTA	1 mM
adjust with HCl to	pH 8.3

Loading buffer	
glycerol	50%
bromophenol blue	1%
EDTA	120 mM
Tris-HCl, pH 8.0	10 mM

A.1.2. Preparation of competent *E. coli* XL1 Blue-Cells

TY agar plates supplemented with tetracycline	
Bacto-tryptone	1.6%
yeast extract	1.0%
NaCl	85.6 mM
agar	2.0%
tetracycline*	0.1%

*After autoclavation and cooling followed addition of the filter-sterilised antibiotic tetracycline.

SOB liquid growth medium	
Bacto-tryptone	2.0%
yeast extract	0.5%
NaCl	10 mM
KCl	2.5 mM
$MgCl_2$*	10 mM
$MgSO_4$*	10 mM

*After autoclavation and cooling followed addition of the indicated components from sterile stock solutions.

PSI liquid growth medium	
Bacto-tryptone	2.0%
yeast extract	0.5%
NaCl	10 mM
KCl	5 mM
$MgSO_4$*	20 mM

*After autoclavation and cooling followed addition of the indicated component from a sterile stock solution.

RF1-solution	
glycerol	15%
RbCl	100 mM
$MnCl_2$	50 mM
KCl	30 mM
$CaCl_2$	10 mM

The pH value was adjusted to 5.8 with acetic acid ($C_2H_4O_2$), before the solution was filter-sterilised and stored at -20°C.

RF2-solution	
glycerol	15%
$CaCl_2$	75 mM
RbCl	10 mM
MOPS (pH 6.8)	10 mM

The pH value was adjusted to 6.8 with NaOH, before the solution was filter-sterilised and stored at -20°C.

A.1.3. Transformation of pGEM®-T Easy Vector into competent *E. coli* cells

SOC liquid medium (pH 6.8-7.0)	
Bacto-tryptone	2.0%
yeast extract	0.5%
glucose*	20.0 mM
NaCl*	10.0 mM
$MgCl_2$*	10.0 mM
$MgSO_4$*	10.0 mM
KCl*	2.5 mM

*After autoclavation and cooling followed addition of the indicated components from sterile stock solutions.

2 x TY liquid growth medium (pH 6.8-7.0)	
tryptone	1.6 %
yeast extract	1.0%
NaCl	0.5 %
ampicillin* [100 mg/ml]	0.1 mg/ml

*After autoclavation and cooling followed addition of the filter-sterilised antibiotic ampicillin.

TY agar plates supplemented with X-gal, IPTG and ampicillin	
Bacto-tryptone	1.6%
yeast extract	1.0%
NaCl	85.6 mM
agar	2.0%
X-gal*	4.0%
IPTG*	0.04 mM
ampicillin* [100 mg/ml]	0.1 mg/ml

*After autoclavation and cooling followed addition of the indicated components from sterile stock solutions.

A.1.4. Restriction digestion of plasmid DNA

Reagent	Volume	Digestion procedure
purified plasmid DNA (from plasmid mini-preparation)	1.0 µl	incubation of the restriction reaction (37°C, 90 min)
enzyme-specific restriction buffer	1.5 µl	
restriction enzyme	1.0 µl	
H_2O_{bidest}	11.5 µl	

A.1.5. Western blot

RIPA buffer (pH 7.4)	
Tris-HCL	50 mM
NaCl	150 mM
TritonX	1%
SDS	0.1%

A.2. List of Oligonucleotides

All primers used in this study were customised synthesised by Sigma-Aldrich and diluted to a final concentration of 20 µM. Except from primers used for IFC chip based real time PCR, that were always delivered in 200 µM dilutions (custom-made by Sigma-Aldrich).

Oligonucleotides used for real time PCR analyses are shown in List A. Besides, the respective real time PCR primers were used for 3'-RACE (forward Primer) and 5'-RACE (reverse Primer) experiments, except from the target genes *EEF1A1B*, *RPL9* and *RPL32*

List A: Oligonucleotides used for real time PCR analyses

Target Gene	5'→3'-Sequence of forward Primer	5'→3'-Sequence of reverse Primer	Primer efficiency [*E*]	Amplicon length [bp]
EEF1A1B	CCTCCACTTGGTCGTTTCG	CGCAGGATGTAGGGCAGCAGA	1.81	189
MAPK3	GTAACGACCACACCTGCTACTT	CTATCCGTGCCAGCCCAAAGT	2.00	156
MAPK1	GTACATCCACTCAGCTAACGTC	GCTACATACTCCGTCAGGAAAC	1.86	153
HSP70	GGCCATGAACCCCAACAACAC	CTCCTCTGGGTTGAAGGATTTG	1.96	176
HSP90	AGATACGAGAGCTTGACAGACC	TGCCAGACTTGGCGATGGTTC	1.95	166
IGF1	TATTGTGGACGAGTGCTGCTTC	CTCTGTCGACGCTTTGCACTG	1.95	158
IGF2	ACCCATGGTGCCCACACTCAA	CTTGATCTTCACCGCCTGCCT	1.84	163
IL1B	AAGGACAAGGACCTGCTCAACT	ACCCAGCTCTTGTTCTCAGAGT	2.00	161
IL6	AGAAGCCTGTGGAAGAGATGTC	ATTGTGGGTATTCAGCCTTAACG	1.93	177
CXCL8	TAGACTCATTAAGAAGGTGGAGAT	TGTTGGCCAGCATCTTCTCAAC	1.95	152
IL12B	GTTCGTCATGCTCCTCTGTGTT	CATTCTCGCCCTCGTACTTCC	1.97	155
NR3C1	GCCCTCGGTCAGTGACAGCT	TTGGACCGCTGGGCTTGGCA	1.97	155
SAA	TTCCCTGGTGAAGCTGCTCGA	TGACTCCTGCTGCCCACCTG	1.95	157
RPL9	ACCACATCAACCTGGAACTCA	CGCATCTTGTAACGGAAACC	1.86	163
RPL32	CAGGCGGTTTAAGGGTCAG	ATCTCAGCAGCATGGGTC	1.83	159
TP53	GAAGAAGCAGCAGGAGACAATC	TTCCCTCGGATCTGAAGAGTGT	2.00	174
TNF	TTTTCCCAGGGTGGGTTCGAG	GGAGTCTGAATAGCGCCAAATAA	2.00	159

List B: Oligonucleotides used for the initial amplification of the respective CDS, 5'- and 3'-regions of the given target genes.

Target gene	5'→3'-Sequence of Primer	T_m [°C]	Specification
MAPK3			
	CGTACAGGACCTGATGGAGACC	63.12	consensus Primer
	TTCCTGGCCTTCATGTTGATG	63.25	consensus Primer
	TTCAGCCAGGATGCAGCCCA	64.34	5'-RACE Primer
	GTGCAGCACGTTGGCAGAGT	63.87	5'-RACE Primer
MAPK1			
	GCTGTTGAAGACGCAGCA	59.85	consensus Primer
	AACGTGTGGCTACATACTCCG	60.07	consensus Primer
HSP70			
	AGACTCATCGGAGACGCAGC	63.05	consensus Primer
	AATGCTGGCCTGGGAGCT	63.25	consensus Primer
	TAACTCCAAACCAYCAAGATGTCATC	62.52	degenerate Primer
	TTAGTCAATCTCTTCAATGGTTGGG	62.61	consensus Primer
	CCTCCAGCTCCCAGGCCAGCATT	62,84	3'-RACE Primer
HSP90			
	TGAAGCACAGGAGCTCATTCTTATC	63.15	consensus Primer
	CAGGCTGAGATCGCCCAG	63.14	consensus Primer
	CAGTCGTTGGTCAGACTCTTGTAGAA	63.15	consensus Primer
IGF1			
	AGATGTGACATTGCCTGCATCTTA	63.07	consensus Primer
	GGGGATGTCTAGCGGTCAT	59.90	consensus Primer
	TTTGCTGGGCTTTGTCGTG	63.30	consensus Primer
	CCCCTGTGTTTCCTCGACT	60.10	consensus Primer
	TCCACCTTTTGTTGTTTTACAGTGAA	62.95	consensus Primer
IGF2			
	AACTGGGAAACTAACTCAACTGCAAC	63.05	consensus Primer
	AACACAAGAATGAAGGTCAAGATG	59.56	consensus Primer
	GCTCAATTGTGGCTGACGTA	59.87	consensus Primer
	GGGAGTTGGGGTGCTGGT	63.35	consensus Primer
IL1B			
	AGGATTCACAAGAACTAAGGACTGA	63.10	consensus Primer
	GTAGAGGTTGGATCCCTTTATGC	63.60	consensus Primer
	CAGTGTTTGCGGCCATCTTAG	62.94	consensus Primer
	TAGAGGATCTCTATTGGAGGCCTTG	63.18	consensus Primer
	AAGGACTGAATACAAGACAACTGCT	60.46	3'-RACE Primer
	GGGCGTGACGTACGAAGACA	62.46	3'-RACE Primer
IL6			
	AGCATCACTGGACACAGAGCC	62.39	consensus Primer
	ACACGCTTCCTCTCACTGGC	62.44	consensus Primer
	GCCTACAAACAATTAGCTGGAACATG	64.00	consensus Primer
	TTGGTTCCGCAAGGTGGTTAC	64.25	consensus Primer
	ACACTGCAAGTTTCTGTTCCAGG	61.49	consensus Primer
CXCL8			
	CAAGATGAGCATCAGAATGTCAG	59.89	consensus Primer
	GTTGTTGGCCAGCATCTTCT	60.26	consensus Primer
IL12B			
	TGACCAGCGCAACTTCAGC	63.72	consensus Primer
	GGTGCAGCCATAAGACTTGGC	64.18	consensus Primer
	GCCAAGTCTTATGGCTGCACC	64.18	consensus Primer
	CTGATCCATCACCTGGCACTTC	64.18	consensus Primer
	GAAGTGCCAGGTGATGGATCAG	64.18	3'-RACE Primer
NR3C1			
	CCAGCAAACTCGAACTGGAGATG	64.00	consensus Primer
	TTGGAGGCGAGTATTGCAG	59.96	consensus Primer
	CTTCCGCAAGTGTCTCCAA	59.97	consensus Primer
	TACTGGTGGGGTTCCTGGG	63.08	consensus Primer
	GATTCACGGTCTAAACACGATTCC	63.03	consensus Primer
SAA			
	GGAGTTCAAACTGCCTGACTGACTAA	64.13	consensus Primer
	TTGTAGGAGCTCAAGCTCAGTGGTAC	64.25	consensus Primer
	TGGTCCTTCAGTTTGGCTAGTAACC	63.80	consensus Primer
TP53			
	CTGCGTGCTGCTTTGAGGTG	64.50	consensus Primer
	GTGGGTGTCATGGCTTGCTG	64.10	consensus Primer
TNF			
	AGACTTTYCCACTGCCACC	60.10	degenerate Primer
	GGCCTGCCTCTCTCTCATC	60.05	consensus Primer
	GCTGACACAGTGCAGTGGAG	61.23	3'-RACE Primer

A.3. Chemicals and media

Agarose	Biodeal, Markkleeberg
Ampicillin	AppliGene, Illkirch Graffenstaden
Antibiotic Antimycotic Solution	Sigma Aldrich, Taufkirchen
Bacto-tryptone	Difco Laboratories, West-Molesey, UK
Boric acid	Carl Roth, Karlsruhe
Bovine Serum Albumin	Sigma Aldrich, Taufkirchen
Bromophenol blue	Serva, Heidelberg
Calcium chloride	Carl Roth, Karlsruhe
Chloroform	Carl Roth, Karlsruhe
dNTPs	Roche, Basel, Schweiz
DMEM (11971-025)	Gibco, Life Technologies, Carlsbad, USA
EDTA	Carl Roth, Karlsruhe
Ethanol	Carl Roth, Karlsruhe
FBS	PAN-Biotech, Aidenbach
Glucose	Carl Roth, Karlsruhe
Glycerol	Carl Roth, Karlsruhe
Hydrocortisone	Sigma-Aldrich, Taufkirchen
IPTG	Carl Roth, Karlsruhe
Isopropanol	AppliChem, Darmstadt
Magnesium chloride	Merck, Darmstadt
Magnesium sulfate	Merck, Darmstadt
Manganese(II) chloride	Merck, Darmstadt
MOPS	AppliChem, Darmstadt
PBS solution	Biochrom, Berlin
Potassium chloride (KCl)	Carl Roth, Karlsruhe
Rubidium chloride	AppliChem, Darmstadt
Sodium chloride (NaCl)	AppliChem, Darmstadt
Sodium dodecyl sulfate	AppliChem, Darmstadt
Succinic anhydride (BSA)	Sigma Aldrich, Taufkirchen
Tetracycline	AppliChem, Darmstadt
Tris	AppliChem, Darmstadt
Triton-X	Boehringer Mannheim (Roche)
Tryptone	Carl Roth, Karlsruhe
Tween 20	AppliChem, Darmstadt
X-gal	Carl Roth, Karlsruhe
Yeast extract	Carl Roth, Karlsruhe
β-Mercaptoethanol	Serva, Heidelberg
2-Phenoxyethanol	Sigma Aldrich, Taufkirchen

A.4. Kits and reagents

CloneJET PCR Cloning Kit	Life Technologies, Carlsbad, USA
Control Line Fluid Kit 192.24	Fluidigm Corporation, South San Francisco, USA
Cortisol Enzyme Imunoassay Kit	DRG Instruments, Marburg
DNeasy Blood & Tissue-Kit	Qiagen, Hilden
DNA Suspension Buffer	Affymetrix, Santa Clara, USA
Exonuclease I	ThermoScientific, Waltham, USA
FastRuler Low Range DNA Ladder	ThermoScientific, Waltham, USA
GeneRuler 1 kb Range DNA Ladder	ThermoScientific, Waltham, USA
GenomeWalker™ Universal Kit	Clontech, Heidelberg
Glucose Colorimetric Assay Kit	BioVision, Milpitas, USA
High Pure PCR Product Purification Kit	Roche, Basel, Schweiz
HotStarTaq Plus DNA Polymerase	Qiagen, Hilden
InsTAClone-Kit	ThermoScientific, Waltham, USA
pGem T-easy Ligation-Kit	Promega, Fitchburg, USA
Q5 High-Fidelity DNA Polymerase Kit	New England BioLabs, Ipswitch, USA
Reverse Transcription & PreAmp Master Mix	Fluidigm Corporation, South San Francisco, USA
RNeasy Plus Universal Kit	QIAGEN, Hilden
RNeasy Mini Kit	Qiagen, Hilden
SensiFast SYBR No-ROX Kit	Bioline, London, UK
Sso-Fast EvaGreen Supermix with Low ROX	Bio-Rad, Hercules, USA
Super Script II Reverse Transcriptase Kit	Invitrogen, Karlsruhe
ZR Plasmid Miniprep Classic Kit	Zymo Research, Freiburg
2nd Generation 5'/3' RACE Kit	Roche,Basel, Schweiz
192.24 DELTAgene Sample and Assay Reagent Kit	Fluidigm Corporation, South San Francisco, USA

A.5. Equipment

ABI PRISM™Systeme	Applied Biosystems, Darmstadt
Array Scanner 428	Affimetrix, Santa Clara, USA
Biological Safety Cabinet Herasafe HS	Thermo Fisher Scientific, Waltham, USA
Biomark HD-System	Fluidigm Corporation, South San Francisco, USA
Block Heater Stuart SBH130D	Bibby Scientific Limited, Staffordshire, USA
Centrifuge Allegra X-12R Benchtop	Beckman Coulter, Krefeld
Centrifuge 5417R	Eppendorf, Hamburg
CO_2-Incubator	Memmert, Schwabach
Confocal laser scanning microscope LSM 780	Carl Zeiss Microscopy, Jena
DNA Thermal Cycler Perkin Elmer Cetus	Scientific Support, Inc, Hayward, USA
DTX 800/880 Series Multimode Detector	Beckman Coulter, Brea, California, USA
Electrophoresis chamber (Electro-4)	FisherScientific, Schwerte
Electrophoresis chamber, Standard Power Pack P25	Biometra, Göttingen
Homogeniser Precellys 24	Peqlab Biotechnologie, Erlangen
IFC Controller RX	Fluidigm Corporation, South San Francisco, USA
Laminar flow hood HERAsafe KS	Heraeus Instruments, Hanau
LightCycler 96 Real-Time PCR System	Roche, Mannheim
Low Voltage Power Supply Power Pack P25	Biometra, Göttingen
Microfuge MicroV	FisherScientific, Schwerte
Micro scale Delta Range® PM480	Mettler-Toledo, Greifensee, Schweiz
Nikon TMS-F inverted phase contrast microscope	Nikon Instruments Inc., Melville, USA
Milli-Q Integral Water Purification System	Millipore, Billerica, USA
NanoDrop 1000	Peqlab Biotechnologie GmbH, Erlangen
Neubauer counting chamber (haemocytometer)	Neolab, Heidelberg
Thermocycler T1	Biometra, Göttingen
Thermocycler Tprofessional	Biometra, Göttingen
ThermoShaker TSC	Biometra, Göttingen
Vortex-Genie 2	Scientific Industries, Bohemia, USA
Water bath Medingen W6	Labortechnik Medingen, Dresden

A.6. Online tools, software, databases

Adobe Acrobat Reader DC, Version 2018.011	Adobe Systems Incorporated, 1984-2017
BioMark HD Data Collection Software v.3.1.2	Fluidigm Corporation, South San Francisco, USA
BioVenn webbased software	http://www.biovenn.nl/index.php
BLAST (Basic Local Alignment Search Tool)	https://blast.ncbi.nlm.nih.gov/Blast.cgi
NPS@:CLUSTALW, multiple sequence alignment of nucleotide and amino acid sequences	Prabi-Gerland Rhone-Alpes Bioinformatic Pole Gerland Site, Institute of Biology and Protein Chemistry, 2016, PBIL-IBCP-Lyon
conversion tool for nucleic acids: weight into mol	http://www.molbiol.ru/ger/scripts/01_07.html
ClustalOmega webbased software	https://www.ebi.ac.uk/Tools/msa/clustalo/
Dict.cc dictionary webpage	https://www.dict.cc
European Nucleotide Archive (ENA) database	European Bioinformatics Institute (EMBL-EBI), Cambridge, UK
ExPASy, Bioinformatics Resource Portal, webpage and linked services	Swiss Institute of Bioinformatics, Biozentrum, University of Basel, Switzerland
Google webpage and services	Google LLC, CA, USA
gplots version 3.0.1, R programming tool	Gregory R. Warnes
GraphPadPrism software version 5.01 and 7.03	GraphPad Software Inc., 1992-2017, CA, USA
HUGO Gene Nomenclature Committee (HGNC) website	https://www.genenames.org
IFC Controller RX software, version	Fluidigm Corporation, South San Francisco, USA
Image Lab Software version 4.1	BioRad, Hercules, USA
Ingenuity Pathway Analysis (IPA) Software version 43605602	Ingenuity IPA, Qiagen Bioinformatics, CA, USA
Ingenuity Target Explorer webpage	https://targetexplorer.ingenuity.com/index.htm
Jalview version 2.10.3b1, MSA editor	Waterhouse, A.M., Procter, J.B., Martin, D.M.A, Clamp, M. and Barton, G. J., 2009
LightCycler 96 Software version 1.0.0.1240	Roche, Basel, Switzerland
Limma version 3.34.9, R programming tool	Gordon Smyth, http://bioinf.wehi.edu.au/limma

Limma version 3.34.9, R programming tool	Gordon Smyth, http://bioinf.wehi.edu.au/limma
Linguee webpage	DeepL GmbH, Cologne, Germany
Lyx, version 2.2.3	LyX, Matthias Ettrich, 1995--2017 LyX-Team
MEGA software Version 7.0.26	MEGA, 1993-2018, Koichiro Tamura, Glen Stecher, Sudhir Kumar
Mendeley Desktop software, Version 1.17.13	Mendeley Ltd., 2008-2018, Elsevier Inc., New York, USA
Microsoft Office 2010 Professional	Microsoft Corporation, Redmond, WA, USA
NCBI database	https://www.ncbi.nlm.nih.gov/
NEB T_m Calculator	New England BioLabs, Ipswitch, USA
Notepad ++ v7.5.6 (64-bit)	Notepad++team; https://notepad-plus-plus.org
Nucleic Acid Sequence Massager	http://www.attotron.com/cybertory/ analysis/seqMassager.htm
PrimaClade Primer Visualization webpage	http://primaclade.org/cgi-bin/primaclade.cgi
Primer3Plus Software	A. Untergasser, Michelstadt, Germany; https://primer3plus.com/
PSQ Primer Design Software 1.0	Biotage AB, Uppsala, Sweden
RealTime PCR Analysis Software v.3.0.2	Fluidigm Corporation, South San Francisco, USA
RStudio Version 1.1.419	RStudio, 2009-2018, Inc., Boston, USA
SignalP 4.1 Server, webbased software	Technical University of Denmark, DTU Bioinformatics, Lungby, Denmark
Swiss-Model, protein structure homology-modelling server	Protein Structure Bioinformatics Group, Swiss Institute of Bioinformatics, Biozentrum, University of Basel, Switzerland
Unipro UGene v1.29.0 64-bit version 2017	UniPro UGENE, 2008–2018, UniPro, Novosibirsk, Russia
Venny 2.1 webbased software	http://bioinfogp.cnb.csic.es/tools/venny/
Windows 8 Pro and 10 Home	Microsoft Corporation, Redmond, WA, USA

B. Supplementary results

B.1. Phenotype characterisation

B.1.1. Ford-Walford plots

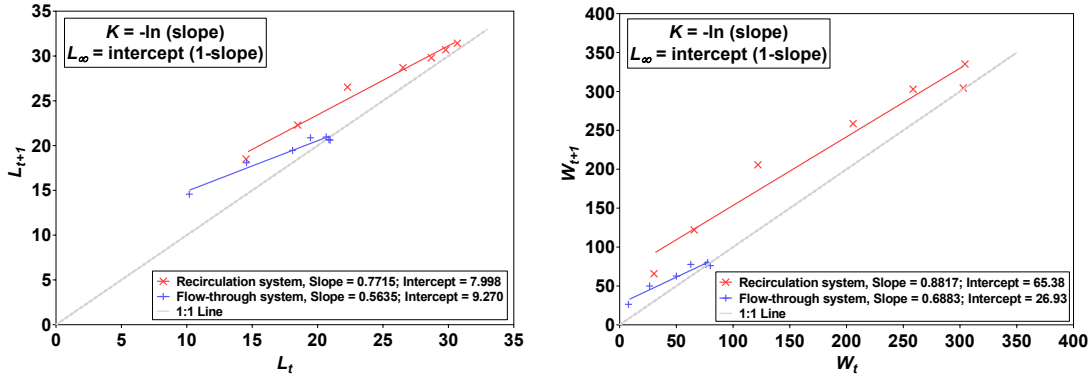

(a) Total length data (b) Total weight data

Figure B.1: **Ford-Walford plots for maraena whitefish length and weight data reared in a recirculation or flow-through system**
Length and weight data obtained from phenotype characterisation (2.1.2) were plotted at L_{t+1} and W_{t+1} against L_t and W_t, respectively to estimate initial values for K, as well as L_∞ and W_∞. Figure B.1a displays Ford-Walford plots for maraena whitefish length data, whereas figure B.1b displays respective plots for maraena whitefish weight data. Linear regression was performed to determine the respective intercept and slope of the resulting line. Subsequently, initial values for unknown Bertalanffy growth equation parameters (K, L_∞ ,W_∞) were calculated according to the formulas given top left in figure B.1a and B.1b.

B.1.2. Water temperatures at sampling in the recirculation and the flow-through system

Table B.1: Water temperatures of the recirculation and the flow-through system

sampling time point	water temperature of the recirculation system	water temperature of the flow-through system
17 wph	20.4°C	22.2°C
22 wph	20.1°C	18.2°C
27 wph	19.2°C	12.2°C
31 wph	19.4°C	8.4°C
35 wph	22.0°C	4.0°C
40 wph	17.9°C	3.9°C
45 wph	19.8°C	1.8°C
48 wph	20.8°C	5.7°C

B.2. Isolation and characterisation of target genes

B.2.1. Isolation of target genes

Table B.2: Overview of orthologous genes used in Primaclade software to derive conserved primers for the initial isolation of maraena whitefish target gene sequences.

Target gene symbol	Target gene orthologues from: Species [Accession]			Oligonucleotides deduced using Primaclade: Forward primer [5'→3']	Reverse primer [5'→3']	Fragment size in *C. maraena* [bp]
HSP70	*O. mykiss* [AB062281.1]	*S. salar* [AJ632154.1]	*O. tschawytscha* [U35064.1]	TAACTCCAAACCAYCAAGATGTCATC	AATGCTGGCCTGGGAGCT	826
HSP90	*O. tschawytscha* [U89945.1]	*S. salar* [KC150878.1]	-	TGAAGCACAGGAGCTCATTCTTATC	CAGTCGTTGGTCAGACTCTTGTAGAA	920
NR3C1	*O. mykiss* [NM_001124730.1]	*S. salar* [GQ179974.1]	-	CCAGCAAACTCGAACTGGAGATG	TACTGGTGGGGTTCCTGGG	2397
TP53	*O. mykiss* [NM_001124692.1]	*S. salar* [AY617117.1]	*C. lavaretus* [EU978857.1]	CTGCGTGCTGCTTTGAGGTG	GTGGGTGTCATGGCTTGCTG	440
IL1B	*O. mykiss* [AJ223954.1]	*S. salar* [AY617117.1]	*S. trutta* [AY853170.1]	AGGATTCACAAGAACTAAGGACTGA	TAGAGGATCTCTATTGGAGGCCTTG	886
IL6	*O. mykiss* [DQ866150.1]	*S. salar* [LN624512.1]	-	AGCATCACTGGACACAGAGCC	ACACTGCAAGTTTCTGTTCCAGG	721
CXCL8	*O. mykiss* [AY160981.1]	*O. mykiss* [AJ279069.1]	*O. kisutch* [XM_020486762.1]	CAAGATGAGCATCAGAATGTCAG	GTTGTTGGCCAGCATCTTCT	249
IL12B	*O. mykiss* [AJ548829.1]	*O. mykiss* [AJ548830.1]	*S. salar* [BT049114.1]	TGACCAGCGCAACTTCAGC	CTGATCCATCACCTGGCACTTC	644
SAA	*O. mykiss* [NM_001124436.1]	*S. salar* [NM_001146565.1]	*S. gairdneri* [X99387.1]	GGAGTTCAAACTGCCTGACTGACTAA	TGGTCCTTCAGTTTGGCTAGTAACC	419
TNF	*O. mykiss* [AJ401377.1]	*S. salar* [AY848945.1]	*S. fontinalis* [AF276961.1]	AGACTTTYCCACTGCCACC	GGCCTGCCTCTCTCTCATC	801
MAPK1	*D. rerio* [AB030903.1]	*C. carpio* [AB006039.1]	-	GCTGTTGAAGACGCAGCA	AACGTGTGGCTACATACTCCG	194
MAPK3	*D. rerio* [AB030902.1]	*C. carpio* [AB006038.1]	-	CGTACAGGACCTGATGGAGACC	TTCCTGGCCTTCATGTTGATG	434
IGF1	*O. mykiss* [M95183.1]	*S. salar* [EF432852.2]	*S. alpinus* [GU933431.1]	AGATGTGACATTGCCTGCATCTTA	TCCACCTTTTGTTGTTTTACAGTGAA	720
IGF2	*O. mykiss* [NM_001124697.1]	*S. salar* [NM_001123647.1]	*S. alpinus* [GU933430.1]	AACTGGGAAACTAACTCAACTGCAACC	GGGAGTTGGGGTGCTGGT	697

B.2.2. Characterisation of immune target genes

B.2.2.1. *IL1B*

(a) Multiple sequence alignment

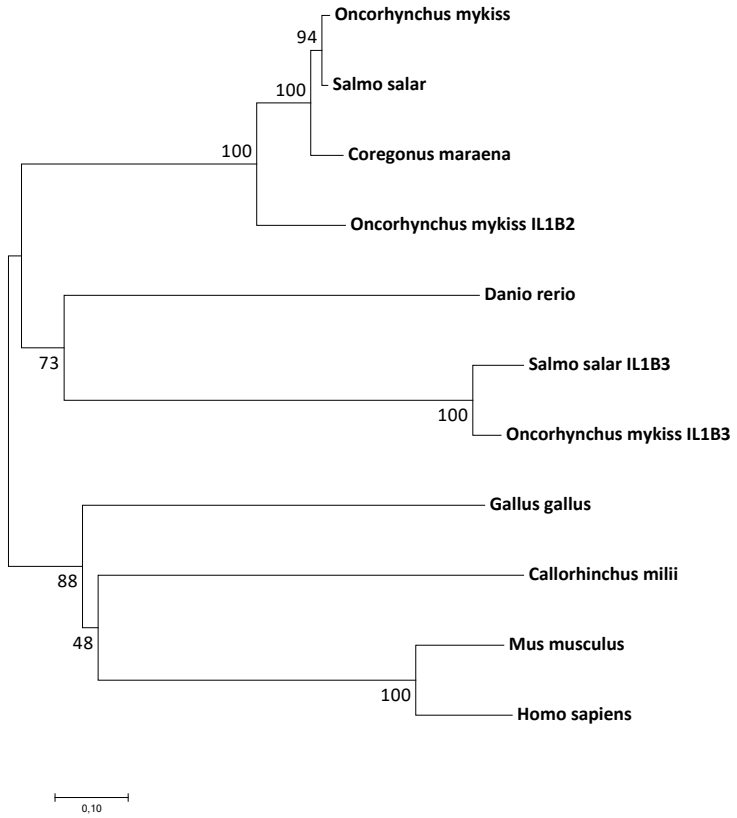

(b) Phylogenetic tree

Figure B.2: **Structural and evolutionary analysis of the putative maraena whitefish IL1B protein**
Figure B.2a shows an alignment of the predicted IL1B aa sequence (*C. maraena*, CEG62716.1) with its homologues from other fish species (bony fish:*Oncorhynchus mykiss*, NP_001117819.1; *Salmo salar*, NP_001117054.1; Danio rerio, CAR66436.1; cartilaginous fish: *Callorhinchus milii*, XP_007905654.1), bird (*Gallus gallus*, NP_989855.1), and mammals (*Mus musculus*, NP_032387.1; *Homo sapiens*, XP_016859477.1). Fully conserved aa residues are printed red, strongly similar residues in blue, weakly similar residues in green, and non-conserved residues in black. The IL1-family signature sequence is boxed in grey, whilst the potential salmonid-specific N-glycosylation site is in a red box and the mammalian cleavage site (an aspartic acid, D) for the mature protein is indicated by a blue box. Further, the predicted start region of the mature *C. maraena* IL1B protein is marked by black asterisks. Based on the given multiple sequence alignment, a phylogenetic tree was constructed as displayed in figure B.2b, which was supplemented by salmonid sequences (*Oncorhynchus mykiss*, CAB53541.3 - IL1B2, CAD89533.2 - IL1B3; *Salmo salar*, XP_013983483.1 - IL1B3) to distinguish between IL1B type I and II.

B.2.2.2. *IL6*

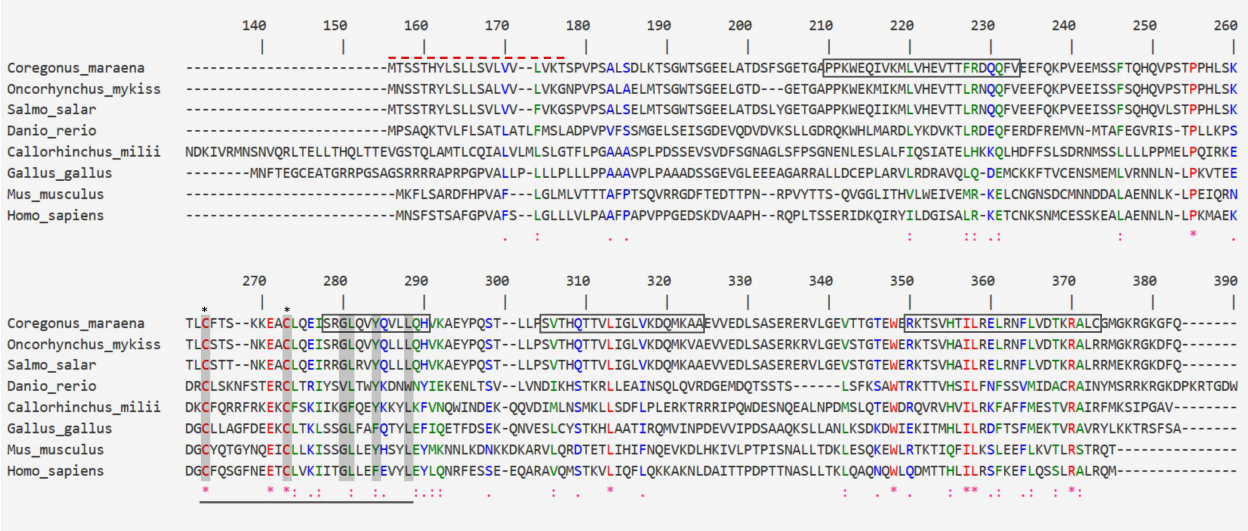

(a) Multiple sequence alignment

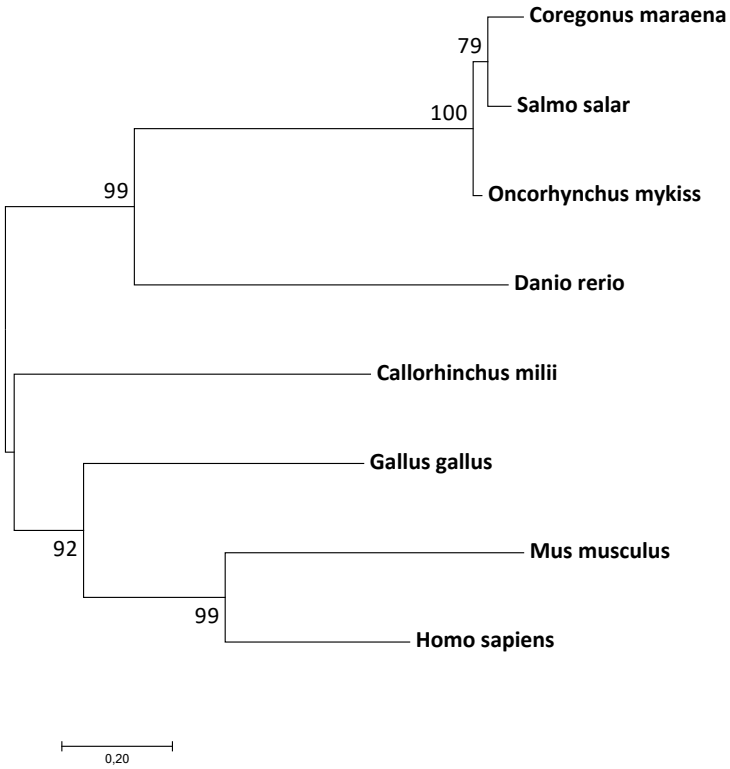

(b) Phylogenetic tree

Figure B.3: **Structural and evolutionary analysis of the putative maraena whitefish IL6 protein**
Figure B.3a shows an alignment of the predicted IL6 aa sequence (*C. maraena*, CEG62714.1) with its homologues from other fish species (bony fish:*Oncorhynchus mykiss*, CCV01624.1; *Salmo salar*, CEH11582.1; Danio rerio, AFC76325.1; cartilaginous fish: *Callorhinchus milii*, XP_007901913.1), bird (*Gallus gallus*, ADL14564.1), and mammals (*Mus musculus*, AAI38767.1; *Homo sapiens*, AAA59154.1). Fully conserved aa residues are printed red, strongly similar residues in blue, weakly similar residues in green, and non-conserved residues in black. The predicted maraena whitefish IL6 peptide structure contains a N-terminal signal peptide (marked by a red broken line), four α-helices (boxed), a IL6-family signature sequence (C–x(9)–C–x(6)–GL–x(2)–[F/Y]–x(3)–L), which is underlined, whereas the highly conserved aa residues are shaded in grey. The two strongly conserved cysteins (C) are marked by black asterisks. Based on the given multiple sequence alignment, a phylogenetic tree was constructed, as shown in figure B.3b.

B.2.2.3. *CXCL8*

(a) Multiple sequence alignment

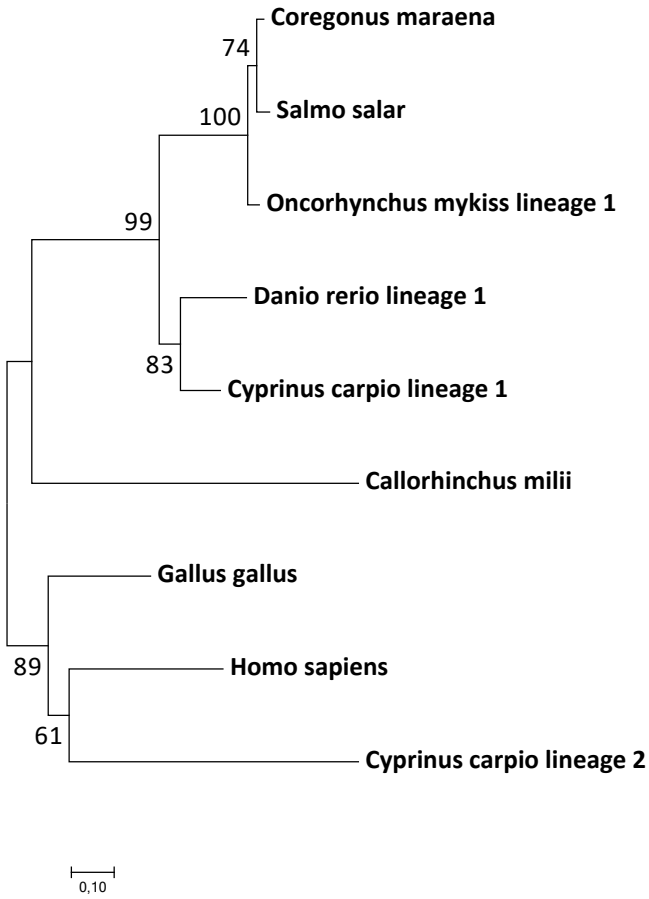

(b) Phylogenetic tree

Figure B.4: **Structural and evolutionary analysis of the putative maraena whitefish CXCL8 protein**
Figure B.4a shows an alignment of the predicted, CXCL8 aa sequence (*C. maraena*, CEG62713.1) with its homologues from other fish species (bony fish:*Oncorhynchus mykiss*,CDM63805.1; *Salmo salar*, NP_001134182.1; Danio rerio, XP_009305130.1; cartilaginous fish: *Callorhinchus milii*, AFK10667.1), bird (*Gallus gallus*, ADU60331.1), and mammal (*Homo sapiens*, AAA59158.1). Fully conserved aa residues are printed red, strongly similar residues in blue, weakly similar residues in green, and non-conserved residues in black. The predicted maraena whitefish CXCL8 protein contains a N-terminal signal peptide (indicated by a red broken line), a DLR motif (instead of the mammalian ELR-motif) that is marked by a grey box, an indicative C-x-C pattern, boxed in blue, and two additional highly conserved cystein residues (C) boxed in red. For evolutionary analyses the given multiple sequence alignment, was complemented with two sequences of common carp (*Cyprinus carpio*, CAD13189-lineage 1; BAH98111-lineage 2), to distinguish lineage 1 and 2 of the CXCL8 chemokines, resulting in the phylogenetic tree shown in figure B.4b.

B.2.2.4. *IL12B*

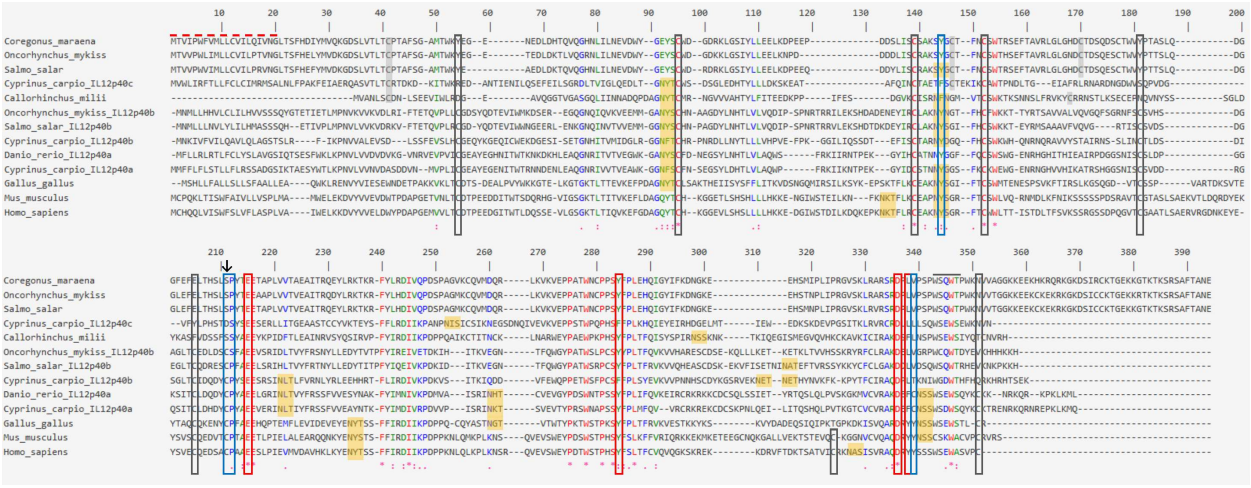

Figure B.5: **Structural analysis of the putative maraena whitefish IL12p40 protein**
Multiple sequence alignment of the predicted, IL12B aa sequence (*C. maraena*, CEG62715.1) with its homologues from other fish species (bony fish:*Oncorhynchus mykiss*, CAD69014.1, CDM74102.1-IL12p40b; *Salmo salar*, XP_014060991.1, CDM74107.1-IL12p40b; Danio rerio, AAI21765.1-IL12p40a, *Cyprinus carpio*, CAF18555.1-IL12p40a, CAF32323.1-IL12p40b, CAF32324.1-IL12p40c; cartilaginous fish: *Callorhinchus milii*, XP_007906151.1), bird (*Gallus gallu*s, NP_998736.1), and mammals (*Mus musculus*, AAF22555.1; *Homo sapiens*, NP_002178.2). Fully conserved aa residues are printed red, strongly similar residues in blue, weakly similar residues in green, and non-conserved residues in black. The predicted N-terminal signal peptide of the maraena whitefish IL12p40 protein is indicated by a red broken line, residues that are crucial or important for the formation of the IL12 hetero-dimer are boxed red or blue, respectively. Mammalian conserved cystein residues (C) are in grey boxes, whilst those cystein residues that are conserved among vertebrates are printed red and cystein residues of fish IL12p40c, that are located near to the mammalian ones are shaded in grey. The one cystein residue, that forms an interchain disulphide bride with the IL12p35 subunit is marked by a black arrow. The identified N-glycosylation motifs (NxT/S) are shaded in orange. The conserved C-terminal WSxWS motif (IL12p40a and IL12p40b) or WSxWT (IL12p40c) is indicated by a black line.

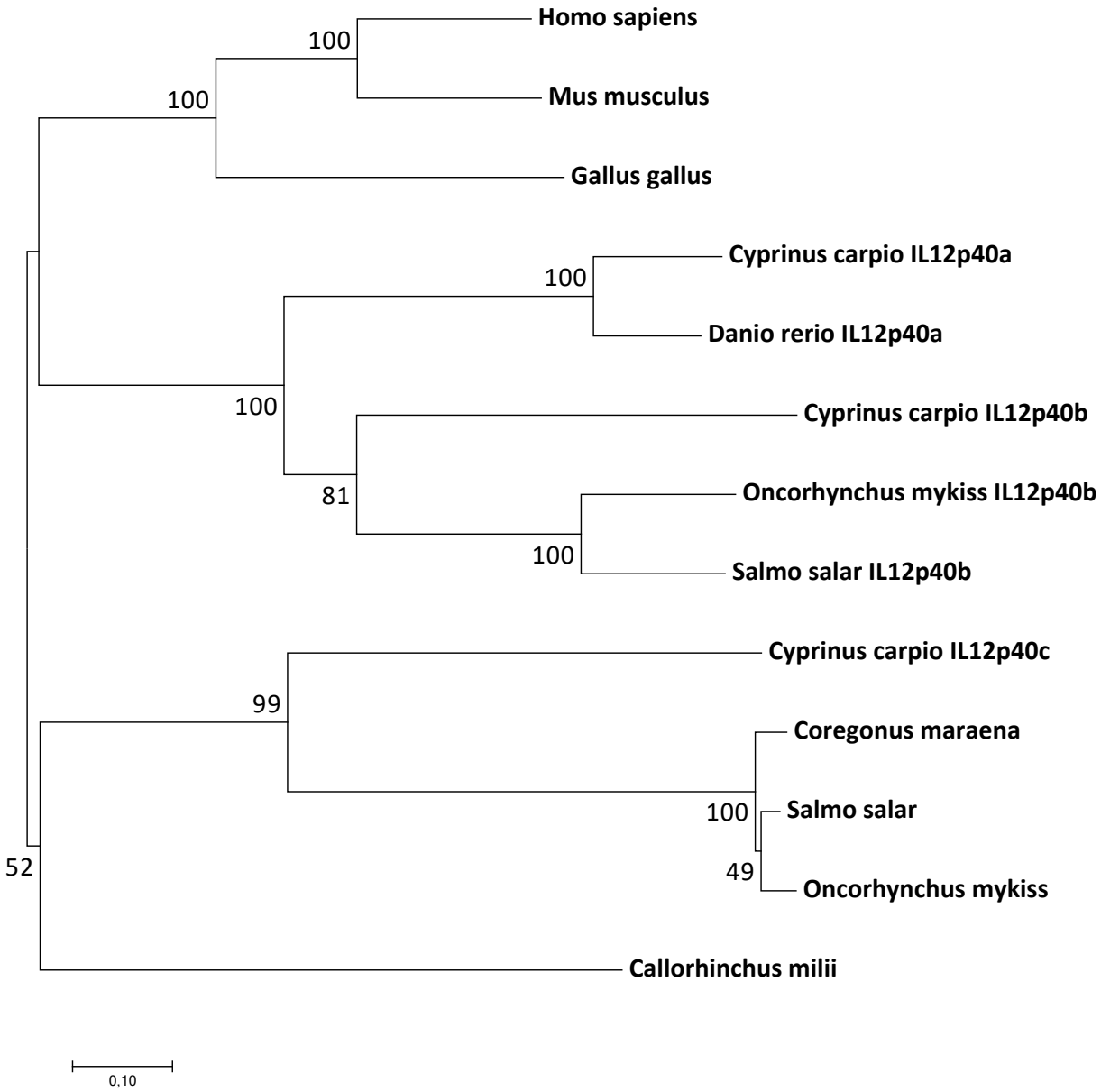

Figure B.6: **Evolutionary analysis of the putative maraena whitefish IL12p40 protein**
The phylogenetic tree was constructed based on the given multiple sequence alignment in figure B.5.

B.2.2.5. *TNF*

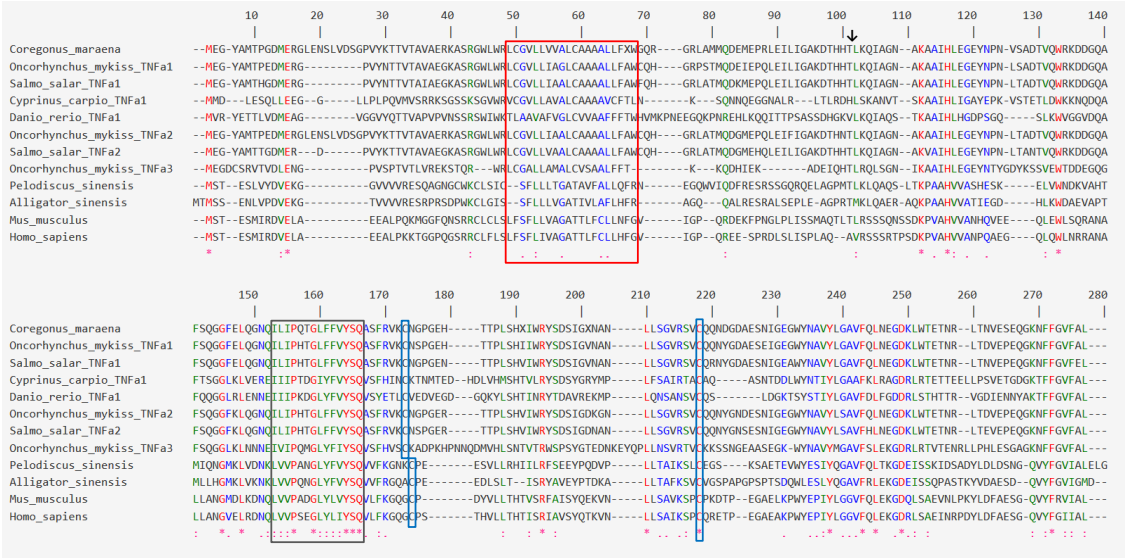

(a) Multiple sequence alignment

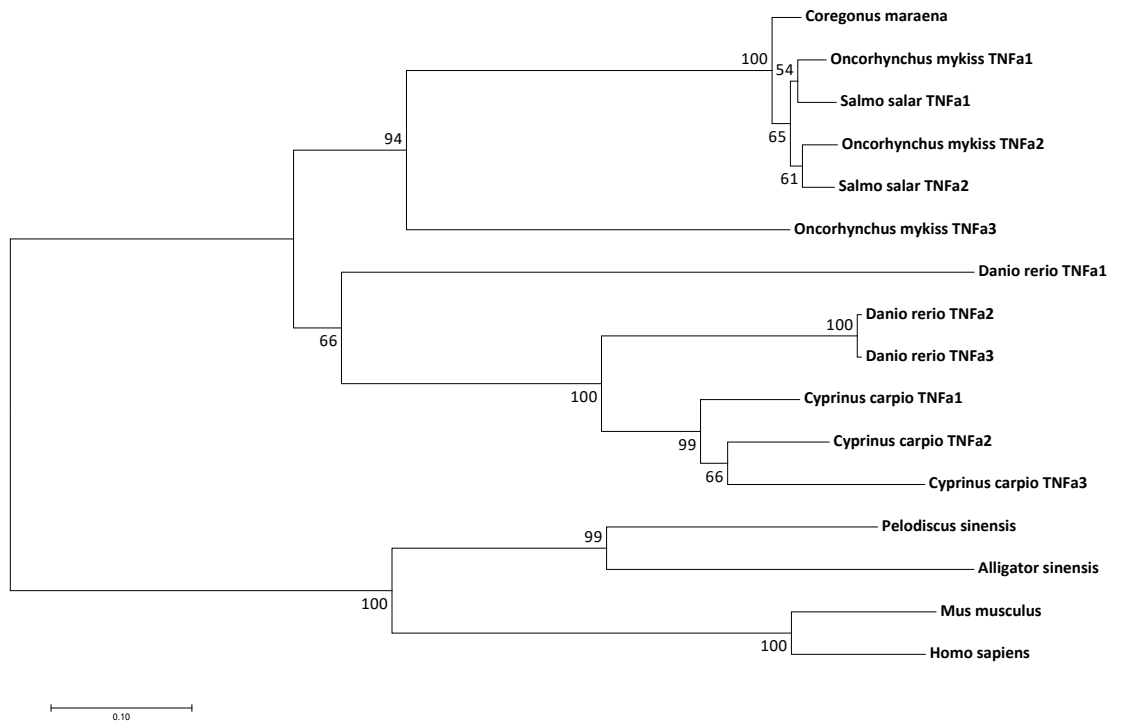

(b) Phylogenetic tree

Figure B.7: **Structural and evolutionary analysis of the putative maraena whitefish TNF protein**
Figure B.7a shows an alignment of the predicted, TNF aa sequence (*C. maraena*, SOX29784.1) with its homologues from other fish species (bony fish:*Oncorhynchus mykiss*, CAB89521.1-TNFα1, CAC16408.1-TNFα2, CCH10518.1-TNFα3; *Salmo salar*, ABG91799.1-TNFα1, ABG91800.1-TNFα2; Danio rerio, Q4W898-TNFα1; *Cyprinus carpio*, CAC84641.2-TNFα1), reptiles (*Pelodiscus sinensis*, XP_014431445.1; *Alligator sinensis*, XP_006036188.1), and mammals (*Mus musculus*, AAA40457.1; *Homo sapiens*, AAA61198.1). Fully conserved aa residues are printed red, strongly similar residues in blue, weakly similar residues in green, and non-conserved residues in black. The predicted transmembrane domain is boxed in red, whilst the TNF-family signature is marked by a black box. The two conserved cystein residues (C), that are predicted to form a disulphide bridge are boxed in blue and the putative cleavage site of the present TNF precursor sequences is indicated by a black arrow. Evolutionary analyses, resulting in the phylogenetic tree in B.7b, were conducted using the given multiple sequence alignment, complemented by additional sequences for *Danio rerio* (Q6T9C7-TNFα2, NP_998024.2-TNFα3) and *Cyprinus carpio* (CAC84642.2-TNFα2, BAC77690.1-TNFα3).

B.2.2.6. *SAA*

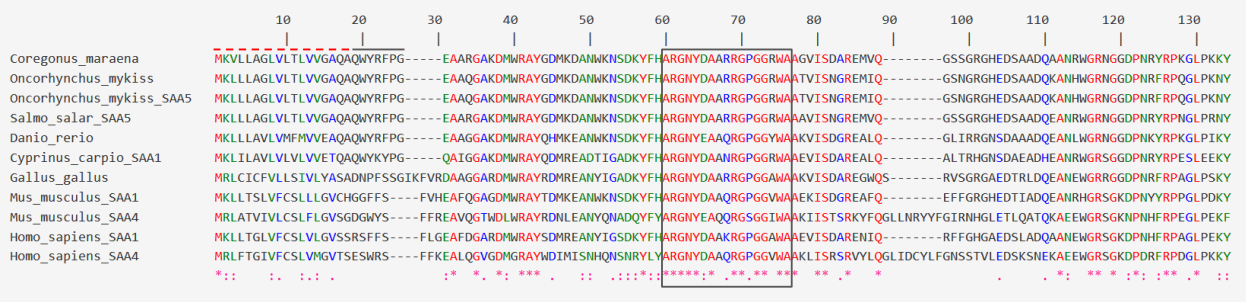

(a) Multiple sequence alignment

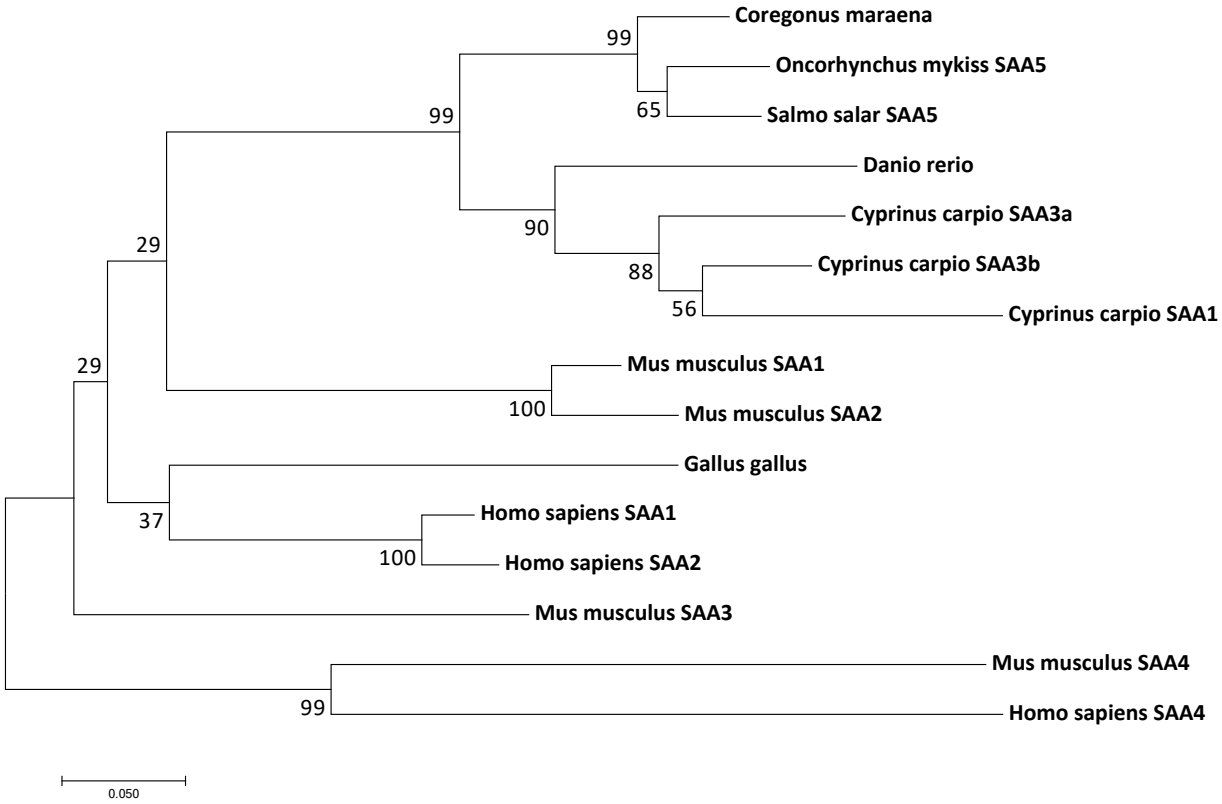

(b) Phylogenetic tree

Figure B.8: **Structural and evolutionary analysis of the putative maraena whitefish SAA protein** Figure B.8a shows an alignment of the predicted, SAA aa sequence (*C. maraena*, CEG62717.1) with its homologues from other fish species (bony fish:*Oncorhynchus mykiss*, XP_021463248.1; *Salmo salar*, NP_001140037.1; *Danio rerio*, NP_001005599.1; *Cyprinus carpio*, ARO38309.1-SAA1), bird (*Gallus gallus*, ADF56353.1), and mammals (*Mus musculus*, NP_033143.1-SAA1- , NP_035446.1-SAA4; *Homo sapiens*, NP_001171477.1-SAA1, NP_006503.2 -SAA4). Fully conserved aa residues are printed red, strongly similar residues in blue, weakly similar residues in green, and non-conserved residues in black. The predicted N-terminal signal peptide and hydrophobic region are marked by a red broken line and a black line, respectively. The conserved SAA-protein-signature pattern is boxed in black. Evolutionary analyses, resulting in the phylogenetic tree in B.8b, were conducted using the given multiple sequence alignment, complemented by additional sequences for *Cyprinus carpio* (ARO38322.1-SAA3a, ARO38323.1-SAA3b), *Mus musculus* (NP_035444.1-SAA2, NP_035445.1-SAA3) and *Homo sapiens* (NP_110381.2-SAA2).

B.2.2.7. *MAPK1* and *MAPK3*

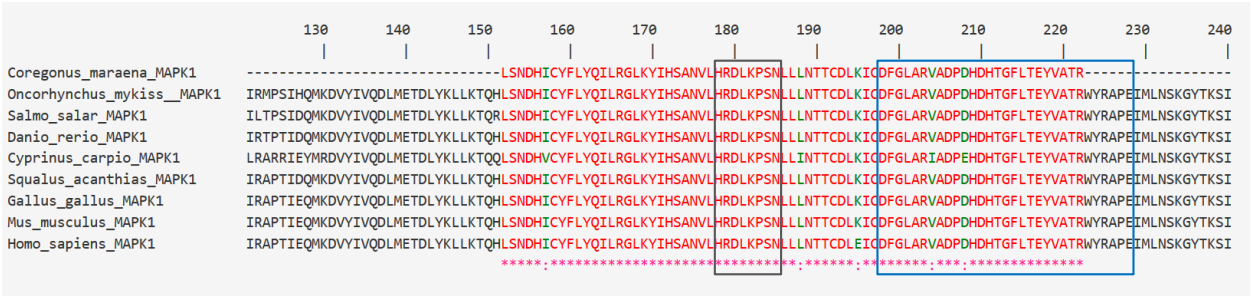

(a) Multiple sequence alignment

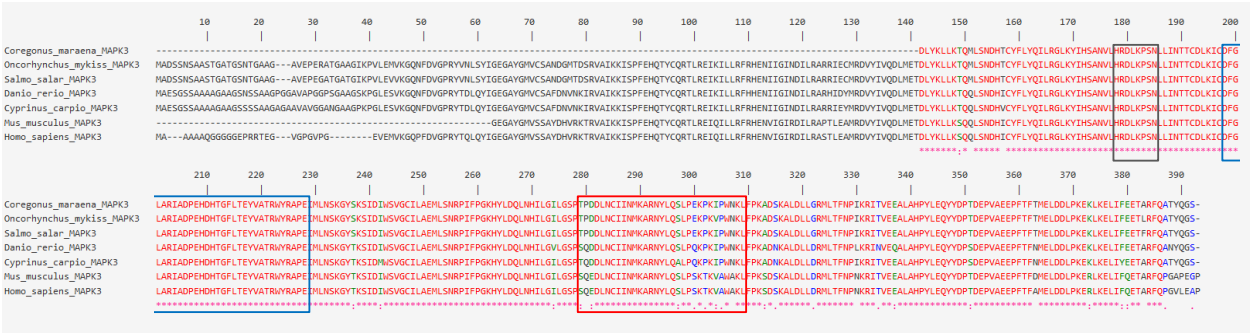

(b) Multiple sequence alignment

Figure B.9: **Structural analysis of the putative, partial maraena whitefish MAPK1 and MAPK3 proteins** Figure B.9a shows a multiple sequence alignment of the predicted, maraena whitefish MAPK1 aa sequence (*C. maraena*, SOX29803.1) with its homologues from other fish species (bony fish:*Oncorhynchus mykiss*, XP_021460756.1; *Salmo salar*, XP_013999028.1; *Danio rerio*, AAH65868.1; *Cyprinus carpio*, BAD23842.1; cartilaginous fish: *Squalus acanthias*, ALD61593.1), bird (*Gallus gallus*, NP_989481.1), and mammals (*Mus musculus*, NP_036079.1; *Homo sapiens*, AAH99905.1), whilst in figure B.9b, the putative, partial maraena whitefish MAPK3 protein (*C. maraena*, SOX29894.1) was aligned with its homologues from other fish species (bony fish:*Oncorhynchus mykiss*, XP_021455507.1; *Salmo salar*, NP_001167267.1; *Danio rerio*, NP_958915.1; *Cyprinus carpio*, BAD23842.1) and mammals (*Mus musculus*, AAH13754.1; *Homo sapiens*, NP_002737.2). Fully conserved aa residues are printed red, strongly similar residues in blue, weakly similar residues in green, and non-conserved residues in black. The predicted catalytic loop is marked by a grey box. The conserved kinase activation segment is boxed in blue and the kinase insert domain in red, while the latter is present only in MAPK3.

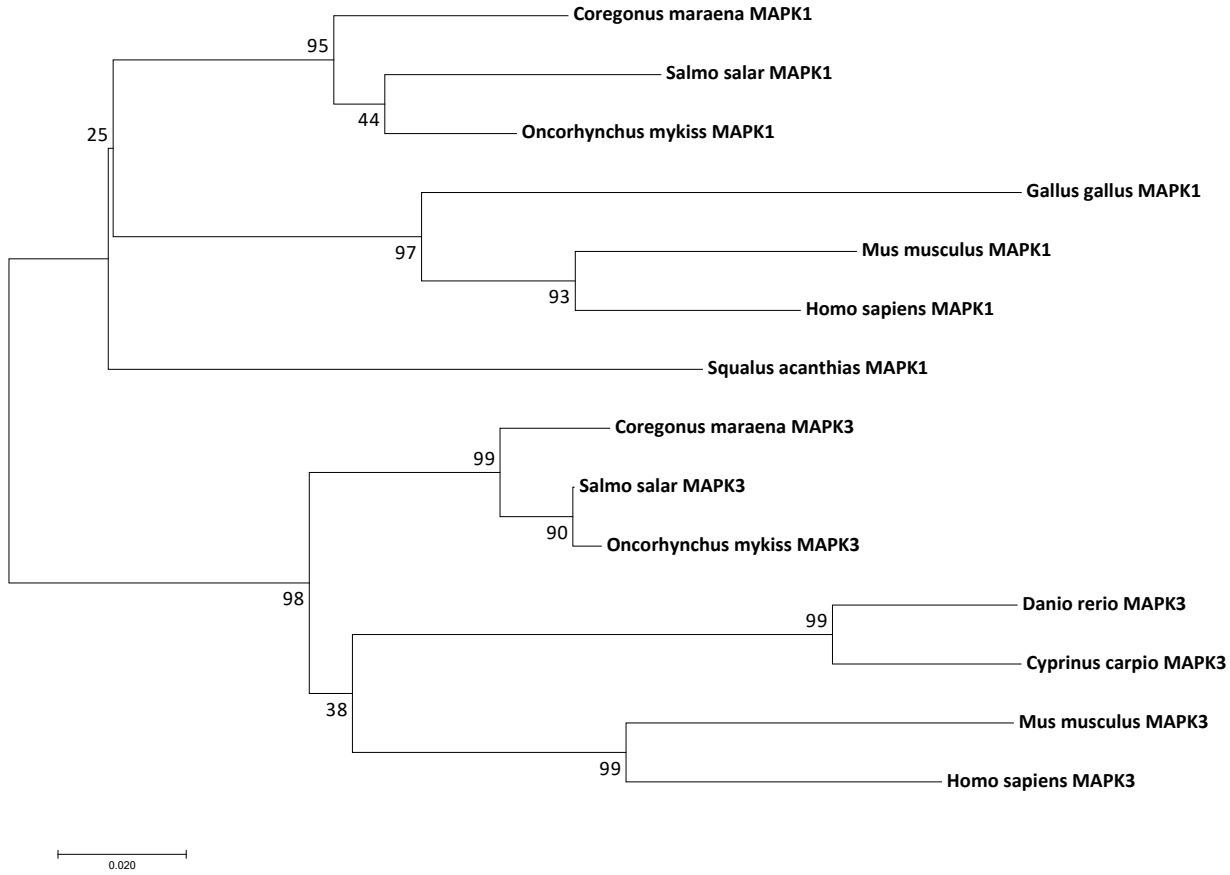

Figure B.10: **Evolutionary analysis of maraena whitefish *MAPK1* and *MAPK3* genes**
Evolutionary analyses, were conducted based on mRNA sequences of *C. maraena MAPK1* and *MAPK3* genes (LT971012.1, LT971391.1), as well as those from other fish species (teleost fish: *Oncorhynchus mykiss*, XM_021605081.1, XM_021599832.1; *Salmo salar*, XM_014143553.1, NM_001173796.1; *Danio rerio*, BC065868.1, NM_201507.1; *Cyprinus carpio*, AB006038.1, AB006038.1; cartilaginous fish: *Squalus acanthias*, KT324594.1), bird (*Gallus gallus*, NM_204150.1), and mammals (*Mus musculus*, NM_011949.3, BC013754.1; *Homo sapiens*, BC099905.1, NM_002746.2).

B.2.3. Characterisation of stress target genes

B.2.3.1. *HSP70*

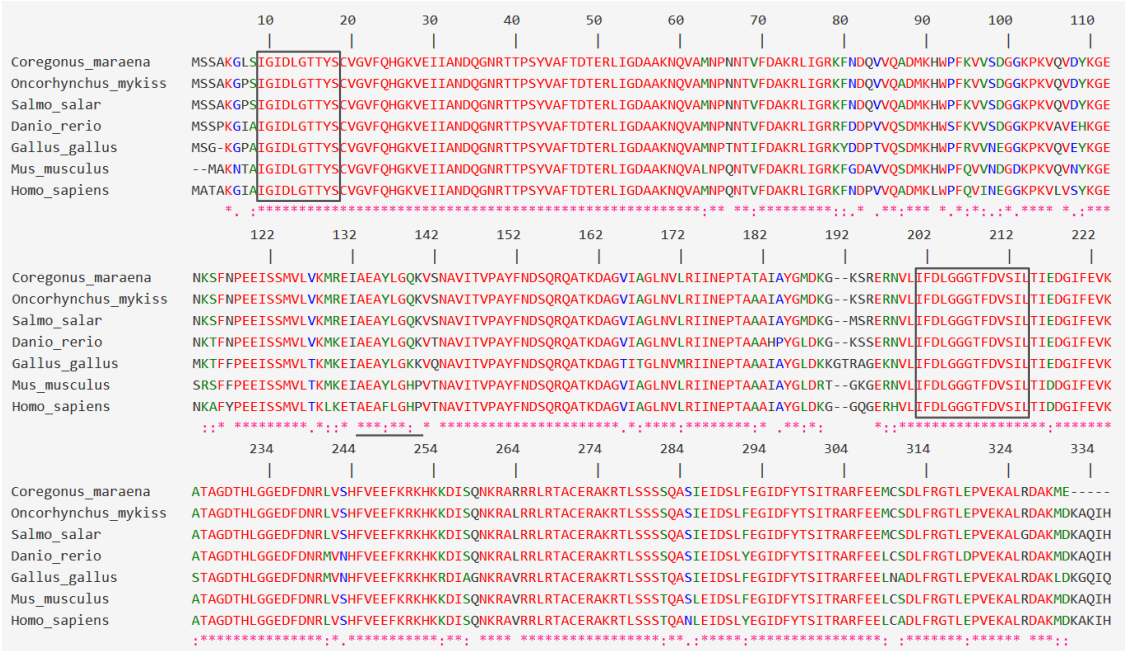

(a) Multiple sequence alignment

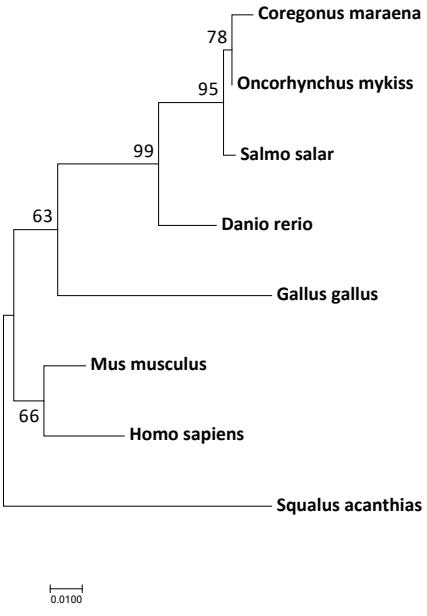

(b) Phylogenetic tree

Figure B.11: **Structural and evolutionary analysis of the putative, partial maraena whitefish HSP70 protein**

Figure B.11a shows an alignment of the predicted, partial HSP70 aa sequence (*C. maraena*, CUU33664.1) with its homologues from other fish species (*Oncorhynchus mykiss*, NP_001117700.1; *Salmo salar*, ACI34374.1; Danio rerio, AAF70445.1), bird (*Gallus gallus*, AAP37959.1), and mammals (*Mus musculus*, AAA57233.1; *Homo sapiens*, AQY76891.1). Fully conserved aa residues are printed red, strongly similar residues in blue, weakly similar residues in green, and non-conserved residues in black. The two conserved HSP70 family signature sequences are boxed and the ATP/GTP-binding site is underlined. Based on the given multiple sequence alignment, which was supplemented by one sequence for the cartilaginous spiny dogfish *Squalus acanthias* (GB: ABI93213.1), a phylogenetic tree was constructed as displayed in figure B.11b.

B.2.3.2. *HSP90*

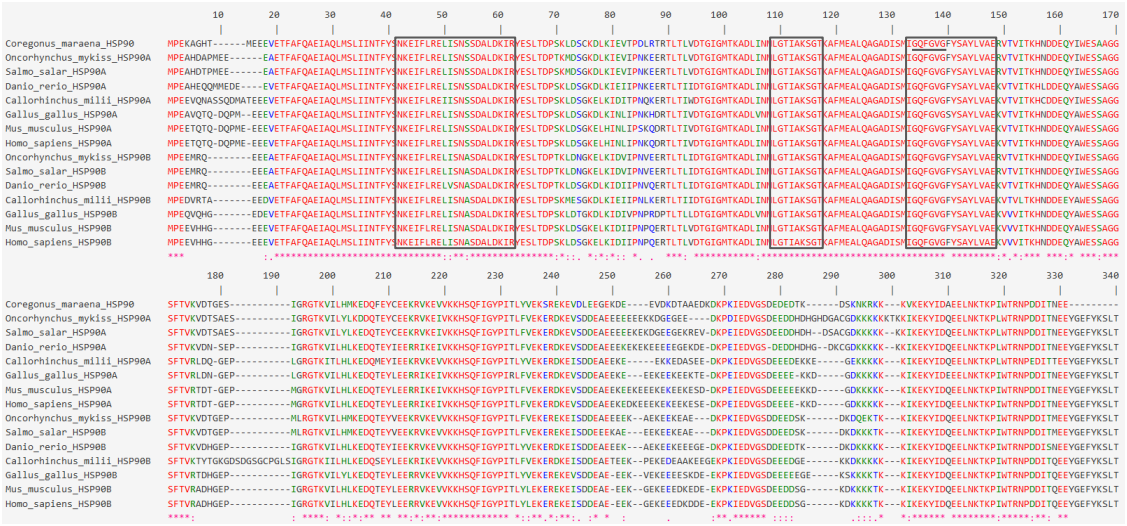

(a) Multiple sequence alignment

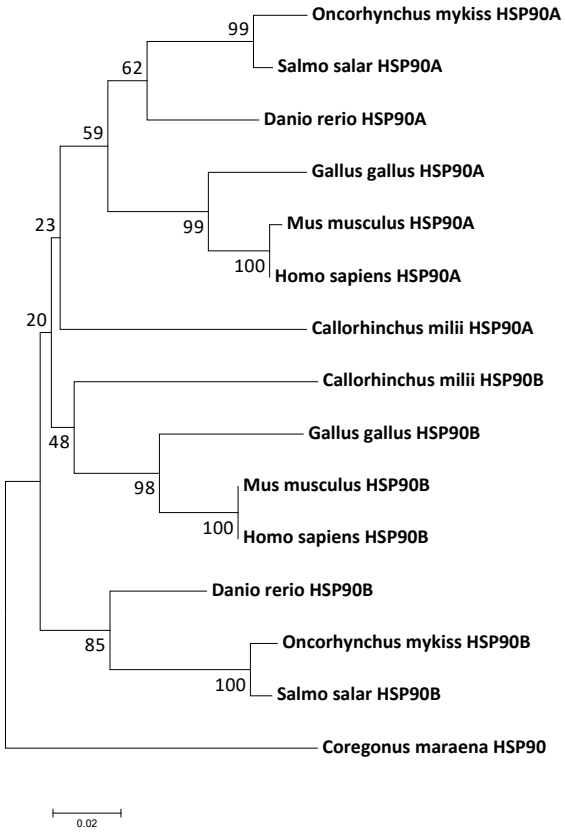

(b) Phylogenetic tree

Figure B.12: **Structural and evolutionary analysis of the putative, partial maraena whitefish HSP90 protein**

In figure B.12a the predicted, partial HSP90 aa sequence (*C. maraena*, CEP28035.1) was aligned each time with homologues of HSP90A and HSP90B from other fish species (teleosts:*Oncorhynchus mykiss*, XP_021456591.1, NP_001117703.1; *Salmo salar*, NP_001167173.1, NP_001117004.1; Danio rerio, NP_001038538.1, NP_571385.2; cartilaginous fish: *Callorhinchus millii*, XP_007886533.1, XP_007896400.1), bird (*Gallus gallus*, NP_001103255.1, NP_996842.1), and mammals (*Mus musculus*, NP_034610.1, NP_032328.2; *Homo sapiens*, EAW81767.1, NP_031381.2). Fully conserved aa residues are printed red, strongly similar residues in blue, weakly similar residues in green, and non-conserved residues in black. The three conserved HSP90 family signature sequences are boxed and the ATP-binding site is underlined. Based on the given multiple sequence alignment a phylogenetic tree was constructed as displayed in figure B.12b.

B.2.3.3. *NR3C1*

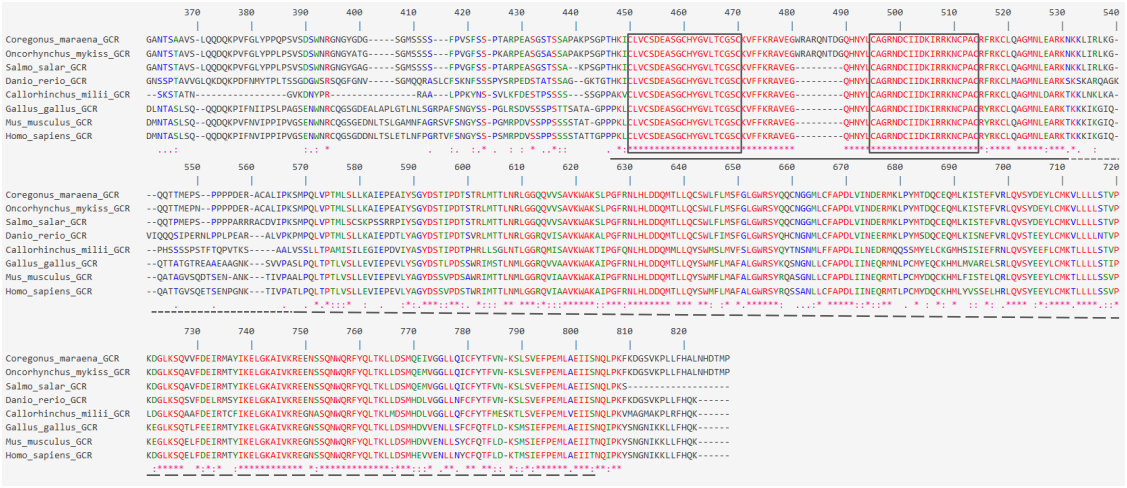

(a) Multiple sequence alignment

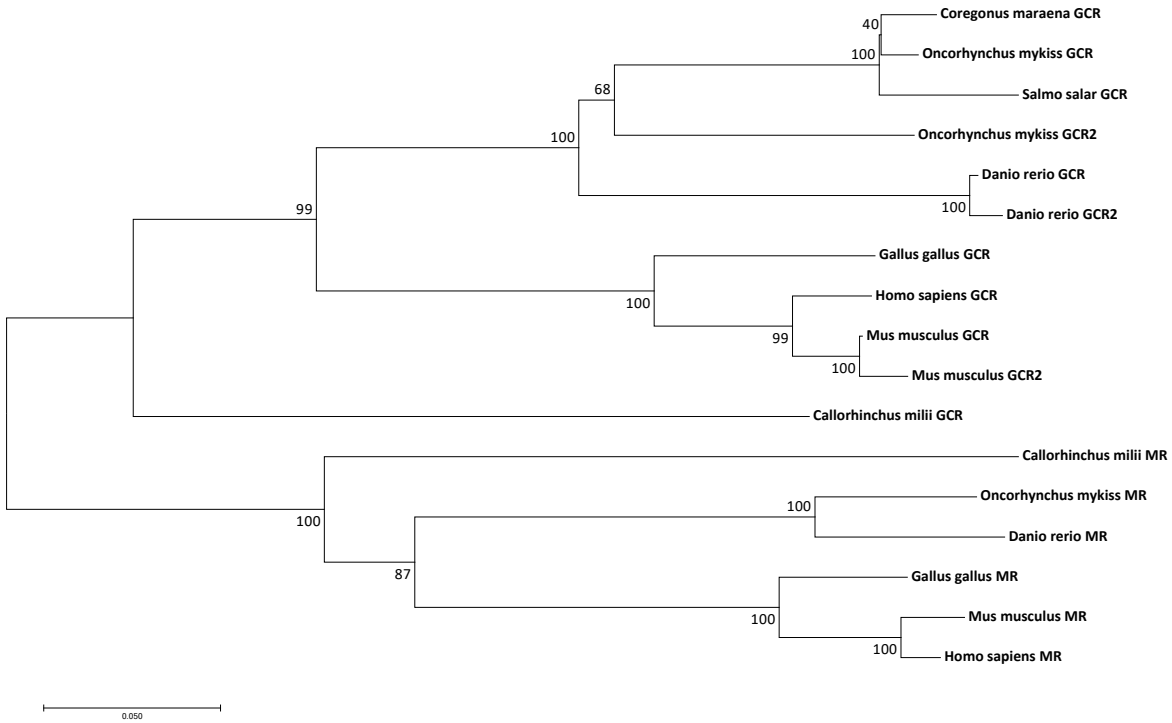

(b) Phylogenetic tree

Figure B.13: **Structural and evolutionary analysis of the putative maraena whitefish Glucocorticoid receptor**

In figure B.13a the predicted, GCR aa sequence (*C. maraena*, CEP28034.1) was aligned with GCR homologues from other fish species (teleosts:*Oncorhynchus mykiss*, NP_001118202.1; *Salmo salar*, ACS91455.1; Danio rerio, NP_001018547.2; cartilaginous fish: *Callorhinchus milii*, XP_007899521.1), bird (*Gallus gallus*, NP_001032915.1), and mammals (*Mus musculus*, NP_032199.3; *Homo sapiens*, BAH02307.1). Fully conserved amino acid residues are printed red, strongly similar residues in blue, weakly similar residues in green, and non-conserved residues in black. The DBD is underlined, containing two zinc finger motifs, which are in boxes. The species-specific hinge region is marked by a dotted line and the LBD by a broken line. For evolutionary analysis, the given multiple sequence alignment was supplemented by putative protein sequences for the GCR2 and/or the MR of teleost species (*Oncorhynchus mykiss*, GCR2: NP_001117954.1, MR: AAS75839.1; *Salmo salar*, ; Danio rerio, GCR2: ABR88076.1, MR: NP_001093873.1), cartilaginous fish (*Callorhinchus millii*, MR: XP_007902220.1), birds (*Gallus gallus*, MR: ACO37437.1;), and mammals (*Mus musculus*, GCR2: ADM18962.1, MR: NP_001077375.1; *Homo sapiens*, MR: AAC63513.1). A phylogenetic tree was constructed as displayed in figure B.13b.

B.2.3.4. *TP53*

(a) Nucleotide sequence alignment

(b) Amino acid sequence alignment

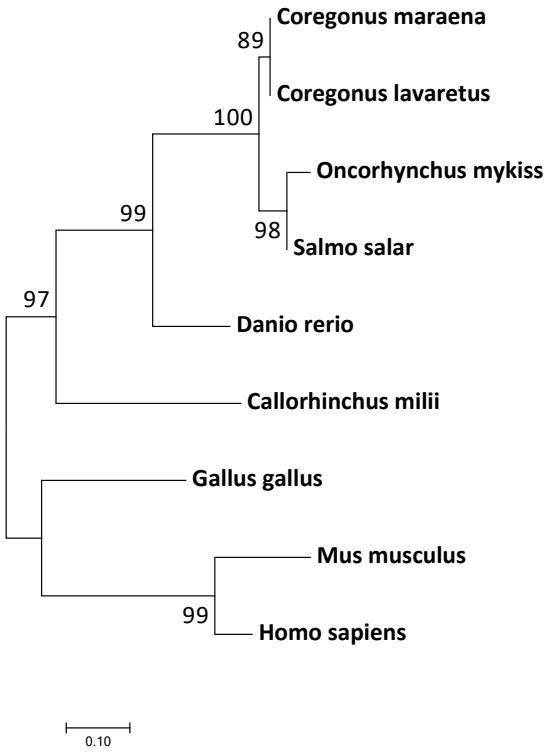

(c) Phylogenetic tree

Figure B.14: **Structural and evolutionary analysis of *TP53* cDNA and the putative, partial TP53 protein** Figure B.14a shows the alignment of the partial maraena whitefish *TP53* cDNA and the *Coregonus lavaretus TP53* cDNA (EU978857.1) from GenBank. In figure B.14b the putative, partial aa sequence for *C. maraena* was aligned with TP53 homologues from other fish species (teleosts:*Coregonus lavaretus*: ACH73252.1; *Oncorhynchus mykiss*, AAF78533.1; *Salmo salar*, XP_014051360.1; Danio rerio, AAH95597.1; cartilaginous fish: *Callorhinchus millii*, AEW46988.1), bird (*Gallus gallus*, NP_990595.1), and mammals (*Mus musculus*, AAA39883.1; *Homo sapiens*, BAD96746.1). Fully conserved amino acid residues are printed red, strongly similar residues in blue, weakly similar residues in green, and non-conserved residues in black. The P53 DBD is boxed in dark grey, whereas the tetramerisation motif is boxed in light grey. For evolutionary analysis, the given multiple sequence alignment was used, and a phylogenetic tree was constructed as displayed in figure B.14c.

B.2.4. Characterisation of growth target genes

B.2.4.1. *IGF-1* and *IGF-2*

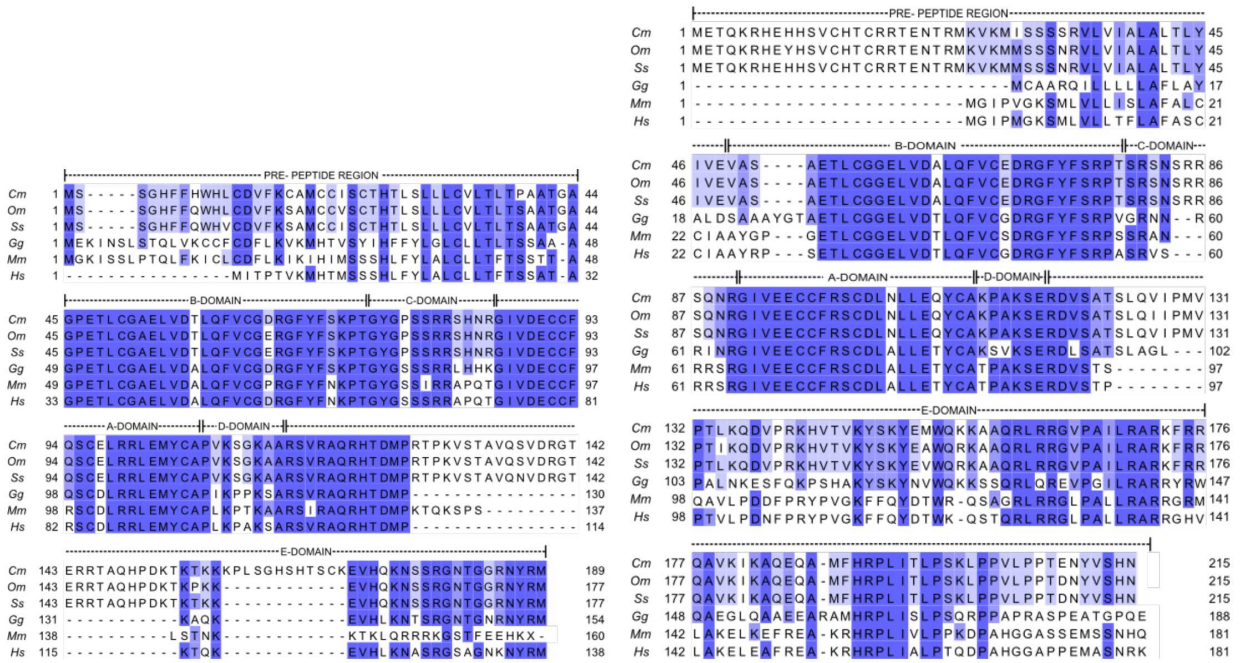

(a) IGF-1 (b) IGF-2

Figure B.15: **Structural analysis of deduced maraena whitefish IGF-1 and IGF-2 proteins**
The figures show multiple sequence alignments of predicted IGF-1 (B.15a) and IGF-2 (B.15b) amino acid sequences (Cm: *C. maraena*, CEP28032.1, CEP28033.1) with its homologues from other fish species (Om: *Oncorhynchus mykiss*, AAA49412, NP_001118169; Ss: *Salmo salar*, ABO36526, ABO36528), bird (Gg: *Gallus gallus*, AAA48828, NP_001025513), and mammals (Mm: *Mus musculus*, NP_034642, AAA37683; Hs: *Homo sapiens*, AAA52789, AAA52545). Fully conserved amino acid residues are shaded in dark blue. Residues that are identical in five or in three to four sequences are shaded in light blue. The B-, C-, A-, and D-domains of the mature protein are marked by dashed lines above the sequences, as well as the pre-peptide region and the E-Domain of the pre-protein. Figures adopted from Nipkow *et al.* (2018).

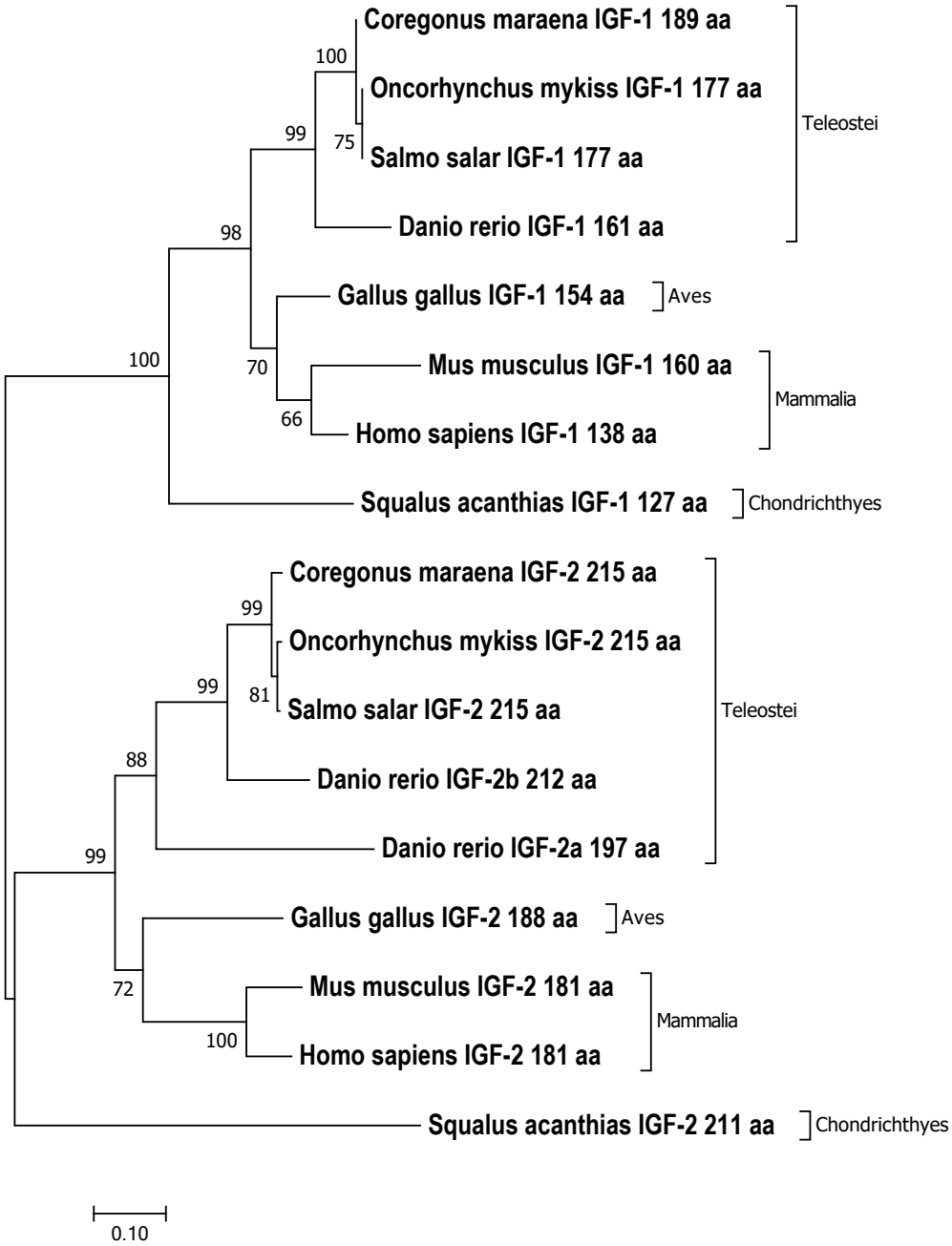

Figure B.16: **Evolutionary analysis of deduced maraena whitefish IGF-1 and IGF-2 proteins**
The evolutionary analysis was based on the multiple sequence alignments shown in figure B.15a and B.15b. It included overall 17 aa sequences for IGF-1 and IGF-2. Directly after the indicated species and gene names, protein lengths are given. Taxonomic classifications of the given species are assigned by brackets. The additionally applied protein sequences were the following: zebrafish *Danio rerio* (AAI14263.1, AAH85623.1, NP_001001815.1) and spiny dogfish *Squalus acanthias* (CAA90412.1, CAA90413.1). Figure adopted from Nipkow *et al.* (2018).

B.3. Tissue Profiling

B.3.1. Tissue profiling of maraena whitefish immune genes

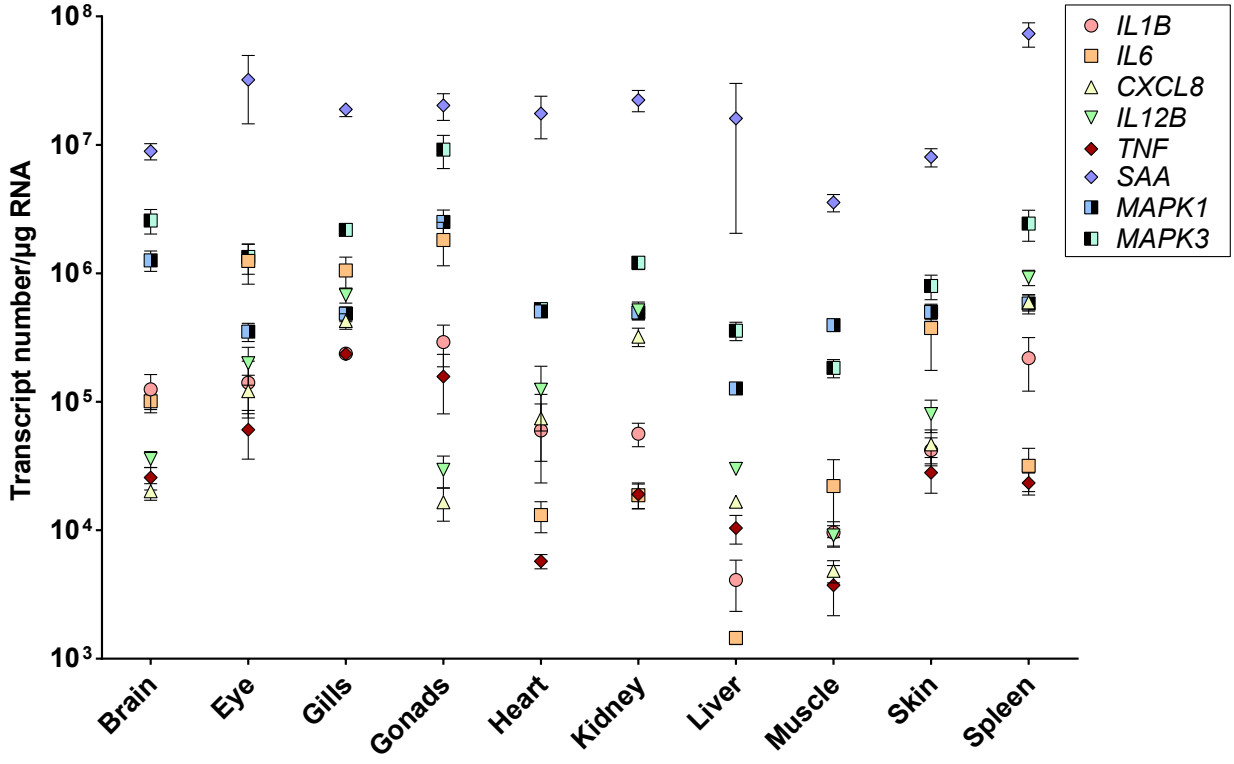

Figure B.17: **Tissue-specific expression of maraena whitefish immune related target genes**
Tissue-specific distribution of mRNA levels of immune related genes in maraena whitefish measured by qPCR. The graph displays means of direct transcript numbers related to 1 µg RNA ±SEM of 4 fish, respectively. One-way ANOVA and Tukey-Kramer multiple comparisons tests were used for statistical analysis. There were no significant differences found in expression levels between tissues of an individual target gene.

B.3.2. Tissue profiling of maraena whitefish stress genes

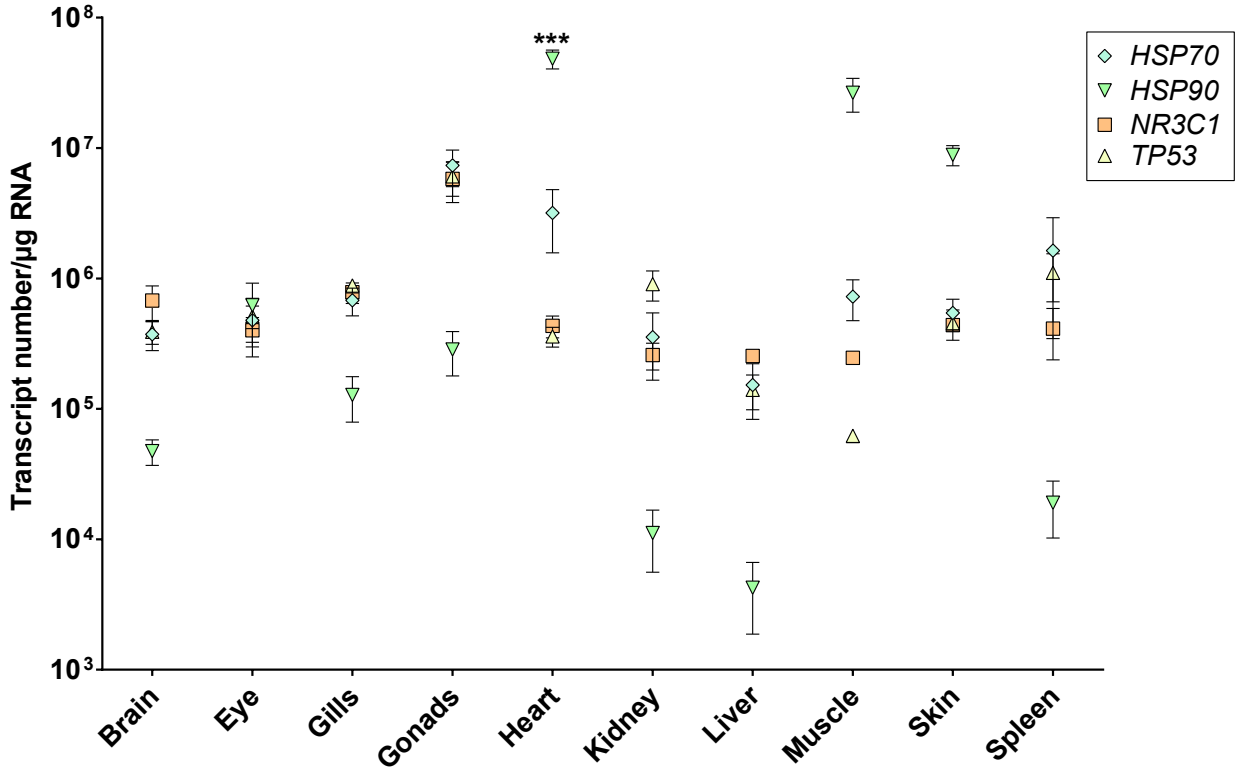

Figure B.18: **Tissue-specific expression of maraena whitefish stress related target genes**
Tissue-specific distribution of mRNA levels of stress related genes in maraena whitefish measured by qPCR. The graph displays means of direct transcript numbers related to 1 µg RNA ±SEM of 4 fish, respectively. Significant differences in expression levels between tissues of each gene, were computed by one-way ANOVA and Tukey-Kramer multiple comparisons tests. Values were considered significant if gene expression in a specific tissue, was determined as significant compared to all other tissues for the same gene. Significant differences are marked with black asterisks above the symbols (***, $p \leq 0{,}001$).

B.4. Density stress

B.4.1. Immune target genes

B.4.1.1. Acute density stress

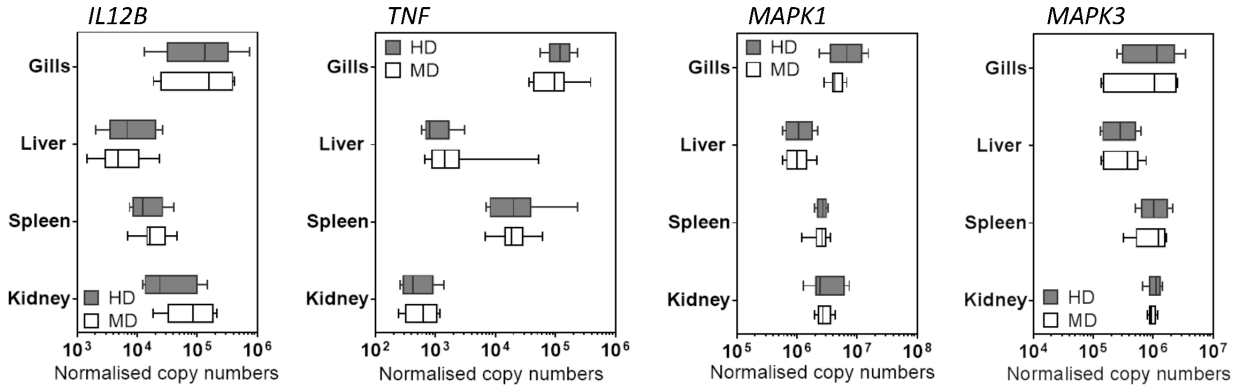

Figure B.19: The box-whisker plots depict copy numbers (x-axis) of the target genes (indicated above the plot) in different tissues (y-axis) measured in each time eight individuals, and normalised by the reference gene *RPL9*. The left to right border of the boxes indicate the 25 to75 percentiles and the vertical line within the box mark the median, whereas the whiskers represent the 10 to 90 percentiles (from left to right). The different treatment categories given in the plot are high density (HD) in dark grey, and moderate density (MD) in light grey.

B.4.1.2. Short-term density stress

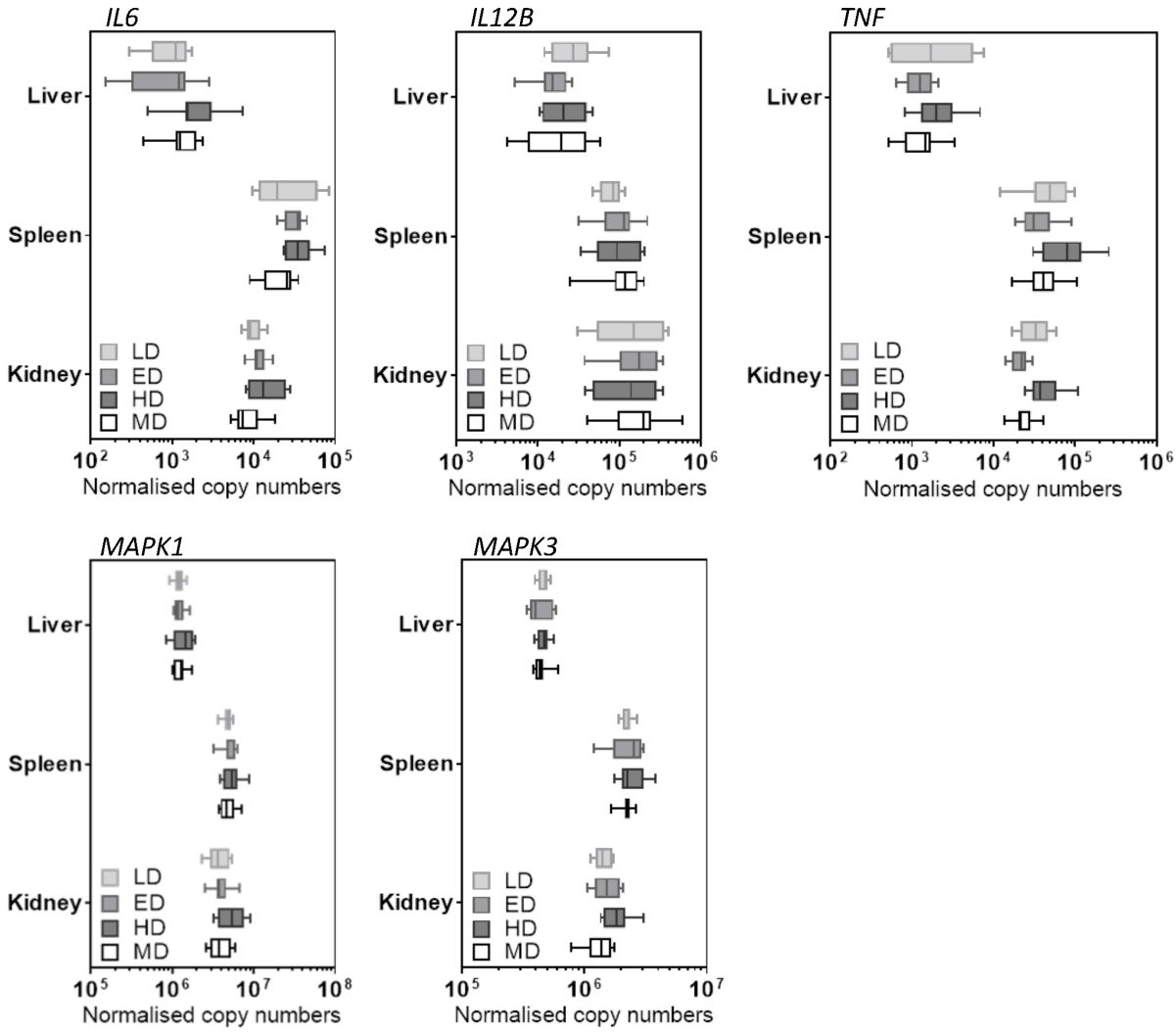

Figure B.20: The box-whisker plots depict copy numbers (x-axis) of the target genes (indicated above the plot) in different tissues (y-axis) measured in each time eight individuals, and normalised by the reference gene *RPL9*. The left to right border of the boxes indicate the 25 to75 percentiles and the vertical line within the box mark the median, whereas the whiskers represent the 10 to 90 percentiles (from left to right). The different treatment categories given in the plot are high density (HD) in dark grey, and moderate density (MD) in light grey.

B.4.2. Stress target genes

B.4.2.1. Acute density stress

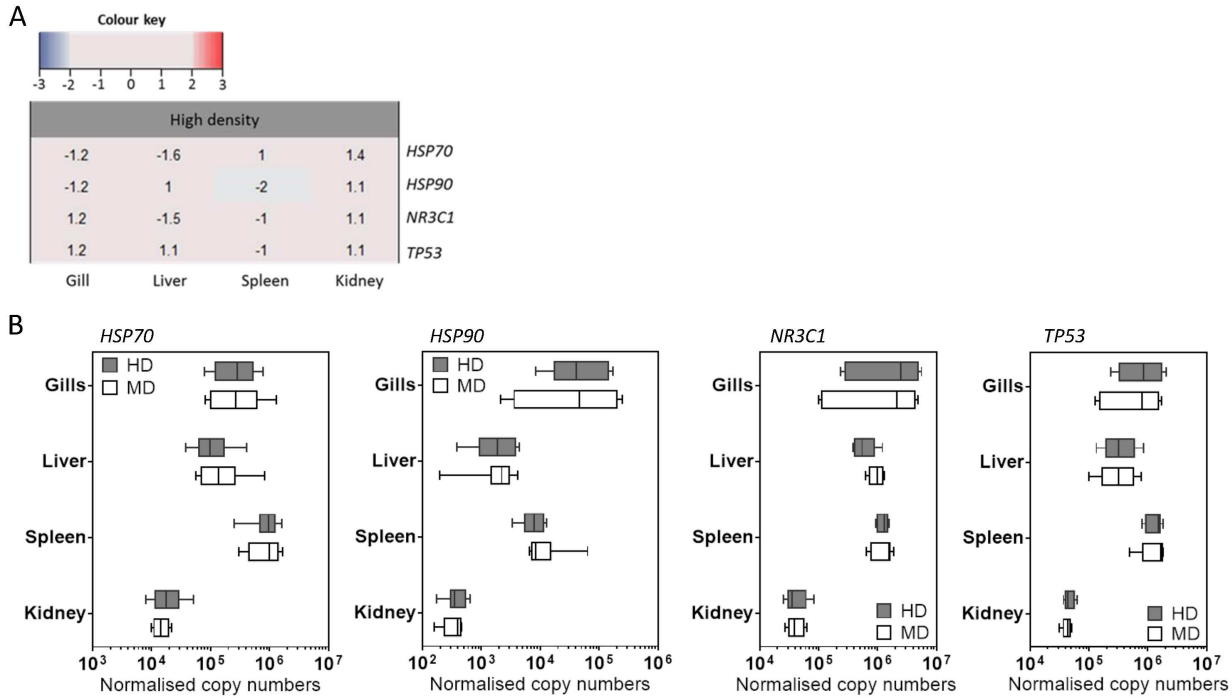

Figure B.21: The given heat map (A) represents average expression ratios as fold changes of high density relative to moderate density for the stress target genes *HSP70*, *HSP90*, *NR3C1*, and *TP53* measured by qPCR (n = 8). The different tested target genes are represented in rows and the tissues in columns. The bar above the heat map indicates the analysed density category. The colour key (on top) indicates the range of values on which the colouring of the heat map is based. The box-whisker plots (B) depict the individual copy numbers (x-axis) of the target genes (indicated above the plot) in the different tissues (y-axis), normalised by the reference gene *RPL9*. The left to right border of the boxes indicate the 25 to75 percentiles and the vertical line within the box mark the median, whereas the whiskers represent the 10 to 90 percentiles (from left to right). The different treatment categories given in the box plot are high density (HD) in dark grey, and moderate density (MD) in light grey.

B.5. Temperature stress

B.5.1. Immune target genes

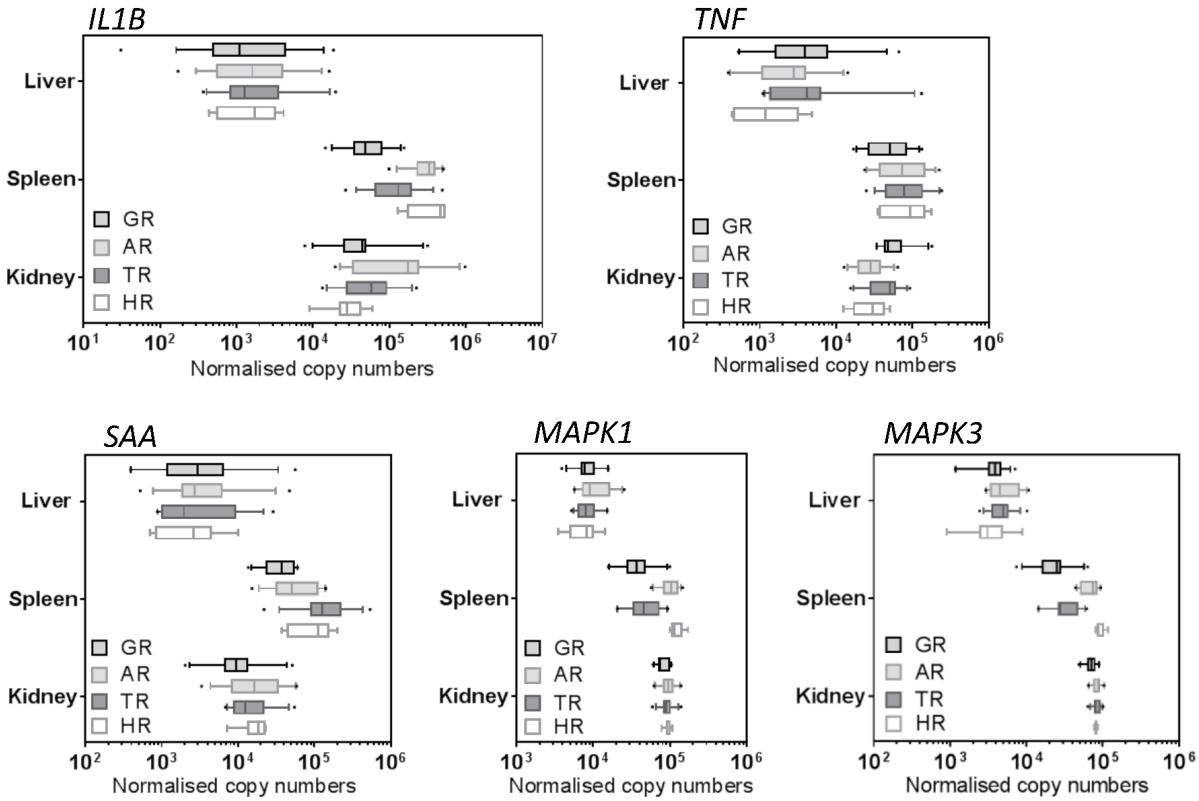

Figure B.22: The box-whisker plots depict copy numbers (x-axis) of the target genes (indicated above the plot) in different tissues (y-axis) measured in each time 14 individuals, and normalised by the reference genes *RPL9, RPL32*, and *EEF1A1B*. The left to right border of the boxes indicate the 25 to 75 percentiles and the vertical line within the box mark the median, whereas the whiskers represent the 10 to 90 percentiles (from left to right). The different treatment categories given in the plot are gradual rise (GR), acute rise (AR), temperature reference (TR), and handling reference (HR), all indicated by different shades of grey.

B.5.2. Handling reference

Table B.3: DE genes shared by liver and spleen after exposure of maraena whitefish to HR conditions (relative to TR).

Treatment Category	Agilent ID	Gene symbol	Function	FC Kid	FC Liv	FC Spl
Handling reference	A_05_P265359	*CSRNP1* (cysteine/serine-rich nuclear protein 1-like)	Transcription regulator	-	2.6	2.3
	A_05_P366767	*TNFAIP2* (tumor necrosis factor, alpha-induced protein 2)	TNF signaling	-	-2.0	-2.4

B.5.3. Gradual temperature rise

Table B.4: List of DE genes shared by kidney, liver, and spleen after exposure of maraena whitefish to GR conditions (relative to TR) and which were subjected to IPA pathway analysis. From the overall 13 DE genes the 12 given in the table below matched to an object in the Ingenuity Knowledge Base and therefore could be assigned to functional pathways.

Treatment category	Agilent ID	Gene symbol	Function	FC Kid	FC Liv	FC Spl
Gradual rise	A_05_P322977	*SERPINH1* (heat shock protein 47)	Chaperone of collagen	3.9	3.3	5.2
	A_05_P366617	*CLU* (clusterin)	Molecular chaperone	2.9	2.6	2.3
	A_05_P247249	*EEF1A1a* (elongation factor 1 alpha)	Translation regulator (delivery of tRNA to ribosome)	2.5	5.6	2.5
	A_05_P450812	*EEF1A1b* (elongation factor 1 alpha-like)	Translation regulator (delivery of tRNA to ribosome)	2.3	5.1	2.4
	A_05_P255059	*EDF1* (endothelial differentiation-related factor 1 homolog)	Cell differentiation	-21.6	-5.9	-50.3
	A_05_P266979	*CEACAM20* (carcinoembryonic antigen-related cell adhesion molecule 20-like)	Regulation of cytokine production	-11.8	-17.9	-34.0
	A_05_P365247	*CIRBP* (cold-inducible RNA-binding protein B-like)	Translation regulator (cellular response to cold)	-4.9	-3.5	-3.5
	A_05_P436147	*YBX2* (Y-box-binding protein 2-A)	Nucleic acid binding protein	-3.5	-2.8	-2.3
	A_05_P251709	*SPCS2* (signal peptidase complex subunit 2)	Protein targeting to ER	-2.5	-2.9	-2.0
	A_05_P275544	*FKBP5* (peptidyl-prolyl cis-trans isomerase FKBP5-like)	Immunoregulation and basic cellular processes	-2.3	-2.3	-2.8
	A_05_P480527	DDX5 (ATP-dependent RNA helicase DDX5)	Helicase and hydrolase activity	-2.2	-3.4	-2.0
	A_05_P473637	*AGT* (angiotensinogen)	Maintaining blood pressure	-2.1	-3.4	-6.3

B.5.4. Acute temperature rise

Table B.5: List of the 11 DE genes shared by kidney, liver, and spleen after exposure of maraena whitefish to AR conditions (relative to TR) and which were subjected to IPA pathway analysis.

Treatment category	Agilent ID	Gene symbol	Function	FC Kid	FC Liv	FC Spl
Acute rise	A_05_P252849	*HSP70* (heat shock 70 kDa protein)	Molecular chaperone	72.5	143.6	109.4
	A_05_P485612	*HSP90* (heat shock protein 90-alpha 1)	Molecular chaperone	6.8	12.2	6.2
	A_05_P410467	*DDIT4* (DNA damage-inducible transcript 4 protein-like)	mTOR signaling	6.2	7.9	8.1
	A_05_P319052	*DNAJA2* (dnaJ homolog subfamily A member 4-like)	Cochaperone of Hsp70	5.2	10.6	5.3
	A_05_P424327	*DUSP1* (dual specificity protein phosphatase 1-like)	Regulation of cellular stress response and proliferation	4.9	3.6	7.3
	A_05_P262354	*DNAJB1* (dnaJ homolog subfamily B member 1-like)	Cochaperone of Hsp70	3.3	3.6	3.2
	A_05_P259219	*PPP1R15A* (protein phosphatase 1 regulatory subunit 15A-like)	Response to DNA damage stimulus	3.1	7.6	7.1
	A_05_P463147	*ZFAND2A* (AN1-type zinc finger protein 2A)	Degradation of toxic or misfolded proteins	2.8	3.2	2.5
	A_05_P276369	*ZFAND2B* (AN1-type zinc finger protein 2B)	Degradation of toxic or misfolded proteins	2.6	4.1	2.3
	A_05_P433692	*AHSA1* (activator of 90 kDa heat shock protein ATPase homolog 1-like)	Chaperone binding	2.6	3.1	3.4
	A_05_P433692	*FOSL2* (FOS-like antigen 2)	Transcription regulator (cell proliferation, differentiation, transformation)	2.4	2.9	4.3

C. Published GenBank sequences

Gene symbol	Organism	Molecule type	Sequence length [bp]	CDS [bp]	Product	Accession number	Date of publication
HSP70	*C. maraena*	linear mRNA	1002	1..>1002	heat shock 70 kDa protein	LN907850	21-NOV-2016
HSP90	*C. maraena*	linear mRNA	920	9..>912	heat shock protein 90kDa	LN812811	20-MAR-2015
NR3C1	*C. maraena*	linear mRNA	2405	43..2340	nuclear receptor subfamily 3, group C, member 1 (glucocorticoid receptor)	LN812810	20-MAR-2015
IL1B	*C. maraena*	linear mRNA	886	66..848	interleukin 1, beta	LN624221	20-OCT-2014
IL6	*C. maraena*	linear mRNA	731	21..689	interleukin 6	LN624219	20-OCT-2014
CXCL8	*C. maraena*	linear mRNA	784	5..298	C-X-C motif chemokine ligand 8	LN624218	20-OCT-2014
IL12B	*C. maraena*	linear mRNA	1130	7..1011	interleukin 12 B	LN624220	20-OCT-2014
SAA	*C. maraena*	linear mRNA	419	38..403	serum amyloid A	LN624222	20-OCT-2014
TNF	*C. maraena*	linear mRNA	801	36..>800	tumor necrosis factor	LT970869	10-JAN-2018
MAPK1	*C. maraena*	linear mRNA	215	<1..>215	mitogen-activated protein kinase 1	LT971012	10-JAN-2018
MAPK3	*C. maraena*	linear mRNA	784	<1..756	mitogen-activated protein kinase 3	LT971391	10-JAN-2018
IGF1	*C. maraena*	linear mRNA	612	6..572	insulin-like growth factor 1	LN812808	20-MAR-2015
IGF2	*C. maraena*	linear mRNA	692	46..690	insulin-like growth factor 2	LN812809	20-MAR-2015

D. Publications and Conferences

Publications

Joan Martorell-Ribera & Mareen **Nipkow**, Torsten Viergutz, Ronald M. Brunner, Ralf Bochert, Raphael Koll, Tom Goldammer, Ulrike Gimsa & Alexander Rebl

Early regulation of immune and endocrine genes after stimulation of salmonid head-kidney cells with stress hormones and Toll-like- receptor ligands. Submitted to Fish and Shellfish Immunology in August 2019

Rebl, A., Verleih, M., **Nipkow**, M., Altmann, S., Bochert, R., Goldammer, T., 2018.

Gradual and acute temperature rise induce crossing endocrine, metabolic and immunological pathways in maraena whitefish (*Coregonus maraena*). Frontiers in Genetics, 9:241.doi: 10.3389/fgene.2018.00241

Nipkow, M., Wirthgen, E., Luft, P., Rebl, A., Hoeflich, A., Goldammer, T., 2018.

Characterization of *igf1* and *igf2* genes during maraena whitefish (Coregonus maraena) ontogeny and the effect of temperature on embryogenesis and *igf* expression. Growth Hormone & IGF Research, 40, 32-43, https://doi.org/10.1016/j.ghir.2018.04.003

Korytář, T., **Nipkow**, M., Altmann, S., Goldammer, T., Köllner, B., Rebl, A., 2016.

Adverse husbandry of maraena whitefish directs the immune system to increase mobilization of myeloid cells and proinflammatory responses. Frontiers in Immunology, 7:631. doi: 10.3389/fimmu.2016.00631

Brietzke, A., Borchel, A., Altmann, S., **Nipkow**, M., Rebl, A., Brunner, R., Goldammer, T., 2016.

Transcriptome sequencing of maraena whitefish (*Coregonus maraena*). Marine Genomics, 29, 27-29, http://dx.doi.org/10.1016/j.margen.2016.05.006

Altmann, S., Korytář, T., Kaczmarzyk, D., **Nipkow**, M., Kühn, C., Goldammer, T., Rebl, A., 2016.

Toll-like receptors in maraena whitefish: Evolutionary relationship among salmonid fishes and patterns of response to *Aeromonas salmonicida*. Fish & Shellfish Immunology, 54, 10.1016/j.fsi.2016.04.125.

Nipkow, M., Rebl, A., Köbis, J.M., Goldammer, T., 2015.

Identifizierung von Serum Amyloid A als potenzieller Marker zur Einschätzung des Gesundheitszustandes von Coregonus maraena (Ostseeschnäpel) in Aquakultur anhand von Genexpressionsanalysen. 16th Day of the Doctoral Student, Schriftenreihe 24, 41-44

Conferences

Rebl, A., Korytář, T., **Nipkow**, M., Altmann, S., Köllner, B., Goldammer, T.,

"The Transcriptional Response to Adversity is conserved throughout vertebrate evolution", poster at the "14th International Conference on Innate Immunity", June 19-24th, 2017, Heraklion, Greece

Nipkow, M., Rebl, A., Köbis, J.M., Goldammer, T.,

"Untersuchungen zur Regulation von Genen des angeborenen Immunsystems nach Infektion von *Coregonus maraena* (Ostseeschnäpel) mit dem aquakulturrelevanten Pathogen *Aeromonas salmonicida",* abstract and presentation at the "Vortragstagung der DGfZ und GfT", September 16-17th, 2015, Berlin, Germany

Nipkow, M., Rebl, A., Korytář, T., Goldammer, T.,

"Healthy fish in aquaculture: Is *SAA* an appropriate marker for description of health in maraena whitefish?", abstract and oral presentation at the "17th EAFP International Conference on Diseases of Fish and Shellfish", September 7-11th, 2015, Las Palmas de Gran Canaria, Spain

Nipkow, M., Köbis, J.M., Rebl, A., Bochert, R., Kühn, C., Goldammer, T.,

"Serum Amyloid A: Ein potenzieller Marker zur Einschätzung des Gesundheitszustands von Ostseeschnäpeln (*Coregonus maraena*) in Aquakultur?", poster presentation at the "VDFF- Deutscher Fischereitag", August 25-27th, 2015, Rostock, Germany

Rebl, A., Köbis, J. M., Verleih, M., Brietzke, A., **Nipkow**, M., Korytář, T., Rebl, H., Krasnov, A., Gjøen, T., Kühn, C., Brunner, R. M., Seyfert, H.-M., Goldammer, T.,

"Charakterisierung der frühen Immunantwort auf *A salmonicida* in Lachsfischen", poster at the "6. Büsumer Fischtag", June 11th, 2015, Kiel, Germany

Nipkow, M., Altmann, S., Köbis, J.M., Goldammer, T.,

"Charakterisierung des Stressverhaltens von *Coregonus maraena* (Ostseeschnäpel) in Aquakultur", abstract and oral presentation at the "Vortragstagung der DGfZ und GfT", September 17-18th, 2014, Dummerstorf, Germany

Nipkow, M., Altmann, S., Köbis, J.M., Bochert, R., Kühn, C., Goldammer, T.,

"Initial Characterization of Immunorelevant Genes as Prerequisite for Stress Analyses in Aquacultured Maraena Whitefish (*Coregonus maraena*)", poster presentation at the "International Congress on the Biology of Fish", August 3-7th, 2014, Edinburgh, Scotland

Nipkow, M., Altmann, S., Verleih, M., Rebl, A., Goldammer, T.,

"Identifizierung und Charakterisierung stressrelevanter Gene des Ostseeschnäpels (*Coregonus lavaretus balticus*)", abstract and oral presentation at the "Vortragstagung der DGfZ und GfT",

September 4-5th, 2013, Göttingen, Germany

E. Acknowledgement

Writing a doctoral thesis is a unique experience, which is in large part exciting and fascinating but sometimes devastating and exhausting, as well. Therefore, I would like to take this opportunity to thank all the people who accompanied, motivated and supported me during the past five years.

First and foremost I would like to express my gratitude to Tom, for taking me under his wings in the Fish Genetics Unit of the FBN, for giving me a lot of freedom to develop myself and for guiding and pushing me if needed, for always having an open door to listen to problems and concerns and for many scientific and even amusing talks.

My sincere thanks also go to Professor Hubert Bahl for being my supervisor at the University of Rostock, for many years of respectful and friendly cooperation, and for reviewing this thesis.

I also want to thank Tomáš, Peter, Elisa, and Andreas Höflich for their support and the friendly and fruitful collaboration. Further, I would like to acknowledge all the past and present members of the LFA Born who were always on the spot whenever a helping hand was needed during the countless fish sampling procedures.

I also would like to thank Alex, Marieke, Judith, and Andreas for their abundant support, encouragement, and constructive suggestions and most of all for being such relaxed, open hearted, cheerful and affectionate colleagues.

I am particularly indebted to Andreas who gave so much time and effort sharing his sheer inexhaustible expertise with me and for his countless patient explanations. Special thanks go to Alex for the thorough proofreading of this thesis and for his guidance and the helpful and highly motivational comments and discussions over the last years. Thank you very much for sharing and spreading your fascination and enthusiasm for research.

Furthermore, I am deeply thankful to our amazing technicians Ingi, Gitti and Luisa, the busy bees and good souls of our lab who made my work so much easier. Without you I could never have obtained this huge amount of data!

I would like to thank all former and current colleagues at the Fish Genetics Unit, the Institute of Genome Biology and the FBN who supported me and contributed to the friendly and pleasant working atmosphere.

I am especially thankful to my friends and fellow sufferers who always understood me and cheered me up, for so many joyful hours and days apart from science but for so many endless discussions about the sense and nonsense of a Ph.D. thesis, as well.

I am particularly thankful to my parents Kerstin and Wilfried for the immense confidence they have shown in me since the very beginning of my school career and for their unconditional support in all my pursuits. I am also deeply grateful to my family for all their understanding, sympathy and support and for braving my mental and/or personal absence over the past months, if not even years.

I owe my deepest gratitude to my dear Tobi for the tireless managing of the daily business around me so that I could completely focus on the writing process over the past months, for the infinite support and encouragement, for sharing so many wonderful moments over the past years and for giving so much love to me and our lovely little Pauli.

F. Selbstständigkeitserklärung

Ich versichere hiermit an Eides statt, dass ich die vorliegende Arbeit selbstständig angefertigt und ohne fremde Hilfe verfasst habe. Dazu habe ich keine außer den von mir angegebenen Hilfsmittel und Quellen verwendet und die den benutzten Werken inhaltlich und wörtlich entnommenen Stellen habe ich als solche kenntlich gemacht.

Rostock, den 18.09.2018

Mareen Nipkow